



UNIVERSITÀ
DEGLI STUDI
DI PADOVA

Università degli Studi di Padova

PhD School in “**HISTORY, CRITICISM AND PRESERVATION OF CULTURAL HERITAGE**”

Doctoral Cycle XXXI

PhD Dissertation

**“NON-INVASIVE METHODS FOR THE STUDY OF WALL DECORATIONS
IN ART HISTORY AND ARCHAEOLOGY”**

Course coordinator: Prof. Andrea Tomezzoli

Supervisor: Prof. Rita Deiana

Co-Supervisor: Prof. Gilberto Artioli

PhD Student: Antonina Chaban

TABLE OF CONTENTS

Abstract	1
Riassunto	3
1. INTRODUCTION	
1.1 Non-invasive approach to wall paintings and wall mosaics: state of the art.....	5
1.2 Objectives of the research.....	10
1.3 Thesis structure.....	12
2. WALL DECORATIONS	
2.1 Wall paintings	
2.1.1 <i>Historical background</i>	16
2.1.2 <i>Materials and execution technique</i>	19
2.2 Wall mosaics	
2.2.1 <i>Historical background</i>	25
2.2.2 <i>Materials and execution technique</i>	27
3. METHODOLOGY AND INSTRUMENTS	
3.1 Contact methods used for on-site tests, principles and applications	
3.1.1 <i>Ground Penetrating Radar</i>	39
3.1.2 <i>Holographic Subsurface Radar</i>	41
3.2 Non-contact methods used for on-site tests, principles and applications	
3.2.1 <i>Infrared Thermography</i>	46
3.2.2 <i>Multispectral Imaging</i>	49
3.3 Other non-invasive methods used in the laboratory simulation tests	57
4. IN-SITU NON-INVASIVE MEASUREMENTS OF WALL PAINTINGS	
4.1 The Frigidarium of Sarno Baths (Pompeii, Italy)	
4.1.1 <i>Case study description</i>	63
4.1.2 <i>Acquisition and analysis of multispectral images</i>	65
4.1.3 <i>Discussion of the results</i>	75

4.2	The Scrovegni Chapel (Padua, Italy)	
4.2.1	<i>Case study description</i>	77
4.2.2		
	a) <i>Acquisition and analysis of multispectral images</i>	82
	b) <i>infrared thermography acquisitions</i>	89
4.2.3	<i>Discussion of the results</i>	90
4.3	The Chapter Hall (Sala del Capitolo) in the Basilica of Saint Anthony (Padua, Italy)	
4.3.1	<i>Case study description</i>	94
4.3.2		
	a) <i>Acquisition and analysis of multispectral images</i>	96
	b) <i>Holographic subsurface radar acquisitions</i>	99
4.3.3	<i>Discussion of the results</i>	100
4.4	The Catholikon of the Dafni Monastery (Athens, Greece)	
4.4.1	<i>Case study description</i>	102
4.4.2		
	a) <i>Acquisition and analysis of multispectral images</i>	104
	b) <i>infrared thermography acquisitions</i>	106
4.4.3	<i>Discussion of the results</i>	108
5.	IN-SITU NON-INVASIVE MEASUREMENTS OF WALL MOSAICS	
5.1	The Church of Santa Maria dell’Ammiraglio, named “La Martorana” (Palermo, Italy)	
5.1.1	<i>Case study description</i>	112
5.1.2	<i>Acquisition and analysis of multispectral images</i>	116
5.1.3	<i>Discussion of the results</i>	133
5.2	The Palatine Chapel in the Norman Palace (Palermo, Italy)	
5.2.1	<i>Case study description</i>	138
5.2.2	<i>Acquisition and analysis of multispectral images</i>	142
5.2.3	<i>Discussion of the results</i>	152

5.3	The main porch of the Basilica of Saint Mark (Venice, Italy)	
5.3.1	<i>Case study description</i>	155
5.3.2	<i>Acquisition and analysis of multispectral images</i>	158
5.3.3	<i>Discussion of the results</i>	162
5.4	The Catholikon of the Dafni Monastery (Athens, Greece)	
5.4.1	<i>Case study description</i>	165
5.4.2		
	a) <i>Acquisition and analysis of multispectral images</i>	165
	b) <i>Infrared thermography acquisitions</i>	169
5.4.3	<i>Discussion of the results</i>	169
5	LABORATORY SIMULATION TESTS	173
6	SUMMARY AND CONCLUSIONS	215
	REFERENCES	225
	<i>Acknowledgements</i>	
	ATTACHMENTS	235

Abstract

Wall paintings and mosaics, especially those of archaeological and art historical interest, represent a complex object of study. They are characterized by the presence of a highly valuable decorated surface and several underlying preparation layers, acting as interface to the structural support. The presence of hidden defects within this structure can be related to the ageing and deterioration of materials, inhomogeneities can be the result of past restoration interventions on the ancient artwork. This thesis project introduces a combined in-situ non-invasive approach to characterize ancient wall decorations and their underlying support in art historical and archaeological field. For this purpose, experimental in-situ and laboratory tests are aimed to evaluate the applicability, potentialities and limitations of the combination of four portable electromagnetic methods:

- Multispectral imaging (MI), using a modified camera with visible, infrared and ultraviolet filters (300-1000 nm), applied to analysis of the decoration layer;
- Holographic subsurface radar (HSR), with 6.4-6.8 GHz antenna), applied to analysis of the shallow subsurface layers;
- Infrared thermography (IRT), applied to analysis of the subsurface structure;
- High resolution ground penetrating radar (GPR), with a full polar 2 GHz antenna for the investigation of the internal structure of the wall.

Operating with different frequencies and related different penetration depth and resolution, these techniques can provide complementary information regarding the surface (i.e. materials, pigments, degradation phenomena, restorations etc.) and its underlying layers (i.e. structural integrity, differences in materials, presence of humidity, detachments, cracks etc.).

The in-situ tests were performed on some representative case studies in Italy and Greece, which date to different periods and are characterized by different site conditions and conservation state of the analyzed decorations.

The in-situ experimental approach, proposed in the thesis, was integrated by laboratory tests, using additional non-invasive methods: Digital Holographic Speckle Pattern Interferometry and Stimulated Infrared Thermography (DHSPI-SIRT).

The experimental approach has shown that the applicability of in-situ methods is strongly conditioned by the intrinsic characteristics of decorated surfaces (high value, geometry, degradation state), to which the use of non-invasive contact methods (GPR and HSR) is limited. The in-situ results are strongly influenced by logistics and acquisition conditions.

The key contribution of this thesis is evaluation of advantages and limitations of the tested in-situ non-invasive investigation approach for the diagnostics of ancient wall paintings and mosaics. This experimental research has shown that portability, remote access, immediate visualization and interpretation of data are crucial in the development of general guidelines (non-invasive investigation protocol) for the diagnostics of wall paintings and mosaics. These characteristics are essential for efficient interdisciplinary collaboration between scientists, art historians, archaeologists, conservators and curators, aimed at correct monitoring and conservation planning of wall paintings and mosaics.

Riassunto

Pitture e mosaici parietali, soprattutto quelli di interesse storico-artistico e archeologico, rappresentano un oggetto di studio complesso. Oltre alla struttura fisica, generalmente costituita da una superficie esterna decorata e preziosa e dai diversi strati di preparazione che fungono da interfaccia con il supporto strutturale e che caratterizzano tutti i tipi di decorazioni parietali senza distinzione di tipologia e di epoca di realizzazione, si deve infatti tener conto anche della componente molto importante legata alla storia e alla vetustà del manufatto. Questo comporta la possibilità che ci siano presenti anomalie legate al degrado dei materiali e dei supporti e disomogeneità legate ai restauri che possono aver interessato l'opera nel tempo. La possibilità di ottenere informazioni preliminari in modo non invasivo su tutti gli strati e sulle eventuali anomalie ivi presenti, costituisce pertanto un punto chiave nella diagnostica in-situ delle decorazioni parietali soprattutto per quelle di interesse storico-artistico o archeologico. Il presente progetto di ricerca, attraverso un approccio di tipo sperimentale, mira a testare le potenzialità e limiti di alcuni metodi elettromagnetici per indagini in situ di tipo non invasivo su pitture e mosaici parietali antichi. A tale scopo, sono stati presi in considerazione quattro diversi metodi di indagine:

- l'Imaging Multispettrale (MI), utilizzando una macchina fotografica modificata e quattro differenti filtri (VIS-UV- e tre bande IR), per analisi, nel range 300-1000 nm, sulla superficie esterna decorata;
- il Radar Olografico (HSR), utilizzando un'antenna con 5 frequenze comprese tra 6.4 GHz e 6.8 GHz, per l'analisi dei primi strati al di sotto della superficie esterna decorata;
- la Termografia infrarossa (IRT), per l'analisi delle anomalie sub-superficiali;
- il georadar (GPR) ad altissima risoluzione, con un'antenna full polar da 2 GHz, per l'analisi della struttura interna dell'apparato murario al di sotto della superficie decorata.

Operando con frequenze diverse, corrispondenti a profondità di indagine e risoluzioni differenti, queste tecniche possono in generale fornire informazioni preliminari sulla superficie (per esempio su materiali, pigmenti, stato di degrado, precedenti interventi ecc.) e sugli strati sottostanti (integrità strutturale, differenze nei materiali, presenza di umidità, distacchi, crepe, ecc.).

Le misure in-situ sono state condotte su alcuni casi studio rappresentativi in Italia e in Grecia, relativamente a manufatti che risalgono a epoche diverse, in differenti contesti e differenti stati di conservazione.

L'approccio sperimentale ha dimostrato che l'applicabilità dei metodi in situ è fortemente condizionata dalle caratteristiche intrinseche delle superfici di pregio (alto valore storico

artistico, geometria, stato di degrado), che limitano l'uso dei metodi non invasivi a contatto (GPR e HSR) e che i dati sono inoltre fortemente dipendenti dalla logistica e dalle modalità di acquisizione.

La sperimentazione in situ proposta nella tesi è stata integrata con test di laboratorio, utilizzando anche altri metodi non-invasivi, quali l'interferometria olografica e termografia infrarossa attiva (DHSPI-SIRT).

Questo lavoro di ricerca ha evidenziato che portabilità, uso a distanza, immediata visualizzazione e interpretazione dei dati sono elementi cruciali nello sviluppo di un approccio non invasivo alla diagnostica di pitture murali e mosaici e risultano fondamentali per la caratterizzazione preliminare, per l'efficiente monitoraggio, la corretta diagnosi e l'adeguata pianificazione degli interventi sulle decorazioni parietali di interesse storico-artistico e archeologico nell'ottica di un'efficace collaborazione interdisciplinare tra componente scientifica e umanistica (storici dell'arte, archeologi) e con conservatori e curatori di questi preziosi beni.

INTRODUCTION

1.1 Non-invasive approach to wall paintings and wall mosaics: current state of the art

Historical and archaeological wall paintings and wall mosaics represent an important human inheritance from the past [1]. They are generally characterized by a visible highly valuable decoration surface and by the presence of several underlying preparation layers, which act as interface between the structural support (i.e. a wall), and the decorative layer (tesserae and binding medium) [2, 3]. The current approach in their diagnostics can foresee several steps: non-invasive full-field characterization (on-site), non-invasive spot analysis (on-site) and very often micro-invasive (usually laboratory) tests [4].

This Ph.D. project is focused on non-invasive methods in the diagnostics of wall paintings and wall mosaics, performed in-situ with the aim to provide a general evaluation of the conservation state of a wall decoration and identification of areas of interest for subsequent detailed, spot-local and micro-invasive analysis.

It should be mentioned that systematic involvement of scientific analysis in the Cultural Heritage field dates back only to a few decades [4]. The first tests were predominantly invasive, performed on samples or later on micro-samples in a laboratory environment [5]. Recently a selection of methods has been developed that help to preserve the integrity of art material. The most recent scientific studies are focused on the development of non-invasive approaches, which minimize and try to exclude sampling of the original artistic material [6-9]. The non-invasive and non-contact approach is of crucial importance for the diagnostics of highly valuable art objects like wall paintings and wall mosaics, in which:

- the micro-invasive analysis is very limited or not allowed at all [7-9];
- direct contact to the surface should be avoided or is not allowed at all [7-9].

This chapter introduces a variety of scientific diagnostic methods, based on the propagation of the electromagnetic signal and used nowadays in diagnostics and conservation practices. This chapter provides their classification and main conservation issues to be addressed by relative instrumentation of these methods.

Methods or analyses are defined as invasive if they induce any type of permanent alteration in the art object or its part [8]. These alterations might refer to chemical or physical alterations inside the material, to extraneous inclusions, to a breakdown of chemical bonds or formation of new molecules. The most common type of alteration is still induced through sampling or micro sampling of the art material, which is implemented in order to perform specific laboratory tests [4-5, 8-9]. The laboratory analyses, performed on a sample or a micro-sample, are already

invasive, at the same time, they can be destructive or non-destructive [4, 8]. After its examination by non-destructive techniques (Optical Microscopy (OM), by Scanning Electron Microscopy integrated with Energy Dispersive X-Ray Fluorescence (SEM-EDX) [4-5, 9-10] and by micro-Raman and Fourier Transform Infrared Spectroscopy (micro-FTIR) [11-12], the sample is identically conserved in its condition prior to the analysis, without any alterations to the material and its integrity [4, 8-9]. The sample can be stored and repeatedly examined by the same or by different techniques. On the contrary, after the examination of the sample by destructive techniques (i.e. X-ray Diffraction (XRD) [13], Gas Chromatography/Mass Spectrometry (GC/MS) and High Performance Liquid Chromatography (HPLC)) [4,5] the sample is altered or destroyed and cannot be used again for further analysis [8].

On-site non-destructive and non-invasive techniques are the methods that do not induce any kind of alterations to the wall decoration and its structural support [8]. This category of methods includes nowadays a variety of techniques, based on electromagnetic waves interaction with matter [4, 8, 14]. These methods can be classified according to the wavelength and energy of the exploited radiation. In this thesis, they are also classified in terms of the size of the analysed area (full-field or spot-local analysis), investigation depth (surface and subsurface) and application mode (contact or non-contact methods).

Up to now, different expert groups involved in the cultural heritage maintenance use non-destructive and non-invasive techniques in a non-standardized way. There is still a lack of commonly agreed classification and standardization of applications and conservation documentation in Cultural Heritage diagnostics [15-16]. In the author's awareness, many of available scientific studies focus whether on the characterization of the uppermost decoration layer or on structural evaluation of deeper levels of wall integrity. The most recent portable non-invasive methods for the characterization of a decorated layer are based on electromagnetic waves propagation [14, 17-18] and include multispectral and hyperspectral imaging [19-22], Fiber-Optics Reflectance Spectroscopy (FORS) [23], portable XRF [24], portable FTIR [25-26], portable Raman spectroscopy [25-26] and Terahertz Imaging (THz) [27-28]. Non-destructive techniques for on-site subsurface structural diagnostics of walls in Cultural Heritage include, among other methods, Infrared Thermography [29-34], Ground Penetrating Radar [35-37] and Optical Holographic Interferometry [38-41].

Nevertheless, the preservation of the decorated surface can be compromised by many factors: by environmental conditions [42-43], failure and deterioration of the supporting structure, as well as by the integrity of the intermediate layer (substrate) [44-47]. In common conservation practices, the advanced non-invasive approaches are still not regularly involved. For example,

a tap test (finger-knocking approach) for in-situ subsurface structural diagnostics of wall decorations is still often used [47]. It can become invasive to fragile historical and archaeological decorated surfaces [46-47]. Furthermore, it is time-consuming for large areas and its execution accuracy and interpretation is subject to individual skills and experience. There is a strong demand for the development of non-invasive combined in-situ approach to wall decorations [7].

The given project is focusing on advantages and limitations of in-situ diagnostics by exclusively non-invasive techniques, the combination of which can provide initial stage information at different depth levels, including surface, shallow subsurface and structural support: Multispectral Imaging, Infrared Thermography, Holographic Subsurface Radar and Ground Penetrating Radar. The physical principle of non-invasive methods, studied in this project, is based on electromagnetic interactions, where the extraction of information about artwork materials and its structure is performed through the study of the reaction of matter to electromagnetic waves at various wavelengths [16-18] (Fig. 1).

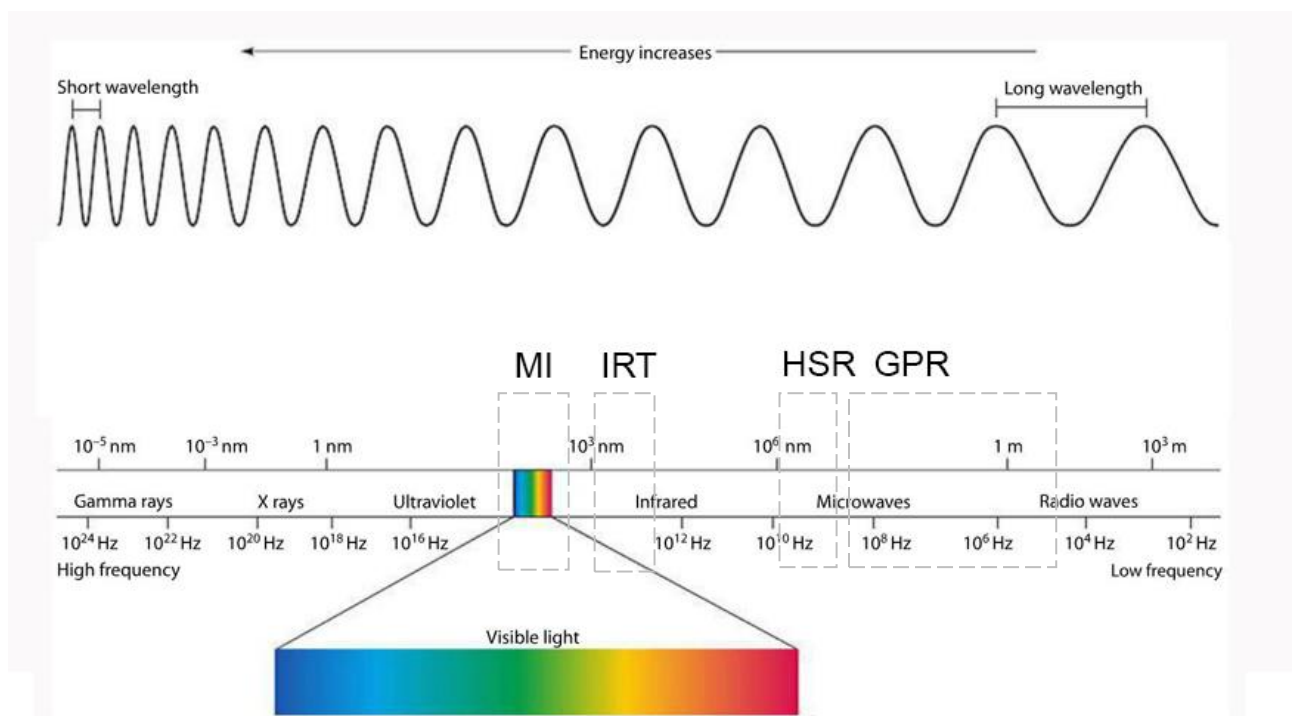


Fig. 1 Electromagnetic spectrum. The image indicates schematically the exploited wavelength range of the examined techniques, after [14]

Electromagnetic waves are typically described by any of the following three physical properties: the frequency f , wavelength λ , or photon energy E . The energy of a photon is proportional to the frequency of the electromagnetic radiation [17-18]. The visible portion of the electromagnetic spectrum covers only a small range within this spectrum with wavelengths

from 0.38 to approximately 0.74 μm (380-750 nm) and is used in laser interferometry techniques as in Digital Holographic Speckle Pattern interferometry (DHSPI) [38-41], in photographic documentation, naked eye and magnified lenses observation, as well as raking light observation and photography. The ultraviolet and near-infrared spectral regions, adjacent to the visible range, have found numerous applications in Cultural Heritage including Multispectral Imaging of decorated surfaces integrated into historical and archaeological buildings and structures [19-22]. The infrared part of the electromagnetic spectrum covers the range from roughly 750 nm to 1 mm (frequency 300 GHz to 400 THz) [29-33]. Holographic subsurface radar (HSR) operates in the microwave range [48-52], high frequency Ground Penetrating Radar, applied to structural diagnostics operates in the radio wave region [34-37]. The list of here evaluated techniques is reported in Table 1.

Table 1. Selected EM methods, relative instrumentation and operating wavelength

Method	Abbreviation	Exploited wavelength	Range	Characteristics of the instruments, used in the project
Ground Penetrating Radar	GPR	Radiowave to microwave	from 10 MHz to 2.6 GHz	IDS system with full polar antenna (2 GHz)
Holographic Subsurface Radar	HSR	Microwave	2 GHz, 4 GHz and 7 GHz	Rascan 5/7000 6.4 – 6.8 GHz
Infrared Thermography	IRT	Infrared	9,000–14,000 nm	FLIR 620BX, B20HS, SC640
Multispectral Imaging	MI	Ultraviolet, visible and near-infrared	300 – 1000 nm	Nikon D800 FR 300-1000 nm
Digital Holographic Speckle Pattern Interferometry*	DHSPI	Visible	380-750 nm, laser beam 532 nm	Custom-built system DHSPI-II, using monocromatic

				laser beam - 532 nm
--	--	--	--	------------------------

*additional method used in laboratory experimental procedure

Multispectral imaging (MI) is already a known tool for on-site diagnostics of wall paintings [19-22], but in author's awareness, no systematical studies can be found in the scientific literature with regards to its on-site applications on wall mosaics. The multispectral systems, which are available commercially, for example, a modified camera Nikon D800 Full Range [53-55], or as custom-built prototypes, like IRIS developed at the Institute for Electronic Structure and Laser at FORTH, Greece [56], largely vary in terms of spectrum range, image resolution, post-processing tools, etc. Multispectral imaging method can be used for preliminary mapping and selection of points of interest for in-situ or laboratory analysis by different analytical techniques [19-22].

Infrared thermography (IRT) is already a recognized technique in the field of non-destructive testing, which has been already widely used for the investigation of cultural heritage and art objects. In particular, it has been applied in different studies to the structural evaluation of wall paintings [30-31], mosaics and plastered mosaics [32, 34, 57-59]. The high interest towards the thermal imaging is related to its capability to obtain subsurface features information without physical contact to the surface and without compromising the structural integrity of the inspected target [16, 31]. When coupled to the Ground Penetrating Radar (GPR), this approach proved to be useful to provide complementary information about the integrity of the structural support of wall and floor decoration [35-36]. Holographic Subsurface Radar is an innovative technique and, until now, it was less known by Cultural Heritage experts. Some preliminary studies on its application to structural diagnostic of buildings [48] and floor stone decorations [51] have been performed and are available in the scientific literature [48-52, 60-64]. Digital Holographic Speckle Pattern Interferometry is already a known technique for on-site non-invasive full-field and non-contact subsurface diagnostics and preventive conservation of wall paintings [38-41, 65-68]. As can be concluded from the bibliographic study, it has not been applied yet to on-site wall mosaic diagnostics. In this project, Digital Holographic Speckle Pattern Interferometry, coupled to Infrared Thermography [68], was selected for complementary laboratory tests on a wall mosaic. Some important advantages of this technique include its applicability and informativity independently from the form and regularity of the surface (it can be applied to non-planar surfaces, reliefs and sculptures). It can be applied even at large distances (up to 15 meters). The system provides real-time images visualization and

raw results are easy to read and interpret. Nevertheless, the system is highly sensitive to surrounding vibrations (movement of operators and other people, other technical and mechanical vibrations).

Table 2 presents a selection of known methods available nowadays as tools for on-site non-invasive diagnostics of wall paintings and mosaics, including full-field and spot-local analysis. The table lists the methods evaluated in this project, additional methods used in the laboratory tests, other methods used in-situ for validation of the results, as well as some further non-invasive methods, which are not examined in the given project.

Table 2. Non-invasive methods for on-site diagnostics of decorated walls

Non-invasive methods		Full-field / area analysis	Spot-local analysis	Portable instrumentation
<i>Methods evaluated in the project</i>				
Multispectral imaging	Visible Light	X		X
	UV Reflectance	X		X
	UV fluorescence	X		X
	UV False Colour	X		X
	IR Reflectance	X		X
	IR Fluorescence	X		X
	IR False Colour	X		X
Passive Infrared Thermography		X		X
Ground Penetrating Radar		X		X
Holographic Subsurface Radar			X	X
<i>Additional methods used in the laboratory tests</i>				
Digital Holographic Speckle Pattern Inrerferometry		X		X
Stimulated Infrared Thermography		X		X
<i>Other methods used in-situ for validation of the results</i>				
Fiber Optics Reflectance Spectroscopy			X	X
X-Ray Fluorescence			X	X
<i>Further methods available for in-situ acquisitions</i>				

Profilometry [69]	X		X
Nuclear magnetic Resonance [70-71]	X		X
Hyperspectral Imaging [72-73]		X	X
FTIR Spectroscopy [25, 26]		X	X
Raman Spectroscopy [25, 26]		X	X
Fiber Optics Reflectance Spectroscopy [23]		X	X
X-Ray Fluorescence [24]		X	X
THz Imaging [26-27]		X	X

Summary

As concluded from the bibliographic study, there is a strong demand for standardization of in-situ diagnostic procedures for wall decorations of high archaeological and art historical value. The methods proposed here for the study of wall decorations by experts in art history and archaeology include:

- Ground Penetrating Radar and Infrared Thermography, already well-known diagnostic tools for subsurface diagnostics of wall decorations;
- an innovative Holographic Subsurface Radar (in author's awareness, never applied in-situ on wall paintings and mosaics) and rapidly developing Multispectral Imaging technique (well-known for wall paintings analysis and still not commonly used for wall mosaics diagnostics and study).

The complementary methods, included in the experimental laboratory tests of this study, are:

- a combination of Digital Holographic Speckle Pattern Interferometry and Stimulated Infrared Thermography techniques (DHSPI-SIRT), well known for wall painting subsurface diagnostics, however, in author's awareness, never applied in-situ for wall mosaic subsurface diagnostics.

The methods, which are not evaluated, but used for documentation and validation in this study, include:

- X-Ray Fluorescence and Fiber Optics Reflectance Spectroscopy, well known in the field of wall paintings study, applied in-situ for validation of Multispectral Imaging results on wall paintings;
- Profilometry (3D laser scanner).

There is a wide range of limitations in in-situ applicability of non-invasive methods to wall decorations of high archaeological and art historical value. As concluded from the bibliographic study, the main limitations of in-situ non-invasive approach can be related to:

- general and technical characteristics of methods and their instruments;
- intrinsic characteristics of wall decorations.

Some preliminary considerations on the main in-situ limitations related to the characteristics of used methods and instruments are presented here. Some considerations on the main problems related to the characteristics of the studied objects (wall decorations) are presented at the end of chapter 2.1 (for wall paintings) and at the end of chapter 2.2 (for wall mosaics).

Limitations and challenges of in-situ non-invasive approach due to the characteristics of the methods and instruments

As concluded from the bibliographic study [1-73], there are relevant issues and limitations in the in-situ diagnostics of the wall mosaics and wall paintings, faced by Cultural Heritage experts. Some considerations, related to the characteristics of available methods and instruments, are reported as follows:

- Availability of the instrumentation.

Many of the most recent techniques are still in constant development and not commercially available. Among the selected methods, this limitation should be taken into consideration when performing in-situ acquisitions with DHSPI system or with new Multispectral Imaging systems and portable modified cameras. These instruments are custom-built and at the current moment available only as prototypes (Holographic Interferometry DHSPI and DHSPI-SIRT workstation used in this study, Multispectral Imaging IRIS, new Microwave Holography Rascan 22 GHz, etc.).

- Costs.

The purchase of some commercially available instruments may lead to elevated costs for an individual or small group of conservator-restorers. The proposed here methods are more affordable for Cultural Heritage experts: approximately 10,000 euros for a modified multispectral camera (Nikon D800 FR) or a holographic subsurface radar (Rascan 5/7000). In comparison, the costs may reach 200,000-300,000 euros for Hyperspectral imaging or THz imaging systems.

- Specific software, individual skills and expertise of operators.

The analysis of acquired data may require specific training and/or become time-consuming. This should be taken into consideration when applying GPR (manual acquisition and the use of specific software), HSR (manual acquisition).

- Necessity of physical contact to the surface. Some techniques of crucial importance in subsurface diagnostics, i.e. Ground Penetrating Radar and Holographic Subsurface Radar. They cannot be applied to highly precious or degraded/fragile wall mosaics and wall paintings.
- Area of the investigation. Many of useful advanced techniques do not provide immediate full-field information. They are point-like analysis (portable XRF, FORS, Raman) or detailed methods (HSR, Hyperspectral and THz imaging), therefore the information during a single acquisition can be extracted only from limited areas. It should be taken into consideration when applying HSR in this study.

1.2 Objectives of the research

The selected non-invasive electromagnetic methods operate with different resolution and depth of investigation and include contact and non-contact techniques. These methods include Multispectral Imaging, Holographic Subsurface Radar, Infrared Thermography and high frequency Ground Penetrating Radar. The experimental work in the thesis is aimed to highlight the limits of each technique in their applications to wall decorations in art history and archaeology. These decorations are characterized by a complex structure: the combination of different original and non-original materials, realization techniques, previous restorations, degradation and ageing of materials. The selected portable methods are evaluated on the basis of their capability to provide immediate information about anomalies in a wall decoration, as well as correlation of these anomalies to specific conservation issues: non-original materials and restoration interventions, presence of defects and degradation, etc.

In particular, the four methods were evaluated in terms of their usefulness to address specific conservation issues of each case study (the full list of case studies can be found in Attachment A), among which:

- applications and enhancement of lost wall painting details to very degraded case studies (Sarno Baths, Pompeii, Italy, and Catholikon of Dafni Monastery in Athens, Greece);
- study of artist's execution technique, attribution issues, revealing of preparatory drawing and hidden paint layers (Giotto's wall paintings in Scrovegni Chapel and in the Basilica of Saint Anthony, Padua, Italy);

- differentiation between visibly similar original and substituted tesserae (figure raffigurations in mosaic case studies);
- general evaluation of object's surface and subsurface conservation state and differentiation between presumably original and substituted areas of the wall decoration (all mosaic case studies).

This project is focusing on the evaluation of applicability, advantages and limitations of the selected methods, employed in-situ by Cultural Heritage experts.

The aim of this study is to address the advantages and limitations of selected non-invasive methods in terms of:

- their applicability to the investigated art objects of high value (in the specific case, wall decorations) due to the site and artwork accessibility, cultural protection regulations, portability and resolution of the methods and related instrumentation;
- usefulness and reliability of data obtained;
- complementarity of the examined and additional methods, used in the experimentation procedure.

The experimental data from the analysed case studies will be useful for the development of recommendations for in-situ acquisitions on each type of decoration: wall mosaic and wall paintings. Finally, these results are aimed to contribute to the development of the most appropriate and completely non-invasive (or if necessary minimally invasive) examination procedure in-situ, obtaining the maximum of reliable information through non-invasive and non-contact methods.

1.2 Thesis structure

Chapter 1 introduces the most common and most advanced practices of in-situ diagnostic campaigns and main problems faced by Cultural Heritage experts when working on wall paintings and wall mosaics of high archaeological and art historical interest.

Chapter 2 is focused on the description of the main characteristics of two types of wall decorations, studied within this project: wall paintings and wall mosaics. It presents a brief history of execution techniques and materials in the decoration layer and the subsurface, focusing on the historical periods and features, particularly relevant for the analysed case studies.

Chapter 3 is aimed at presenting the fundamental operation principles of the selected electromagnetic methods, evaluated in this project, subdividing them in two categories: the methods that can be applied at a distance from the decoration surface (non-contact) and the methods that require contact with the investigated surface (contact methods).

Chapters 4 and 5 present the results of experimental in-situ acquisitions on wall paintings and wall mosaics respectively, performed during three years of the project on case studies in Italy and Greece. For each case study, the subchapters start with introducing to the historical context and main conservation issues, the applied methodology and analysis of the results.

Chapter 6 presents the procedure and the results of laboratory simulation tests, performed on fresco samples and on a custom-built mosaic model, with hidden defects and complex subsurface structure. In this experimental part, additional laboratory methods are used.

Taking into consideration the results of experimental in-situ and laboratory tests, chapter 7 contains a general summary of the results, draws some important conclusions and proposes an outline for further research.

2. WALL DECORATIONS IN ART HISTORY AND ARCHAEOLOGY

Ancient wall paintings and mosaics are essential assets of tangible Cultural Heritage. They have been cultural expressions of human creation throughout history and must be preserved for future generations. Their deterioration, accidental or intentional destruction constitutes an important loss for the world's human inheritance [1-3]. Their characteristics and conservation state (constituent materials and degradation problems) must be investigated, in order to assure correct and on-time conservation planning.

However, the diagnostic and conservation challenges presented by decorated wall surfaces are complex for numerous reasons. Wall paintings and mosaics are inherently different from easel paintings (on wood, canvas etc.) or movable mosaics since they are organically connected with a thick structural support (wall, vault, etc.). The decorations generally are made with materials that include earth, lime, cement, and gypsum plasters, various paints, glazes, coatings, stone and glass tesserae, which can be applied to a variety of primary supports [2-3]. The layering of different materials creates a surface that is often of high quality and refinement, imbued with decorations that maintain artistic, historical and technical values, cultural significance and meaning, which should be preserved for future generations. The decorated surface is at the interface between the wall and the surrounding environment (outdoor or indoor) and is particularly vulnerable because it is both exposed to external deterioration factors and can be directly affected by the preservation state of the structural support. In their complexity, these characteristics represent the fundamental challenges in the diagnostic and conservation of decorated surfaces of historical and archaeological structures [46-47].

2.1 Wall paintings

2.1.1 Historical background

The experimental study of this project is focused mainly on the applicability of methods to fresco wall paintings from the Roman, Medieval and 16th century periods in Italy and Greece. However, there is a wide range of artistic techniques and materials use for decoration of walls and vaults during centuries [74].

The first wall paintings were the positive and negative imprints of hands applied to the surfaces of caves. These paintings are dated to 30.000 B.C., the beginning of the Upper Palaeolithic period [75]. The principal pigments were natural oxides of iron and manganese, hematite and limonite. A colour range from brown ochre to yellow was provided by these pigments. Charcoal and bone were used to produce black, while clays were used for white colour. On the

paintings of Lascaux cave (France), the pigments were applied in a dry state to a possibly damp support [75]. Water circulating in the wall cavities contains dissolved limestone, and this solution, crystallizing on the walls, forms a thin, transparent calcium carbonate layer which holds the pigment on the wall [76-77].

It was in the Neolithic period wall painting began to be finally associated with architecture [74, 77]. Paintings started to be applied onto clay based plasters, instead of irregular and rough surfaces of caves.

In Ancient Egypt, wall paintings were applied on one or two layered plaster according to the smoothness of the wall. Generally, the first layer of this plaster was composed of silk and the second layer was composed of calcium sulphate mixed with calcium carbonate. Calcium sulphate dries quickly, hence it was not suitable for fresco application. As far as it is known, arabic gum, gelatine, egg white and beeswax were used as binding media in Ancient Egypt. The fresco technique of painting was not used in Egypt, where painting in tempera was popular [78].

In the prehistorical period, a great variety of painting techniques were already used in Mesopotamia. While the traditional clay plaster technology was still in use, lime plaster technology was developed (around 2000 A.D.). The wall paintings of Yarim-Lim palace at Atchana (Syria) belong to the earliest known examples of fresco paintings. The decoration was first applied on a fresh surface of two-layered lime rendering with the finishing highlights applied on the dried surface [74].

Nevertheless, the real fresco technique can be found even earlier, in ancient Crete and Mycenae around 2500 A.D [79-80]. During the second millennium A.D., paintings were applied over two layers of plaster, with the lower layer being of coarser grains and with the upper layer being of a finer quality. It is thought that the painted plaster of ancient Greece was executed in the fresco technique, where additionally the painting was sometimes burnished to ensure the proper fixing of pigments [74]. The technique referred to as *fresco secco* (mixed) was also sometimes applied. Wall paintings of Knossos, being one of the most important sites of this period, were executed on a support composed of mud and rubble [79]. This support was covered with two layers (1.2 cm and 0.6 cm thickness) calcium carbonate plaster with impurities. Different techniques were used, among which: lime fresco, lime painting (a secco), lime caseinate (tempera) and application of pigments on a fresh rendering of lime and gypsum, which was similar to the technique used in Egypt in that period [70, 74, 80].

Also in Ancient Greece, secco and fresco techniques were sometimes used together. The plasters of Greek wall paintings in the archaic period were lime-based and did not include gypsum [74].

The fresco technique reached its perfection in the Roman period. The most important source about the fresco technique that came to us from that period is the seventh Book of Vitruvius [2]. Wall paintings in Rome, Pompeii and Herculaneum represent the common and characteristic feature of wall decorations of the Roman period. The use of the tempera technique in the Republic period was reduced by the rise of the fresco technique but it was not abandoned. Binding materials used in secco in this period are animal glues, gums, egg, honey and milk [81]. Plasters used in Byzantine period show differences from those used in the Roman period and Western Europe [82]. Basically, plasters were composed of lime, straw, chopped hog bristles, and contained only a small quantity of sand. More, Masonry walls were very common as wall decoration support. But since bricks absorb much moisture from the plaster, the thickness of plasters was increased to provide the moisture needed for frescoes [74].

During the Renaissance period, the fresco technique achieved its apogee in Italy. Scientific research has confirmed that the paintings by Michelangelo Buonarroti in the Sistine Chapel (Vatican) were executed in buon fresco [83-84]. The high level of the technique's skillfulness can be observed in the Giotto's frescoes of the Scrovegni Chapel (Padua, Italy), with very high accuracy of thin and fine plaster layers [85].

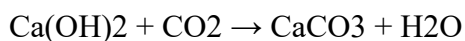
In the 13th century, important developments on the preparation of siccitative oils were introduced. For example, in France (Hesdin Castle, Conflans Castle and Marais Chapel) and in England (Ely Cathedral built in 1325-1358 in Ely, Cambridgeshire, England), oil was used as a binder in wall paintings in the 13th and 14th centuries [81, 86]. Vegetable oils became widespread after the 15th century, making the paintings more transparent and less opaque [86]. Tempera and oil allowed the use of pigments which cannot be used in fresco paintings (e.g. orpiment, cinnabar, azurite, minium, verdigris and lead white) [2, 81, 83]. Oil painting became popular from the 16th century until nowadays, with the most employed linseed oil [86].

In the Baroque period, for example, rough intonaco surface was used for oil painting, in order to enhance the vibrating effects of tones. During the 19th century in Europe, the great majority of wall paintings were executed a secco (on a dry surface) using tempera or oil as a binder [84]. During the 20th century, many synthetic pigments and innovative binders were rapidly introduced, leading to many debates on their future conservation and on the compatibility of new materials for restorative interventions on historical and archaeological wall paintings [87-88].

2.1.2 Materials and execution technique

The term “al fresco” or “affresco” has been used since 14th century, though the technique was used since antiquity. In order to be applied, the pigment is first mixed with lime and water, and then applied to the surface being painted, which consists of damp lime plaster. During the carbonation process of the lime, i.e. calcium hydroxide being carbonated to produce calcium carbonate, the pigments attach to the plaster and become incorporated with the hardened plaster [2, 83, 86].

The process of application involves mixing pigments with lime water, which in turn reacts with the carbon dioxide in the air and the colours are then fixed by the precipitation of calcium carbonate. The lime mixed with the pigments acts as a binder [74, 83, 86]. Pigments remain permanently bound to the plaster because of a chemical change after the fresh lime becomes calcium carbonate upon drying (equation):

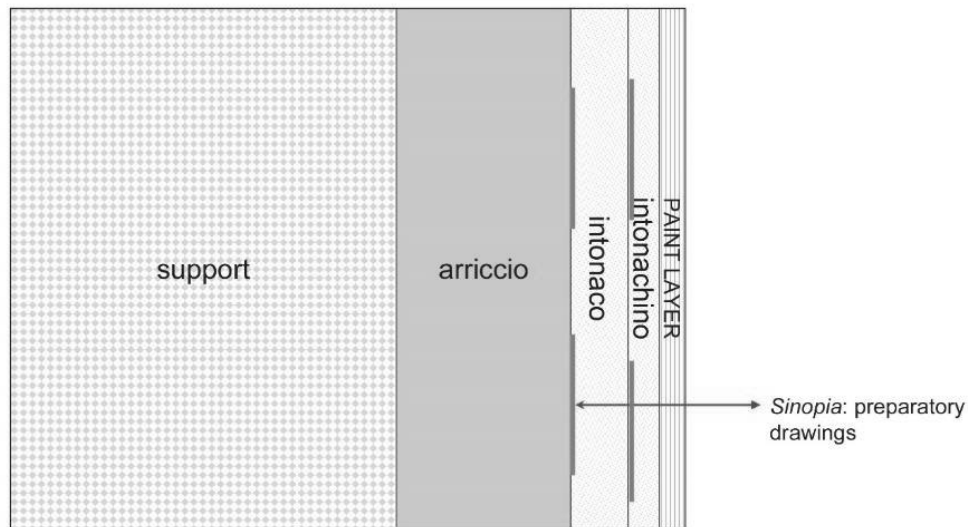


For achieving a good result (or “buon fresco”), the wall backing, as well as the plaster undercoats, should not be too dry that would allow them to absorb the water required in the setting of the fresco paint layers, which in turn should not become dry too fast [2, 83]. Painting on a wall requires the preparation of a suitable uniformly flat, smooth and white ground layer. At least two preparation layers are therefore generally applied to the wall before it can be painted (Fig. 2):

1. a medium-fine plaster directly applied to the rough water-wetted surface of the wall;
2. a fine plaster made up of fine-grained sand and lime.

According to Vitruvius (first century A.D.) [2], the Romans applied up to six preparation layers of plaster before painting (three medium-fine grained layers called *arriccio*, and three more, fine-grained, layers. More, in his book “De Architettura” [2], Vitruvius mentions that the Romans used sheets of lead inserted in the wall to prevent the capillary action of water from attacking the fresco.

In the case of fresco technique, a very fine-grained pigment dispersed in water was laid on a fresh fine-grained plaster; while in the case of lime-paint, also called lime wash, lime-resistant pigments were mixed with slaked lime or limewater and spread on the dry plaster [89]. In order to achieve a smoother finish and for stucco and render technique, the top layer contained rather powdered marble than the sand [89-91].



<u>Arriccio</u> =	slaked lime $[\text{Ca}(\text{OH})_2]$ and coarse sand
<u>Intonaco</u> =	slaked lime and fine sand
<u>Intonachino</u> =	slaked lime and finest sand
<u>Paint layer</u> =	“true fresco” (pigments diluted in water and applied while the intonachino is still damp)

Figure 2. Section of a fresco wall painting on a structural support. Image credits: Rocco Mazzeo

Plasters only conserve their optimal characteristics for use as a background in fresco painting for a very short time (6–8 hours), called the ‘golden-hour’ [4]. Therefore, the plaster is only applied to the portion of the wall to be painted on the same day, called “giornata”, which means “day” in Italian. Only during this period of time, calcium carbonate forming in the plaster by reaction between intergranular limewater (saturated in calcium hydroxide) and dissolved atmospheric carbon dioxide guarantees the binding of the pigment to the surface [4, 81]. Alterations can be made only by immediate washing or scratching of the plaster. Minor retouchings to the dried plaster are possible with tempera or casein [81].

Most probably, initially ancient wall painting compositions were sketched directly on the plaster (by carbon black or earth pigments) that had to be painted. The use of sinopia (red pigment found in Minor Asia) was common from the middle of the 13th century until 1430 (when it was largely replaced by cartoons) [74]. Cennino Cennini (1370-1440) [83] recommended using sinopia for drawing the figures on arriccio and to make a preliminary charcoal sketch to be brushed off afterwards. In the Renaissance period, sinopia was not used anymore for underdrawing on the penultimate layer. It was substituted by black, cinnabar and vermilion, red earth and yellow ochre. Since the middle of the 20th century, the term sinopia

has been used to denominate underdrawings made with other pigments [74]. From the 15th century, the use of cartoons (sheets of paper with the applied full-scale preparatory drawings) became an essential part of artists' practice. There were two main methods of transferring a drawing from a cartoon to the support. The first method is tracing, which consists in the application of the sheet of paper onto the fresh lime-based render and following the contours with some pressure, using a stick or the handle of a brush, so that the lines remain imprinted on the preparation layer. In this case, the incisions guide the artists in the application of the decorative layer. The second method is called pouncing. The contours or principal lines of a full scale drawing on paper are pierced with a pin at regular intervals. The sheet of paper is set onto the wall and a gauze bag containing a pigment in powder is padded over the paper surface so as to transfer the pigment through the holes onto the render, called *spolvero* technique. Sometimes cartoons were combined to *sinopia* technique [74, 81].

The decorative layer is represented by paint, consisting of pigments and binding medium. Most of the paint pigments even nowadays are inorganic compounds [88-96]. In the traditional wall painting techniques, only lime-resistant pigments can be used [2,4,83, 88-96]. The palette was limited and when dried, the colours appear matt and lighter in tone [96]. The retouching by "a secco" technique was used to highlight details. Some pigments degrade on contact with lime. Therefore, white and red lead, malachite, azurite, cinnabar, orpiment and organic pigments cannot be applied by fresco technique. Blue azurite $Cu_3(CO_3)_2(OH)_2$, if in contact with lime water, converts to green malachite [96]. Therefore, these pigments could be applied as a "secco" finishing over the earth pigment, when the plaster was dry. The best pigments for fresco technique are natural earth and mineral pigments [88-96]. The list of the pigments most commonly used in Roman, Middle Ages and Renaissance frescoes is reported in Table 3 [88-96].

Table 3. Pigments used in buon fresco technique

Colour	Pigment(s) used in fresco technique
Yellow	yellow ochre
Red	red ochre
Blue	egyptian blue
Purple	haematite
Green	Green Earth rich in glauconite or celadonite
White	carbonated minerals: cretes, aragonites, marbles
Black	black-ivory, black-carbon and black-vine

Main degradation problems

As to the conservation of wall paintings, excessive moisture is one of the most hazardous factors to all the wall surface and internal structure [97-99]. Damp may rise through the wall, originating at the level of ground contact and spreading upward. Prevention of rising damp is sometimes achieved by cutting into the wall beneath the mural and inserting a “damp course” of water-impermeable material or a high capillary tube that draws and deflects the harmful accumulation of moisture. Damp may also come from the outside wall, where direct infiltration of rainwater may penetrate through the substrate to the face of the painting, evaporating at the paint surface. Moisture may also result from condensation on a cold wall surface, which is a common phenomenon for churches, or buildings that are subject to excess ambient moisture generated by the respiration of crowds of visitors. More continuous and uniform heating of the wall may adjust this situation, provided that ambient air is not dried so rapidly, otherwise, the “efflorescence” (formation of salts) may occur [97]. Water damage can be caused by leaking roofs, clogged drainpipes, and faulty plumbing. This damage may be very hazardous and quick, therefore these problems must be detected and repaired immediately.

Damages to wall paintings, which are caused by moisture, may include blanching, staining and delamination of paint layers due to efflorescence [4, 9, 97, 99]. Crystallized salts may form above or below, even within the painted layer, resulting in disintegration and loss of the image scene, sometimes creating a salty “veil.” If the surface is coated with a water-impermeable material, such as wax or resinous products, the ways for evaporation are blocked, moisture will move laterally and this will expand areas of damage [99]. Also, such problems as mold growth and mildew are also often related to the presence of moisture [100-101].

As to the outdoor wall paintings (on facades or integrated into archaeological structures), due to the increasing worldwide use of fossil fuels and sulfur gas emissions, the so called “acid rains” may rapidly erode the calcium-carbonate component of most cement-based and lime-based wall paintings, converting it to calcium sulfate [97]. The volume of the sulfate crystal is almost twice larger than that of the original carbonate of the mural. It causes fragility and disintegration of the upper decoration layer, including the internal pressure within the pores and leading to fracturing [4, 97]. Further, the sulfate has a greater capacity to absorb moisture. Polluted environments can produce sooted patinas and discolour certain pigments, which are traditionally found in Renaissance paintings: white or red lead, malachite and azurite [99].

Many innovative conservation treatments were developed in the second half of the 20th century for cleaning, reduction of salt deposits and consolidation. There have been recently emerging studies on the use of nanotechnology for consolidation of wall paintings [102].

The conservators often face a challenge of the need for a specific solution in a given situation. In the past, conservators used drastic methods to transfer frescoes from the decaying walls, in order to protect them. Sometimes the frescoes are detached and reattached in-situ. The methods range from the *strappo* technique to so called *stacco a massello* [103]. The so called *strappo* (taking off, tore up) is the more radical procedure, used sometimes in the past, can be found on real case studies nowadays. It consists of gluing canvas firmly to the surface of the fresco and then pulling away a thin layer of the plaster containing the pigment particles of the fresco. The bond between the facing and the fresco must be stronger than the internal cohesion of the plaster. This thinned pictorial layer can be fixed to a stable support. Unfortunately, much of the original surface characteristics of the wall and density of the pigment layer is sometimes irreversibly altered by this technique, it is not commonly used anymore. Less intrusive is the *stacco* method. In this case, a thicker layer of plaster is retained along with the fresco decoration layer. It is then smoothed flat on its back surface before the composite rigid layer is mounted to a prepared support. Finally, in the procedure called *stacco a massello*, the least intrusive to the fresco but more challenging transfer procedure due to mass and weight, the wall painting is removed with the entire portion of the original substrate (preparation layer). These interventions could have been performed in the past and could be not documented. Nowadays, the minimum necessary conservation and restoration treatments carried out in-situ are preferred [103-104].

Main conservation problems of wall paintings to be detected in-situ

As described above, for the efficient in-situ diagnostics of wall paintings, the complete in-situ non-invasive approach is expected to provide preliminary and reliable information about:

- efficient and fast detection of moisture and related risk areas;
- diagnostics of the structural support and decoration subsurface layers (detachments, voids, cracks, deterioration of materials, presence of structural restoration interventions etc.);
- identification of previous restorations (reattached fresco layers, presence of metal rods, etc.)
- presence of surface alterations (blanching, staining and delamination of paint layers, mold growth, salt formation).

In terms of art historical and archaeological study of wall decorations, it is important that the applied methods are can contribute to the knowledge about:

- materials and construction technique in the subsurface and bearing structure;
- materials and general execution technique in the decoration layer;
- mapping and (if possible) identification of pigments;
- artist execution technique and (if necessary) attribution studies;

- revealing the underdrawings, stylistic features, lost details due to degradation etc.;
- identification of retouched areas and previous restorations.

Limitations of in-situ applicability of electromagnetic methods due to the characteristics of wall paintings

The methods, applied in-situ to wall mosaics of high archaeological and art historical value, should be portable, non-invasive and very often non-contact techniques.

Since many archaeological and historical sites are not easily accessible, the relative instrumentation must be capable to operate in challenging work conditions: contrasts in temperature, humidity, lighting, distance from the object of investigation, safety and support stability, etc. The informativity level of the acquired data can be influenced by:

- distance, shape and geometry of the wall painting support (vaults, domes, sometimes access is inhibited from one or more sides);
- surface irregularity (if not properly documented and considered, uncontrollable lighting and surface non-planarity can lead to the creation of artefacts and to the misleading interpretation of acquired data);
- conservation state of the wall painting surface (often physical contact to the surface is normally not allowed);
- High value, uniqueness and irreplaceability, as well as National Cultural Heritage Law (time-consuming issue of specific authorizations for data acquisition and results dissemination, physical contact and micro-sampling are not allowed).

As to the application of one or two non-invasive methods to the study of a wall painting (whether only to its decorated layer or to its subsurface), we find a wide range of available and already published scientific studies. The interest in the development of non-invasive methods for in-situ diagnostics of wall paintings shows a strong progress in the last years. Scientific experts work on the development of multispectral, hyperspectral imaging systems to the characterization of a painted layer of a fresco decoration, application of non-invasive material characterization methods (portable XRF, portable Raman, etc.). Many examples are available in the literature to the use of infrared thermography for efficient in-situ subsurface monitoring. As described in this chapter, each fresco painting is a complex structure including the underlying preparation layer and structural support. The development of a non-invasive approach to analyse the system as a whole (at different levels by a combination of methods) is of crucial importance for the preservation and monitoring of wall paintings. Some first studies,

when applied to historical buildings with integrated wall paintings or other cultural heritage artefacts can be already found in the scientific literature.

The penetration depth of each of the tested electromagnetic method, applied to wall paintings, is shown in Attachment B.

2.2. Wall mosaics

2.2.1 Historical background

Mosaic art in its broadest sense of the term is related to different decorative forms: inlay (l'intarsio), incrustation (l'incrostazione), commesso work and intarsia (or la tarsia) [105]. All these artistic techniques are based on the same principle, i.e. placing and fixing together, side by side, of small pieces of one or several materials (marble, coloured stones, glass, and ivory, wood). They are often of different colours and form a geometric or figurative pattern on a flat surface [105-107]. Whereas inlay work is composed of closely fitted pieces, cut into specific shapes, according to the elements of the design, a mosaic is built up from small, regular, but always neutrally shaped fragments, known as tesserae, which are held in space by mortar and separated by visible interstices. This study is focused on integrated wall and vault mosaics from the Byzantine period, which are characterized by a very complex underlying supporting structure.

First, mosaic art flourished in a form of floor covering, within the cultural and geographical boundaries of the ancient Greco-Roman world, later becoming a major pictorial art form in the Christian and Byzantine era [106-107]. During the late Republic period of the Roman Empire (133–31 A.D.), the walls and vaults of nymphaea, natural or artificial grottos, were studded with shells, volcanic pumice, marble chips and fragments of glass vessels. The need to provide a richer polychrome decoration led to the introduction of glass-cut tesserae, which gradually replaced the earlier materials [105]. During the Roman period, glass mosaic decoration attained a high degree of technical refinement; nevertheless, it remained a subordinate art form serving the purposes of architecture [106].

Though the earliest stage large wall mosaics, which have come down to us, date back to the age of Constantine of the Roman Empire, it is possible that the wall and vault decoration with glass tesserae (opus musivum), which was employed to embellish Christian churches, derived from earlier pagan examples, only traces of which have been preserved [105]. In a tomb under the Vatican Basilica of St. Peter, there is one of the earliest mosaics to be preserved till now, dating from the 3rd century A.D., which portrays Christ as Apollo, the Sun God, ascending into heaven in a chariot [106].

Wall mosaic became the preferred artistic technique in the decoration of Christian basilicas, and especially in the decoration of walls [107- 108]. The Byzantine mosaic art gradually became a spiritual language, called the “expression of absolute authority, superhuman greatness, mystical inaccessibility”. The tendency to endow architectural space with a transcendent and spiritual character is also clear through extensive use of golden tesserae. In the Justinian Period (520-565 A.D.), mosaic almost entirely replaced painting in the embellishment of churches. In the 12th century, mosaic art flourished in the Byzantine Empire and expanded far beyond its boundaries [106, 108]. It experienced brilliant development in Kievan Rus (with magnificent examples in Kiev), in the Middle East (Damascus, Jerusalem) and especially in Italy, both on the Apennin Peninsula and in Sicily. Among them, there are wall mosaics of Venice, Trieste, Florence, Palermo and Cefalù. The style of Byzantine mosaics in Cefalù, Palermo (12th c.), Venice and Trieste (12th-14th c.) may suggest to experts that mosaic masters, and sometimes even mosaic material itself, frequently came directly from Byzantium [108-111].

The 13th century signed a decline in both wall and floor mosaic art decoration and already by the 15th century mosaic was not considered an independent artistic technique anymore. The revival came in the 16th century, thanks to the great artists like Titian, Tintoretto, Veronese and Raphael, which furnished cartoons for major mosaic decorations in the churches of Venice, Florence and Rome. These works were called “painting in stone” [105].

It was in the 16th century that the revival of mosaic art started, with the opening of local mosaic schools in Venice and Rome. In Venice, the new mosaic workshops were mainly engaged in the restoration works on the mosaic decorations in St. Mark’s Cathedral [106]. At the same time, the Catholic Church promoted the revival of mosaic as means “of formally reasserting the spiritual values of early Christianity” [112], but only in 1727, the Studio del Mosaico Vaticano was founded. This workshop is still active nowadays, involved both in manufacture and restoration of mosaics [110]. In Venice, the mosaic masters started to use the so called “indirect method” when the tesserae were set upside down on a temporary pare base and the mosaic was then transported to its destination and installed in-situ [107-108].

The mosaic decoration was extensively used throughout Europe in the 19th century, in the most important buildings of Neo-Gothic and Neo-Romanesque style and in the restorations from the 19th century [105].

In the 20th century, the mosaic art schools were set up in Spilimbergo (1922), Ravenna (1959), Monreale and Venice (1968) and they focus either on the study and restoration of ancient mosaics or on the execution of mosaic replicas [106].

2.2.2 Materials and execution technique

The tesserae materials, which have been used for the execution of ancient wall mosaic and for subsequent replicas and restorations, may be divided into two main groups: stone and glass. The natural stone comprised all types of minerals and rocks, which may be easily worked and cut into tiny tesserae. Glass was mainly consisting of a variety of coloured smalti (Italian term for opaque glass paste) and gold and silver smalti [110-116].

Stone tesserae

Since antiquity, stone has been mainly employed in mosaic pavements [105-107]. However, occasionally, marbles and coloured stones have also been employed in wall mosaics. In antiquity, the most important quarries were located in Greece (white Pentelic marble, verde atracio, rosso antico, Hymettian marble, nero antico), in Asia Minor (pavonazzetto, africano), in Egypt (porphyry, granite, alabaster), in Lybia (giallo antico) and in Italy (Carrara marble). However, up until the 1st century A.D., mosaic production mostly employed extremely common local stone, such as limestone, tufa and flint. Most of the quarries worked in antiquity have been exhausted in the course of centuries, for this reason, the stones used in Greco-Roman times are referred to as “ancient marbles” [105-106].

Glass tesserae

Glass paste as tesserae material is almost exclusively employed in wall and vault mosaics. Consisting of a variously coloured glass substance, glass paste made its first appearance in the 4th millennium B.C. in a geographic area from Mesopotamia to Egypt. The use of glass paste tesserae was introduced into mosaic art around the middle of the 1st century A.D. With the decline of Roman Empire, the use of mosaic art was increasingly conditioned by the difficulties in finding vitreous materials [106]. Glass tesserae, however, continued to be produced and became the most widely used material in mosaic decoration in Early Christian and Byzantine Ages. More than 200 colours were produced in that period, comprising thirty hues of green and almost twenty different shades of red. In the Middle Ages, glassware had its major centre of production in Byzantium.

After the 13th century, however, Venice started to acquire increasing importance in the field of glass technology. Many furnaces were being opened in Venice and on Murano. They created a wide range of colour shades, extending from a few hundred to several thousand different hues, and introduced the term “smalto” [112-115]. This term, in its original meaning, describes a particular decorative technique involving the application of coloured glass either to a metallic or ceramic surface by firing, a technique which is commonly known in English rather by the “enamel” term or glaze.

Tesserae glass material is obtained by the fusion and subsequent cooling of a mixture of silica, alkali and metal oxides as colouring agents. Glass is an inorganic material, amorphous solid. It lacks the long-range order that is characteristic of crystalline materials. There is no regularity in the arrangement of its molecular constituents on a scale larger than a few times the size of these groups [113].

During the Roman period and in the early Medieval period in Europe, glass was made from either soda-rich plant ash and pure sand, or natron (mineral hydrated sodium carbonate) mixed with calcareous sand [105], both resulting in a glass with a composition close to the contemporary recipes.

In soda-lime-silica glass, commonly used throughout centuries, the oxides in the network are sodium oxide, calcium oxide and silica [116].

The method of coloured glass paste manufacture has remained mostly unchanged since late antiquity [105]. The basic procedures for glass-making can involve five main steps:

- 1) The selection and preparation of raw materials;
- 2) Making the glass involving fritting the raw materials;
- 3) Mixing the batch and melting the glass;
- 4) Working the glass to form the glass objects;
- 5) Annealing the objects.

In order to facilitate the manufacturing process by reducing the melting point of silica to lower temperatures, fluxes (potassium or sodium carbonate, lead oxide) are usually added to the glass compound. As for colouring agents, mainly metal oxides were used.

Starting from the Roman period up until the 14th century, pure colours obtained from a single metal oxide were preferred. After the 14th century, colours were made from a mixture of several oxides, thereby considerably enriching the chromatic range of the tesserae. In antiquity, the most popular colouring agents were cobalt oxide for blue, copper oxide for green, cuprous oxide for red and zinc oxide for white [105-107]. The lead was used already in ancient Egyptian glass, but high lead opaque red glasses were introduced in the eighth century B.C., at about the same time as the change from high magnesia to low magnesia soda-lime glasses occurred. It was used in the manufacture of generally prestigious yellow, emerald green and opaque red medieval glasses [107]. The ultimate source of cobalt blue coloration in ancient glasses was cobalt-bearing mineral. It is commonly found in association with other minerals, like copper. For Roman cobalt blue glasses, the sources rich in manganese were used. There were only some chronological changes in the use of cobalt sources during medieval times in Europe. In fact, the same impurities, such as lead and zinc, were found in the medieval western and islamic glasses

[116]. Opacity in the ancient glasses was due to the presence of dispersed crystals in a translucent glass matrix. It is the density of crystals that makes the glass opaque to wavelengths of light. Opaque white glass contained masses of white calcium antimonate crystals. Opaque yellow glass, often of a somewhat paler yellow color, can be produced by lead stannate crystals. In the most recent glass production, the opacity can be produced by the presence of tin oxide crystal. Opacity used in the 17th century glasses included lead arsenate crystals, probably first introduced by Venetian glass-workers [115].

Two compounds were used in antiquity, in order to produce colourless or nearly colourless glass: antimony trioxide or manganese oxide. The method of manufacture for gold and silver smalti, probably from the period of Alexander the Great, was employed in Rome around the 3rd century A.D. to produce “glass of martyrs”, namely golden glass discs which were mortared into the enclosing walls of the locules in the catacombs. Between the 4th and the 5th century the use of golden tesserae for the background in mural mosaics became widespread [116]., and it ultimately became a characteristic feature of Byzantine mosaics up until the Middle Ages [116-117].

In this type of smalti the colour is obtained by sandwiching a very thin metal leaf – of gold, silver or, more recently, platinum, between two layers of either transparent or coloured glass, one acting as a base, the other as a protective glass film, called cartellina. The bottom layer is approximately 8-10 mm thick, while the upper one is extremely thin (0,8-1 mm) [118].

Along with the artificially manufactured and coloured glass paste, natural glass was used for the precious details of wall mosaic decorations. Obsidian is a volcanic glass, formed when lava is cooled rapidly, often at the margins of a flow. It is normally shiny in appearance, and dark in colour (black or grey), but may be colorless, red, green, or brown, depending on the composition and circumstances of formation. Obsidian became widely used already in antiquity, in different parts of the Aegean in the Neolithic (beginning around 7 000 A.D.) and Early Bronze Age (beginning around 2500 A.D.). It can be still observed in byzantine wall mosaic decorations [107-108].

Binders

Different substances have been employed as binders in mosaics execution, ranging from the bituminous glues of the Sumerian Civilization to gypsum plaster in Egypt, and from natural resins in ancient Greece to, finally, the materials used by ancient Romans, which have been used also later, throughout the history of mosaic art: hydrated lime, pozzolana and hydraulic lime. In more recent times, Portland cement (from the mid 19th century) and modern synthetic resins (since the 20th century) were added [105].

Hydrated lime, either in pure form or mixed with a variety of fillers, was undoubtedly the most commonly used material in the past and even today. A non-hydraulic binder was also widely used. While hydraulic lime sets by hydrolysis, the non-hydraulic lime sets by carbonation [119-120]. Since late antiquity, the fillers have been used in order to improve its resistance to humidity and water. Hydraulic fillers were extensively employed from Roman times up until the 19th century when the development of building industry led to the invention of real hydraulic lime [105].

During centuries, other types of binders have been employed. A very strong binder obtained from a warm mixture of beeswax, paraffin and rosin was used in Byzantine portable mosaics which have come down to us perfectly preserved [101,102]. In mosaic decorations made with stone tesserae, a compound of slaked lime and casein, with good hydraulic and adhesive properties, was preferred. The binder was made by mixing lime putty with the phosphoprotein of milk, previously dried and pulverized, and adding water [119].

Gypsum plaster was widely used in Egypt and in all countries with dry climates because it is highly susceptible to humidity and is soluble at ambient temperatures. Since the Renaissance period, an oily binder of particular strength, “stucco” or “oil mastic” has been exclusively employed in glass mosaic, since stone tesserae tend to absorb the vegetable oil and become discoloured. The binder is made from a mixture of powdered marble, slaked lime and raw linseed oil, which is dried, pulverized and then added to boiled linseed oil [110-111].

In the year 1824, a binder known as “Portland cement” was patented, which is well suited for mosaic art. It is produced by burning a mix of clay (22%) and limestone (78%) in rotary kilns at a very high temperature (1500°C) [105]. The resulting product, known as clinker, is then finely ground and mixed with a small amount of gypsum (3%). Cement mortar, made by adding water and sand to the powder, in the proportion of 3 to 1, hardens in 28 days and finally sets over a period of a few years.

The portland cement, which was used for restoration or reproduction of historical wall mosaic, represents an important issue in conservation. It may frequently contain soluble salts which, in the presence of moisture, might appear on the mosaic surface in the form of whitish efflorescences, altering the color of the tesserae; these salts might be dissolved by water containing carbon dioxide and sulphates, increasing the porosity of the binder and causing its deterioration [105].

Portland pozzolana cements and slag cements have been furtherly used to overcome these problems. Pozzolana or slag react with the salts produced during the setting process and form insoluble compounds.

Nowadays, many synthetic resins can be used in mosaic decorations (acrylic, vinyl and epoxy resins). The most commonly used acrylic resin is PRIMAL AC 33 (better suited for indoors due to its limited resistance), Vinyl resin is represented mostly by polyvinyl acetate. The epoxy resins are the most suited for outdoor mosaics [105].

Mosaic execution techniques

Two main execution procedures have been used in the history of mosaic decoration application: direct and indirect (or reverse) method. The direct method of mosaic work was used since antiquity and it involves gluing the mosaic tesserae directly on the latest preparation layer covering the wall. The indirect application is the more recent method that has been used in Venice since the 18th century and is still used now, for example, at the San Marco restoration workshop. The tesserae are placed face down (using a removable adhesive) on a temporary paper, following the drawn design on it (mirror image). The mosaic is then transported to its destination and installed in-situ.

It is believed that the original Byzantine mosaics were applied in stages directly on the wall (using the direct method). The surface of the masonry wall was first usually covered by three layers of lime mortar. The total thickness of the three lime mortar layers was usually in the range of 4-6 cm, it could be slightly thicker on the edges of the vaulted parts [105, 119]. The most underlying layer was applied usually thicker than the other two (Fig. 3). On example of the Byzantine mosaics in Hossios Loukas Monastery (Greece), we know that the first two layers were commonly made of lime, bricks and cut straw, while the third contained only lime and marble powder. The cut straw served to improve the binding characteristics and to balance the migration of moisture between pores (Fig. 3a and Fig. 4a-c). The final (bedding) layer of mortar contained linseed oil and adhesive substance, in order to ensure the slowing down of mortar setting while plaining the tesserae.

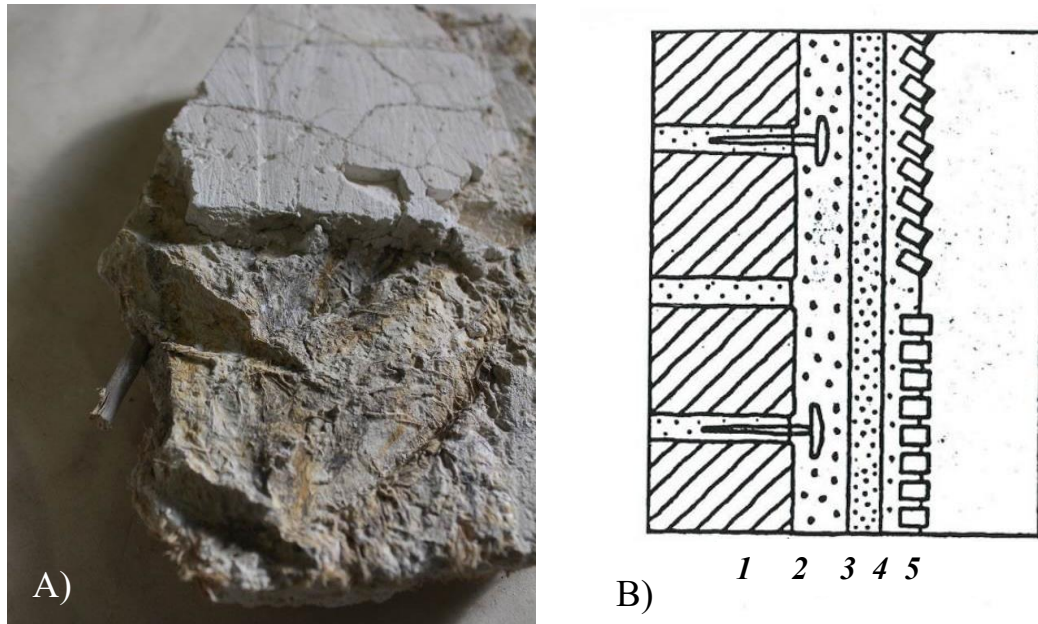


Figure 3. Structure of the byzantine mosaic wall decoration: a) mortar fragment from the Byzantine period in the Basilica of Saint Mark, Venice, image credits: V. Cantone; b) section of the Byzantine wall mosaic with the supporting structure: 1 – brick wall; 2 – the first plaster layer with flat-headed nails; 3 – the second plaster layer; 4 – setting bed; 5 – tesserae [105]

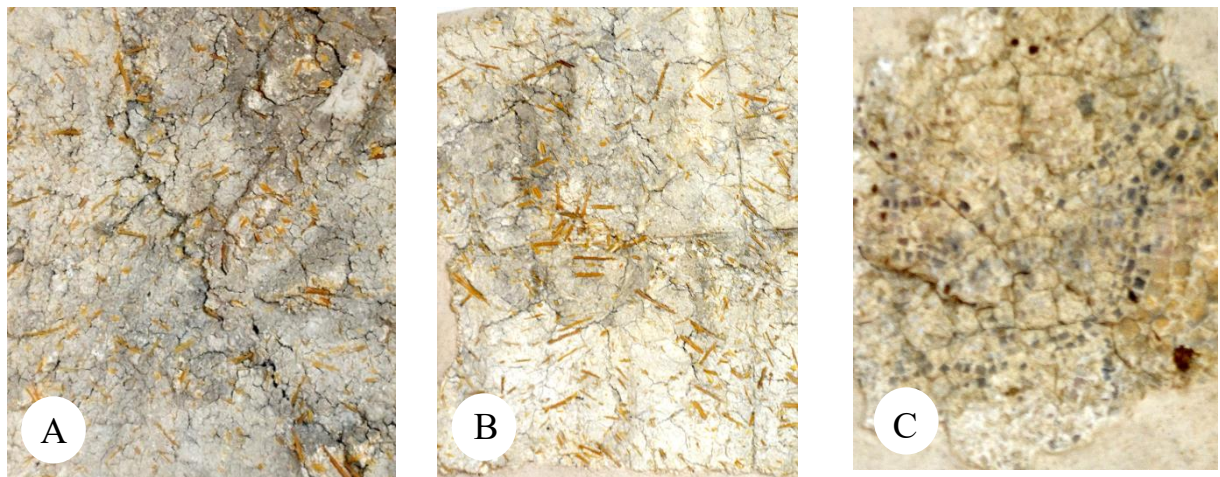


Figure 4. Examples of mosaic substrate layers, exhibited at the museum of Hosios Loukas Monastery, Distomo (Greece): a) the first substrate layer: clear lime plaster, sand and straw; b) the intermediate layer: pure lime plaster and a few straws; c) the final coating, setting bed for the tesserae: Pure lime plaster with linseed oil and an adhesive substance.

The final coating was sometimes attached to the intermediate one with large pointing jagged tesserae set vertically and functioning as wedges (3.5-4.3 cm), placed inbetween the other

tesserae. Fig. 3b shows a section of the described possible internal structure of mosaic decoration support and its fixing to the wall [119].

In order to secure even better fixing of the layers, the first and the second layer had a rough surface, in the form of deep bumps or ripples made by the tip of the trowel. This kind of surface was called “scaletta”, which in Italian means “stepladder” (Fig. 5). To furtherly secure the positioning of the mortar on the wall, in particular, on the vaults, strong steel flat-headed nails were often placed on the wall, so that the nails protruded lightly from the wall surfaces. This structure was found in many examples of mosaics from 11-12th century, for example during the restoration works in the Basilica di San Marco (Venice) and in the Nea Moni Monastery (Greek: *Νέα Μονή*, located on the Chios island, Greece) [122]. In the wall mosaics of Nea Moni Monastery, the revealed heads of the nails have the diameter of 4 to 5 cm, their length is in the range of 8 to 10 cm. In this case, the thickness of the first mortar layer is about 2,5 cm, the second one is from 1,5 to 2 cm and the third one is applied with the thickness of 1 to 1,5 cm. The total thickness is between 5 and 6 cm. The first and the second layers could contain old ash-powder, lumps, marble and fine straw [105, 119, 122]. During the works for the maintenance of the mosaics in the Nea Moni Monastery in Chios, coloured preliminary designs, executed with fresco technique, were found beneath the mosaic decoration layer [122].

During the past restorations at St. Mark’s Basilica mosaics, different composition of mortar and other types of “scaletta” surface were used for support of new mosaics, new or reused mosaic tesserae. The Fig. 5 shows a comparison between two original pieces preserved at the restoration workshop of Saint Mark’s Basilica: the older (byzantine) supporting layer used for the first mosaics and an example of the supporting layer used for the execution of mosaics in the 16th century.

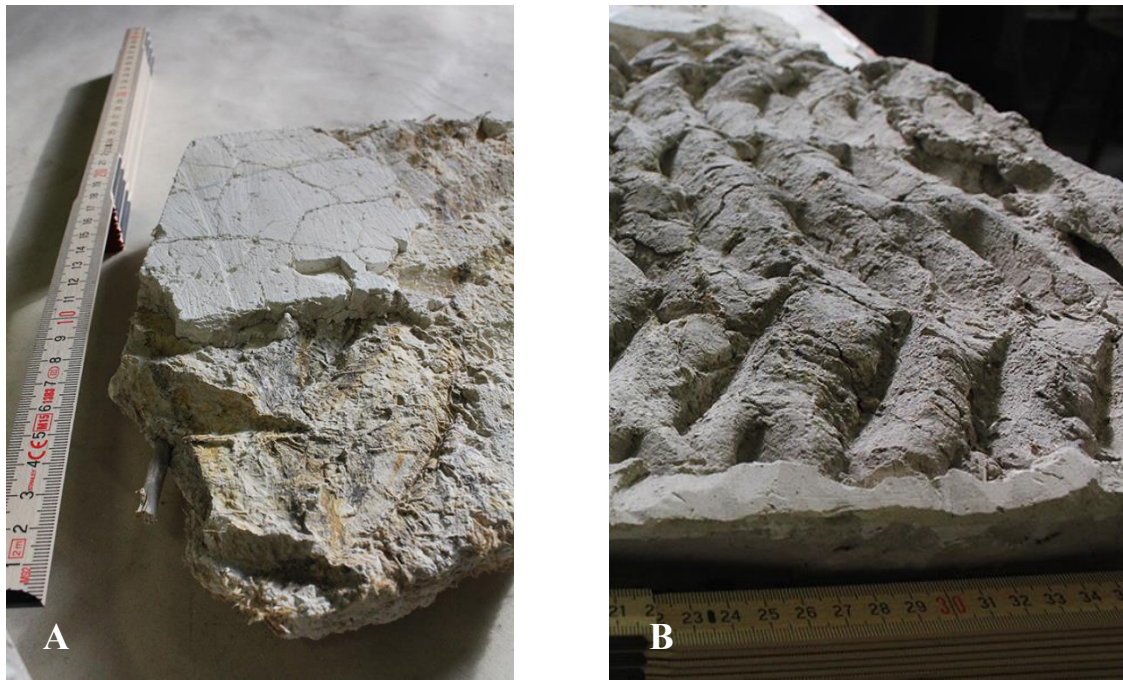


Figure 5. Internal mortar structure *scaletta* (from Italian: “stepladder”), restoration workshop of Saint Mark Cathedral: a) Byzantine period; b) 16th century restorations. Image credits: Valentina Cantone

Main degradation problems

The preservation of the precious decorative layer is subject to the condition of the wall mosaic as a whole system: tesserae, binding and preparation layers, supporting structure, as well as the adhesion between them.

Glass paste is an inert material, it is considered stable. Only fluoridic acid can dissolve it. But for long-term exposure, even the glass tesserae enter in contact with the degradation agents, which may come both from the environment (in contact with the front side of the decoration layer) and from the substrate, in contact with the back side of the tesserae.

The degradation problems of historical and archaeological mosaic decorations include surface alterations, detachments of tesserae, loss of adhesion between layers, presence of moisture, deterioration and damages in the subsurface and supporting structure.

The patinas of the superficial layer can be of two main morphological types [123]:

- white opaque encrustations of spongy and distorted structure, which cause whitening to the superficial layer;
- iridescent lamellae of several overlapping thin layers of micrometers scale, creating a general nacre effect.

The main causes of degradation and loss of the tesserae decoration layer include the interaction with humidity and environmental conditions, restorations by incompatible or irreversible materials which may lead to material irreversible transformations and/or deposition of salts [123-126].

Furthermore, the preservation of the integrity of the decoration layer can be affected by the condition of the underlying substrate layers, their bond to the structural support and by the bond at the interface between different substrate layers.

The detachments can be present different depth levels (Fig. 6):

- detachment and loss of tesserae (uppermost decoration level);
- Loss of adhesion between different substrate layers;
- Detachment at the interface between the first mosaic preparation substrate layer and the structural support (wall or vault structure).

The cleaning of the wall mosaics is generally performed through chemical action, mostly through the removal of soluble salts. In the case of resistant encrustations, cleaning must be performed through mechanical operations. The consolidation of degraded tesserae is usually performed using acrylic or silicone resins. Regarding the preparation layers, which generally suffer the problem of adhesion loss of the tesserae, the detachments and cavities in the support are usually filled by injecting mortar. In the past and still nowadays, the anchoring of preparation layers is used, in the case of big detachments' areas, because injection or filling the cavity may cause damage or collapse, due to the heaviness of detached layers. Metal anchors were used in the past, nowadays ceramic or plastic materials are preferred [126].

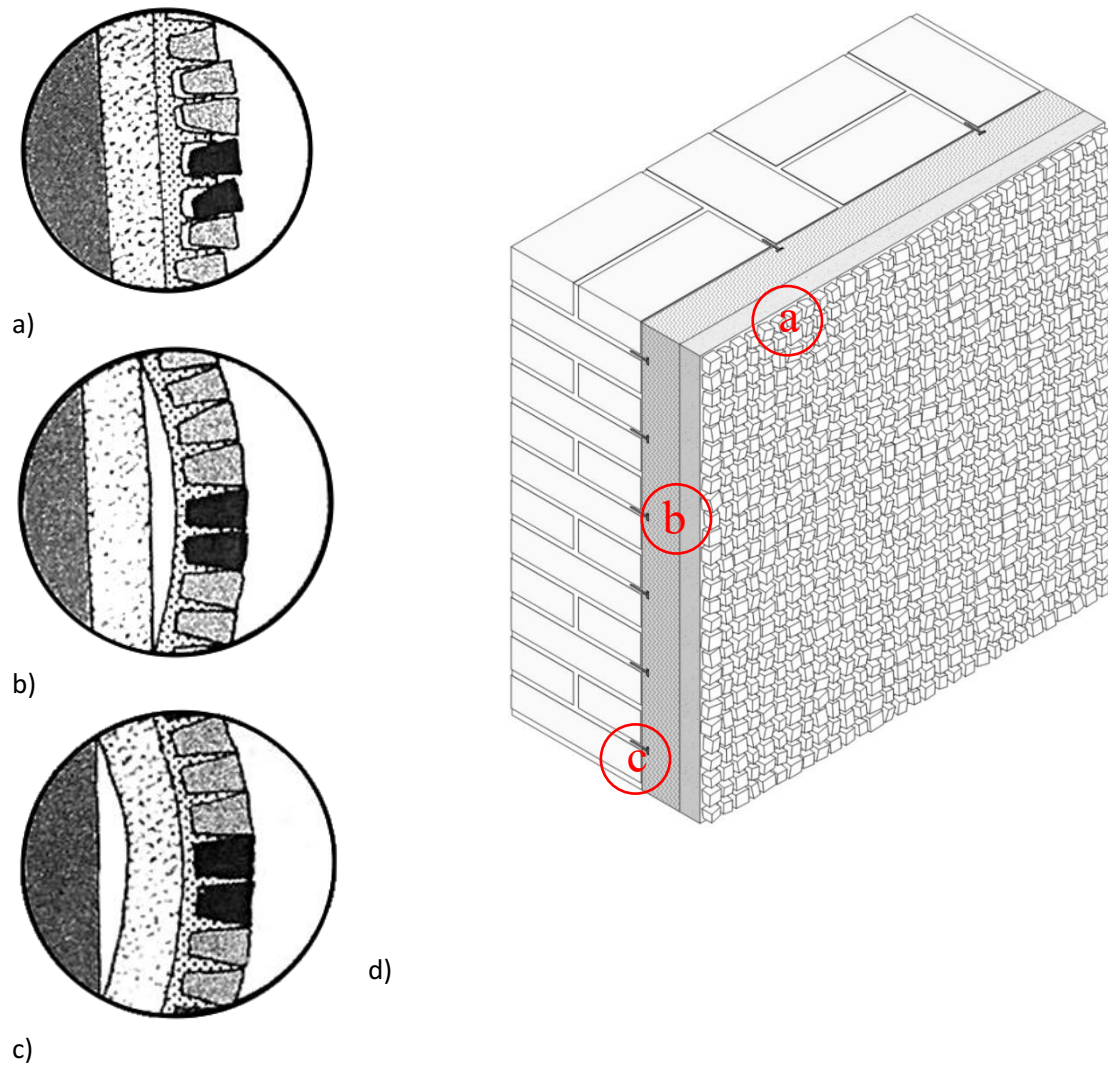


Figure 6. Three types of detachments in mosaic conservation. a) detachments of tesserae; b) loss of adhesion between preparation layers; c) detachments between the first substrate layer and structural support; d) structure of a wall mosaic, after [45].

Main conservation problems of wall mosaics to be detected in-situ

As illustrated before, for the efficient in-situ diagnostics of wall mosaics, the complete in-situ non-invasive approach is expected to provide preliminary information about:

- efficient and fast detection of moisture and related risk areas;
- diagnostics of deterioration and damages in the structural support and decoration subsurface layers (detachments, voids, cracks, deterioration of materials etc.);
- identification of previous restorations (refilling of mortar, presence of metal rods, etc.)
- presence of tesserae surface alterations (patinas, loss of tesserae material, etc.)

In terms of art historical and archaeological study it is important that the applied methods can contribute to the knowledge about:

- materials and construction technique in the subsurface and structural support underneath the mosaic layer;
- materials and general execution technique in the decoration layer;
- differentiation between tesserae and (if possible) their characterization;
- identification of reintegrated areas (tesserae and binding medium) and previous restorations.

Limitations of in-situ applicability of electromagnetic methods due to the characteristics of wall mosaics

The methods, applied in-situ to wall mosaics of high archaeological and art historical value, should be portable, non-invasive and very often non-contact techniques.

Since many archaeological and historical sites are not easily accessible, the relative instrumentation must be capable to operate in challenging work conditions: contrasts in temperature, humidity, lighting, distance from the object of investigation, safety and support stability, etc. The informativity level of the acquired data can be influenced by:

- distance, shape and geometry of the mosaic support (vaults, domes, sometimes access is inhibited from one or more sides);
- surface irregularity (if not properly documented and considered, uncontrollable lighting and surface non-planarity can lead to the creation of artefacts and to the misleading interpretation of data);
- conservation state of the wall mosaic decoration (often physical contact to the surface is not allowed);

- High value, uniqueness and irreplaceability, as well as National Cultural Heritage Law (time-consuming issue of specific authorizations for data acquisition and results dissemination, physical contact and micro-sampling are not allowed).

As concluded from the bibliographic research, unlike the in-situ characterization of floor mosaics ([32, 35-37] and many other references not presented later in the relative chapters), less attention has been dedicated to non-invasive study of mosaics integrated into a wall structure. It can be related to the limitations already described above and summarized as follows:

- limited accessibility to the historical and archaeological sites;
- high costs and limited portability of the instruments;
- Limited availability until most recent period of non-invasive full-field non-contact in-situ characterization methods.

Various studies until now have been dedicated to the surface and subsurface study of archaeological floor decorations. At the same time, relevant sources can be found about the material study and characterization of glass tesserae of wall mosaics ([122-123]. Simultaneously to the experiments performed within the frames of this thesis project, some first tests have been performed on the wall mosaics by the means of multispectral imaging, using the Nikon D800 camera modified to full range (300-1000 nm), used in this thesis [127]. No published studies about the mosaic decoration as a whole (tesserae, preparation layer and structural support), in the author's awareness, at the moment of this thesis project implementation could be found.

The penetration depth of each of the tested electromagnetic method, applied to wall paintings, is shown in Attachment C.

3. METHODOLOGY AND INSTRUMENTS

3.1 Contact methods used for on-site tests, principles and applications

3.1.1 Ground-penetrating radar (GPR)

Ground-penetrating radar (GPR) is a well known and common subsurface radar system. It is a geophysical method that employs electromagnetic radiation, transmitting and receiving radio waves to test the subsurface structure. One of the earliest successful applications in the development of this technique included large scale prospections, for example, estimating ice thickness on polar ice sheets in 1960s [128]. In 1970s and 1980s, the detection of subsurface objects was possible at the depth of a few meters, using the frequency range of 100-500 MHz, accessible at the time. Since then, after numerous developments in hardware and analysis techniques, the method started to be extensively used in other fields, such as forensics, geology, utilities detection, archaeology and finally civil engineering [129].

Depending on the frequency of the antenna, the GPR applications can be divided into two main categories. The first one (less than or equal to 500 MHz) refers to geological and archaeological prospections and the second category (200 MHz - 2 GHz) is applied to non-destructive testing of buildings structures. The application of the second category of GPR is particularly important for the wall structures bearing highly valuable paintings and mosaics.

Operating principle of a GPR system

This technique allows the identification of discontinuities in the subsurface medium due to the presence of layers or buried targets that have different dielectric properties compared to the surrounding environment [128-129]. *Dielectric permittivity* (ϵ) is thus the primary diagnostic physical property of this technique, which characterizes the degree of electrical polarization which material experiences under the influence of an external electric field. Electric conductivity is the measure of a material's ability to allow the transport of an electric charge, while *electrical resistivity* is a fundamental property that quantifies how strongly a given material opposes the flow of the induced electric current.

The GPR operating system consists of three main components: transmitting and receiving antenna and a control unit (Fig. 7). The operating principle of any GPR system is based on electromagnetic signal propagation in inhomogeneous subsurface media. The system repeatedly transmits one period of sine wave signal and records the amplitude and time. GPR systems that transmit an impulse and receive the reflected signal from the target in the subsurface medium are called impulse-type radars. In particular, the buried targets partially

reflect the electromagnetic radiation, emitted by the transmitting antenna of the GPR system, towards the receiving antenna of the same GPR system. The detected discontinuities highlight the presence of gaps, fractures or different materials inside the propagation medium. Finally, the software provides vertical sections of the investigated medium called radargram.

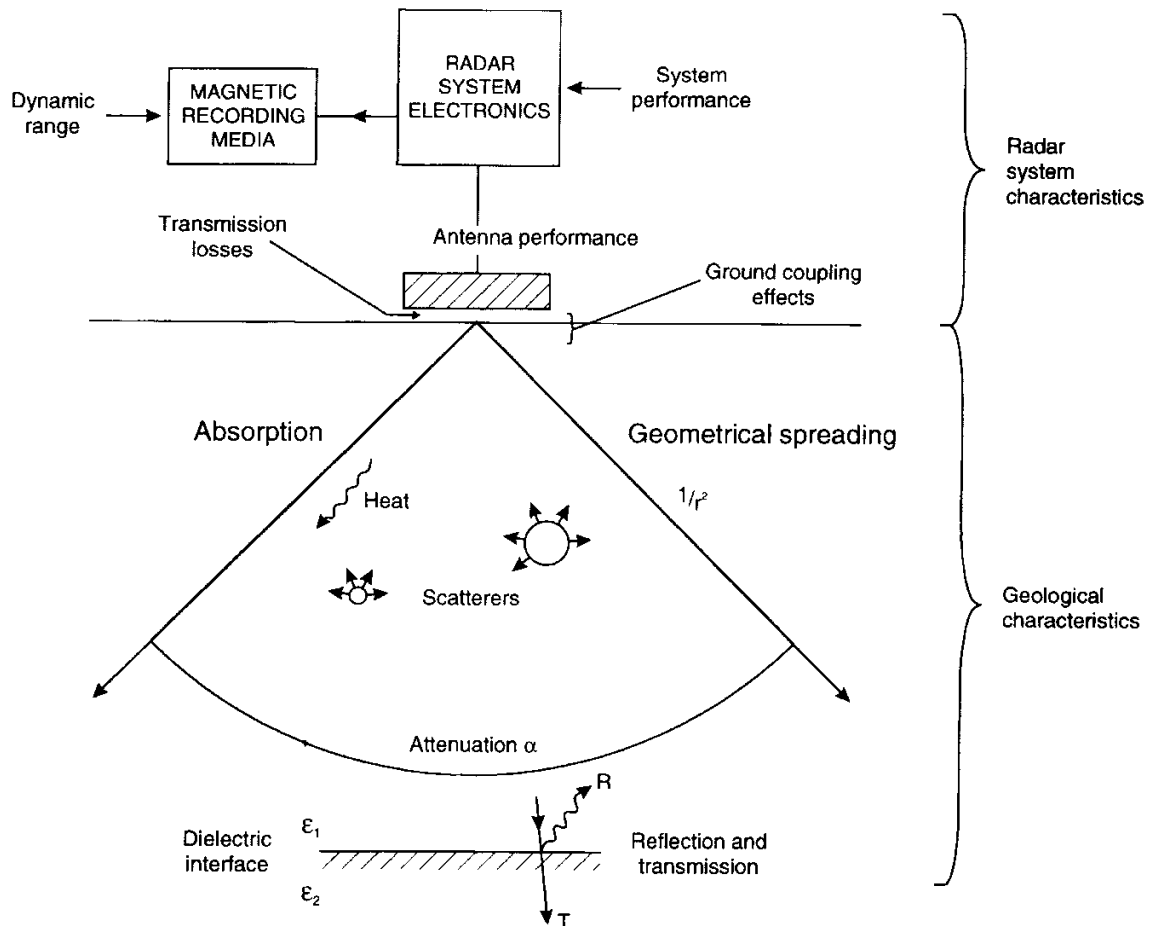


Figure 7. Scheme of the operating principle of a common GPR system [129]

The common GPR systems can be subdivided into:

Time-domain impulse radars, which send a short nonsinusoidal waveform with a wide bandwidth [129];

Frequency-modulated continuous wave radars, which sweep a narrowband signal through a wide frequency range [130].

The operating performance of the GPR is expressed in terms of its maximum penetration depth and resolution. The first parameter refers to the maximum depth at which a target inside the investigated medium can be detected, whereas the second one concerns the minimum separation between two bodies before their identities are lost. The building materials elements are often characterized by a high absorption of electromagnetic energy, due to high conductivity. As the

conductivity increases, the penetration depth decreases [129-131]. In highly conductive materials, like concrete and other cement based materials (which might be present in the structural support), the electromagnetic energy is more quickly dissipated and transformed into heat, causing a decrease in signal strength with the increase of the depth [132, 133]. The presence of salts in the wall constituent material can increase material conductivity and therefore can also decrease the penetration depth of the GPR signal.

The main advantage of this technique when applied to the wall decoration is high penetration into the support and possibility to estimate the depth of the target. Signal processing can estimate the depth of subsurface objects by measuring the time-of-flight of the reflected signal and factoring in the electromagnetic wave speed in the dielectric medium. The main disadvantage of the impulse-type penetration radar is the resolution the high attenuation of electromagnetic radiation, characteristic for most media of interest for Cultural Heritage and Structural Diagnostics [50, 132].

Instrumentation used in the project

High resolution IDS Georadar with full polar 2 GHz antenna was applied for the experimental part of the given study. The instrument is the property of the Department of Cultural Heritage: Archaeology and History of Art, Cinema and Music of the University of Padova. It is a portable system consisting of an antenna head and a control unit (laptop), which can be transported manually to historical buildings and even to hardly accessible archaeological sites. Its operation requires, however, certain physical skills and accuracy. For the performed in-situ acquisitions on wall paintings on wall mosaics, a soft transparent PVC film was used, in order to protect the artistic surface from direct contact with the instrument and with the operator's hands. A regular grid of acquisition lines was applied on the external surface of the transparent film, in order to maintain the precise step of acquisitions during the manual operation of the instrument.

3.1.2 Holographic Subsurface Radar

Nowadays Rascan radars do not represent yet a commonly applied technique for subsurface structural diagnostics. They represent an innovative subsurface radar system that operates with continuous narrowband systems, at several close frequencies around 2 GHz, 4 GHz or 7 GHz, depending upon the model [48-52, 134-144] and use interference techniques for the image formation.

The first mock-up of the MiRascan subsurface sounding radar was developed at the Remote-sensing Laboratory of the Bauman Moscow State Technical University (Russian Federation), with the aim to detect mines in the ground [139]. The custom-built software program produces plan view grayscale images of the internal structure of examined areas, using five simultaneous frequencies [48-52]. The holographic principle refers exclusively to image formation since reflected signals are mixed with an internally generated reference signal that has not been transmitted to the medium (Fig. 8). The technique can be also referred to as Microwave Holography [142].

The fundamental difference of the HSR from the GPR systems is that it provides plan-view subsurface images. HSR uses signal processing methods analogous to the optical hologram technology first proposed by D. Gabor in 1948 [138]. Unlike an optical photograph, the optical hologram records not only the intensity of the waves scattered by the object but also the information on the phase of these waves. In the case of a point object shown in Fig.8, the resulting interference pattern on the hologram recording medium forms a set of concentric rings like a Fresnel zone plate. Illuminating by coherent light, with the same wavelength used for recording, a virtual three-dimensional image of the object is created (Fig. 8).

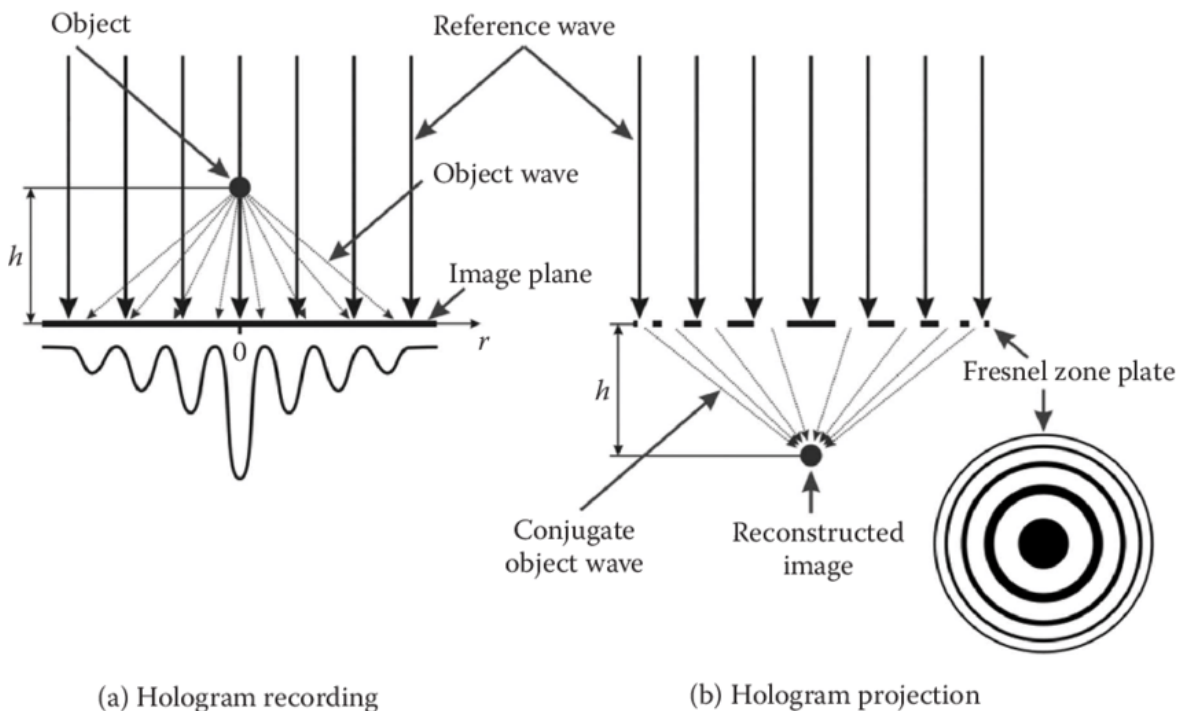


Figure 8. The principle of simplest optical hologram proposed by D. Gabor: a) the interference pattern resulting from coherent light reflected (diffracted) from a point and the reference wave forms an interference pattern on a hologram recording medium; b) Passing the same frequency light wave through the hologram produces a virtual image on the other side of the hologram [138].

The main difference between optical holography and subsurface radar holography is the relative dimensions of the recording systems in the two cases. Both the reflected signal and reference signal have the same frequency but the reflected signal has a phase shift depending on the distance (depth) to the reflector. Thus, the reflected signal and reference signal interfere constructively or destructively depending on the target or the depth of its position. The phase shift of the reflected signal depends on the distance to the reflector, which allows the estimation of the defect depth.

The RASCAN-type holographic radar consists of a transmitting antenna and two receiving antennas for parallel and cross polarizations [143]. It emits unmodulated, continuous wave signals. The system operates at five simultaneous frequencies within the microwave range in order to ensure that a target (contrast in dielectric properties) will be visible on at least one of the frequencies, regardless of its depth. In the case of only one frequency used, the so called “blind depths” may appear for a particular target depth due to sinusoidal variation with depth in the phase difference between the reference and target beams [138]. Therefore, the multi-frequency mode is essential for HSR because, in the monochromatic mode of operation, it is possible to miss objects at certain depths. These five frequencies are automatically switched during scanning and their values are very close (within 10%) to the nominal frequency. At the end of each acquisition, 10 images are obtained (five frequencies, two antenna polarizations) [137-138].

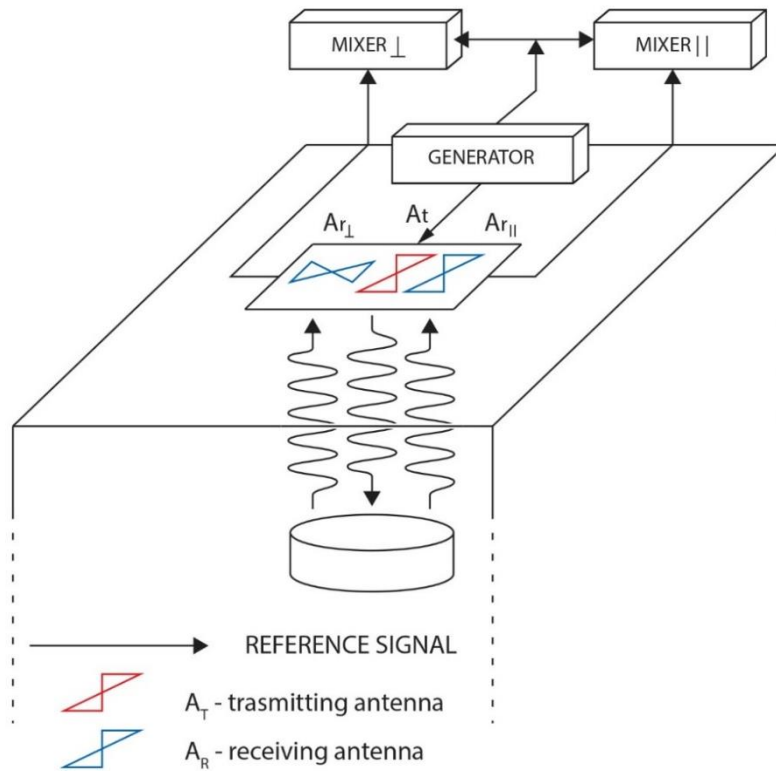


Figure 9. Operating principle of the holographic subsurface radar system, after Vladimir Razevig [134, 140-141].

The detectability of targets in the subsurface is based on contrasts in dielectric permittivity, therefore, the system proved its high effectiveness in the detection of hidden metallic, plastic elements under the planar concrete and wooden surfaces, as well as in the detection of moisture and water pipes [138]. Experiments with RASCAN HSR have demonstrated that the main factors that deteriorate the quality of HSR holograms result from attenuation and inhomogeneities in the medium in which the electromagnetic wave propagates. Moisture frequently has the greatest influence on both of the factors. Concrete and clay represent examples of media that have high levels of conductivity and attenuation in moist conditions.

The system has been applied various times to the building structural surveying, including walls and floor stone coverings (marble medallion) of high historical value [51]. In the author's awareness, however, no publications refer to the application of HSR and RASCAN HSR systems to the analysis of highly valuable wall paintings and wall mosaics surfaces.

The system has been applied to the structural diagnostics of objects that are characterized by planar surfaces, encountering difficulties while evaluating irregular or non-planar (for example,

curved) surfaces. Currently, the scientists of the Remote Sensing Laboratory are working on further development of microwave scanning system by integration of video tracking and Photoscan [130]. Both of these innovations are aimed to improve the informativity of the images and remove eventual artefacts in the signal while investigating under irregular surfaces. At the same time, a new prototype of Rascan system operating at the frequency of 22 GHz is under construction at the Remote Sensing Laboratory of the Bauman Technical University in Moscow (Russian Federation).

The instrument, used for the experimental part of this project, is RASCAN 5/7000, the most recent commercially available model, which is operating at the frequencies 6.400, 6.500, 6.600, 6.700 and 6.800 GHz. Table 4 reports its main technical characteristics [141].

Table 4. Technical parameters of the instrument Rascan 5/7000 (6.4-6.8 GHz)

Parameters	Value for the Rascan 5/7000
Maximum sounding depth (depends on medium properties), mm:	
in concrete	75
in brick wall	150
in wall board	180
in wood	180
Resolution in plane of sounding at shallow depths, cm	0.5
Number of frequencies	5
Productivity, m ² per hour	4...6

Note: * Maximum sounding depth is given for homogeneous and dry materials. Moisture and heterogeneity in the medium cause the decreasing of the penetration ability [144]

The Rascan instrument is a lightweight, portable holographic radar system. It consists of an antenna head and a control unit (Fig. 9). It can be easily portable by hand to the acquisition site, even in hardly accessible conditions of an archaeological site. The manual acquisition by Rascan is time-consuming and requires high skills ability from the operator since the irregularity and inaccuracy of acquisition lines influence strongly the resulting Rascan image. For this purpose, a special robotic scanning system was developed [145], which can be applied only to horizontal surfaces.

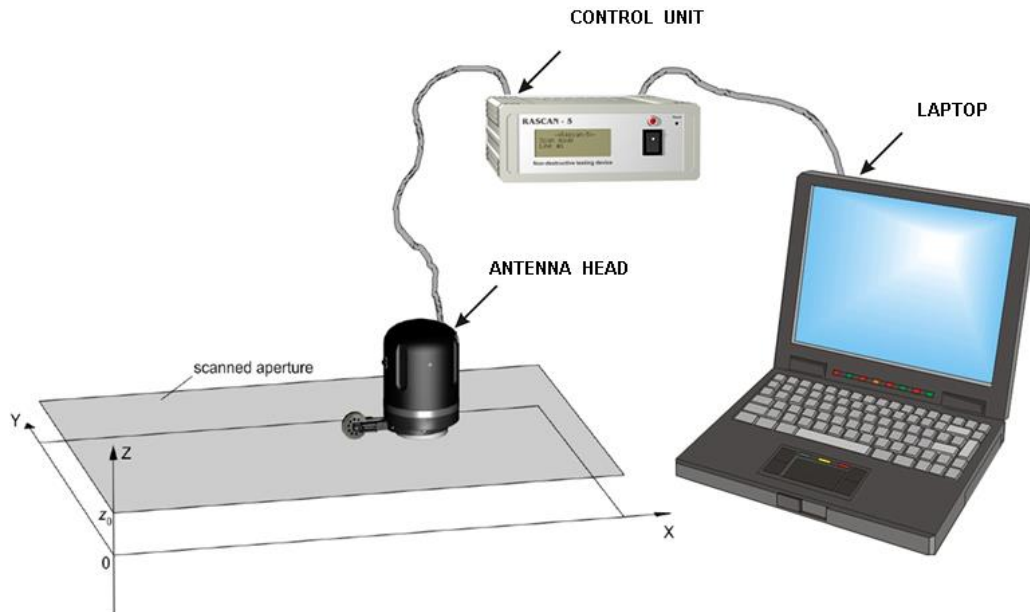


Figure 9. Operating scheme of Holographic Subsurface Radar RASCAN 5/7000, after Vladimir Razevig [138].

The Q-Rascan dedicated software was used for visualization and examination of acquired data. If the dielectric permittivity constant of the constituent materials is known, the software program:

- allows focusing the holographic image at different depths inside the investigated medium;
- can provide indications on the distance from the antenna to the detected target inside the medium.

3.2 Non-contact methods used for on-site tests, principles and applications

3.2.1 Infrared Thermography

The infrared thermography measures and records variations in thermal radiation from the surface of a body in the infrared range of the electromagnetic spectrum, see Fig. 10. The retrieved result from such controls is a thermal image (or thermogram), which reflects any spatial variations in temperature on the surface of the body through different color (using colour palette) or brightness value (using grayscale). In other words, as indicated by its name, “thermography” can produce the distribution map of the temperature on the surface of the target under investigation.

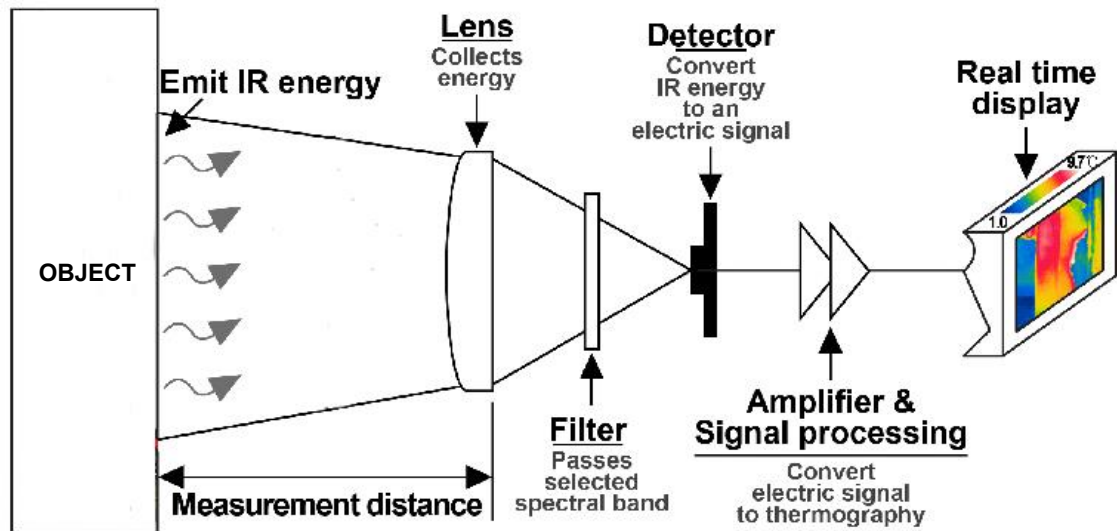


Figure 10. Operating principle of the Infrared Thermography, after Young Hoon Jo [146]

The existence of the infrared portion of the electromagnetic spectrum was accidentally discovered

around 1800 by *Sir William Herschel (1738-1822)*, while searching for new optical filters to reduce the brightness of the sun's image in telescopes during solar observations. In 1860, the concept of a *blackbody* (perfect radiator) was defined by *Gustav Robert Kirchhoff (1824-1887)*, as an object which absorbs all radiation that is directed to it, independently of direction or wavelength [147]. The degree of similarity of a real object to the black body is measured through the parameter called *spectral emissivity*, which represents the relationship between the energy emitted by the real object and the energy that would emit a black body at the same temperature.

When considering the total radiant flux, incident on the surface of a real object, some fraction of this total radiant energy is absorbed, some is reflected and some is transmitted through the real object.

The radiative behaviour of real objects depends on many factors: body temperature, chemical composition, surface roughness and geometry, temperature, wavelength of the radiation and angle at which the radiation is emitted [148]. In order to describe the emission of thermal radiation from the surface of a real object, the term *emissivity* (ϵ) has been introduced as a fundamental radiative property of real objects. Absorptivity (α) is the parameters that correspond to the fraction of the absorbed energy by surface and can be defined as the ratio of the spectral radiant energy absorbed by an object to that incident upon it. As in the case of emissivity, absorptivity depends on the direction and wavelength, but it is practically unaffected

by surface temperature. Reflectivity (ρ) measures the fraction of the incident radiation reflected by a real surface and can be defined as the ratio of the spectral radiant energy reflected by an object to that incident upon it. Surfaces may be defined as diffuse or specular, according to the manner in which they reflect radiation. *Transmissivity* (τ) measures the fraction of transmitted radiation after passing through the medium and can be defined as the ratio of spectral radiant energy transmitted through an object to that incident upon it.

Another crucial parameter, which must be taken into account during the investigation by infrared thermography, is the *heat transfer* phenomena. Whenever there is a temperature difference inside the medium or between two media, heat transfer occurs. The heat energy always moves from the medium with a higher temperature to the medium with lower temperature. There are three basic properties which lay the foundation of any conduction analysis of a material and these are the *thermal conductivity* k , the *specific heat* cp , and the *mass density* ρ . *Thermal conductivity* k [$W/m\ ^\circ C$] is a property that indicates the transfer rate by conduction for a specific material. The higher is the thermal conductivity of a material, the greater is the heat transfer rate by conduction. These three thermophysical properties can be combined into the property of *thermal diffusivity* α [m^2/s] which measures the material's ability to conduct heat in relation to its capacity to store it [148-149].

The knowledge of the influence of the thermophysical properties and understanding of heat transfer problems are very important since they can provide information about observed phenomena such as abnormal temperature patterns detected on the surface by the means of an infrared camera.

The two main approaches to thermography are those of the passive and active approach respectively.

Passive thermographic inspection, employed in on-site acquisitions within this project, measures the heat flux, generated from the surface of the test object under natural conditions. Passive thermographic inspection aims at the detection of subsurface and/or surface features, through temperature differences (ΔT) observed on the investigated surface during the monitoring with an infrared camera [150]. Nevertheless, the accuracy of temperature measurements is limited when the inspected surface consists of various types of materials with different emissivity values and if there are no naturally occurring thermal contrasts, passive thermography will not provide efficient results.

For on-site acquisitions in Italy and in Greece, several models of FLIR ThermoCAM was used, coupled to the camera dedicated software FLIR ResearchIR.

The areas of interest (defects) may appear sometimes as subtle signatures or not appear at all when examining raw thermal images, some information might be missed [151]. If defects or some features of interest are detectable, some image processing algorithms may be applied for their enhancement, compensating or discriminating between real features and artefacts.

3.2.2 Multispectral Imaging

Multispectral imaging is a non-invasive and non-destructive technique used to observe the surface of an object using selected ranges of wavelengths of the electromagnetic spectrum, including and extending beyond the capabilities of a human eye, sensitive in the range from 380 to 750 nm approximately [152]. As suggested by its denomination, it is an imaging technique and, when coupled to a specific software, can include point and spot analysis.

The wavelength range that can be observed using modified commercially available cameras, typically employing silicon-based sensors, is in the range from approximately 350 nm to 1100 nm.

In Multispectral or Hyperspectral Imaging systems, the images are produced by sensors that measure reflected energy within specific sections (called bands) of the electromagnetic spectrum [153]. The difference between the two systems consists in the number and width of examined bands. In Multispectral Imaging, the collection of reflectance spectra for each point of the field of view is performed between several bands (from 3 to 30). At the same time, hyperspectral sensors measure energy in narrower and more numerous bands (up to 200 or more) [72-73, 154].

The quantity of bands and the exact spectrum may vary for different multispectral and hyperspectral imaging systems. Key performance characteristics (bandwidth, number of bands and image resolution) of some recent developments in this field are presented and compared in Table 5 [24-25, 142].

Table 5. Comparison of multispectral and hyperspectral imaging systems

Name	Country	Type	Range	Number of bands	Camera Information
Profilocolore Nikon D800 FR* [53-54]	Italy	Multispectral	300-1000 nm	7	Nikon D800 FR modified to Full range + Filters; 36 megapixel

Antonello [155]	Italy	Multispectral	400-925 nm	18	unknown
MUSIS [156]	Greece	Multispectral	420-1000 nm	30	CCD and photocathode 1600x1200 + Filters
ISIS - I [157]	Greece	Multispectral	380-950 nm	15	Color CCD 1600x1200 +Filters
ISIS- II [157]	Greece	Multispectral	350-1200 nm	28	Monochrome CMOS sensor 2560x1920 +Filters
Hypex VNIR160 0 [158]	Norway, France	Hyperspectral	414–994 nm	160	SSI CCD 1600 ×1200
Specim Corp [159]	Finland, USA	Hyperspectral	1000–2500 nm	256	ImSpector N25E spectrograph
Specim V10E [160]	Finland, USA	Hyperspectral	394–1009 nm	776	Monochrome sCMOS linear 2184 pixels
Syddarta [161]	Spain, Greece, Netherla nds	Hyperspectral	400-900, 900-2500 nm	around 300	Basler ace ACA2040-25gm CMOS camera, 25 fps, 2048 x 2048 and Xenics custom MCT camera, 320x256 pixel resolution

*multispectral system used in the experimental part of this project

A modified commercial reflex camera, which is used in this project, makes use of seven bandpass filters covering a range of 300-1000 nm [72-73], as shown in Fig. 11.

Generally, a multispectral imaging system is composed of three main components:

- incoming radiation, which is generated by a radiation source and is directed towards the object;
- the object, which interacts with the incoming radiation;

- outgoing radiation, which, following the interaction between the incoming radiation and the object, travels from the object back to the recording device.

The radiation ranges used for on-site Cultural Heritage inspections typically may include ultraviolet radiation (UV approximately 200-400nm), visible light (VIS approximately 400-700nm) or near-mid infrared radiation (IR approximately 760-1700nm) [152]. At the same time, the UV range can be subdivided into UVA (315-400nm), UVB (280-315nm) and UVC (100-280nm).

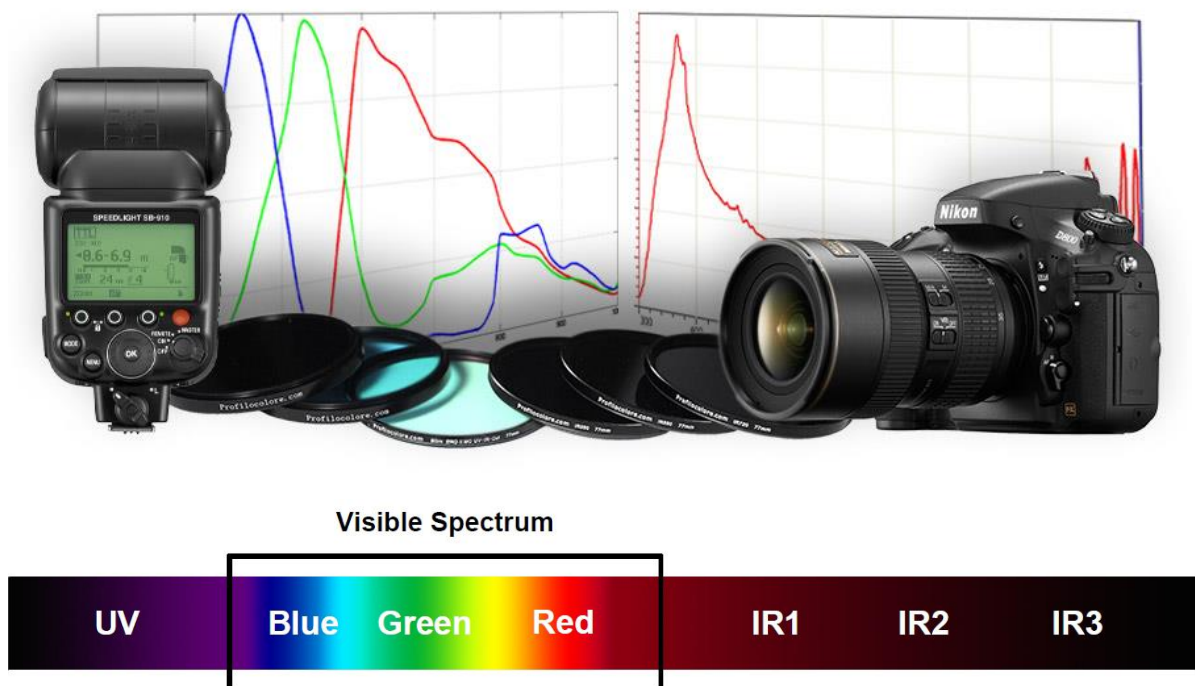


Figure 11. The camera Nikon D 800 FR and the spectral range used in Multispectral Imaging. Image credits: Marcello Melis [19]

The penetration depth of investigation depends on the incoming radiation wavelength and on the absorbance of the materials, which compose the object under investigation. Longer wavelengths of radiation generally penetrate further into the depth. For example, when examining a wall painting, longer wavelengths (IR) can pass through the varnish and interact with the pictorial film and sometimes underlying preparatory drawings [20, 162].

The incoming radiation reaching the surface of a wall decoration can be absorbed and/or reflected, absorbed and re-emitted as fluorescence (luminescence) at longer wavelengths [152]. The spectral reflectance of a surface is the relationship between the incident radiation and the reflected radiation, as a function of wavelength, with an angle of incidence of 45 ° and reading angle 0 ° from normal. The incoming and the recorded outgoing radiation can be in the same

range (Reflectance Mode) or in different ranges (called Fluorescence or Pholuminiscence mode).

Table 6 reports the main applicability features of each acquisition mode and relative wavelength, when applied to painted surfaces (on-site or in a museum environment).

Table 6. Multispectral imaging and its applications

Acquisition mode		Wavelength range	Applicability to painted surfaces
Reflected images	Ultraviolet-reflected (UV-R) images	approx. 200-400 nm	Superficial distribution of material, such as varnishes and coatings.
	Visible-reflected (VIS-R) images	approx. 400- 700 nm	Documentation. Reference image to interpret the other image sets.
	Infrared-reflected (IR-R)	approx. 700-1100 nm	Underdrawings and concealed features. This is because infrared radiation is usually highly penetrative and many materials, such as organic binders and colorants, are generally transparent to infrared wavelengths.
False-colour reflected images	Ultraviolet-reflected false-colour (UVRFC) images	approx. 200-400 nm, 400-700 nm	The combination can result in distinctive “false” colours that may aid the characterisation or differentiation of materials.
	Infrared-reflected false-colour (IRRFC) images	approx. 400-700 nm, 700-1100 nm	The combination can result in distinctive “false” colours that may aid the characterisation or differentiation of materials.
Photo-induced luminescence images	Ultraviolet-induced luminescence (UVL) images	Emission of light (luminescence) in the visible region (400-700 nm) from a subject when this is illuminated with UV radiation	Distribution of luminescent materials, such as organic binders and colorants [163, 164]. Some inorganic materials also show luminescence properties, such as, for example, some inorganic pigments including zinc oxide with impurities. The absence of luminescence does not imply the absence of organic materials.

	Visible-induced infrared luminescence (VIL) images	Emission of radiation (luminescence) in the infrared region (700-1100 nm) from a subject when this is illuminated with visible light	This image characterizes the spatial distribution of pigments such as Egyptian blue, Han blue, Han purple [163] and cadmium-containing pigments [164] This technique is very sensitive and can reveal even single particles of such pigments.
--	--	--	--

Ultraviolet-reflected false-colour (UVRFC) images are produced in post-processing when splitting the image into its red, green and blue (RGB) channels and shifting the blue and green components into the green and red channels respectively. The UVR image is inserted into the blue channel. The reflective properties of the object in the UV range are described by blue colour on the B channel [152].

Infrared-reflected false-colour (IRRFC) images are produced in post-processing when splitting the visible image into its red, green and blue (RGB) components and shifting the red and green components into the green and blue channels respectively. The IRR image is inserted into the red channel. The reflective properties of the object in the IR range are described by red colour on the R channel. Ultraviolet-induced luminescence (UVL) images record the emission of light (luminescence) in the visible region (400-700 nm) from a subject when this is illuminated with UV radiation [152].

The exact maximum penetration depth and informativity of multispectral imaging technique vary for different types of the decoration (painting or mosaic) and for their characteristics (constituent materials and thickness of layers). The expected penetration depth for each type of acquisition/analysis mode is presented in the Fig.12 for wall paintings and in the Fig.13 for wall mosaics.

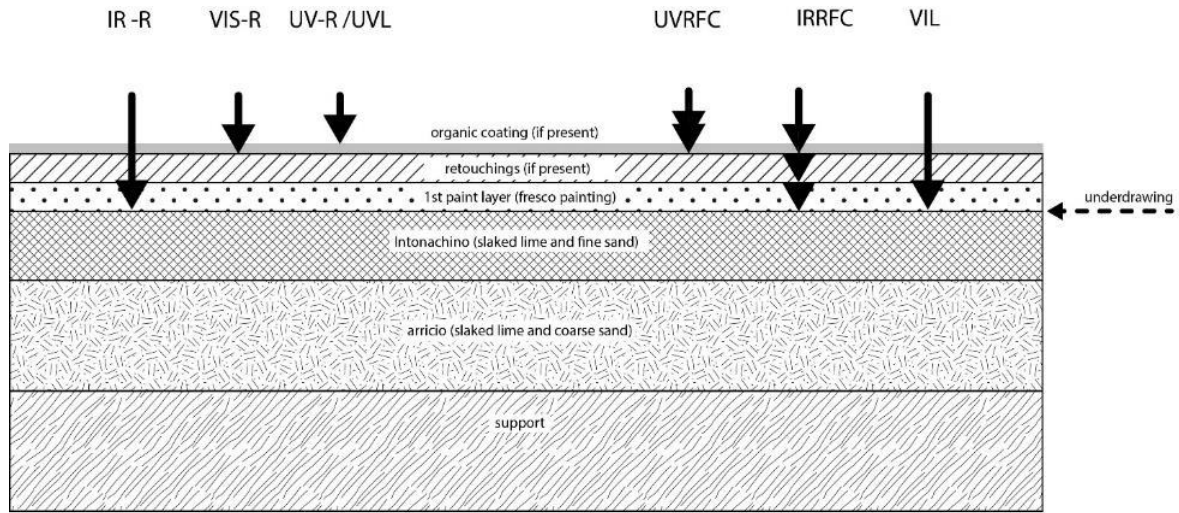


Figure 12. Penetration depth of non-invasive investigation by Multispectral Imaging technique applied to wall decorations

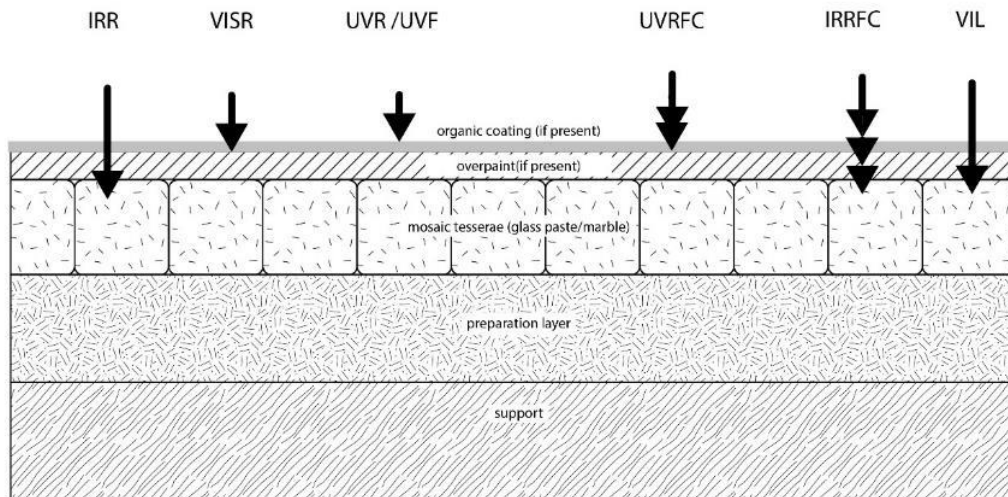


Figure 13. Penetration depth of non-invasive investigation by Multispectral Imaging technique applied to mosaic decorations

Instruments used in this thesis project

Nikon D800 FR (full range) camera with a 36-megapixel sensor was modified in a common project by Nikon/Profilocolore to widen the range of its sensitivity to ultraviolet and infrared bands (300-1000 nm) [72-73]. The camera is equipped with two Nikon SB- 910 flashlights, each modified to excite a full range spectrum, and a set of bandpass filters: UV (transmission of 30-60% between 320- 400 nm), VIS (transmission of 90% between 400-700 nm), IR1 (transmission >95% above 715 nm), IR2 (transmission >95% above 840 nm), IR3 (transmission

>95% above 920 nm) [53]. More information can be found on the relative website [73], the spectral curves of the used filters can be found in the uploaded documents [165]. The instrument is easily portable, allows rapid data acquisition and is suitable for operating in hardly accessible archaeological sites. The system is in constant development. New variations of modified cameras (Sony) are currently under development by the experts of Profilocolore company. It is therefore highly recommended to check the updates on the website [73]. The functions presented and evaluated in this thesis are last updated in 2017.

During the acquisition, two flashlight sources are placed on both sides of the camera, with a 45° angle to its main optical line [19,53, 72-73] (Fig. 14). Where possible, a color reference chart (e.g. Profilocolore color reference chart or a Macbeth color checker) for calibration of the light conditions should be used.

In the given project, different types of software tools were tested. Since dedicated software tools are more complex to use and are characterized by higher costs, they are not always directly available to Cultural Heritage experts. In this thesis the potentialities of this multispectral imaging system are evaluated:

- information obtainable through the observation of raw images;
- qualitative image analysis by alternative free and commonly available software tools;
- qualitative and quantitative image analysis through dedicated Profilocolore software.

Before using alternative software tools, the raw images (NEF) should be converted to Tagged Image File Format (TIFF) with minimal processing (without white balance and brightness corrections or stretching or pixel rotations) using the dedicated NX Viewer or DCRAW free software.

The software tools including Image Enhancer, Adobe Photoshop, NIP2 and ImageJ for qualitative analysis of wall paintings. It should be emphasized that NIP2 requires the presence of a Macbeth Color Checker in the photographic capture (Fig. 14b). Macbeth Color Checker is a standard color rendition chart, initially designed to deliver true-to-life color reproduction for photographers [162].

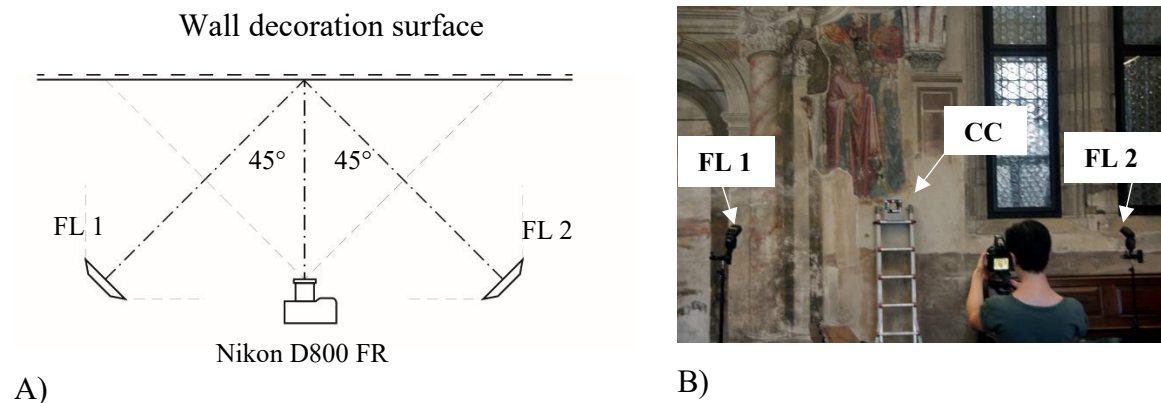


Figure 14. Acquisition of multispectral images: a) scheme of recommended acquisition geometry (horizontal view); b) photographic representation during the acquisition procedure, image credits: Rita Deiana. FL 1 and FL 2 – flashlight sources; CC - color rendition chart.

Image Enhancer is a recent desktop application, open source, based on 64 simple and complex Image Processing concepts [166]. It is an easy-to-use and simple tool for the application of fundamental image filters and image transformations (convolution, RGB channels rotation, etc.). This software tool does not provide any option of quantitative or spectral information.

Adobe Photoshop and GIMP (open source alternative to Photoshop) represent already two routine tools in the field of digital image processing and digital manipulation industry. Apart from improving visual presentation of results, they have already proved to be useful for art examination, segmentation and visualization of multispectral images [167-168]. They represent an essential tool for comparison, overlay and qualitative statistical mapping for different spectral images.

Recently a free Technical Photography Kit software was introduced by Dr. Antonino Cosentino, an alternative to Photoshop and GIMP, which is based exclusively on free software tools dedicated to Cultural Heritage images examination [167].

ImageJ is an open source image processing program, a well-known image calibration and analysis toolbox for scientific purposes, introduced and widely used in microscopy examination [169]. It can be also applied in multispectral imaging for art examination [21-22].

Moreover, the examination included NIP2, a graphical interface of the free processing system VIPs, with a specific workspace, developed by the British Museum for the needs of cultural heritage community, under the EU CHARISMA project [142]. The use of this software is only possible when the images were acquired in the presence of Macbeth Color Checker, which is a classic color rendition chart, initially designed to deliver true-to-life color reproduction so photographers [162].

As for the quantitative analysis, spectral analysis by means of ENVI image analysis software [170] was introduced, which is originally dedicated to remote sensing geological applications, such as classifications of minerals and mapping.

Many of the developed multispectral imaging systems, commercial and custom built, are equipped with a dedicated software, which provides qualitative and quantitative analysis possibilities. The use of dedicated software tools is necessary for obtaining scientifically correct results [72-73]. It is, however, possible, to improve the informativity of raw non-elaborated images in-situ by the means of alternative free and commonly available software tools. The preliminary information obtained without the use of dedicated software can indicate the areas of interest for further qualitative and semi-quantitative analysis, for which the specific software tools and/or other methods can be used.

The recommended workflow, tested within the experimental part of this thesis project, is shown in Attachment D.

3.3 Other non-invasive methods used in the laboratory simulation tests

The simultaneous application of Digital Holographic Speckle Pattern Interferometry (DHSPI) and Stimulated Infrared Thermography (SIRT) is already a recognized combined approach for subsurface structural diagnostics of art works [38-41, 65-68, 171]. The experimental tests on a custom-built mosaic model were performed at the Holography Metrology Laboratory of the Institute for Electronic Structure and Laser, Foundation for Research and Technology (IESL-FORTH), Heraklion (Crete, Greece) during March-April 2018.

Digital Holographic Speckle Pattern Interferometry (DHSPI) is a non-invasive full field, remote control and non-contact optical technique aimed to evaluate the structural condition of objects evaluating the presence of ageing, structural failure and material's deterioration. It is based on the combination of Holographic Interferometry (HI) and Electronic Speckle Pattern Interferometry (ESPI) [171-172], which are well-known non-destructive techniques used in the industrial sector for quality control [172]. The history of optical holography is briefly introduced in chapter 3.2 (see Fig. 8). It should be added that the Holographic principle of DHSPI consists in recording phase variations of two mutually coherent laser beams, produced by a laser source of monochromatic light at the single wavelength of (532 nm): in the recording plane, the object beam OB (reflected from the surface) interferes with the reference beam RB. The superposition of holographic wave fields gives rise to visible interferometric fringes which indicate the out-of-plane displacement of the surface. The data acquisition is based on an interferometric comparison of the two states of the surfaces under examination: the reference

state and the excitement state [38]. The white-light image is captured before the excitation and the subsequent acquisitions are performed with a defined regular interval after the excitation (Fig. 15). The images are captured using a 5-frame algorithm and each set of 5 images is compared to the first initial set.

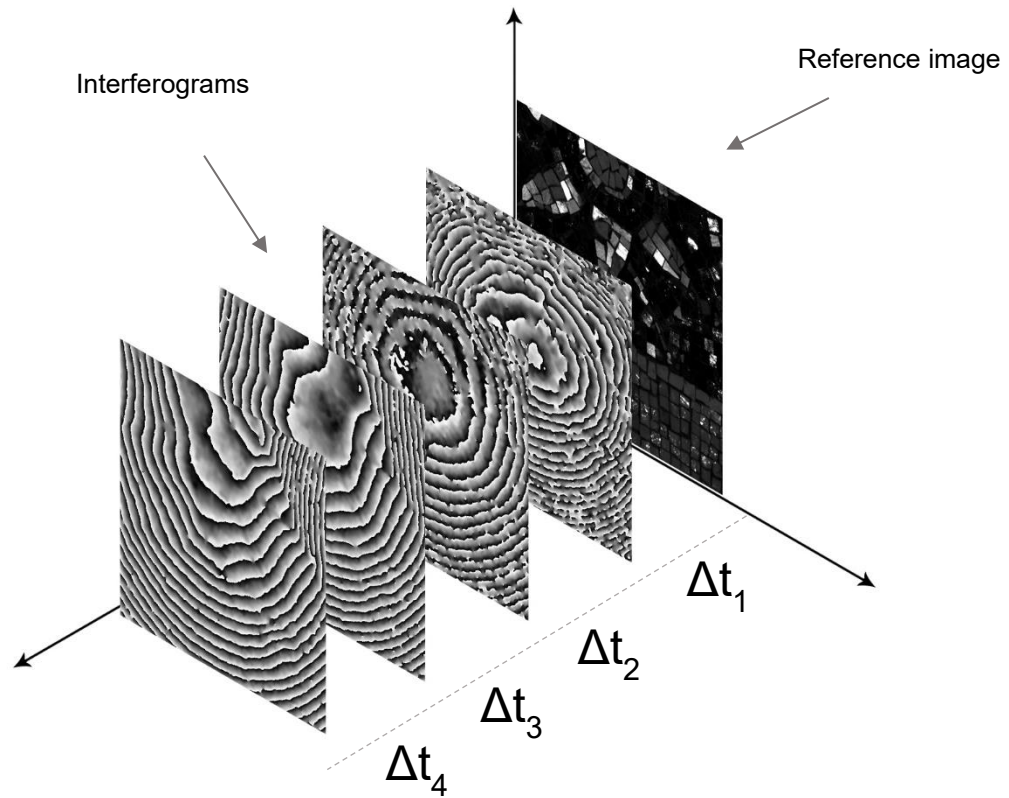


Figure 15. Acquisition of interferograms by Digital Holographic Speckle Pattern Interferometry at a regular interval (where each Δt indicated the time interval from the start of acquisition).

Different types of excitation source can be used: mechanical impact, thermal excitation, etc. When applied in combination with the Stimulated Infrared Thermography, thermal excitation is used as a stress source. The differences in surface microdeformations are induced by differences in thermal expansion behavior of the materials and elements in the object's subsurface structure. Moreover, the technique can be applied to temporal monitoring of structural changes on the basis of environmental and climatic changes, conservation treatments, natural or stimulated ageing, transportation or handling.

Coupled to custom-built dedicated software, the technique can provide quantitative information on microdeformation, allowing detection of defects' location, size measurement and exact positioning within the structure of the object. The magnitude of surface displacement, expressed in μm or fractions of micrometers, corresponds to the number of fringes multiplied by $\frac{1}{2}\lambda$ laser wavelength employed by the system. Quantitatively, the displacement resolution (distance between two pairs of interferometric fringes) is 266 nm ($1/2$ wavelength) [65-68], while it is

possible to obtain the displacement resolution of 1/10 of the wavelength by subfringe interpolation.

When used in combination with the Stimulated Infrared Thermography, thermal excitation is used as a stress source [38, 68]. The detectability of discontinuities is due to the differences in microdeformation of the surface upon excitation, caused by distinct thermal expansion behavior of different materials underneath. This technique, however, can be applied, without the use of induced stress, to temporal monitoring of structural changes on the basis of environmental and climatic changes, conservation treatments, natural or stimulated ageing, transportation or handling.

The fundamental principles of passive Infrared Thermography were introduced in chapter 3.2.1. For Stimulated Infrared Thermography, an external energy source is used, in order to produce a thermal contrast between the features of interest and the background. This approach is necessary in the conditions where the studied object is normally in a thermal equilibrium and no natural temperature are detectable, absent or not sufficiently strong, for the identification of internal inhomogeneities beneath the investigated surface [33].

Defect detection principle in a stimulated thermography is usually based on the heating (sometimes, cooling) of the studied object's surface. The process of the thermal energy inside the sample provides a transient temperature gradient. Different external excitation sources can be used to stimulate the object under investigation: flash lamps, heat lamps, forced hot or cold air, electromagnetic induction and ultrasonic energy [33].

Regardless the stimulation source used and the way that the test object is being excited, the basic operational principle in all stimulated thermographic inspections is the sequential monitoring of the thermal response of the surface with respect to time, during and /or after the application of a heating excitation (Fig. 16). When the studied object cools down after flash heating, and any flaws present will cause changes in the cooling rate of specific areas (called regions of interest or ROIs). The cooling rate is recorded by the infrared camera as an image or as a sequence of images.

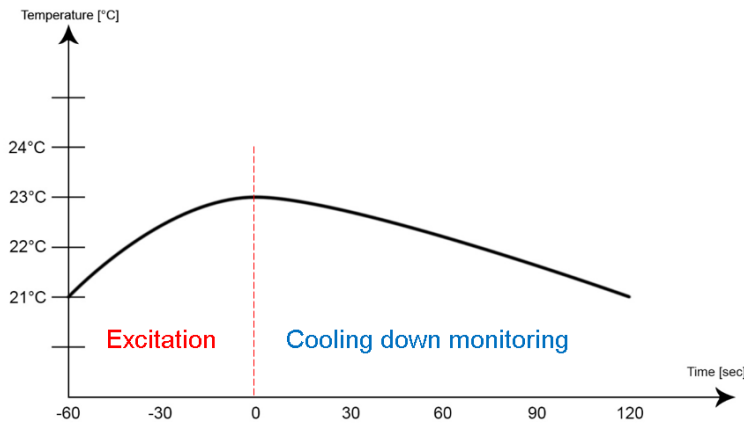


Figure 16. Scheme of acquisition procedure by Stimulated Infrared Thermography.

The general experimental procedure implemented by DHSPI-SIRT system is described in Table 7, after Vivi Tornari [68]. More details on the acquisition geometry and parameters, used in this thesis, can be found in chapter 6.

Table 7. Experimental procedure of DHSPI-SIRT acquisition

<p>STEP 1 Reference values and excitation</p>	<p>1a. DHSPI measurement starts - <i>the reference of the initial surface position is measured</i> 1b. Thermal excitation starts - <i>temperature increase for a pre-specified duration</i> 1c. Thermal excitation stops - <i>cooling down starts</i></p>
<p>STEP 2 Monitoring of cooling down process</p>	<p>2a. DHSPI and SIRT measurements in sequential recording during cooling down 2b. DHSPI and SIRT keep recording for as long as ΔT° fluctuates, or till initial surface value</p>
<p>STEP 3 Processing and post-processing</p>	<p>3a. Raw data evaluation and processing 3b. DHSPI and SIRT data post-processing - <i>quantitative/qualitative, post-processing tools and routines for data exploration and demonstration</i> 3c. DHSPI and SIRT comparison - <i>raw and post-processed data are compared and evaluated</i></p>

Instrumentation used in this project

In this project, a custom-built Digital Holographic Speckle Pattern Interferometry system DHSPI-II was used [38-41, 65-68, 171]. The workstation on operation and its instrumental set-up is shown in Fig. 17. It consists of an optical head that makes use of 300 mW DPSS (Diode Pumped Solid State) 532 nm laser with a coherence length higher than 30 m for illumination.

The image is captured by a 5 Megapixel CCD and is further processed. This optical configuration provides a sensitivity of 144 lines/mm and a displacement resolution of 266nm (1/2 of the wavelength 532 nm). The system is controlled remotely via an external laptop PC, the operation, processing and post-processing dedicated software applications have been developed in LabVIEW environment. The post-processing software provides several functions, aimed at enhancement and quantification of measurement results, the dimensioning and positioning of structural defects to generate risk-maps.

The system used for Stimulated Infrared Thermography operation comprises IR lamps (excitation device), an infrared camera (detection device) and electronic and computing instrumentation for monitoring. The detection system is constituted of an infrared camera FLIR B20 (20° x 15°/0.3 m Field of view, 1.1 mRad Spatial resolution, 50 mK at 30°C Thermal sensitivity, 7.5 to 13 μm Spectral range), working in a synchronous way with the excitation system (infrared lamps). The measurement can be done in the range of temperature -40°C to 120°C, with the thermal sensitivity 0.05° C or 50 mK. More details on experimental geometry and laboratory acquisition procedure are provided in chapter 6.

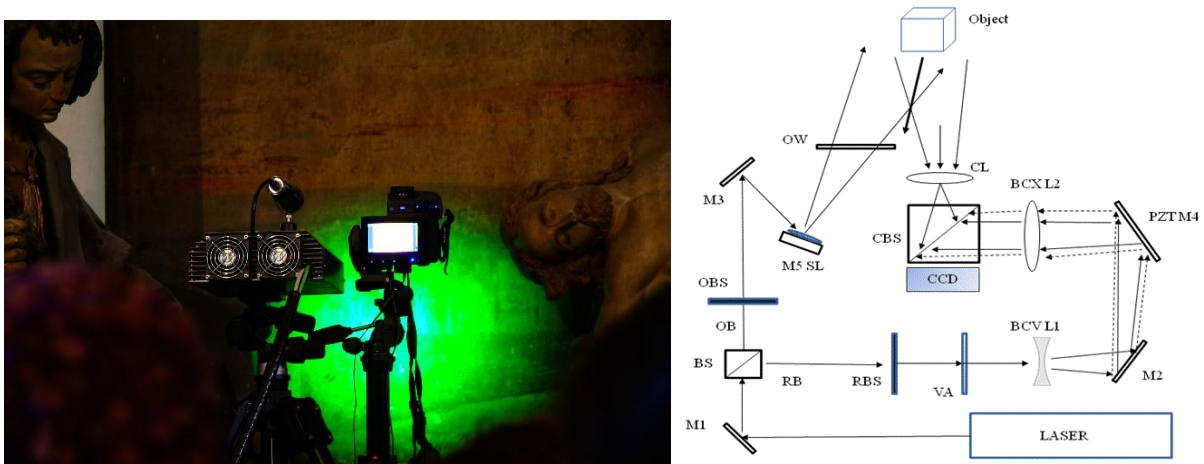


Figure 17. DHSPI-SIRT system: a) in-situ operation, image credits: Anna and Sergey Sirro; b) scheme of optical geometry of DHSPI system. M: Mirrors, OB: Object Beam, RB: Reference Beam, L: Lenses, RBS: Reference Beam Shutter, OBS: Object Beam Shutter, VA: Variable attenuator, BS: Beam Splitter, OW: Optical Window, PZT: Piezo transducer, CVX: Convex, SL: Surface Lens, CBS: Combine Beam Splitter, CL: Combined Lens, image credits: Vivi Tornari.

4. IN-SITU NON-INVASIVE MEASUREMENTS OF WALL PAINTINGS

The selected case studies are part of interdisciplinary research projects held by the scientific staff of the Department of Cultural Heritage and Geosciences department of the University of Padova, in collaboration with international research groups from the National Technical University of Athens and other international research groups of IPERION-MOLAB. The examined wall paintings are representative in terms of high historical and archaeological value and main conservation challenges to be faced by Cultural Heritage experts in these or similar cases.

Table 8. List of case studies and main conservation challenges

Case study	Period	Main conservation challenges
Frigidarium, Sarno Baths (archaeological site of Pompeii) - Italy	Roman wall paintings	Very advanced state of degradation, salt growth and fast loss of pictorial layer, high archaeological value, reconstruction of original painting layout and identification of pigments, contribution to the need urgent conservation treatments
Scrovegni Chapel (Padova) - - Italy	Proto-Renaissance and later additions/restorations	Many undocumented restorations of the pictorial layer and building structure, high value, artist technique and attribution issue of some parts of wall paintings
Sala del Capitolo, Basilica Saint Anthony (Padova) - Italy	Proto-renaissance, later additions/restorations 18th century	Lack of historical documentation, study of the artist technique and attribution the hand of Giotto, detection of hidden underlying fresco layer, degraded areas, loss of pictorial layer, restoration interventions,
Catholikon, Dafni Monastery (Athens) -- Greece	16th century	Loss of details and pictorial layer, lack of documentation, no recognition and interpretation of depicted figures

4.1 Frigidarium of Sarno Baths (archaeological site of Pompeii, Italy)

4.1.1. Case study description

Terme del Sarno (Sarno Baths) complex is situated on the Southern slopes of ancient Pompeii, one of the most important and most studied archaeological sites of the Roman period. Its exact location is at the junction of the Via delle Scuole and the Via della Regina (Regio VIII, insula II, civ.17-21) [173]. The baths were installed by extending an existing residential block of houses during the early Dynasty of Claudius, occupying approximately one third of the *insula* itself [174]. In 62 A.D., 17 years before the catastrophic eruption, a powerful earthquake struck the area, and the Sarno Baths, like many other buildings in that area, were still under restoration when Vesuvius erupted [173].

The Sarno Baths complex (Fig. 18) remained buried until the end of the 19th century. The excavations began in 1888 and, after some interruptions, concluded between 1894 and 1900. The volcanic materials around the exterior walls were completely dismissed in the 1950s. Following exposure, interventions were employed in order to stabilize the building and conserving the wall paintings decorations within the complex, using cement for stabilizing and rebuilding the walls of the Terme, and some frescoes were re-attached. Nowadays, the wall paintings in the Frigidarium are progressively affected by re-deposition of sulphates on the surface, which are growing fast and the loss of pigments from the pictorial layer is irreversible (Fig. 19).

At the end of 19th century, the brothers Fausto and Felice Niccolini produced drawings of some of the wall paintings of Sarno Baths, among many other buildings, statues, views and ground plans of the excavated Pompeii [175]. In the Frigidarium, Niccolini brothers documented only the North Wall painting. Some details are reported precisely, but there are some simplifications, for example, the absence of human figures in the frame under the *lunetta*, which have been preserved until now [175]. (Fig. 20).

The crucial art historical and conservation questions of this case study are strongly connected to the advanced degraded state of the wall paintings. In particular, the non-invasive acquisitions performed in-situ, were aimed at materials characterization and correct planning of urgent interventions.

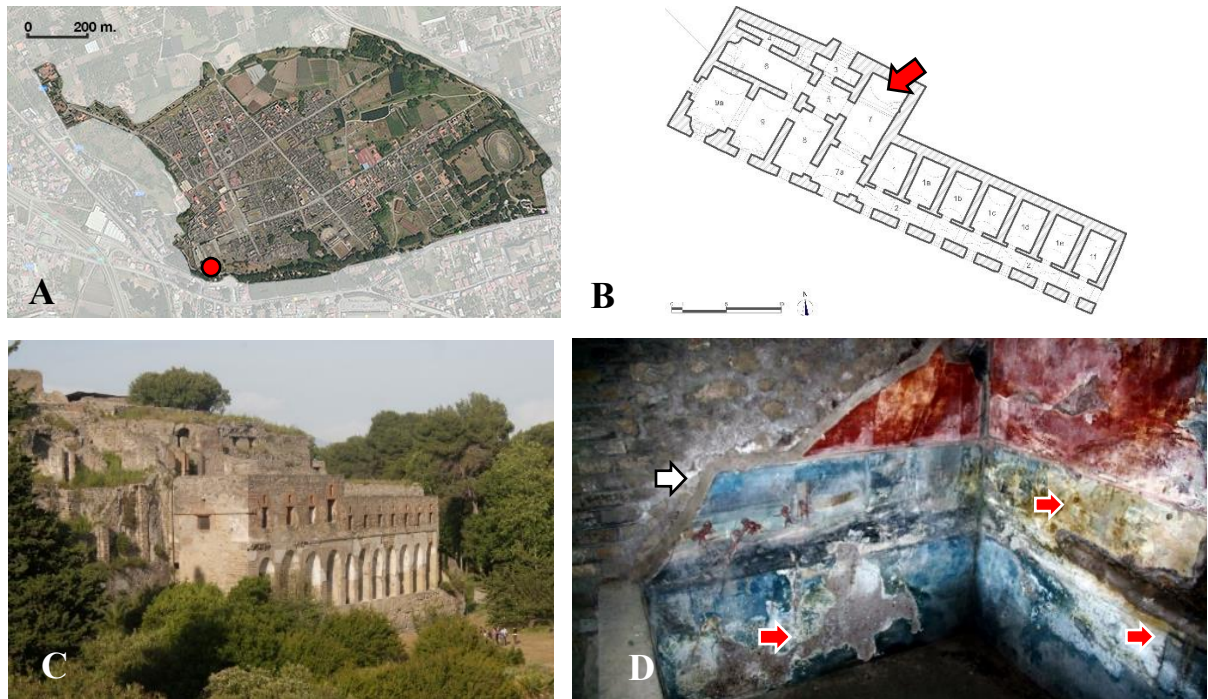


Figure 18. Sarno Baths: a) plan of the excavated Roman city of Pompeii and the location of the Sarno Baths indicated by a red spot (regio: 8, insula: 2, civico: 14,16-20), image source: google maps; b) 3rd level floor plan containing the Frigidarium, indicated by a red arrow. Image credits: L. Bernardi e F. Panarotto; c) external view of the Sarno Baths complex; d) interior view of the Frigidarium. Image credits: Yotam Asscher. A white arrow marks the location of cement used for re-attaching the frescoes and wall reinforcements, and red arrows mark the salts depositions.

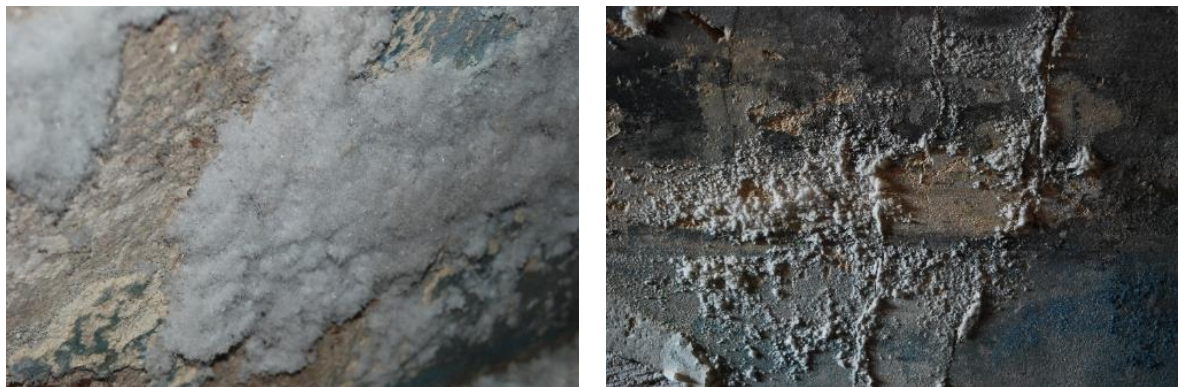


Figure 19. Details of salts growth on the Western wall painting. Image credits: Yotam Ascher.

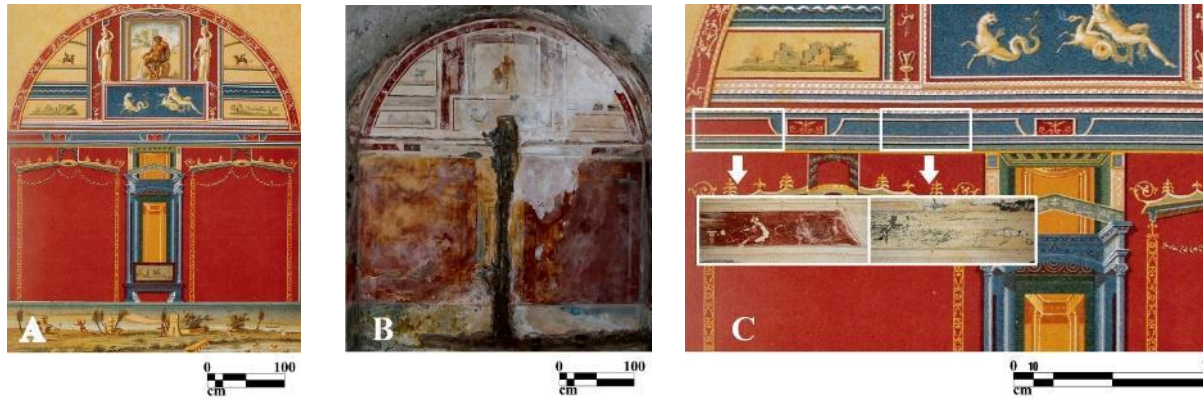


Figure 20. Northern wall painting in the Frigidarium of Sarno Baths: a) documentation by the brothers Fausto and Felice Niccolini [175]; b) current state of conservation; c) comparison between the drawing and current state, showing mismatching details.

Multispectral Imaging method was evaluated as a preliminary qualitative tool for differentiation between different pigments, detection and mapping of specific Roman pigment Egyptian blue. The multispectral imaging results were compared and validated by XRF and FORS in-situ tests, performed in collaboration with the Geosciences Department of the University of Padova and GeoMEB S.r.l.s. Several in-situ subsurface diagnostic tests were performed by the means of Passive Infrared Thermography. They did not produce a contribution to the study, hence the results are not presented in this thesis.

In particular, the main research questions of this case study are the following:

- Can Multispectral Imaging be used to enhance lost details in a very degraded wall painting?
- Can Multispectral Imaging be used to differentiate between Egyptian blue and other blue pigments?
- Can Multispectral Imaging be used to identify different mineral pigments of the Roman palette?
- Can Passive Infrared Thermography provide information on the subsurface structure of the wall paintings in partially underground archaeological in-situ conditions?
- What are the main limitations of these techniques applied in-situ in this case study?

4.1.2 Acquisition and analysis of multispectral images

In this case study, the experiments were focused on the analysis of the preserved Western (primarily) and Eastern wall paintings. The Western and Eastern wall paintings of the Frigidarium have approximate dimensions of 3 m width (2.5 m width inside the bath tub) and

5 m height. The analyzed area with the depiction of pigmies, very degraded, is located in the inferior part of the Western wall over the tub with cold water (the analysed area 1.5 m width and 1 m height). The acquisitions of the Eastern wall painting were focused on the central framed wall painting fragment, very degraded, probably depicting Nereide with a dolphin (the analysed area 1.5 m width and 1 m height, the depicted fragment approximately 40x40 cm) (Fig. 21).

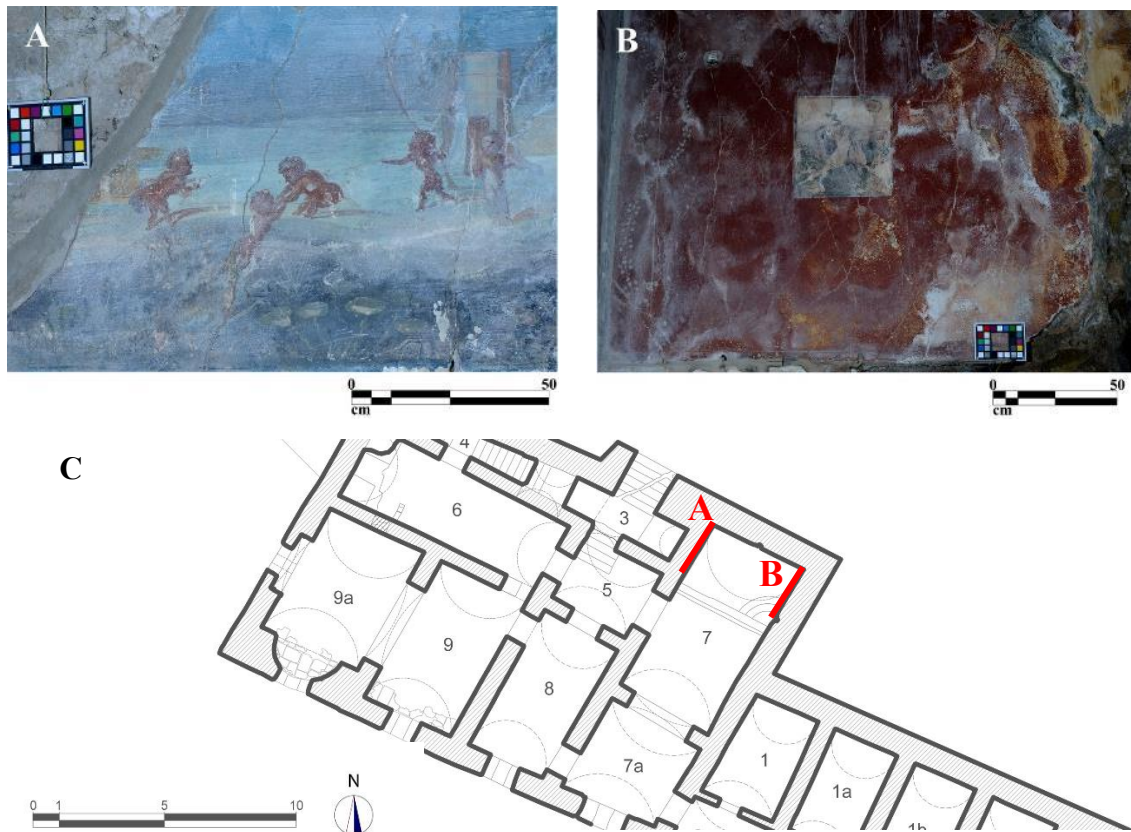


Figure 21. Non-elaborated visible images of the Western (a) and Eastern (b) wall paintings, their location in the Frigidarium of the Sarno Baths complex (image credits: L. Bernardi e F. Panarotto)

The instrument Nikon D800 FR (Full range) camera with a 36-megapixel sensor was used. The camera has been modified, removing the internal UV and IR filters, to collect different images in the UV-VIS-IR range using specific external band-pass filters. A couple of modified Nikon speedlight flashes (Nikon SB 910) including excitations in the UV and NIR ranges was also used. During the acquisition, these flashes are in general positioned at 45° with respect to the measured surface, whereas the camera is placed between the flash lights and pointed orthogonally to the surface. The camera was placed at approximately 1,5 m height from the

ground and the horizontal distance of the camera from the wall painting was approximately 2 m for the Western wall painting and 2 m for the Eastern wall painting.

The multispectral images were then calibrated using a colorchecker provided with the camera (Profilocore Color Checker) and Macbeth Color Checker and placed close to the wall paintings during the acquisition. Five external band-pass filters were used in this case to take the pictures in the UV-Vis-NIR ranges: one for the UV range (350-420 nm), one for the visible range (about 400-700 nm) and three different filters for the near infrared range (IR1= 720 nm, IR2= 850 nm, IR3= 950 nm). Before analysing in alternative software tools, the collected photos were converted from raw images to 16-bit Tagged Image File Format (TIFF) with minimal processing (without white balance and brightness corrections or stretching or pixel rotations) using the NX Viewer free software.

In the given case study, no retouchings and no restorations are expected to be found in the pictorial layer of the wall paintings inside the Frigidarium. It was confirmed by the reflected ultraviolet photography (UVR) which did not provide information about the presence of organic materials on the surface of the wall painting. It was impossible to darken completely the environment, therefore, acquisitions of images in UV fluorescence could not be performed.

The experimental procedure of image analysis was performed in two steps: qualitative (visual enhancement and preliminary characterization) and quantitative analysis (statistical analysis of spectral similarity and intensity of reflection). Different editing software programs (open source: NIP2, Image Enhancer; ImageJ, commercial: Photoshop) were evaluated for calibration, enhancement and preliminary examination of acquired images.

The whole set of Image Enhancer filters [166] for separate spectral images and the subtraction, difference, addition functions of ImageJ [169] between two spectral images (VIS and IR), were tested in this case study. Adobe Photoshop was used for transformations in separate spectral images (contrast, brightness, saturation corrections, changes in RGB channels) and for a combination of different spectral images (VIS and IR), using the blending function of layers [168]. The analysis and enhancement of details in the UV spectral image did not help obtain more information about the characteristics of the studied wall paintings with a limited palette of inorganic pigments, therefore, it is not presented here.

Acquisition and image analysis procedure tested for revealing underdrawings and lost details

Reflected infrared photography (IRR), proved in this case study, its well known usefulness to reveal underdrawings beneath the pictorial layer, due to the contrast between the infrared light

reflected by the ground and the light absorbed by the underdrawings. The near-infrared band IR2 (more than IR1 and IR3) in reflected light photography has shown to be the most informative for revealing underdrawings and details, which became invisible for the naked eye due to degradation.

In order to facilitate and improve simple comparison of visible and infrared images, several methods were tested to enhance the contrast, allowing locating better the finer details in the paintings. Combinations between different wavelengths were tested. They are performed by the means of software tools that allow multiplications and additions of RGB values, that encapsulate the luminosity, hue and saturation between different images, pixel-by-pixel. By comparison of all the possible combinations (image processing functions in ImageJ and blending of layers in Photoshop), an easy and efficient solution for combining in one image the information from both visible and infrared bands was found in blending of layers using luminosity mode (see attachment F).

Figure 20 shows the results of enhancing the contrast, using the blending function in Photoshop, which applies the luminosity values from the infrared image with the IR2 filter to increase the contrast values in the RGB of the visible image (luminosity mode). This enhancement relies on the fact that pigments may show different absorption values in the infrared region (depending on both depth and reflectivity), and therefore show different luminosity. Using these features, it was possible to locate more accurately the shapes and the details of the palm trees in the underdrawing. Probably, the higher contrast in these features is due to the preparatory drawing absorption and the reflectivity of the background (Fig. 20b). Some further ways to increase the contrast in the combined spectral images were experimented, by changing the saturation and contrast values in the raw images in Image Enhancer or Photoshop before combining them one with another. It should be noted that by increasing the contrast in the IR2 image and inverting the tone curves values in the visible image (by the means of Adobe Photoshop or in Image Enhancer), details in the darker areas in the fresco, that include the black and blue areas that represent the Nile River in the painting, are enhanced. Inverting the tone curves in the visible image prior to its combination with the infrared, the darker areas were converted to lighter tones, so that the underlying traces of more absorbing pigment became even better highlighted over the background (Fig. 20d). This is how the traces of an animal figure (appearing dark in the infrared) on the bottom of the wall painting (dark area which became bright) started to be identified. It is thought to represent an alligator or some other animal (a dog?) in the Nile River. For locating better underdrawings it is, therefore,

recommended to use luminosity blending mode on brighter areas of a wall painting and to use luminosity blending mode with the inversion of the tone values on dark areas of a wall painting.

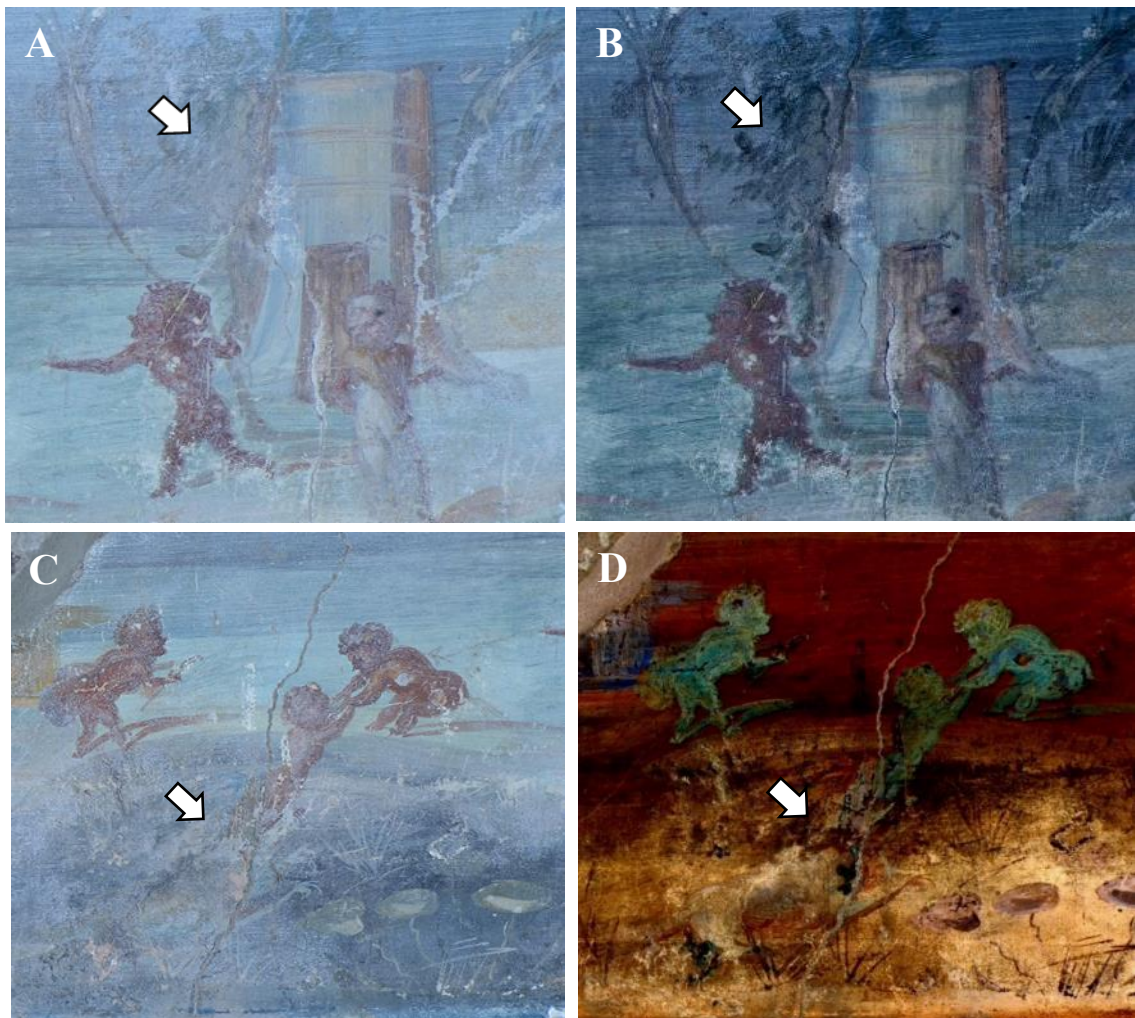


Figure 22. The appearance of new details in the elaborated images by Image Enhancer and Adobe Photoshop: a) non-elaborated visible image of the upper right part of the wall painting; b) IR2-VIS blended image (luminosity mode) of the upper part of the wall painting. The arrows show the enhancement of vegetation details; c) non-elaborated VIS image of the bottom part of the wall painting; d) IR2 (enhanced contrast) -VIS (inverted curves) blended image (luminosity mode) of the bottom part of the wall painting. The arrows indicate the areas where new details appear in elaborated images.

Image analysis for differentiation between similar pigments

Simple image processing filters of Image Enhancer did not provide more information about the differences between similar pigments. The false-colour IR (IRRFC) mode in non-calibrated images by the means of Adobe Photoshop (RGB channels) and in calibrated iamges by the means of NIP2 provided useful information for differentiation between similar pigments. The

false colour images combine the properties associated with reflectivity, absorption and colour of pigments at different wavelengths (visible and infrared range), due to their composition. Figure 23 shows different blue areas in the Western wall painting as IRRFC images, acquired through NIP2 image processing software [152](see attachment H). The IRRFC image emphasises different hues of blue, presumably differentiated according to the pigments concentration, depth and presence of other pigments (Fig. 23b). It can be clearly seen that there are two similar dark blue areas on the Western wall painting (indicated by white and red arrows) that are obtained by application of different pigments, which vary in their chemical composition and therefore show different hue in the generated IRRFC image (Fig. 23b).

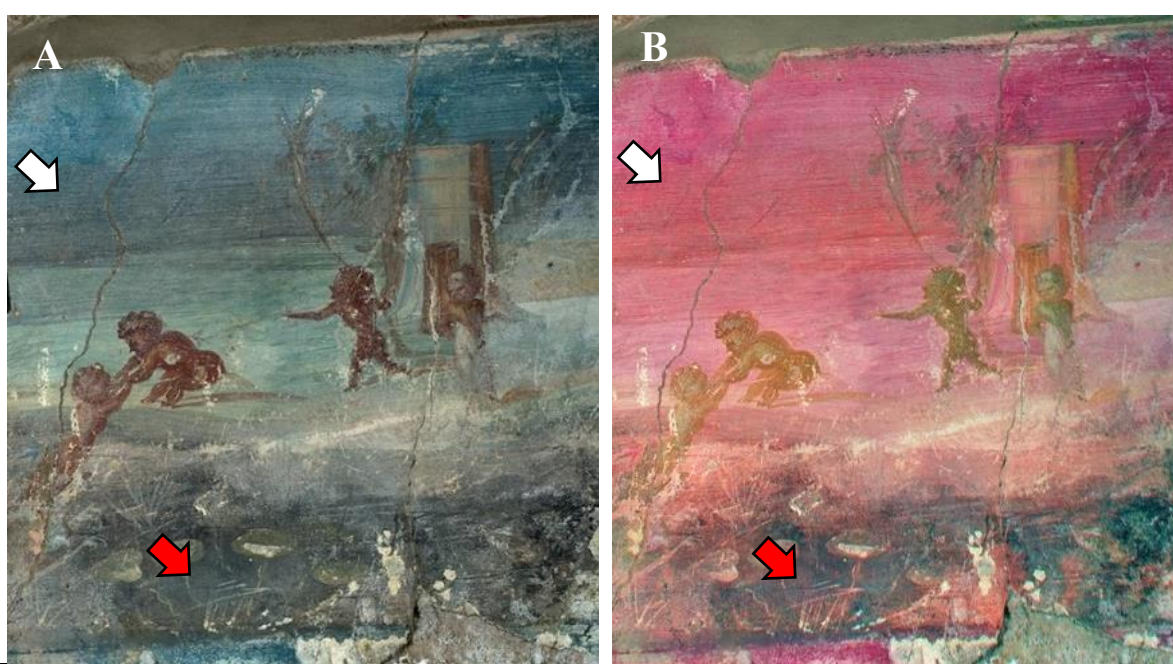


Figure 23. Differentiation between similar pigments (or their concentration) by the generation of a false-colour IR image. Application to the Western wall painting. A) Calibrated visible image of the Western wall painting; B) generated IRRFC image of the Western wall painting. The arrows show the areas of interest.

Image acquisition and analysis for the identification of Egyptian Blue and revealing underdrawings

The Egyptian blue, one of the first synthetic pigments having the chemical formula $\text{CaCuSi}_4\text{O}_{10}$ and commonly used in Roman times, was found in the frigidarium abundantly [174]. The Egyptian Blue shows the strongest visible induced near- infrared fluorescence at around 910 nm [176]. Therefore, the bandpass filter IR2 (with the central wavelength at 850 nm) was selected for the experimentation. Photo-induced luminescence imaging, after series of laboratory tests (see Chapter 6), was used to perform in-situ analysis of multi-spectral images

by different software programs, in order to detect, quantify and estimate different concentrations of the same pigment. Taking into consideration the results of laboratory tests (described in Chapter 6), two T8 fluorescent tubes, colour temperature of 4000 K, model F38T8 of CH lighting, based on a portable power source and a power inverter, were used as visible light illumination source. Two images of the Eastern wall painting were collected from the same acquisition area, at the distance of 2 m, using the same band filter (IR2). The first image was acquired under natural light conditions (Fig. 24a), the other when illuminated from both sides by two lamps that emit light only in the visible range (Fig. 24b).

The ImageJ software was evaluated for the qualitative analysis of photo-induced luminescence images. Both images, acquired under natural light conditions and when illuminated from both sides by two fluorescent tubes, were converted to grey scale by the means of Image Enhancer. Each pixel in these images is marked by a luminescence property that shows the reflectance from stray light and the fluorescence of the Egyptian blue, as recorded through the infrared band filter. Then, using ImageJ, the image, acquired under natural low light conditions (Fig. 24a), was subtracted from the image, acquired when illuminated from both sides by two lamps (Fig. 24b), in order to enhance the traces of fluorescent pigment on the wall painting (Fig. 24b). In this way, the traces of Egyptian blue are stronger highlighted on the dark background of the fresco, which is believed to be a representation of Nereid, preceded by a sea horse and, probably, by a dolphin [174] (Fig. 24b).

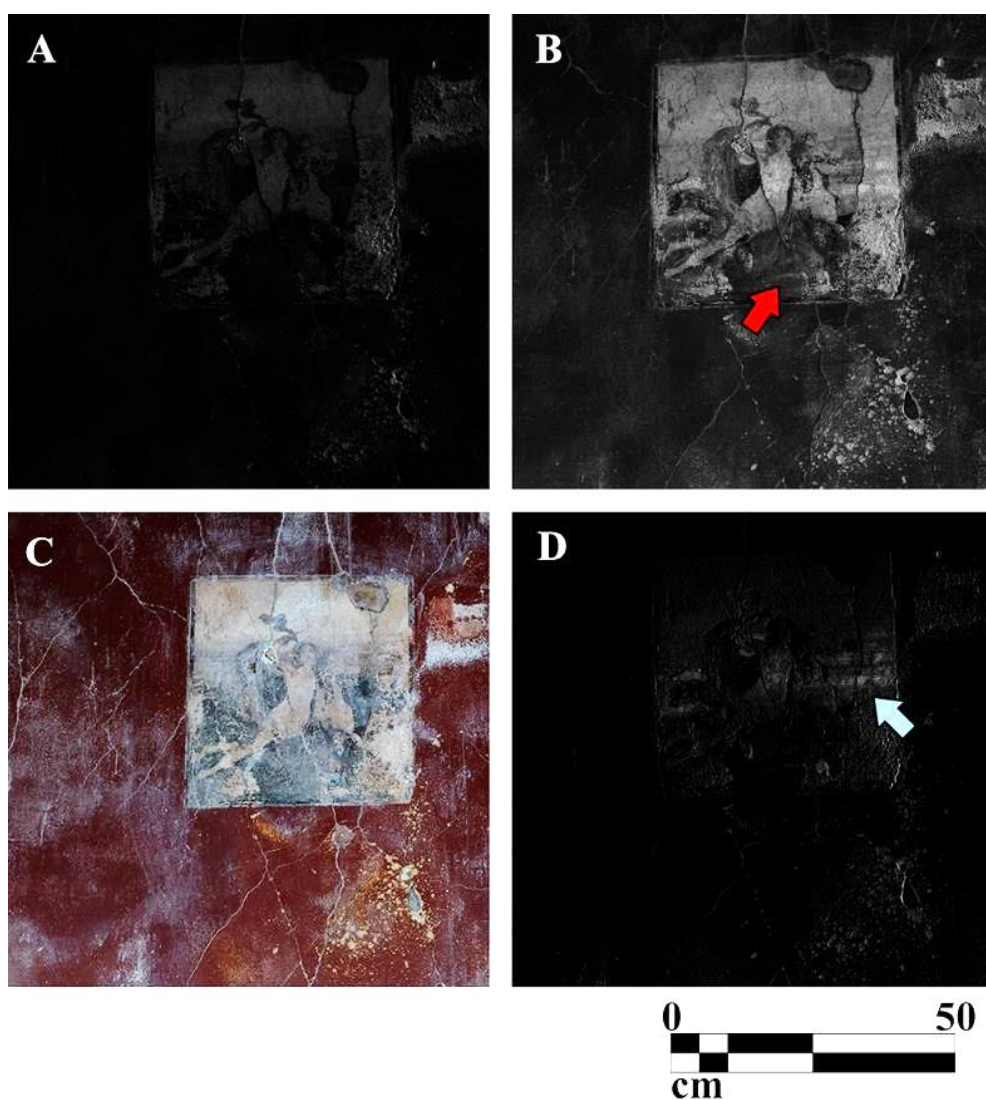


Figure 24. Analysis of visible-induced IR luminescence, applied to the Eastern wall painting: a) IR2 image, acquired under natural low light conditions; b) IR2 image, acquired when the wall painting is illuminated by two fluorescent lamps. The red arrow indicates the presence of an underpaint; c) Non-elaborated visible image; d) subtracted IR2 image. The blue arrow indicates the traces of Egyptian Blue.

Identification and semi-quantitative analysis of Egyptian blue

The quantitative analysis of the relative concentration of Egyptian blue was performed using the Profilocolore (license property of the Department of Cultural Heritage). These results were compared to the results of quantitative analysis by the means of ENVI software (in collaboration with Dr. Yotam Asscher, Geoscience Department, University of Padova).

Profilocolore software uses a statistical tool (PCA) [19, 53] to verify spectral similarities, by comparing the intensities of different bands (UV, VIS, IR1-3) in different locations, to the intensities in a reference point set by the user. ENVI software allows to semi-quantify the

intensity of the fluorescence emission of Egyptian blue. Both methods of multispectral analyses showed a reduction in spectral similarities (Profilocolore) and fluorescence (ENVI) from the upper to the lower part of the fresco.

In the given experiment, the selected reference point of a blue pigment is shown by a red arrow in Fig. 25a. The measured areas are $T1 = 1.6941 \text{ cm}^2$, $T2 = 1.6720 \text{ cm}^2$, $T3 = 2.9232 \text{ cm}^2$, $T4 = 4.1664 \text{ cm}^2$, $T5 = 3.3492 \text{ cm}^2$, as shown in the Fig. 25c.

By the means of Profilocolore software, the spectral similarities showed a clear decrease of intensities towards the lower part of the wall painting, between 0.9-1, as the amount of blue pigment is reduced (Fig. 25b), suggesting a reduction of the concentration of Egyptian blue.

By the means of ENVI image processing software, the emission of the stray infrared light, when the wall painting was in the dark, was subtracted from the emission that occurs when using visible fluorescent light, to obtain an image that represents the emission of Egyptian blue due to fluorescence (Fig. 25c), following the protocols for photo-induced luminescence imaging [176]. The intensity of the fluorescence was semi-quantified in an image processing software (ENVI), in which the values of reflected light in different locations were measured. In figure 23d, the x-axis shows the intensity of fluorescence, associated to Egyptian blue, and the y-axis shows the frequency of counts per area that show this intensity. It can be clearly seen the areas in the upper part of the wall painting show higher concentrations of Egyptian blue.

By the means of Profilocolore software, a high inhomogeneity of spectral similarities in the areas of interest was observed, presumably due to the degradation processes of the pictorial layer. Also by the means of ENVI software, it was noted that there is a large variability in the fluorescence values, as quantified by the histogram in ENVI.

These results were confirmed in-situ by XRF spectroscopy [55]. The portable XRF spectrometer was employed, in collaboration with GeoMEB S.r.l. in the same locations to measure the content of copper. A neat gradient was observed, showing higher concentrations of copper in the upper parts of the fresco, and as the locations of sampling went to lower areas, the concentrations decreased significantly. Moreover, traces of iron are present, as well as potassium and sulfur. Potassium and sulfur can be associated with the deposition of salts and other degradation products. These degradation products could be the reason for the fragmentary image that shows a large variability in the fluorescence intensity (Fig. 25c) and spectral similarities (Fig. 25b).

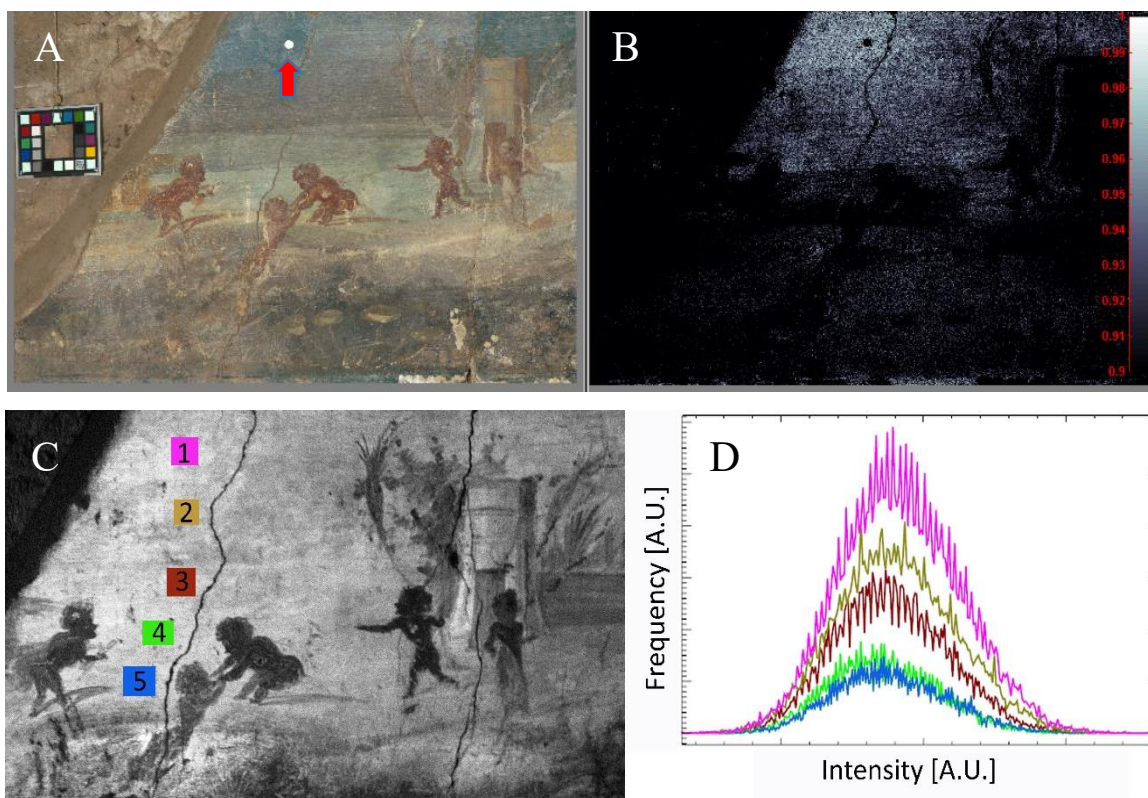


Figure 25. Quantitative analysis of the relative concentration of Egyptian blue. Image credits: Yotam Asscher. A) A visible image of the Western wall painting in Profilocore, showing the color checker used for calibration, and the blue point used as a reference to quantify the spectral similarities (marked with a red arrow). B) Different locations having spectral similarities in Profilocore, showing a gradient between the upper part (with spectral similarities of 1) to the lower part (spectral similarity of 0.9). C) Greyscale intensity image of the western wall painting in ENVI, representing the intensity of fluorescence after illuminating the fresco with a visible light, and recording the image with an IR filter. Each pixel greyscale value is a result of the fluorescence value, after removing stray light when the fresco is not illuminated. The locations of analyses are numbered and color-coded. D) The frequency of pixels (counts per area), showing the fluorescence intensity range associated to Egyptian blue, in different locations marked in Fig. C, the graphs following the same color-codes. It is higher in the upper part of the wall painting. The frequency is normalized to the size of the area that was analyzed (more than 1 cm² in each location).

4.1.3. Discussion of the results

The obtained in-situ experimental results showed that multispectral analysis can map the distribution of pigments and, when coupled to specific softwares, can semi-quantitatively characterize them, as well as their uniformity along the wall paintings.

The proposed workflow for in-situ acquisition and analysis of multispectral images includes predominantly free or commonly available software programs (Image Enhancer, NIP2, ImageJ, Adobe Photoshop or its alternative GIMP). The qualitative analysis of multispectral images can be easily understood and applied by art historians and conservators to enhance lost details, to

map specific pigments (in limited palettes) and to differentiate between them. Moreover, combinations of different bands, such as visible and infrared, can be useful to enhance distinct iconographic features that help reconstruct the original wall paintings. It is particularly important for very degraded wall paintings, for which historical documentation is missing and conservation interventions must be planned.

As concluded from the image processing tests on the spectral images acquired in this case study, the combination of information from visible and infrared spectral bands by the means of commonly available Adobe Photoshop software program can be helpful to locate and enhance finer details of the underdrawings and degraded iconographic features. For this purpose, therefore, it is recommended to use luminosity blending mode on brighter areas of a wall painting and to use luminosity blending mode with the inversion of the tone values on dark areas of a wall painting (see attachment E). The false-colour IR (IRRFC) mode by the means of NIP2, Adobe Photoshop or dedicated Profilocolore software is recommended for differentiation between visibly similar pigments (see attachment G).

The semi-quantitative analysis of concentrations of pigments, even if limited to specific types of minerals with unique spectral properties, when using modified camera Profilocolore Nikon D800, it can be performed by the means of Profilocolore dedicated software or by the means of ENVI image processing software (see attachments D and E). The outcome of this experimentation is that relative concentrations of Egyptian blue, as measured and confirmed by a portable XRF on the wall paintings of Sarno Baths, could be mapped also using multispectral analysis, and could bring forward new information on the materials used by the artists, the combinations/concentrations used to achieve specific hues and colors, and in the framework of these studies to understand past technology of the wall painting execution technique. The multispectral data for semi-quantifying concentrations of Egyptian blue should be used in case studies where the pigments' mineralogical composition is known and distribution maps of the pigments could be produced.

It should be emphasized that, from one side, the study of underdrawings and revealing lost details could be performed equally in the absence of a color reference chart, i.e. without calibration or statistical analysis, while semi-quantitative approach requires calibration of lighting conditions in multispectral images.

The recommended image acquisition and analysis workflow and the selected image processing procedure can be found in attachments D and E respectively. The detailed description of each of the image processing functions, tested in this project, is reported in the attachment G.

The in-situ investigations by Passive Infrared Thermography did not produce useful results, due to the absence of sufficient temperature contrasts in the semi-buried archaeological structure.

The brief answers to the research questions of this case study are summarized in Table 9.

Table 9. Results of the acquisitions in the Sarno Baths, Pompeii

Research question	Results and observations
Can Multispectral Imaging be used in this case study to enhance lost details in a very degraded wall painting?	Yes, even in absence of a color reference chart, by simple comparison of spectral images (reflected mode VIS, IR), improved and facilitated by the means of free or commonly available software tools
Can Multispectral Imaging be used in this case study to differentiate between Egyptian blue and other blue pigments?	Yes/no. Adequate visible light sources are needed to induce infrared fluorescence of the Egyptian blue.
Can Multispectral Imaging be used in this case study to identify different mineral pigments of the Roman palette?	Yes/no. It is possible only if coupled to appropriate software tools (dedicated Profilocore or ENVI)
Can Passive Infrared Thermography provide information on the subsurface structure of the wall paintings of this case study in partially underground archaeological in-situ conditions?	Yes/no. It is possible only in the presence of an adequate thermal gradient. The optimal difference is around 10-15 °C. In this specific study case and during acquisitions in February 2017, it was not possible.
What are the main limitations of these techniques applied in-situ in this case study?	For MI: Absence of sufficient natural light, impossibility to darken completely the environment for acquisitions in fluorescence mode, limited accessibility to the archaeological site and to the wall decorations, logistical problems (distance, limitations in space and geometry of positioning the camera and the flashlights, absence of scaffoldings);

	For IR: Absence of sufficient natural thermal gradient in the month of February 2017
--	---

4.2 Scrovegni Chapel (Padua, Italy)

4.2.1 Case study description

The *Cappella degli Scrovegni* (Scrovegni Chapel) is considered a masterpiece in the history of painting in Italy and Europe, as the vaulted roof and walls are completely painted with outstanding unique frescoes, framing episodes in the lives of the Virgin Mary and Christ. This fresco cycle was executed by Giotto da Boldone, completed around 1305 [177].

The history of the site of Scrovegni Chapel starts between 60 and 70 D.C. when the Roman amphitheater was built. Its archaeological remains are now commonly referred to as the *Arena* (Fig. 26). Until the 5th century A.D., the amphitheater should have still maintained its function as the venue for performances. It was followed by a period of abandonment of the site, related to the general decline of the city, earthquakes of the years 1117 and 1222 and some fires, with the particularly strong one of 1174 [178]. In 1300, it became the property of the Scrovegni family [177]. The dedication of the Chapel to the Virgin of Charity is mentioned by historical sources from 1304 in which Pope Benedict XI granted indulgences to those who visited "Santa Maria del Carità de Arena" [177].

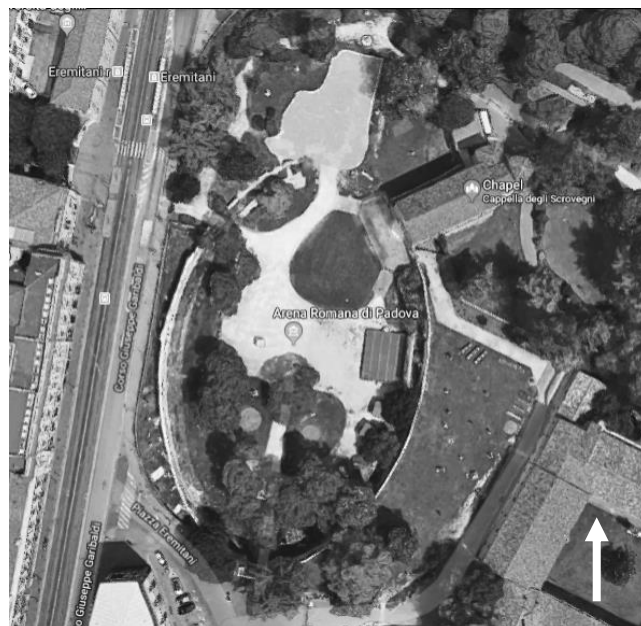
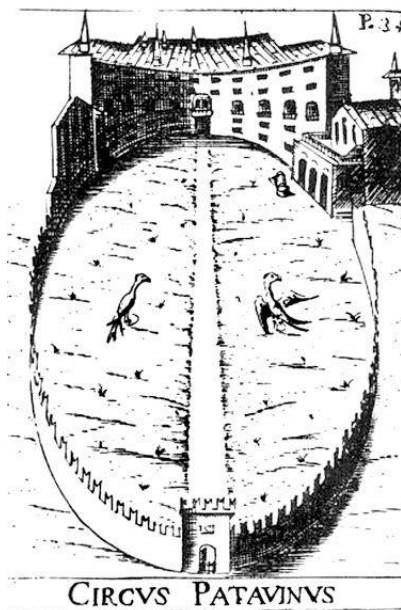


Fig. 26. The Roman Amphitheater and Scrovegni Chapel. a) 17th century view on the Arena, Foscari Palace and adjacent Scrovegni Chapel, engraving 1669 [179]; b) modern aerial view on the Arena and Scrovegni Chapel, google map 2018.

The forty scenes of the wall paintings represent the Old and New Testaments, culminating in Christ's crucifixion and resurrection, and the Last Judgement. They follow three main themes: episodes in the lives of Joachim and Anna; episodes in the Virgin Mary's life; episodes recounting Christ's life and death. The lower parts of the walls contain a series of frescoes illustrating Vices and Virtues in allegory.

After the death of Enrico Scrovegni, the history of the Chapel is characterized by a continuous chain of property changes: Capodilista and Trevisan families, brothers Alvise e Giovanni Foscari, Gradenigo family. The small portal in front of the Chapel (see Fig. 27) collapsed and in 1827 the building of the adjacent Foscari Palace was demolished. The necessary precautions were not taken to protect the walls that were adjacent to it. The intervention resulted in leaving the north wall exposed to the elements and humidity, with consequent deterioration of the fresco wall paintings.



Figure 27. South-western façade of the Scrovegni Chapel. a) fragment of a historical engraving (1842) showing the facade with the portal in front of it [180]; b) current state of the façade [181]

In 1828, the presence of alarming cracks was documented by Arch. P. Selvatico, which were probably caused by the demolition of the palace [182]. From 1829 to 1835 two masonry chains in the sacristy walls were inserted, along with the restoration of the roof. However, after the demolition of Foscari-Gradenigo Palace, in 1837 a new and more modest residence was built,

connected to the chapel through a part of a wall that is still partly visible today. This building was also demolished in 1906.

In 1867 the Municipality of Padova (il Comune) started preliminary studies aimed at restoration planning. They were based on the guidelines approved in 1857: removal of the causes of humidity, restoration of the roof and the walls, re-plastering the walls outside, removing the gutters in the northern and eastern walls.

The restoration works started in February 1868 led by Guglielmo Botti, a Tuscan restorer, who prepared a detailed report to the Commission examining the state of conservation of the frescoes and the possible interventions that could be carried out on them. In the following years, Botti was commissioned for an urgent conservative intervention on the fresco depicting Last Judgment; in 1870 [183], the frescoes of the arch were removed and reattached after its consolidation. In 1870, the presence of a large masonry iron chain above the vault of the presbytery was discovered, at the height of 1.50 m above the arcade of aisle" More, in 1871 an alarming crack in the same area was reported, together with other minor injuries, stains, breakdowns and nail holes [184].

In 1880 The Municipality acquired the property from the Gradenigo family. Archaeological excavations and cognitive investigations started to guarantee the conservation of the whole complex. The restorations were led by Eugenio Maestri and Antonio Bertolli. In 1884 the restoration of the gap in the wall above the arch between the nave and presbytery and the apse was performed, by inserting an iron chain inside the masonry above the arch and repairing the thrust of the aisle closest to the arcade [177]. Subsequently, in 1885 the external plasters were removed. 1890 was a year of continuous heavy rains that caused extraordinary flooding and, despite the excavation and works that had been carried out in previous years, the crypt found itself constantly flooded.

In 1892 the restorer Antonio Bertolli carried out the detachment of the most deteriorated damp areas on the north wall of the nave of the church. They were reattached on copper frames, with an interspace between the wall and the support in order to avoid contact between the damp wall and the fresco decoration layer [182].

After the first World War, the vault of the crypt was consolidated at the point of contact with the southern wall by inserting three chains covered by transversal wooden chaining beams positioned. During the second World War, eight walls were placed transversely to the longitudinal walls, in order to strengthen the structure and to support the military aerial protection works.

Following the diagnostic campaigns carried out in 1953 and 1956 that observed the opening of old fissures and appearance of new ones, in the apse, in sacristy and loggia, three new chains were added on the external walls of the Scrovegni Chapel in 1957 [182].

In 1957 Leonetto Tintori proceeded with the urgent restoration of the fresco of the Last Judgement to improve the adhesion to the support, using three different types of synthetic resins, never used before in the restoration field. In 1961-63, he was in charge of interventions on the whole cycle of Giotto's frescoes. But already 8 years later, some visible damage to the frescoes was observed, due to the pollution that accelerated the deterioration [184-185].

Recent long planning scientific research was aimed at the definition of the future restoration of the frescoes, directed by the Istituto Centrale per il Restauro from Rome (Italy). The project is divided into two phases: the first, from 1989 to 1994, and the second, from 1994 to 2001. In the 90s, the study was dedicated to the execution techniques, the previous interventions and the conservative status of all the frescoes; all the information was documented in detail. In 1994, the first pilot project on the removal of the salts present on the surfaces was launched. The restoration on the entire Giotto cycle began in July 2001 and is expected to end on March 18, 2028.

According to G. Basile [85, 182-183, 185], two similar preparatory layers of plaster, consisting of lime and fine-grained sand, were applied on brick walls in the nave. Their total thickness was of maximum 2-2.5 cm, divided into 1-2 cm for the arriccio and 0.5 cm for the "intonachino" (finishing coat). However, the thickness is not homogeneous. The preparatory layers were sometimes very thin. The nave consists of about 850 "giornate" (days work). The lacunar in the preparatory layers on the left wall of the presbytery, in the scene "Announcement of the Death", made it possible to observe the sinopia. In the lunette above the door to sacristy (wall painting, presented in this project), the traces of cord snapping were observed. In some areas, direct incisions were used [85, 182].

Generally, the fresco technique was employed. However, there are many areas with a "secco" finishing: the sky of the ceiling, blue backgrounds of the narrative paintings and behind the Saints. The reason for the employment of the secco technique is the extended use of azurite, which is not alkaline-resistant. In all the halos and in several details of the scenes, gilded tin leaf fixed with mordant was used.

There are many unsolved art historical and conservation issues related to the origins of the building of the Chapel, the undocumented restorations, artist's technique, attribution and conservation challenges.

The main research questions analyzed in this specific case study are related to:

- study of Giotto's technique, use of pigments, revealing the underdrawings and painting details, lost with time;
- differentiation between original and non-original parts of the wall painting, mapping of the restoration interventions;
- preservation state of the wall decoration, its subsurface and structural support; structural stability;
- scientific proof and support to the historical studies.

Multispectral Imaging was evaluated as an immediate in-situ method for the study of a pictorial layer: revealing underdrawings and study of artist's technique, differentiation between pigments and, if possible, between original and restored/retouched areas.

The potentialities of Infrared Thermography applied in passive mode were evaluated as an in-situ subsurface diagnostic method for the recognition of discontinuities within the shallow subsurface and structural support of a wall painting.

Some first in-situ subsurface diagnostic tests by the means of Holographic Subsurface Radar were performed. Due to in-situ accessibility limitations and high value Cultural Heritage protection regulations, the first tests could be performed only on lateral areas of the wall painting, not of particular interest for the given study. Hence, the HSR results are not presented in this thesis.

In particular, the main research questions of this case study are the following:

- Can Multispectral Imaging be used to reveal more details about the artist's technique and underdrawings?
- Can Multispectral Imaging be used to differentiate between original and retouched areas?
- Can Multispectral Imaging be used to identify and to differentiate between pigments?
- Can Passive Infrared Thermography be applied to reveal subsurface and structural discontinuities underneath the decoration layer? If yes, what are the necessary conditions?
- What are the main limitations of these techniques applied in-situ in this case study?

4.2.2 a) Acquisition and analysis of multispectral images

A wide range of acquisitions was performed, in order to address the research questions by art historians and conservators (Department of Cultural Heritage – University of Padova, Institute

Superior of Conservation and Restoration – Rome). In particular, the acquisitions were performed on:

- crypt wall and vault paintings (eastern wall);
- lunette wall painting above the sacristy entrance door (northern wall of the presbytery, presented here and shown in Fig. 28);
- Giotto's iconographic scenes (northern and southern wall);

- Vices wall paintings (northern wall): *Stultitia, Inconstantia, Ira, Iniustitia, Infidelitas, Invidia, Desperatio* (presented in this thesis, see Fig. 28);

- Virtues wall paintings (southern wall): *Prudentia, Fortitudo, Temperantia, Iustitia, Fides, Caritas, Spes* (presented in this thesis, see Fig. 28);

The instrument Nikon D800 FR (Full range) camera with a 36-megapixel sensor was used. The camera has been modified, removing the internal UV and IR filters, to collect different images in the UV-VIS-IR range using specific external band-pass filters. A couple of modified Nikon speedlight flashes (Nikon SB 910) including excitations in the UV and NIR ranges was also used. During the acquisition, these flashes are in general positioned at 45° with respect to the measured surface, whereas the camera is placed between the flash lights and pointed orthogonally to the surface. The multispectral images, where it was possible (e.g. in *Lunette* wall painting), were then calibrated using a colorchecker provided with the camera and placed close to the wall paintings during the acquisition. Five external band-pass filters were used in this case to take the pictures in the UV-Vis-NIR ranges: one for the UV range (350-420 nm), one for the visible range (about 400-700 nm) and three different filters for the near infrared range (IR1= 720 nm, IR2= 850 nm, IR3= 950 nm). Before analysing in alternative software tools, the collected photos were converted from raw images to 16-bit Tagged Image File Format (TIFF) with minimal processing (without white balance and brightness corrections or stretching or pixel rotations) using the NX Viewer free software.

The informativity of images, acquired without a color checker, was compared to the information obtainable from calibrated images. Some additional methods, using common or free software tools (Image Enhancer, ImageJ, Adobe Photoshop), were tested for enhancement of the detected features.

In this thesis, several representative examples are presented, showing simple procedures of non-invasive examination, which is recommended in this or similar case studies for art historians, conservators-restorers and other Cultural Heritage experts.

The wall painting “Fides” from the Virtues series is shown here to illustrate the elaboration results of single spectral bands by the means of free software tools (Image Enhancer, ImageJ), using simple image processing filters, aimed at enhancement of details, underdrawings, artist’s brush movements and characteristics of the surface.

The wall painting “Inconstancia” from the Vices series is shown here to illustrate the elaboration results of combined analysis of two or more spectral bands by the means of common or free software tools (Image Enhancer, Adobe Photoshop), aimed at enhancement

The wall paintings and their fragments, presented in this thesis, are shown in Fig. 28.

The images of the “Lunette” wall painting were acquired in the presence of Proficolore Color Checker and without it. The comparison is aimed at showing potentialities of information obtainable from calibrated and non-calibrated images.

The whole building structure was examined by passive IR thermography. Some representative results are presented here.

The acquisitions of multispectral images on the wall paintings Fides and Inconstancia, located in the lower parts of the interior walls (2 m above the ground level) were performed with a camera positioned at the height of 1,7 m from the ground level and at the distance of approximately 2,5-2,7 m from the object.

The acquisitions of multispectral images on the “Lunette” wall painting was performed with the camera positioned at the height approximately 1.5 m from the ground level at the distance of approximately 2 m from the object.

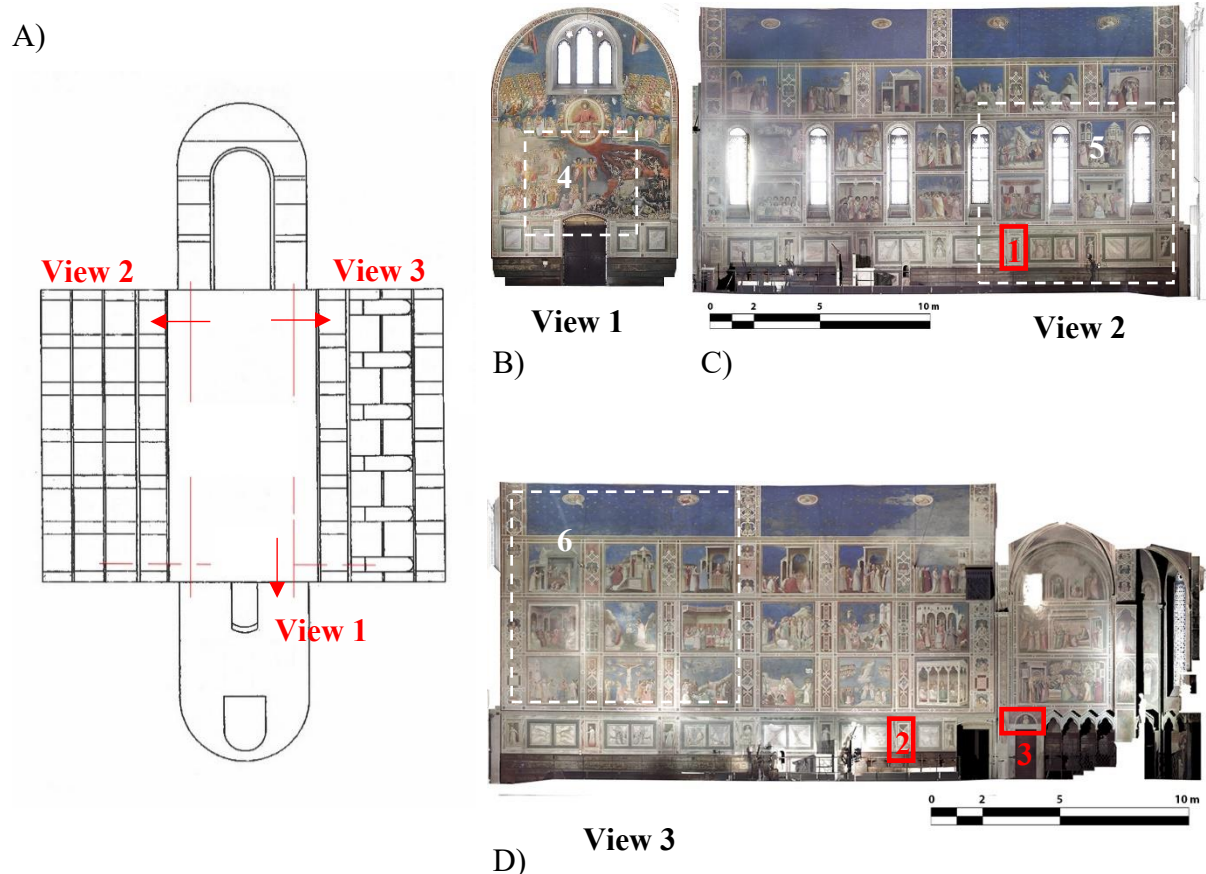


Fig. 28. Acquisitions in the Scrovegni Chapel: a) Scheme of the interior; b) South-Western wall from the survey by ISCR* (view 1); c) South-Eastern wall from the survey by ISCR (view 2); d) North-Western Wall from the survey by ISCR (view 3). The fragments of wall decorations examined by Multispectral Imaging and presented in this thesis are indicated in red: 1) Wall painting Fides (from the series of Virtues); 2) Wall painting Inconstantia (from the series of Vices); 3) Wall painting „Lunette“. The fragments of wall decorations examined by Infrared Thermography and presented in this thesis are highlighted in white: 4, 5 and 6.

*ISCR – Superior Institute of Conservation and Restoration

Examination and analysis of multispectral images

In this case study, particular interest was dedicated to the comparison and critical analysis of the informativity of multispectral data:

- raw non-elaborated images;
- after processing in commercial camera-dedicated software Proficolore;
- after processing in alternative free or open source software tools.

Qualitative analysis of separated spectral images

The brightness and contrast changes (by the means of Image Enhancer or Adobe Photoshop, see attachment G) and convolution filter (by the means of Image Enhancer software, see

attachment G) were used for enhancement of details readability in visible, infrared and ultraviolet images. Convolution is a simple mathematical operation which is fundamental to many common image processing operators [153]. It is performed by multiplying a pixel's and its neighboring pixels color or brightness value by a matrix. Application of this function by the means of Image Enhancer software allowed further enhancement of surface details in separate bands, see Fig. 29 and 30.

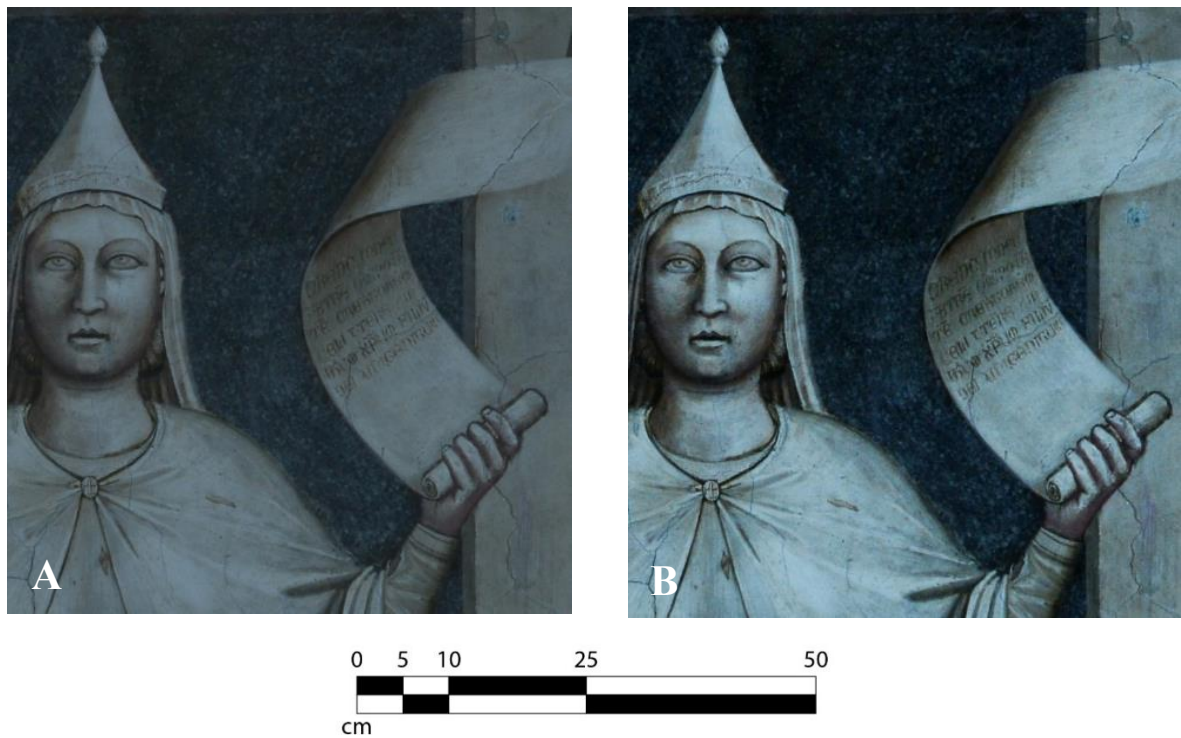


Figure 29. Enhancement of details on the example of the wall painting “*Fides*”: a) non-elaborated visible image; b) the same image after enhancement of contrast (in Adobe Photoshop).

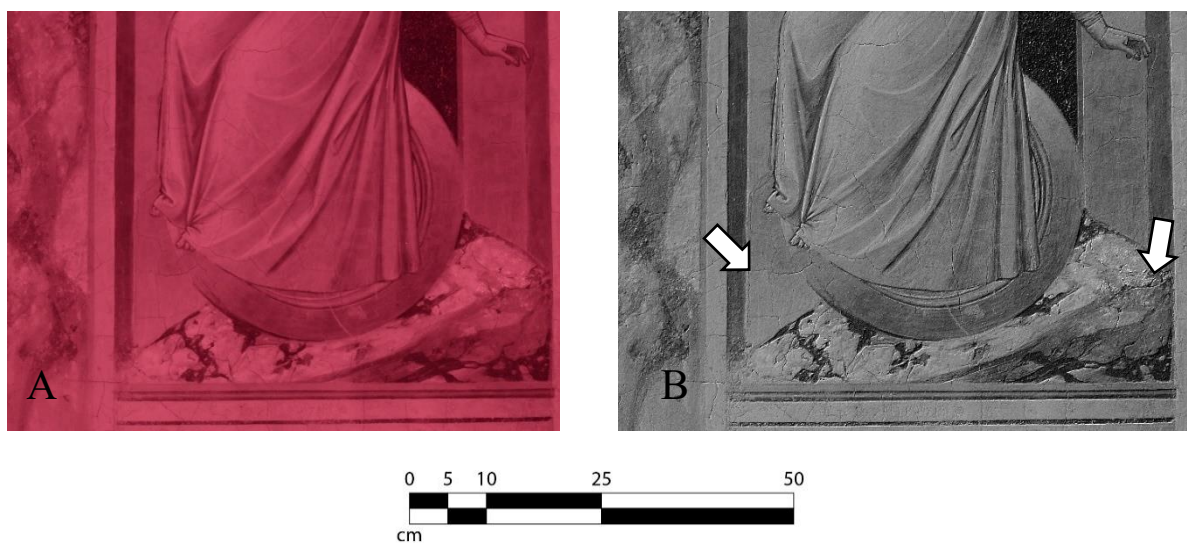


Figure 30. Enhancement of contrast and minor surface irregularities on the example of a wall painting “Inconstantia”: a) non-calibrated and non-elaborated infrared image (IR1); b) convolution filter applied to the infrared image (IR1) by the means of Image Enhancer. The arrows in Fig. 30b indicate the surface irregularities detectable by naked eye observation (shallow fractures and thickness of paint layer), enhanced in the elaborated image.

Qualitative analysis of combined spectral images

The tests on analysis of combined visible and infrared images were performed by the means of different software tools: Image Enhancer and ImageJ as programs available for free, Photoshop as a commercial but commonly available software, commercial Profilocolore dedicated software. Fig. 31 shows the combined image in Adobe Photoshop, obtained by blending of visible and infrared bands in luminosity mode (IR1), after enhancing the contrast in each of the bands separately. The resulting combined image preserves the color, hue and saturation values from the visible image (Fig. 31b), but enhances the differences in pixels luminosity between the visible and infrared bands. Infrared reflected light photography allows identification of materials with different composition, which absorb and reflect the infrared light differently. The difference in infrared reflectance values corresponds to the differences in the composition of pictorial layer (pigments) or background (final plaster layer). Since the differences are not observed in the ultraviolet image, it can be assumed that the difference is not related to the presence of superficial organic materials or binders. Application of this simple image processing operation allowed mapping of presumably reintegrated (with the application of background material) or retouched areas (only painting layer).



Figure 31. Revealing the hidden details and areas of presumed retouchments by combined analysis of visible and infrared images, on example of “Fides” from the series of Virtues wall paintings: a) visible image (VIS), after contrast enhancement; b) visible (VIS) and infrared (IR1) blended image, using luminosity mode in Adobe Photoshop. The red arrows on the blended VIS-IR1 image indicate the presence of presumably retouched areas.

Qualitative and semi-quantitative analysis of spectral images by dedicated and alternative software tools

The stack of spectral images, acquired on a lunette wall painting above the entrance door to the sacristy, was analysed before and after calibration of lighting conditions. The results, obtained by simple observation and by qualitative analysis, were evaluated by comparison to the semi-quantitative analysis performed by the means of camera dedicated Profilocolore software.

The hidden paint layers in the lunette wall painting were revealed already by simple observation of the raw infrared reflected light image and by its comparison to the raw visible image (Fig. 32b compared to Fig. 32a). The background of the lunette shows high inhomogeneity in the application of the paint layer, which can be related to the application of lime plaster and to the brush movements. More, the details of the preparatory drawing were enhanced in different ways, since it was performed not only by infrared absorbing pigments (charcoal), but also by cord or by snapping [85]. If the upper layers consist of the pigments, transparent or partially transparent in the infrared range, then the infrared light penetrates underneath it, it is reflected differently in the traces of cord snapping, while infrared absorbing pigment shows high contrast on the white background. Some new features, which appeared beneath the IR-transparent pigment of the upper paint layer, are shown in the non-elaborated IR image (Fig. 32b).

The Profilocolore IR2 image shows the enhancement of the same details, already observed in the non-calibrated IR image, with even higher contrast and definition (Fig.32d).

The efficiency of details enhancement, detected in the infrared band, was tested by the means of blending function in Adobe Photoshop, applying luminosity values of each pixel from the infrared image (IR2) to increase the contrast values in the visible image. This procedure proved its efficiency when applied both to calibrated and non-calibrated images (see Fig. 33). Combination of visible and infrared images enhanced the presence of brighter areas underneath the pictorial layer, which may indicate the presence of retouched or reintegrated areas and can be furtherly compared to the anomalous areas, detected in the other wall paintings. However, a difference in illumination homogeneity distribution, color saturation, luminosity and hue is evident between the calibrated and non-calibrated images (Fig. 33a and 33b).

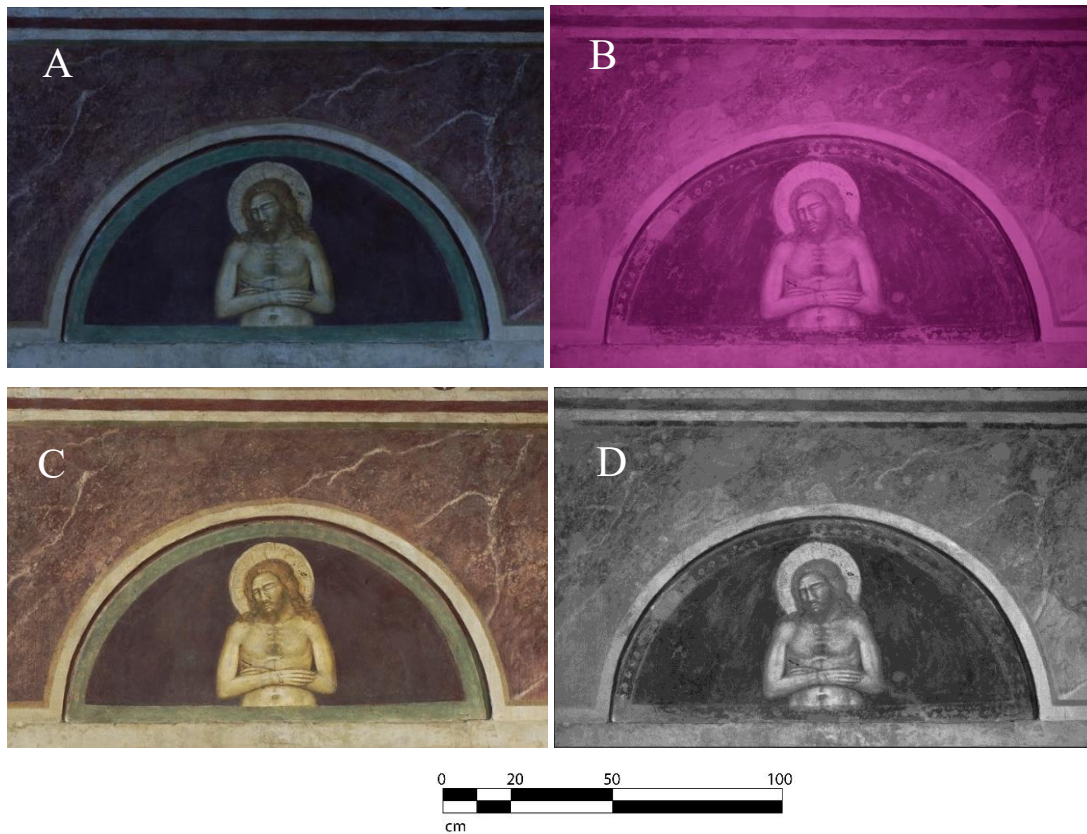


Figure 32. Comparison of calibrated and non-calibrated spectral images of the “Lunette” wall painting. a) Non-calibrated and non-elaborated visible reflected light image; b) Non-calibrated and non-elaborated infrared image (IR2); c) Profilocolore calibrated visible reflected light image; d) Profilocolore calibrated infrared (IR2) image. The arrows indicate the presence of hidden paint layer, which appears in the infrared light image, as well as brush movement details and presumable differences in the plaster (intonachino) composition.

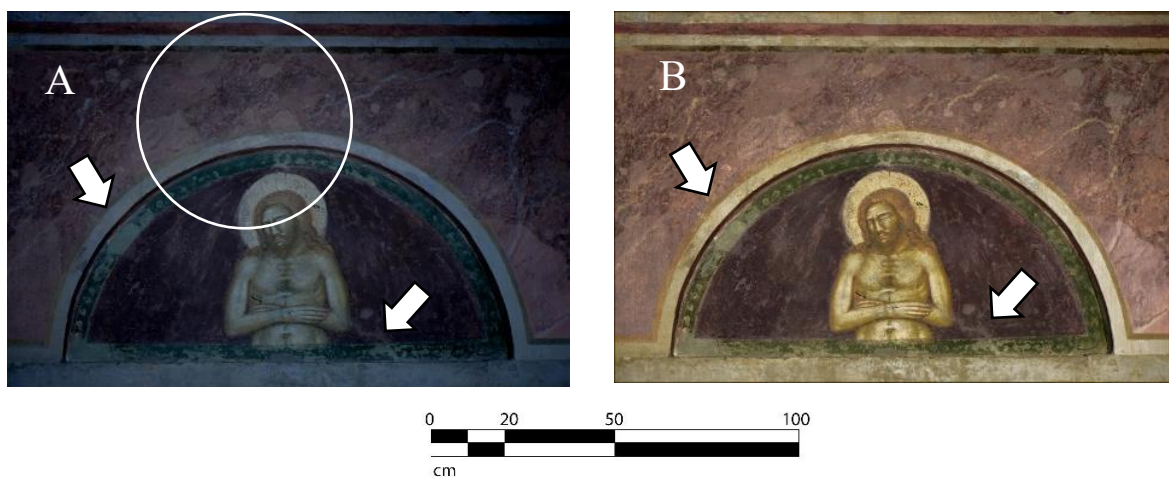


Figure 33. Revealing hidden details. Combination of visible and infrared images, using blending function in luminosity mode of Adobe Photoshop: a) stack of non-elaborated images VIS-IR2; b) stack of Profilocolore calibrated images VIS-IR2.

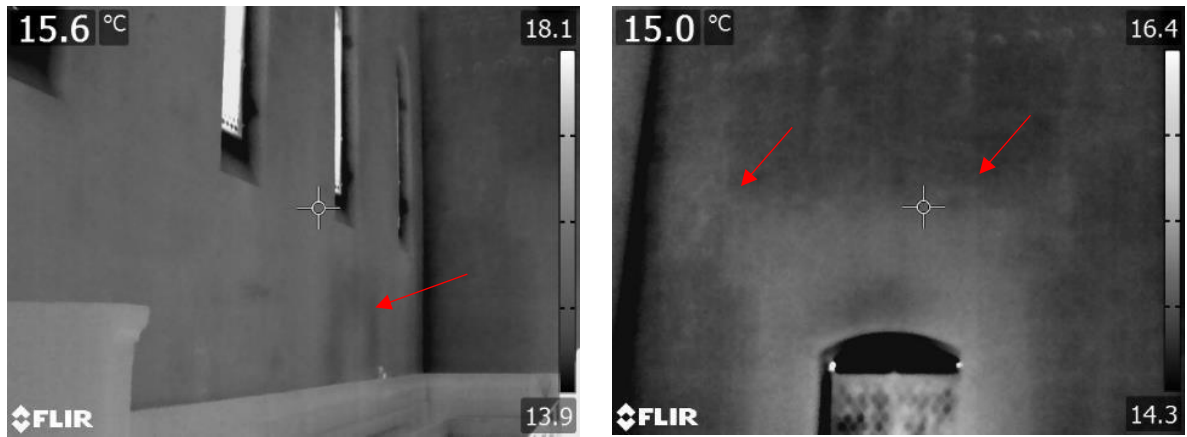
4.2.2 b) *Infrared Thermography acquisitions*

Infrared Thermography inspections were performed in passive mode in the month of January and November 2016. The distance from the camera to the investigated objects was in the range of 10-20 m. Some important subsurface characteristics were immediately identified by in-situ passive infrared thermography inspections. These issues are related to the structural stability of the building and to the conservation state of the wall decorations.

The passive infrared thermography inspections helped identifying areas of high inhomogeneity in the underlying subsurface and structure. The examination of thermal images allowed mapping of the areas of most probable future structural and deterioration risk, resulting in higher or lower temperature values on the surface, without the need to use external excitation sources

In particular, the difference in thermal properties of materials and high contrast of temperature inside and outside the building allowed to locate the presence of structural changes within the architecture of the building. It was possible to locate the infilled entrance door (Fig. 34a) and the original form of the portal on the northern facade, demolished at the beginning of the 19th century (Fig. 34b). The door is detectable through a region of lower temperature values in the presumable contact area between the building wall and infilling material (indicated by a red arrow in Fig. 34a). It could be explained by humidity infiltrations and/or by different thermal behavior of the adjacent construction materials. At the same time, the original form of the portal, as well as the consolidated cracks and weak areas due to its demolition (indicated by red arrows) may be traced through a warmer area around the door, due to the wall thickness and material thermal properties variations.

By visual observation of thermal images, some inhomogeneities in the subsurface underneath the wall painting layer were detected. In particular, it was possible to recognize the position of frescoes on the Eastern wall, which were reattached on copper frames in the 19th century. They are revealed through areas of higher surface temperature (Fig. 35a). Furthermore, the presence of good contrast in temperature and humidity between interior and external areas allowed mapping of so called putlog holes (Fig. 35b), which were made to receive the beams supporting scaffldings during the realization of wall paintings. The presence of these discontinuities is not detectable by naked eye observation.



A)

B)

Figure 34. Revealing of hidden structural inhomogenities by on-site Passive IR Thermography inspections. a) South-Eastern wall (Fig. 28), the red arrow indicates the position of the plugged door; b) South-Western wall, the red arrow indicates the higher temperature area in the position of the demolished external portal.

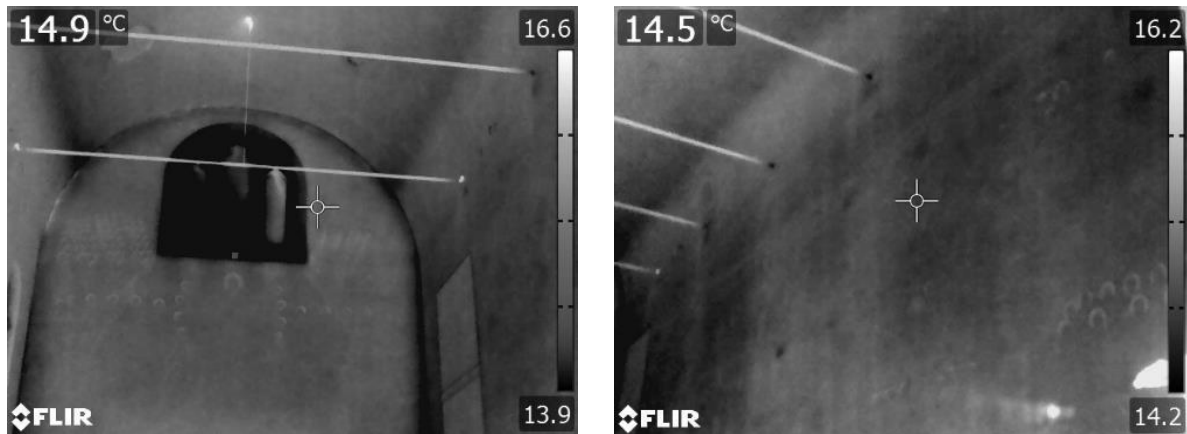


Figure 35. Revealing of hidden structural inhomogenities by IR Thermography inspections in passive mode. North-Western wall painting (Fig. 28), a) The position of reattached wall paintings (higher temperature areas); b) appearance of putlog holes (lower temperature areas).

4.2.3 Discussion of the results

Both Multispectral Imaging and Passive Infrared Thermography, full-field and non-contact, showed rapid efficiency during in-situ monitoring and preliminary investigation campaign inside the Scrovegni Chapel. The application of Ground Penetrating Radar and Holographic Subsurface Radar were limited to the areas that are not covered by highly valuable wall decorations and are not presented in the given project.

Multispectral Imaging was applied only in reflectance mode. The possibility to use the color reference chart on some of the wall paintings in these acquisitions allowed subsequent

calibration and more detailed analysis of on-site multispectral images. Both calibrated and non-calibrated images were useful for on-site mapping of presumably retouched areas and in revealing hidden decoration layers (lunette wall painting). Simple enhancement functions, blending of spectral images and RGB values transformations allowed to enhance the contrast between different bands. The comparison and differentiation between pigments in images without the calibration of lighting conditions was, however, not possible. Irregular and uncontrollable lighting, surface small irregularities or general non-planarity may lead to the creation of artefacts and to the misleading interpretation of the results.

The first preliminary results of in-situ multispectral images observation can provide indications on the areas of higher interest for further laboratory or on-site investigations, whereby also more sophisticated instrumental (FORS, XRF) or image processing tools (ENVI software) can be applied.

The recommended image acquisition and analysis workflow and the selected image processing procedure can be found in attachments D and E respectively. The detailed description of each of the image processing functions, tested in this project, is reported in the attachment G.

Infrared Thermography inspections, performed in different periods, showed different levels of informativity. In the presence of a big contrast of climatic conditions between the interior of the Chapel and outside it, this technique proved high usefulness in the detection of inhomogeneities in the walls, which communicate with the exterior. It was possible to detect the presence of deep structural and shallow subsurface inhomogeneities (cold areas due to the moisture rising and warmer areas due to the presence of refilled cracks inside the wall structure and risk of formation of new detachments).

Simple observation of thermal images (without any further processing of data) revealed itself useful to support structural monitoring of the building and art historical study on the details of Giotto's execution technique. It allowed quick identification of the exact position of the demolished external small portal on the north wall of the Chapel. More, it was possible to map in-situ the shallow subsurface discontinuities, for example, the location of reattached wall paintings. The inspection by Passive Infrared Thermography provided rapid and non-invasive identification of structural and subsurface areas that require immediate intervention or should be monitored for further evaluation of stability risks. All this information is useful for correct conservation planning of wall paintings, their underlying subsurface and structural support.

The brief observations of the research questions of this case study are summarized in Table 10.

Table 10. Results of the acquisitions in Scrovegni Chapel, Padua

Research question	Results and observations
- Can Multispectral Imaging be used in this case study to reveal more details about the artist's technique and underdrawings?	Yes, even in absence of a color reference chart, by comparison of different spectral bands, enhanced and assisted by the means of free or commonly available software tools
- Can Multispectral Imaging be used in this case study to differentiate between original and retouched areas?	Yes, even in absence of a color reference chart and by the means of free or commonly available software tools. It can be used
- Can Multispectral Imaging be used in this case study to differentiate between pigments?	Yes/no. In the case of a wide range of used pigments and undocumented restorations, it should be performed only on calibrated images by the means of dedicated software tools (Profilocolore or ENVI)
- Is it possible to extract useful preliminary information about the wall paintings in-situ, without the use of dedicated software (by simple observation or alternative software tools) in this case study?	Yes, simple comparison of different spectral bands (VIS and IR) can help to locate underdrawings and presumably retouched areas; the informativity can be improved by the means of simple and combined image processing functions
- Can Passive Infrared Thermography be applied in this case study to reveal subsurface and structural discontinuities underneath the decoration layer? If yes, what are the necessary conditions?	Yes/no. It is possible only if adequate thermal contrast is naturally present.
- What are the main limitations of these techniques applied in-situ in this case study?	For MI: Limited access (opening hours and tourist presence groups), long distance from the objects in the upper part of the chapel, low natural lighting conditions, impossibility to

	<p>darken completely the environment (for the use of MI in fluorescence mode) and impossibility to use the complete set of recommended acquisition arrangement (color checker and placement of flashlights)</p> <p>For IRT:</p> <p>Distance from the investigated surfaces, presence of adequate natural thermal gradient</p>
--	---

4.3 The Chapter Hall (Sala del Capitolo) of the Basilica of Saint Anthony (Padua, Italy)

4.3.1 Case study description

The *Basilica di Sant'Antonio* (Basilica of Saint Anthony) or *Il Santo* (The Saint), is with its architectural decoration one of the most important monuments of the city and one of the outstanding examples of architectural and art historical heritage. The name of the architect is unknown, however, it is believed that he was a Franciscan friar. The construction of Basilica started in 1232, and its principal part was completed towards the end of the 13th century [186]. It was dedicated to Saint Anthony of Padua, who was born around 1195 in Lisbon, Portugal, and who died in Padua on June 13, 1231.

The so called *Sala del Capitolo* (Chapter Hall), part of the Basilica's architectural complex (Fig.36a), was presumably completed shortly before the second translation of the body of Saint Anthony (around 1310) or soon afterwards [187]. The wall paintings, executed by fresco technique, are attributed to Giotto, probably even before the pictorial cycle in the Scrovegni Chapel. More, it is maintained by a historian Vittorio Sgarbi [186], that it could be Giotto's work in the Chapter Hall that led to his meeting with the Scrovegni family. For a long time period, the main wall of the Chapter Hall remained covered by the 16th century wall painting depicting a portal. In 1842 Pietro Selvatico, while investigating some washed out patches, discovered underneath them several fragments of a Martyrdom of the Franciscans raffiguration in the Chapter Hall of St. Anthony of Padua and, due to outstanding quality and stylistic features, recognised them to look like Giotto's paintings. In the next years, the findings became more extensive and in the long walls of the hall, a Crucifixion and a Stigmatisation scene, besides the Martyrdom, came to light, as well as some full-figure representations of Franciscan Saints and Prophets, painted on the short walls forming part of the complex architectural layout. The rediscovery of these wall paintings could confirm the many and various indications in the historical sources of Giotto's presence at the site: by Riccobaldo Ferrarese (1312) and Michele Savonarola, who in 1440 speaks clearly about decorations for the convent chapter. Particularly worth considering is a detailed note by Marcantonio Michiel (an authoritative source for Giorgione too) who in 1550 speaks of a fresco of the Passion done by the hand of Giotto the Florentine, also in the Chapter hall. Vasari, for his part, in the 1568 edition of the Lives attests to Giotto's activity in several of the chapels inside the church [188].

The historical sources are poor and a multidisciplinary scientific campaign is now under process. Regarding the frescoes in the Chapter, the scholar Flores d'Arcais prefers to attribute

them rather to some of Giotto's collaborators. However, in the *Cappella delle Benedizioni* of the Basilica (Chapel of blessings), Flores d'Arcais has recognised Giotto's hand in the decorations inside the arch with busts of Saints, which belonged to the Scrovegni family, who commissioned also the Scrovegni Chapel. A multidisciplinary scientific campaign is now being carried out by the University of Padua, aimed at studying the remaining fresco fragments attributed to Giotto and his school. The focus is set on testing the hidden presence of the original pictorial layer and its integrity below the subsequent paint layers. The acquisition campaign is part of the interdisciplinary study "Recovery Giotto at the Basilica of Saint Anthony, Padua", coordinated by Prof. Gilberto Artioli (co-tutor of this Ph.D. project). The research is conducted in collaboration with researchers from the Department of Geosciences, of the Department of Cultural Heritage of the University of Padua, in collaboration with the researchers of the international network IPERION-MOLAB. Specifically for this project, the experiments concerned integrated data acquisitions of other groups with Nuclear magnetic resonance profiling, THz Imaging, Stimulated IR Thermography and Holographic interferometry, carried out through MOLAB access, for shallow subsurface integrity characterization.

The Multispectral Imaging, FORS, Portable XRF were applied for the study of the pictorial layer.

GPR, HSR were used for structural and subsurface diagnostics.

The analysis is aimed at the creation of a basis for the future restoration and management of this poorly known Giotto's work. In the frame of the non-invasive characterization carried out through the MOLAB access, the integrity of the underneath original fresco was tested by THz imaging, NMR profiling, Digital Holographic Speckle Pattern Interferometry (DHSPI) and Stimulated Infra Red Thermography (SIRT).

In this case study, only the results of two methods: Multispectral Imaging (MI) and Holographic Subsurface Radar (HSR), performed on the Eastern wall painting (Fig.36b) by the research group of the University of Padua (Italy), are presented.

The research questions considered in this thesis include the following:

- Can Multispectral Imaging be used in this case to reveal more details about the artist's technique, underdrawings and degraded details?
- Can Multispectral Imaging be used to differentiate between original and retouched areas?
- Can Multispectral Imaging be used to identify and differentiate between pigments?

- Can HSR be helpful to reveal subsurface and structural discontinuities underneath the decoration layer?
- What are the main limitations of these techniques applied in-situ in this case study?

4.3.2 a) Acquisition and analysis of multispectral images

The acquisitions were performed only on the Eastern wall painting fragments. The instrument Nikon D800 FR (Full range) camera with a 36-megapixel sensor was used. The camera has been modified, removing the internal UV and IR filters, to collect different images in the UV-VIS-IR range using specific external band-pass filters. A couple of modified Nikon speedlight flashes (Nikon SB 910) including excitations in the UV and NIR ranges was also used. During the acquisition, these flashes are in general positioned at 45° with respect to the measured surface, whereas the camera is placed between the flash lights and pointed orthogonally to the surface. The multispectral images were then calibrated using a colorchecker provided with the camera and placed close to the wall paintings during the acquisition. However, in this thesis, only the results of the analysis of non-calibrated spectral images are presented. Five external band-pass filters were used in this case to take the pictures in the UV-Vis-NIR ranges: one for the UV range (350-420 nm), one for the visible range (about 400-700 nm) and three different filters for the near infrared range (IR1= 720 nm, IR2= 850 nm, IR3= 950 nm). Before analysing in alternative software tools, the collected photos were converted from raw images to 16-bit Tagged Image File Format (TIFF) with minimal processing (without white balance and brightness corrections or stretching or pixel rotations) using the NX Viewer free software.

The fragments of multispectral images presented in this thesis are acquired on the Eastern wall painting at the distance of approximately 2.5 (bottom part of the wall painting) to 4.5 m (upper part of the wall painting fragments) from the camera, positioned at approximately 1.5 m above the ground level. Non-calibrated images were analyzed by simple image processing tools and compared for qualitative analysis for the study of original fresco fragments, which are attributed to the hand by Giotto da Boldone. Simple image processing tools were applied and evaluated to differentiate between different fresco fragments (presumably original, retouched or overpainted areas).

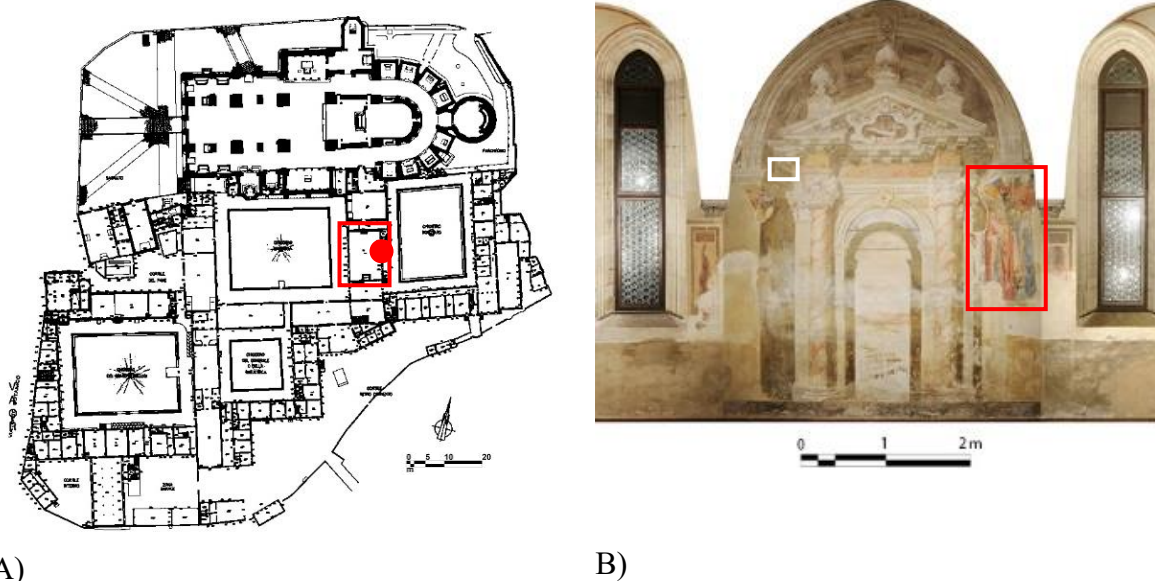


Figure 36. Sala del Capitolo in the architectural complex of the convent and the basilics: a) groundplan map, the location of the Chapter Hall (Sala del Capitolo) and the Eastern wall painting are highlighted in red [189]; b) survey of the Eastern wall painting, after Luca Baggio [188], showing the area of HSR acquisition, highlighted in white, and the area of MI acquisition, highlighted in red.

Reflected infrared photography (IRR) is well known to reveal underdrawings beneath the pictorial layer (due to the contrast between the infrared light reflected by the ground and the light absorbed by the underdrawings) and to differentiate between similar pigments (due to the different IR light absorption properties as function of differences in chemical and mineralogical composition). In this specific case study, however, simple observation of visible and infrared images did not reveal areas with pronounced discontinuities in reflectance values distribution. The comparison of wall painting fragments one by one was also time consuming and not efficient.

The enhancement in informativity of the infrared image was achieved by blending spectral bands as layers in Adobe Photoshop, using luminosity mode, already described in the previous chapters 4.1 and 4.2. In this case study, the IR1 band showed differences in the reflectance values, while IR2 and IR3 did not show significant results. The combined visible (VIS) and the first infrared (IR1, 700-800 nm) image allowed rapid localization of visibly homogeneous painted areas with differences in infrared range.

The red arrows in Fig. 37 indicate areas of similar colour/brightness in the visible image that shows differences in the infrared range. The white arrows in Fig. 37b indicate the presence of continuous division (stitch) in brightness across the 16th century and late medieval wall painting fragments.

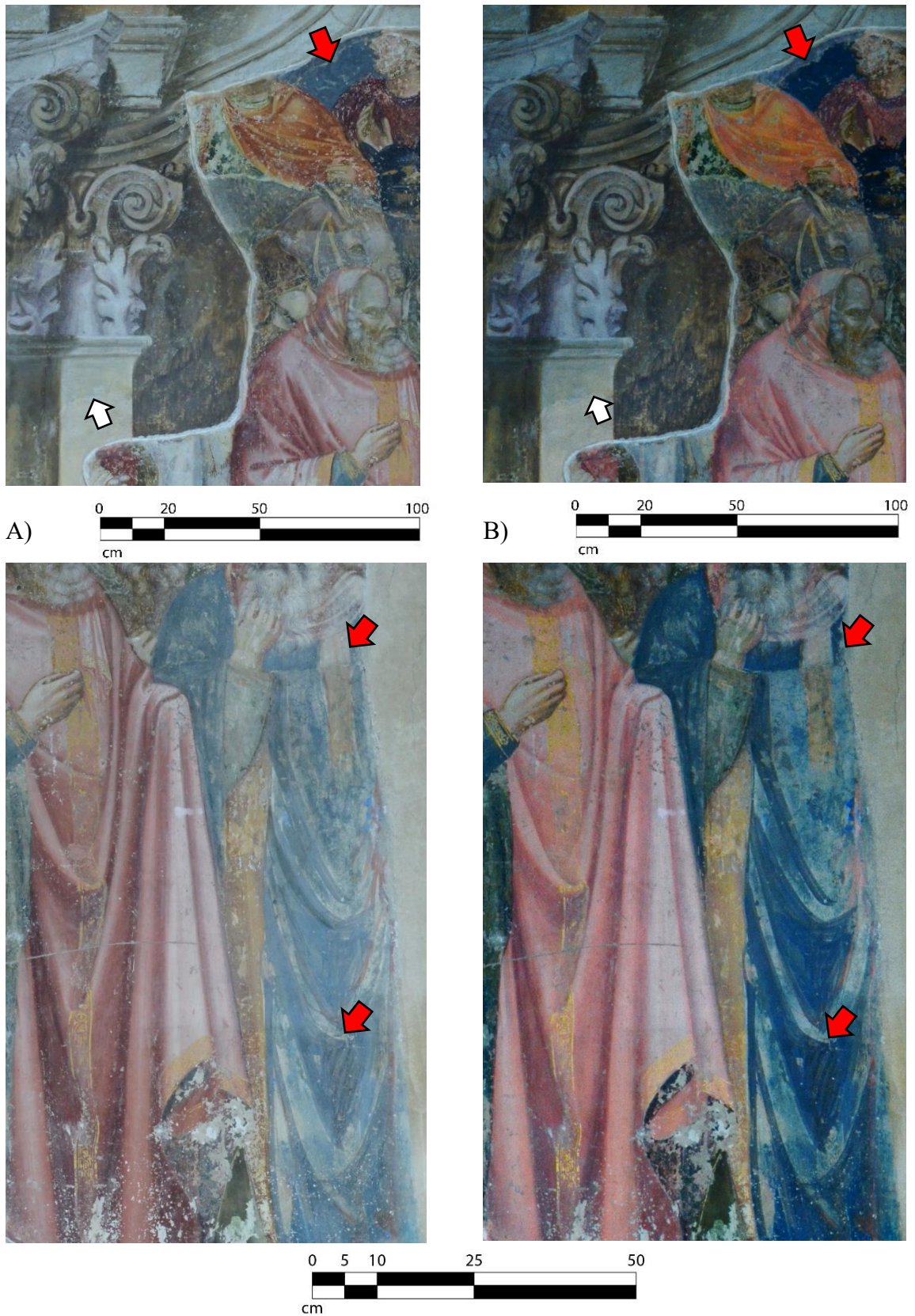


Figure 37. Differentiation between similar pigments or their concentration in degraded wall painting areas: a) upper fragment, non-calibrated and non-elaborated VIS image; b) upper fragment, IR1-VIS blended image (luminosity mode); c) bottom fragment, non-calibrated and non-elaborated VIS image; d) bottom fragment, non-calibrated IR1-VIS blended image (luminosity mode).

The procedure showed its efficiency in revealing the lost details in the pictorial and preparatory layer. Fig. 38 shows the fragment of the acquisition frame that helps better recognition of face's details and reconstruction of possible details in the original wall painting.

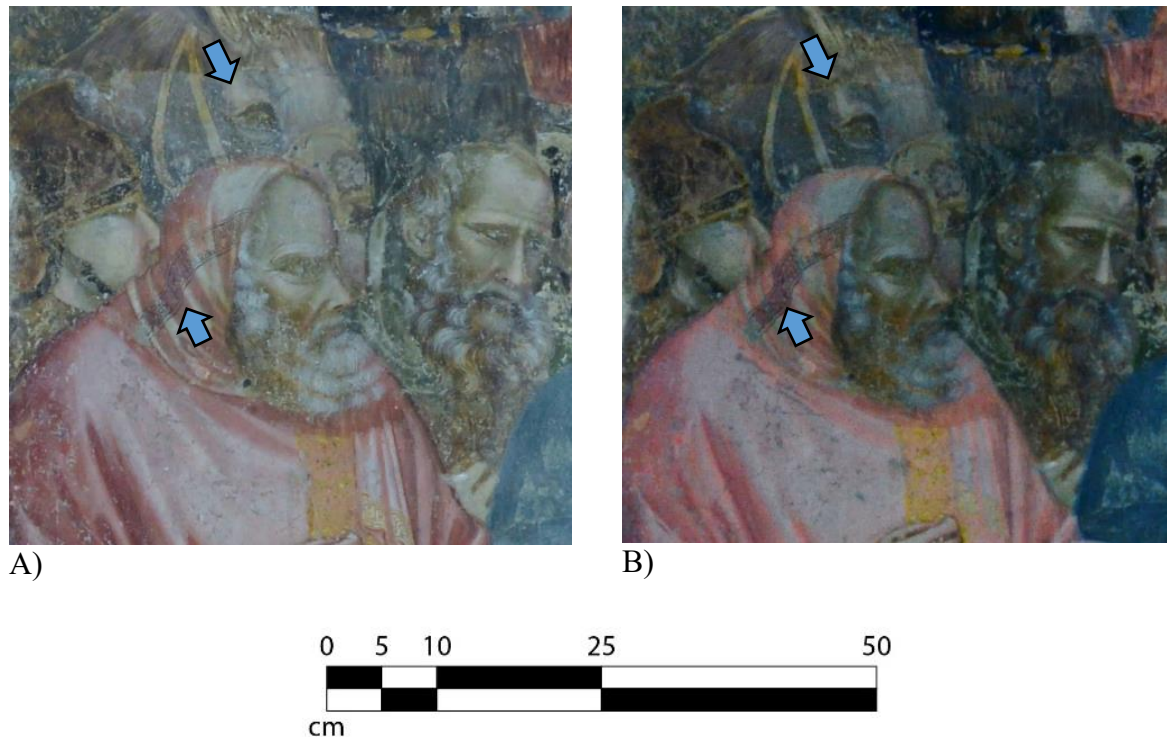


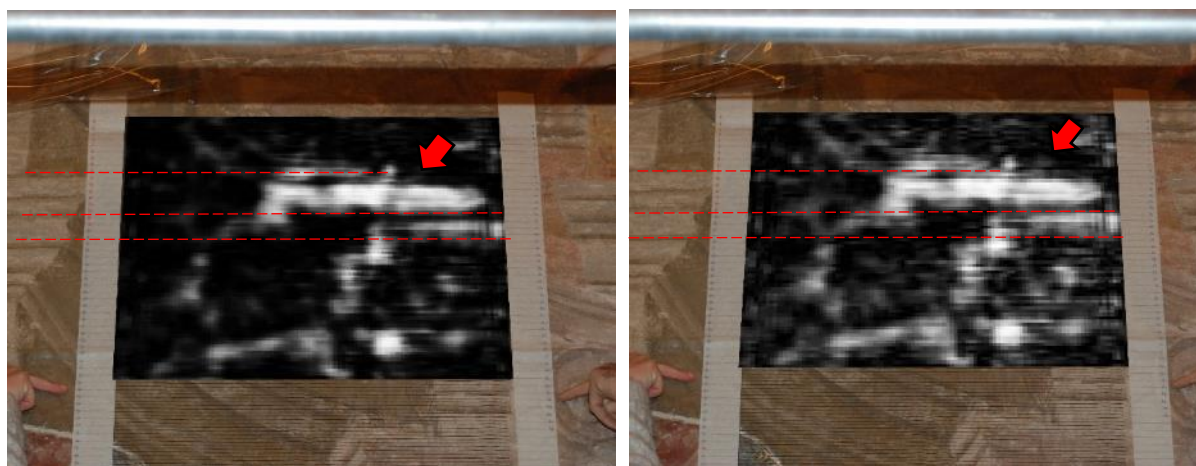
Figure 38. Enhancement of figures face details, horse's eyes and drapery pattern lines in a wall painting fragment. a) non-elaborated visible image. b) non-calibrated IR1-VIS blended image (luminosity mode)

4.3.2 b) Holographic subsurface radar acquisitions

The areas of interest for detailed acquisition by the Holographic Subsurface Radar were selected after preliminary full-filed examination by DHSPI-SIRT full-filed investigations (MOLAB, Holography Lab from IESL-FORTH, Greece).

Fig. 39 illustrates the result of HSR acquisition (6.4 GHz), focused at the depth of 1.5 cm and 2.5 cm inside the wall subsurface. The Rascan image was scaled and presented in overlapped on the photo of the analyzed area. The HSR system detected the presence of a material with different dielectric permittivity properties, indicating the geometry and dimensions of the anomaly seen in its planar view parallel to the painting surface. As can be seen from Fig. 39, the position of the identified anomaly in the subsurface coincides with the level of columns raffiguration on the wall painting on the surface. The anomalous signal reflection is well defined at the depth of approximately 1,5 cm beneath the surface, but the exact depth of its position can vary depending on the exact composition of the subsurface medium. This structural

discontinuity was not clearly confirmed by the GPR results. Further tests may be needed, in order to trace the presence of anomalous material in the subsurface of this and adjacent areas.



A) B)
Figure 39. Result of Holographic Subsurface Radar acquisition. 50x40 cm, its location is shown in Fig. 36. Overlay of the Rascan image on the picture showing the position of acquisition lines: a) Rascan image focused at the depth of 1.0 cm inside the medium, 6.4 GHz; b) Rascan image focused at the depth of 2.5 cm inside the medium, 6.7 GHz.

4.3.3 Discussion of the results

The multispectral imaging technique showed its usefulness in the enhancement of wall painting details, partially lost due to degradation and ageing (golden leaf lines, eyes, etc.) Some areas with different reflectance values, identified by the multispectral camera, may indicate the presence of retouched areas. Qualitative analysis of multispectral images, acquired in reflectance mode by a modified camera, showed to be a good pre-screening tool for the identification of areas of further scientific interest. According to the art historical question (in this case, authenticity studies), the presumably original areas can be indicated for subsequent semi-quantitative (Profilocore, ENVI) or quantitative in-situ point analysis (portable XRF, Raman, etc.) or laboratory tests.

The recommended image acquisition and analysis workflow and the selected image processing procedure can be found in attachments D and E respectively. The detailed description of each of the image processing functions, tested in this project, is reported in the attachment G.

Within the collaboration between different international research groups, several subsurface structural diagnostic tools were tested in terms of their usefulness and complementarity for identifying hidden discontinuities in the very shallow subsurface and in the deep structure of the wall support. The innovative Holographic subsurface radar was tested for a detailed area study on a fragment of 16th century painting, in proximity to a fragment of original wall painting.

The technique was capable to provide information about the presence of a complex discontinuity pattern underneath the 16th century wall painting. The results of HSR, applied to the given case study, are only qualitative since, in the absence of knowledge about the materials and lack of historical documentation, it is however impossible to estimate the depth of presumable changes in the medium material.

The brief observations of the research questions of this case study are summarized in Table 11.

Table 11. Results of the acquisitions in the Chapter Hall, Basilica of Saint Anthony, Padua

Research question	Results and observations
- Can Multispectral Imaging be used in this case study to reveal more details about the artist's technique, underdrawings?	Yes, even in the absence of a color reference chart by comparison of spectral images (VIS and IR), enhanced and facilitated by the means of free or commonly available software tools
- Can Multispectral Imaging be used in this case study to differentiate between original and retouched areas?	Yes, even in the absence of a color reference chart by simple comparison of spectral images (VIS and IR), facilitated and improved by the means of free or commonly available software tools
- Can Multispectral Imaging be used in this case study to identify and differentiate between pigments?	Yes/no. In the case of a wide range of used pigments and undocumented restorations, it should be performed only on calibrated images by the means of dedicated software tools (Profilocore or ENVI)
- Can HSR be helpful in this case study to reveal subsurface and structural discontinuities underneath the decoration layer?	Yes/no. The interpretation of the results can be difficult in the absence or insufficient historical documentation about the materials and previous interventions. More, the direct physical contact to the decorated surface in most of the cases upon the areas of interest is not allowed

<p>- What are the main limitations of these techniques applied in-situ in this case study?</p>	<p>For MI: Limited access (opening hours and tourist presence groups), long distance from the objects in the upper part of the chapel, low natural lighting conditions, impossibility to darken completely the environment (for the use of MI in fluorescence mode) and impossibility to use the complete set of recommended acquisition arrangement (color checker and positioning the flashlights)</p> <p>For HSR: Limitations of physical contact to the surface, time-consuming manual acquisitions and difficulties in the interpretation of holographic images</p>
--	--

4.4 Catholikon of the Dafni Monastery (Athens, Greece)

4.4.1 Case study description

The Monastery of Daphni (Μονή Δαφνίου), the Monastery of Hossios Loukas (Ἅγιος Λουκάς) and Nea Moni (Νέα Μονή) are outstanding examples of the middle period of Byzantine religious architecture [190], representing its most significant monuments preserved until today. The Monastery of Daphni is considered to be the Parthenon of the Byzantine era and is internationally protected by UNESCO. It is built on the site of the ancient sanctuary of Apollo Daphnaios which was destroyed during the invasion of the Goths in 395 A.D. (that is where its name “Daphni” comes from). Only one Ionic column still remains in the colonnade of the narthex from the old temple, while the rest were removed by Lord Elgin in the 19th century. The monastery, dedicated to the Dormition of the Virgin, was founded in the 6th century A.D. and in spite of its great wealth and fame, it was soon abandoned. It was reconstructed at the end of the 11th century [191].

The Monastery is situated in the South-Eastern part of Attica near Athens, in the centre of its area the majestic central church is situated, called catholikon or katholikon (from Greek: καθολικόν).

The catholicon is a cross-in-square church of the octagonal type, surmounted by a broad and high dome. It has a narthex, in the form of an open portico in which the Ionic columns of the ancient temple of Apollo initially had been. The exonarthex was built some time later, in the early 12th century, the porch was added in the 13th century and the chapel to the west was added in the 18th century. The interior of the church is decorated with wall mosaics, dating from the end of the 11th century. These are unique and fine examples of Middle Byzantine art. But only a small part of mosaics and wall decorations, representing narrative scenes from the life of Christ and the Virgin, have been preserved till now. The lower section of the walls was dressed with marble slabs which were replaced by wall paintings around 1650 [190]. To the north of the church lies the refectory, an oblong rectangular building with an apse, also decorated with wall paintings.

Deconsecrated in 1821, the monastery has been undergoing continuous restoration works since 1888, with two earthquakes in 1889 and 1897. In 1936-39, the Greek Architect John Travlos carried out excavations at the ancient temple of Apollo.

Another earthquake struck the area recently. It happened on 7th September 1999 and caused severe damage to the catholicon and to the rest of the buildings of the monastery. The Ministry of Culture immediately decided to take strong measures in order to protect the monument (Fig. 40a). The recovery works, led by the Ephorate of Antiquities, continue till now. The Monastery is now open to the public only for several hours, two days per week.

The non-invasive acquisitions presented in the given project were performed in July 2017 within the frames of regular monitoring activities held by the Ministry of Culture, Ephorate of Antiquities of West Attika, Pireus and Islands, in collaboration with the Non-Destructive testing techniques Laboratory of the National Technical University of Athens (NTUA, Greece).

The research issues include the following questions:

- Can Multispectral Imaging be used to in-situ reveal underdrawings and degraded details to support the art historical and material study in this specific study case?
- Can Multispectral Imaging be used to identify and to differentiate between pigments?
- Can Infrared Thermography, applied in passive mode, provide immediate information about the condition of subsurface and structural support underneath the wall paintings in this study case?

Some of the wall paintings inside the Catholikon are strongly degraded (Fig. 40b).



A)

B)

Figure 40. Monastery of Daphni A) Catholikon under restoration, 2013-2014 [192]; B) Interior, detail of the wall painting St. Apostle Andrew, northern wall of the main aisle. Image courtesy: Maria Koufi

4.4.3 a) Acquisition and analysis of multispectral images

Fig. 41 shows the location of the wall paintings that were selected for the experimental multispectral analysis. In this case study, the experiments were focused on the preserved fragments of wall paintings from the second half of the 16th century, with particular interest to reveal underdrawings and lost details.

The instrument Nikon D800 FR (Full range) camera with a 36-megapixel sensor was used. The camera has been modified, removing the internal UV and IR filters, to collect different images in the UV-VIS-IR range using specific external band-pass filters. Five external band-pass filters were used in this case to take the pictures in the UV-Vis-NIR ranges: one for the UV range (350-420 nm), one for the visible range (about 400-700 nm) and three different filters for the near infrared range (IR1= 720 nm, IR2= 850 nm, IR3= 950 nm). Before analysing in alternative software tools, the collected photos were converted from raw images to 16-bit Tagged Image File Format (TIFF) with minimal processing (without white balance and brightness corrections or stretching or pixel rotations) using the NX Viewer free software.

The wall paintings are located in the lower part of the walls, therefore, acquisitions at a comparably short distance from the wall painting were possible. The camera was positioned at the height of approximately 1.5 m and the distance to the vault painting (numbered 1 in Fig. 35b) was approximately 1.75-2 m. Due to the geometry of structural support and limited accessibility to the wall paintings inside the catholikon, color reference chart could not be used in this case study. As a result, the calibration of lighting conditions and semi-quantitative analysis were not possible. A couple of modified Nikon speedlight flashes (Nikon SB 910)

including excitations in the UV and NIR ranges was also used. During the acquisition, these flashes are in general positioned at 45° with respect to the measured surface, whereas the camera is placed between the flashlights and pointed orthogonally to the surface for all the wall paintings except the niche painting of Virgin Mary, because of its location on the lateral side of the niche. This situation represents a common case in conservation practice, when the correct acquisition conditions are not possible due to restrictions in site accessibility and regulations. The collected stack of images was analysed using different software and image processing algorithms for qualitative analysis: ImageJ, Image Enhancer and Adobe Photoshop.

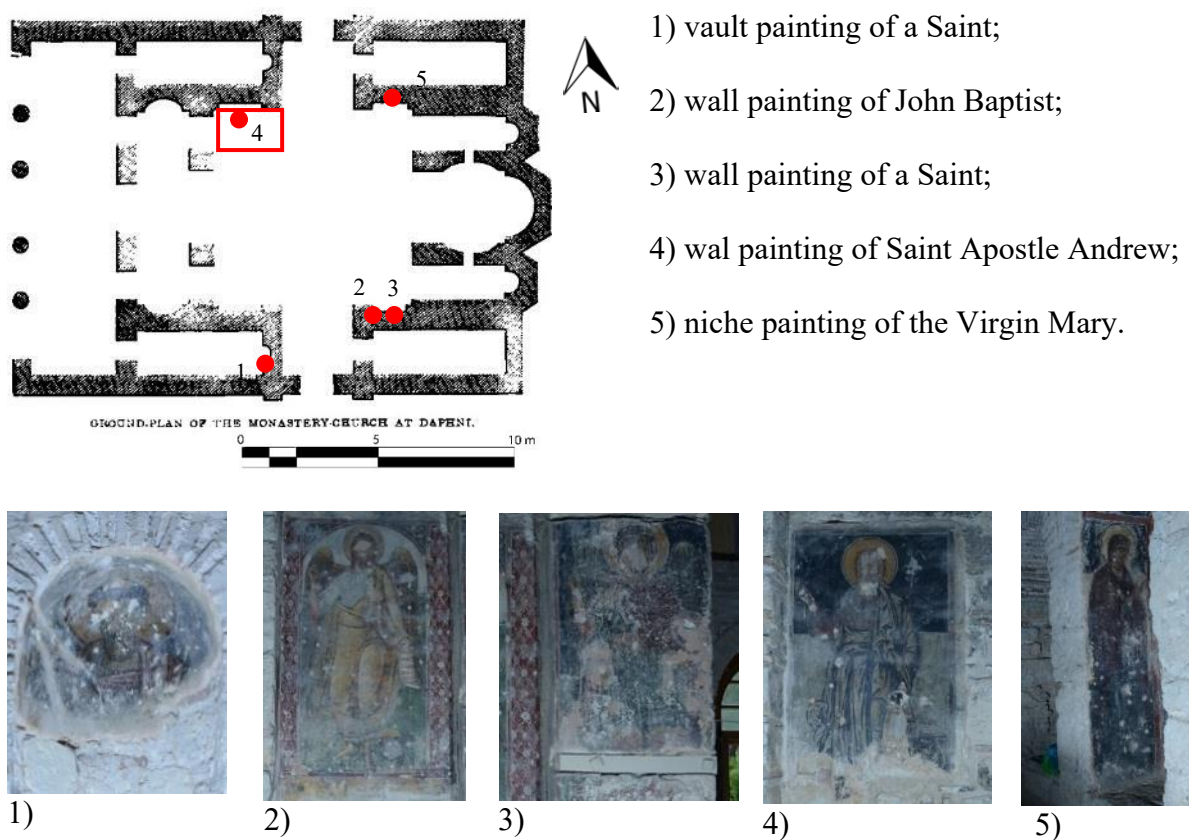


Figure 41. Acquisitions on wall paintings inside the Catholikon of Dafni Monastery. a) Ground plan with the indicated location of examined wall paintings by the means of Multispectral Imaging (indicated by a red dot and a number) and of the areas, examined by the means of Infrared Thermography, presented here [191]; b) Non-elaborated visible images of the examined wall paintings.

Reflected infrared photography (IRR) showed its known usefulness to provide information about the underdrawings underneath the pigments of the decoration layer that are transparent to infrared light. Simple observation and comparison of visible and infrared images provided preliminary information about the areas, in which the lost or hidden details became enhanced outside the visible region (Fig. 42a and 42b). Several methods were tested to enhance the

contrast between the visible and infrared bands, allowing locating better the details in the paintings, using Image Enhancer and Adobe Photoshop or ImageJ. The experimental procedure, combining information from different bands, multiplications and additions of RGB values, luminosity, hue and saturation, was applied and evaluated. Figure 42c shows the results of revealing underdrawings and lost details in a degraded wall painting of an unknown Saint, using Image Enhancer and Photoshop for combined qualitative processing of visible and infrared images. This procedure has been explained in chapter 4.1 on the example of the Western wall painting in the Frigidarium of the Sarno Baths in Pompeii. In this case, in order to improve the readability of the underdrawing, the curves of the visible image were inverted (using Adobe Photoshop and/or Image Enhancer), prior to its overlay with the infrared image. The dark areas were transformed into bright ones (VIS) and, as a result, the underlying traces of more absorbing pigment (IR2) appeared more highlighted over the background. More details in the paintings, the contour and the details of the face and of the arm shield, were immediately highlighted in the combined image, as it can be seen in Fig. 42.

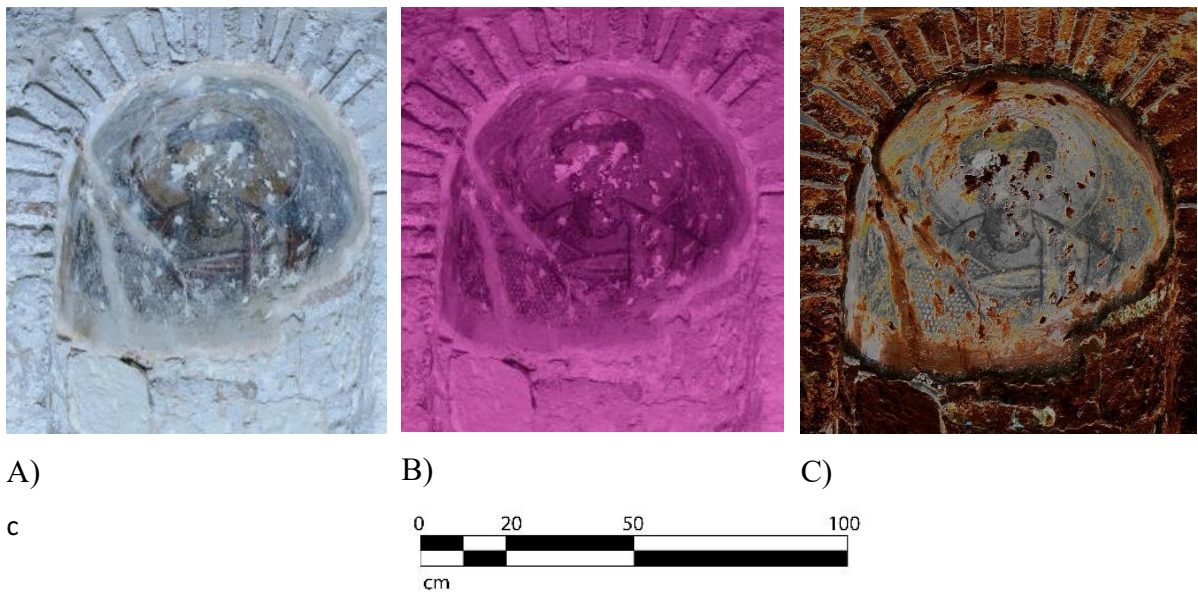


Figure 42. Enhancement of underdrawings in a vault painting raffiguration of an unknown Saint (presumably, a warrior): a) non-elaborated visible image; b) non-elaborated infrared image (IR2); c) non-calibrated IR2 (enhanced contrast) and non-calibrated VIS (inverted curves) blended image (luminosity mode) image.

4.4.2 b) Infrared thermography acquisitions

The in-situ tests were performed with the FLIR ThermaCAM SC640 in July 2017. This IR camera is the property of the Non-Destructive Testing techniques Laboratory of the National

Technical University of Athens (Greece) and the acquisitions were performed in collaboration with the Ephorate for Antiquities of Attica Region, in charge for the preservation of Daphni Monastery. The distance from the examined wall painting and wall masonry surfaces varied in the range of 2 (lower parts of the wall structure) to 6 m (upper part of the building). It was observed that the informativity of IRT acquisitions in passive mode in the absence of an adequate thermal gradient can strongly limit the informativity of acquired thermal images. No information about the condition of the wall subsurface underneath the painted surfaces could be extracted.

Nevertheless, the tests showed the efficiency of the technique to evaluate and to confirm the general thermal equilibrium of the building structure in this case study. According to the results of preliminary passive IR Thermography inspection, the preserved wall paintings and their underlying structural support did not show temperature inhomogeneities that can be correlated to integrity risk and humidity. Additional tests, with the use of external thermal excitation source (IR lamps), may be needed to confirm the equilibrium of the church walls' condition.

However, some areas of moisture capillary rise in the low part of the building structure were revealed by the Passive IR Thermography on-site inspection. As illustrated in Fig. 43, acquired within the temperature range 27.1 – 29.1 °C, at the distance of approximately 2 m, the areas showed high contrast in thermal distribution and can be detectable without the use of external excitation sources. This type of information can be obtained immediately in-situ, with or without subsequent thermal images analysis and post-processing.

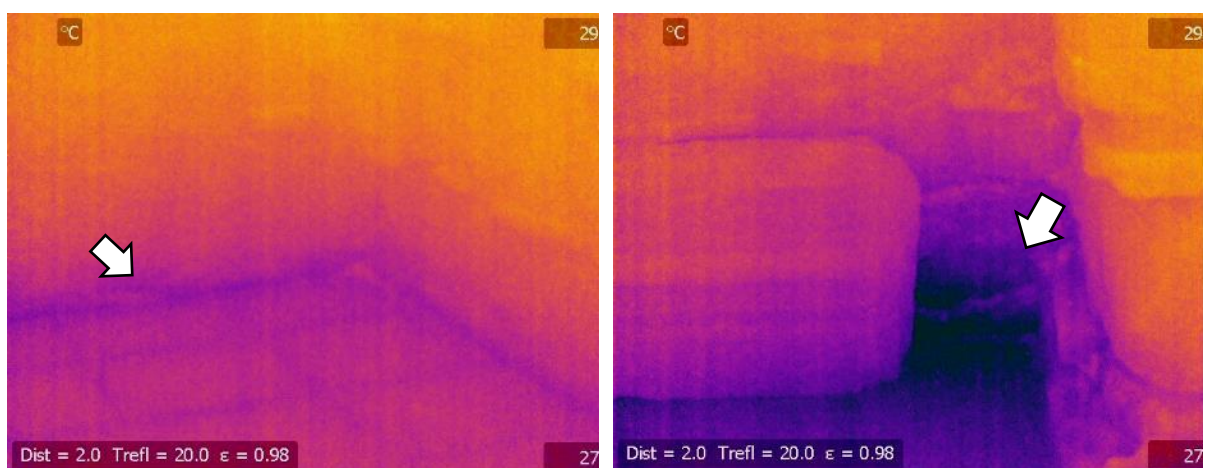


Figure 43. Wall moisture rising (floor level) detected by Passive Infrared Thermography inspection. The area of acquisition is indicated in Fig. 39.

4.4.3 Discussion of the results

Multispectral Imaging and Passive Infrared Thermography, both full-field and non-contact techniques, were applied in this case study with several limitations, due to the given in-situ acquisition conditions.

These methods proved, however, their capability to provide preliminary information for monitoring of surface and subsurface conservation state of integrated wall paintings after structural damage and subsequent restoration interventions.

The acquisition and analysis of multispectral images was performed in the absence of color reference chart. This case study is representative and challenging in terms of site conditions, which can be faced by Cultural Heritage experts: limited opening hours (just a few hours per week), strict accessibility regulations, impossibility to use scaffolding, control the lighting conditions and use thermal excitation sources.

The stacks of spectral images, acquired in reflected mode on a selection of wall paintings from the 16th century inside the Catholikon, was analysed using exclusively qualitative image processing tools. The methodology applied in this case study confirmed the applicability of RGB transformations and blending functions on non-calibrated images for the revealing of underdrawings and enhancement of lost details in degraded areas. As concluded from the image processing tests on the spectral images acquired in this case study, the combination of information from visible and infrared spectral bands by the means of commonly available Adobe Photoshop software program can be helpful to locate and enhance finer details of the underdrawings and lost details. In this or similar case studies, luminosity blending mode with the inversion of the tone values on dark areas of a wall painting is recommended (see attachment G). The differentiation between similar pigments and mapping of certain pigments would not produce reliable results, due to irregular surface characteristics and uncontrolled lighting conditions in the absence of a color reference chart.

The recommended image acquisition and analysis workflow and the selected image processing procedure can be found in attachments D and E respectively. The detailed description of each of the image processing functions, tested in this project, is reported in the attachment G.

The in-situ passive infrared thermography inspection inside the Catholikon of Dafni Monastery (Athens, Greece) was performed in the absence of sufficient thermal gradient between and outside the church. The technique showed its limited applicability for rapid in-situ structural and subsurface diagnostics by solely visual observation of thermal images. However, even in natural conditions, the technique was capable to detect the presence of the moisture capillary

rise at the bottom level of the building structure, lower than the decorated part of the walls. Further tests might be needed for in-depth study and confirmation of the subsurface and structural condition of the wall decoration support.

Both techniques, Multispectral Imaging (applied only in reflectance mode) and Infrared Thermography (applied in passive mode), full-field and non contact, within site condition limitations, proved to be useful for regular monitoring of general conservation state, highlighting the main areas of interest for further art historical study (decorated layer) and risk areas of possible structural damage (subsurface and structural support).

The brief observations to the research questions of this case study are summarized in Table 12.

Table 12. Results of the acquisitions in the Catholikon of Dafni Monastery, Athens

Research question	Results and observations
- Can Multispectral Imaging be used to in-situ reveal underdrawings and degraded details to support the art historical and material study in this specific case study?	Yes, even in the absence of a color reference chart: by comparison of different spectral bands (VIS and IR), facilitated and enhanced by the means of free and/or commonly available software tools.
- Can Multispectral Imaging be used to identify and/or to differentiate between pigments in this case study?	Yes/no. It should be performed only on calibrated images by the means of dedicated software tools (Profilocore or ENVI). It was not possible due to in-situ acquisition conditions.
- Can Infrared Thermography, applied in passive mode, provide immediate information about the condition of subsurface and structural support underneath the wall paintings in this case study?	Yes/no. It is possible only in the presence of an adequate thermal gradient. It depends on the season and environmental conditions. Repetitive tests might be necessary.
- What are the main limitations of these techniques applied in-situ in this case study?	For MI: Limited access (open just a few hours during the week), impossibility to completely darken the environment (for the use of MI in fluorescence mode) and the impossibility to

	<p>use the complete set of recommended acquisition arrangement (color checker and positioning the flashlights)</p> <p>For IRT:</p> <p>Insufficient natural thermal gradient</p>
--	---

5. IN-SITU NON-INVASIVE MEASUREMENTS OF WALL MOSAICS

The selected case studies are part of interdisciplinary research projects held by the scientific staff of the Department of Cultural Heritage of the University of Padova (Italy) in collaboration with the National Technical University of Athens (Greece). These wall mosaic decorations are representative in terms of high historical and archaeological value and main conservation challenges to be faced by Cultural Heritage experts in these or similar real cases.

Table 13. List of case studies and main conservation challenges

Case study	Period	Main conservation challenges
Church of Santa aria dell’Ammiraglio, called “La Martorana” (Palermo, Sicily – Italy)	Byzantine wall mosaics (with later restorations and reshufflements)	Heavily reshuffled mosaic panels, undocumented restorations and reintegrations of tesserae in vault and wall mosaics
Palatine Chapel (Palermo, Sicily – Italy)	Byzantine wall mosaics (with later restorations and reshufflements)	Different periods, undocument restorations and reshufflements
Catholikon, Dafni Monastery (Athens, Greece)	Byzantine wall mosaics	Lack of historical documentation, loss of decoration material (only a few mosaic fragments preseved), regular monitoring after recent restoration (conservation problem due to effluorescence of tesserae)
Main porch of Saint Mark Basilica (Venice, Italy)	Byzantine and 16th century wall mosaics	Lack of historical documentation, study of material and execution technique, acquisitions during the restoration campaign

5.1 Church of Santa Maria dell’Ammiraglio, called “La Martorana”

5.1.1 Case study description

The church of Santa Maria dell’Ammiraglio (church of St. Mary’s of the Admiral) was the pious foundation by George of Antioch, Admiral of the Fleet of Roger II (Second) of Sicily (Fig. 44). The precise date when the Admiral began to build the church is not known. In the only preserved historical document, Admiral’s charter, which bears the date 1143, the founder speak about the building of the church in past sense and refers also to its embellishment. No precise dates are provided about the mosaics, though they were certainly concluded by 1151 when George of Antioch died.

After this date, there were several milestones in the history of the church.

1193-94: the foundation of the Benedictine convent of the Martorana on the land directly adjacent to the Admiral’s church.

1433-34: the absorption of the church by the Benedictine convent and the first changes.

16th century: drastic architectural changes.

From 1683 until the middle of the 18th century: building activity involving extensive redecoration in baroque style, with numerous interventions.

1770-73: Restoration work directed by Giuseppe Patricolo.

1870: another drastic restoration of the church.

Some tesserae were reused but relocated away from their original position. Mosaic tesserae replicas at the end of the 19th century were commissioned from Murano glass foundry (Venice), led in this period by Lorenzo Radi. The examples of mosaic tesserae were sent to Venice, with a request to reproduce the exact colour of the historical tesserae. The mosaics were restored using mortar with the addition of linseed oil, which subsequently was the cause of the appearance of stains on the white tesserae (porous stone) [194-195].

However, the last restorations of the end of the 20th century and beginning of the 21st century, are documented in details. There were several restoration campaigns: 1939, 1946, 1952, 1968, 2010-2012.

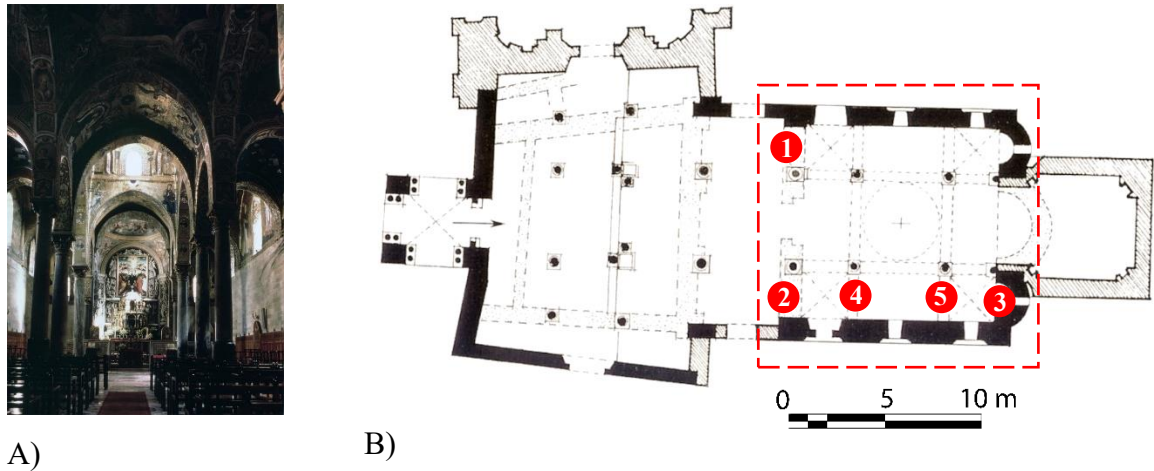


Figure 44. Church of Santa Maria dell'Ammiraglio, current state: a) interior of the main nave [196]; b) groundfloor plan [197], the original byzantine nucleus is highlighted by the dashed red rectangle. The red dots indicate the location of investigated wall mosaic decorations, presented in this thesis: 1) mosaic panel "Dedication of the Church to the Virgin"; 2) mosaic panel "Coronation of King Roger II"; 3) Saint Anna; 4) Saint Apostles Andrew and Peter; 5) Saint Apostles Jacobus and Paul.

It is believed that the atelier that executed the mosaics of the church of Santa Maria dell'Ammiraglio was a separate entity distinct from the one, which was operating during the same period in the sanctuary of the Palatina Chapel [194]. The atelier must have been procured from a metropolitan Byzantine milieu (social environment) and it is possible that the team working on the mosaics of the church of Santa Maria dell'Ammiraglio came from Constantinople [194].

The mosaic decorations can be divided into categories:

- **Individual figures** (the Pantocrator and the adoring archangels, the Virgin, the chorus of the Prophets, the Evangelists, the Apostles, the Saints).
- **Scenes** (the Annunciation, the Presentation of Christ at the temple, the Nativity and the Dormition of the Virgin). All belong to the so-called "Feast Cycle" (it corresponds to the most important festivals in the Greek liturgical calendar), that is to the canonical series of images that in Byzantine art represents the salient facts of the life of Christ and the Virgin. They are called dodekaorton, a canonical series of twelve scenes that begins with the Annunciation and ends with the Dormition. From this cycle the creator of the mosaic program, resumed the scenes that see the virgin protagonist, thus stopping the focus more on her than on Christ.
- **Dedicatory panels** (the two mosaics representing the coronation of King Roger by Christ and the dedication of the church by George of Antioch to the Virgin Mary).

The main questions by art historians, in this case, are related to the execution technique, comparison of materials and techniques to other examples of Byzantine art, to possible reshufflements and restorations on mosaic decorations inside the church. Particular attention was dedicated to the Dedicatory panels. These mosaics are believed to have been transferred and rearranged during the 16th century. Since the documentation about the past restoration interventions is missing, the informativity of applied non-invasive techniques is crucial for differentiation between the original and integrated parts of the mosaics: original tesserae in place, original tesserae reused and relocated and more recent integrations.

The two mosaics showing George of Antioch prostrating himself in front of the Virgin Mary, called further *Dedication scene*, and King Roger being crowned by the Christ, called further *Coronation scene*, are now located respectively in the northern and southern lateral aisles of the New Church. They occupy eastern walls of the spaces, framed in baroque settings. They are roughly of the same size and, compositionally, they balance each other. Also, in the Cathedral of Monreale, where the wall mosaics show many similarities to those in La Martorana church, the two dedicatory panels, featuring King William II, the founder, with the Christ and the Virgin respectively, were placed and remain till now facing each other on opposite walls of the church [186]. At the Church of Santa Maria dell'Ammiraglio, the original location of the two panels cannot be determined with certainty, but it is believed that they had been in the inner narthex [194]. Despite the heavy damage undergone by the dedicatory panels, especially in the lower parts of the mosaic panel, some studies help reconstruct possible original appearance of the mosaics (Fig. 45 and 46).

Some studies revealed its possible original appearance of George from Antioch in the Dedication scene. Its pose, called proskynesis, is similar to numerous examples in Byzantine art. E. Kitzinger [194] assumed that the bent knee, lower leg and foot of George from Antioch were originally visible beneath the cloak. His head and hands have not been materially affected by restoration. The figure of the Virgin, Hagiosoritissa type, holds a scroll with a long text, which is a poem in which she intercedes with her son on behalf of "him who lies at my feet" [198].

At the left edge of King Roger in Coronation scene mosaics, there are remnants of what must be considered as the original frame and the original mosaic surface may have extended somewhat further to the right. Altogether, the composition seems lopsided, being crowded on the right when to the amount of empty background on the left. Both mosaics, definitely, suffered distortion because of the transfer to their present locations and the creation of their present framework. Both panels are supposed to be originally less tall.



Figure 45. Presumed reconstruction of the original state of the mosaic “Dedication of the Church to Virgin” after E. Kitzinger [194].

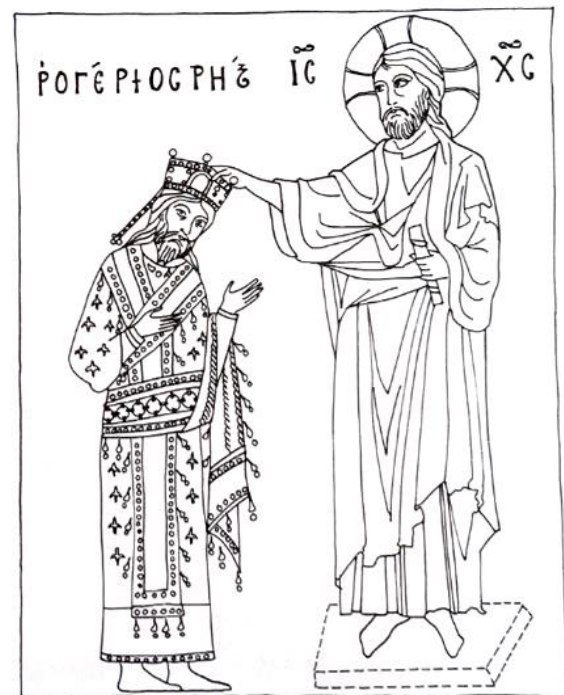


Figure 46. Presumed reconstruction of the original state of the mosaic “Coronation of King Roger” after E.Kitzinger [194].

The access to the church was allowed only during opening hours and in the presence of tourists. The in-situ tests were performed by the means of multispectral imaging and infrared camera. The thermal gradient was not sufficient for revealing discontinuities by passive infrared thermography. The results are not presented here.

5.1.2 Acquisition and analysis of multispectral images

The instrument Nikon D800 FR (Full range) camera with a 36-megapixel sensor was used. The camera has been modified, removing the internal UV and IR filters, to collect different images in the UV-VIS-IR range using specific external band-pass filters. A couple of modified Nikon speedlight flashes (Nikon SB 910) including excitations in the UV and NIR ranges was also used. During the acquisition, these flashes are in general positioned at 45° with respect to the measured surface, whereas the camera is placed between the flash lights and pointed orthogonally to the surface. The multispectral images, where it was possible (e.g. in *Dedication panels*), were then calibrated using a colorchecker provided with the camera and placed close to the wall paintings during the acquisition. Five external band-pass filters were used in this case to take the pictures in the UV-Vis-NIR ranges: one for the UV range (350-420 nm), one for the visible range (about 400-700 nm) and three different filters for the near infrared range (IR1= 720 nm, IR2= 850 nm, IR3= 950 nm). Before analysing in alternative software tools, the collected photos were converted from raw images (.NEF) to 16-bit Tagged Image File Format (TIFF) with minimal processing (without white balance and brightness corrections or stretching or pixel rotations) using the NX Viewer free software.

The list of multispectral acquisitions, according to the research questions of art historian Professor Beat Brenk (University of Basel, Switzerland), performed inside the Church of Santa Maria dell'Amiraglio is reported as follows:

- Dedication scene (“Dedication of th Church to the Virgin”), without (no CC) and in presence of Profilocolore color checker;
- Coronation scene (“Coronation of King Roger”), without (no CC) and in presence of Profilocolore color checker;
- Apse mosaic of Saint Anna (no CC);
- vault mosaics of Saint Apostles Andrew and Peter, Jacobus and Paul (no CC);
- wall mosaic Nativity scene (no CC).

The experimentation was focused on the potentialities of the technique as a non-invasive tool to support the iconographic and material study of the wall mosaics as an easy portable prescreening tool in analytical investigation.

The qualitative examination procedure started with the observation of raw images using Nikon dedicated visualization software (NX Viewer). Subsequently, after conversion of the images to TIFF format, several common image editing software programs (free software: Image Enhancer; ImageJ, commercial software: Photoshop) were tested for calibration, enhancement and preliminary examination of acquired images. The multispectral images acquired in the presence of a Profilocore color checker on the two Dedicatory panels were analysed by the means of dedicated Profilocore software.

The main research questions of this case study are the following:

- Can Multispectral Imaging be used in this case study to differentiate between original and restored/reintegrated mosaic areas (tesserae and binder)?
- Can Multispectral Imaging be used in this case study to differentiate between similar tesserae of distinct composition?
- Can Multispectral Imaging be used in this case study to identify the composition of the tesserae?
- Can Multispectral Imaging be used in this case study without a color reference chart? If yes, what are the potentialities and limitations?
- Can Infrared Thermography be used in this case study to reveal information about the homogeneity in the mosaic subsurface and about stability/preservation state of the structural support (wall, vaults etc.)?
- Can Holographic Subsurface Radar be used in this case study to reveal discontinuities and defects in the mosaic subsurface layers?
- What are the main limitations of Multispectral Imaging, Infrared Thermography and Holographic Subsurface Radar techniques when applied in-situ to wall mosaics?

Additional questions by art historian Prof. Beat Brenk were related to the potentialities of Multispectral Imaging to enhance the differences in mosaic execution technique and provide information about the original composition/preparatory drawing if available etc.

Acquisition and analysis of multispectral images of the Dedicatory Panels

The first acquisitions were focused on the Dedication and Coronation scenes (Fig. 47 and 48). The multispectral camera was placed at the height of 1.5 m at the distance from 2.5 – 3 m from the panels, following the standard acquisition geometry and using Profilocolore color checker. As described above, there is no historical documentation about their restorations, rearrangements and relocation within the church interior. The mosaic panels are planar, unlike the curved surface of the most part of the vault mosaics inside the Church “La Martorana” and they are easily accessible. The distance from the camera to the decoration can be changed and significantly reduced. The surface can be observed by the naked eye at a close distance with no need of scaffoldings.

Main problems that were observed during the examination of raw non-elaborated images of the mosaic panels are related to:

- irregular surface of the decorations, due to the orientation of mosaic tesserae, previous rearrangements and due to the characteristics of underlying substrate;
- distance from the camera to the examined wall decorations (many mosaics are located in the vaults and apses of the church and the distance reaches more than 5 m).
- acquisition conditions, i.e. artificial illumination, which cannot be switched off during opening hours of the church, impossibility to darken completely the environment in order to use MI in fluorescence mode, continuous flow of tourists within the interior area.

The tesserae are opaque but very glossy. Even if standard geometry of flash lights illumination is maintained (45°), it is almost impossible to avoid artefacts created by glares and shadows on the surface, due to the general geometry of the surface and small irregularities in tesserae placement. Therefore, as stated almost immediately, complementary methods are necessary to discriminate between real anomalies (i.e. different material composition) and those, related to the surface characteristics of the wall decoration.

Some visibly homogeneous tesserae (of equal color) revealed to reflect and to absorb light differently in the infrared range. Such differences are clearly observed in the cloak of George from Antioch from the Dedication scene (Fig. 49). As the mosaic panel was transferred, some tesserae were probably reused and other ones were substituted by replicas. Both artificial and natural black glass tesserae (obsidian) could be used in Byzantine wall mosaic decorations.



A)

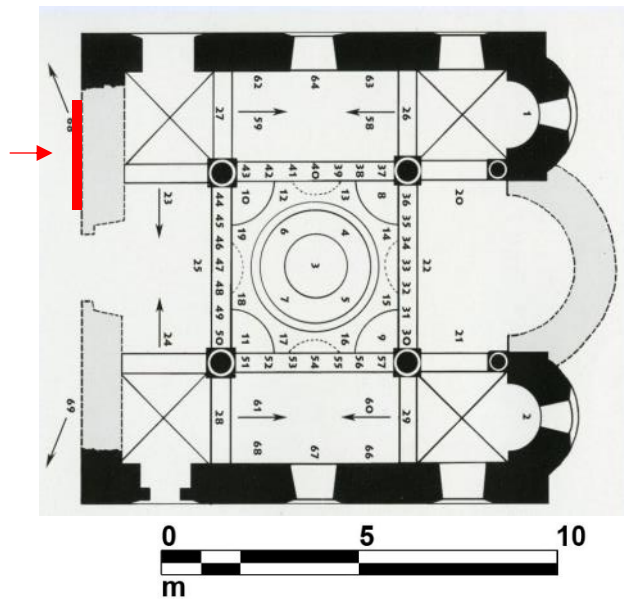


Figure 47. Mosaic panel “Dedication of the Church to the Virgin” (Dedication scene): a) visible light image; b) location of the investigated mosaic panel inside the church.



A)

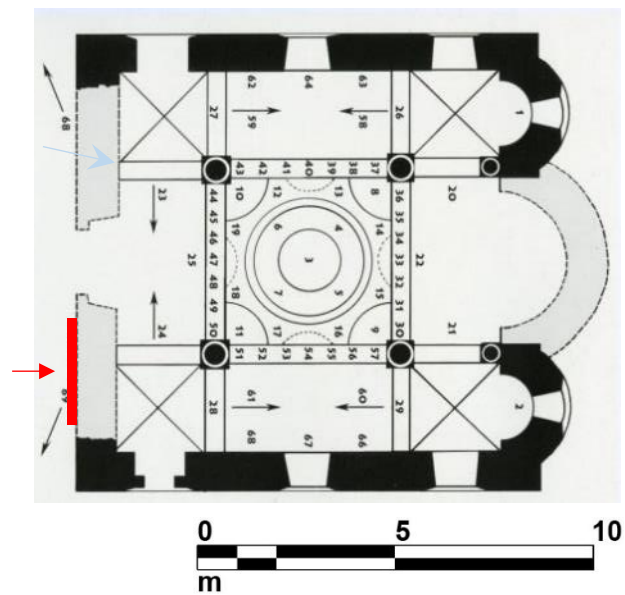


Figure 48. Mosaic panel “Coronation of King Roger II” (Coronation scene): a) visible light image; b) location of the investigated mosaic panel inside the church.

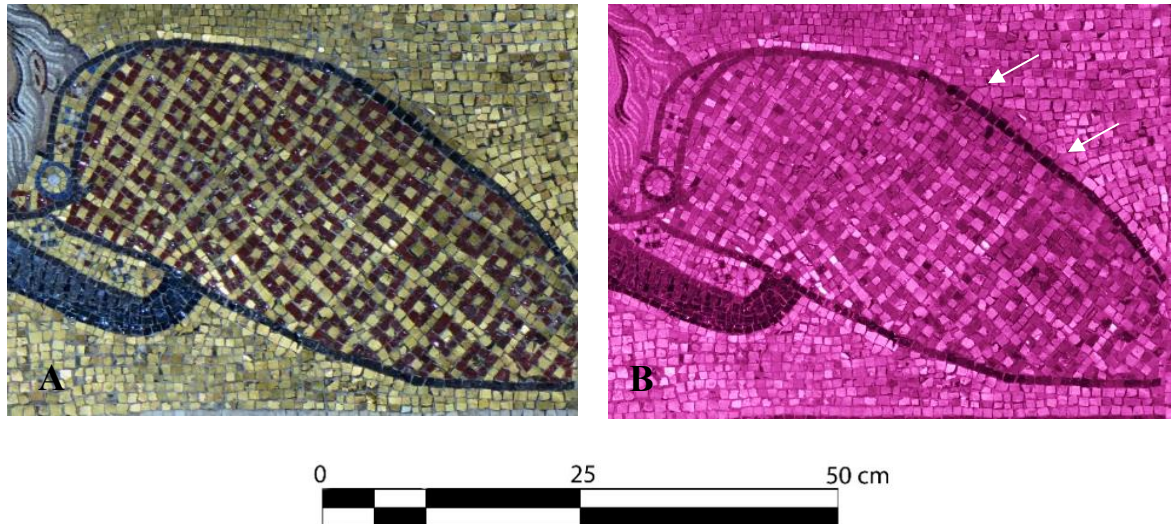


Figure 49. Fragment of the mosaic panel, a reshuffled area of the figure: a) non-elaborated visible image; b) non-elaborated infrared image (IR2).

In the visible range, we can observe wide and smooth gradation of skin brightness and tone on the cheeks of the Virgin's face in the Dedication scene (Fig. 50a). The infrared image, on the contrary, reveals the presence of a clearly outlined frame, consisting of darker, i.e. more absorbing in the infrared range, surface material. The absence of reflectance gradations in the infrared image (within the outlines schematic frame all the tesserae show homogeneous pixel brightness), as shown in Fig. 50b, can be related to different factors:

- the same stone material/the same composition of glass paste tesserae was used for cutting the tesserae, with minimal differences in tone and colour, which cannot influence the tesserae reflectance/absorption values in the infrared range;
- there is an overpaint by infrared transparent pigment, which may have been used to enrich the palette of the tesserae underneath.

Furthermore, a darker stain can be observed on the neck of the Virgin (indicated by a blue arrow in Fig. 50c), is detectable in the visible and enhanced in the ultraviolet band. It can be related to the restorations of the end of the 19th century when mortar with the addition of linseed oil was used. With time, the linseed oil, which does not polymerize quickly, penetrates into the pores of stone tesserae used for the face areas, resulting in staining of the decoration surface.



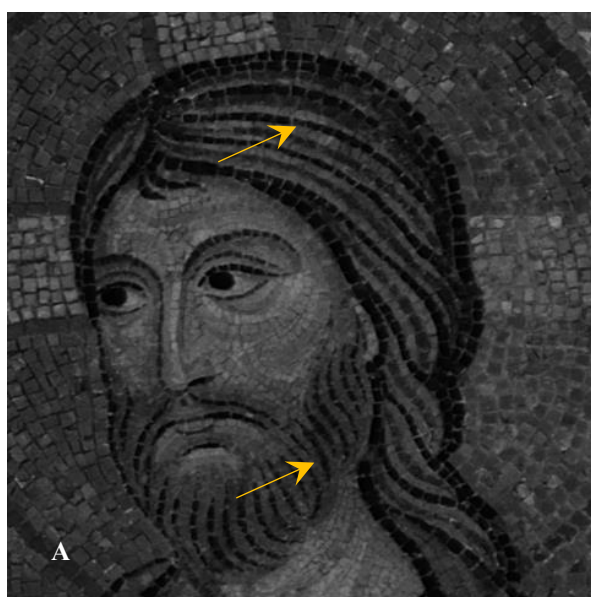
A)

B)

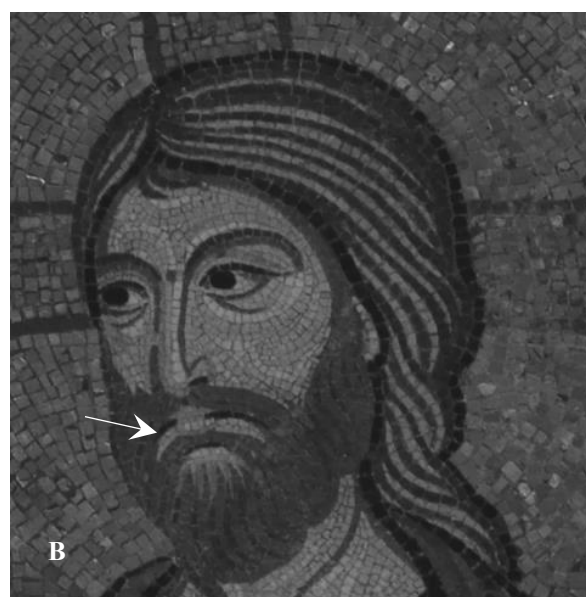
C)

Figure 50. A stack of raw non-elaborated spectral images. Fragment of the Virgin's face: a) visible image; b) infrared image (IR2); c) ultraviolet image (UV). The yellow arrow indicates the variations in colour and brightness of the face tesserae, observed in the visible and ultraviolet range, not detectable in the infrared range. The white arrow shows the discontinuities in the golden tesserae of the background. The light blue arrow indicates a darker stain on the neck of the Virgin.

Detailed observation of the face of Christ (Coronation scene) in different spectral bands helped to reveal some inhomogeneities. As shown in Fig. 51, the grayscale visible and infrared images present significant differences: some of the visually black tesserae appear darker in the infrared range while other visually black tesserae show the same brightness as the surrounding tesserae, seen as grey in the visible range. This difference in the infrared range clearly indicates the use of black tesserae of at least two types for the face of Christ. The qualitative multispectral approach cannot provide further information but can help differentiate between these groups of tesserae.



A



B

Figure 51. Fragment of the face of Jesus Christ. Comparison of a grayscale visible image (a) and a grayscale infrared (IR2) image (b). The raw images were converted to greyscale using Image Enhancer software. The white arrow indicates the differences, which are detectable in the infrared and not detectable in the visible range. The yellow arrows indicate the visible differences that are not detectable (or less distinguishable) in the infrared range.

Subsequently, several commonly used editing software programs (free software tools: Image Enhancer; ImageJ, commercial software tools: Photoshop) were tested for the improvement of the results of qualitative examination of the acquired images (see attachment E and G).

False colour images were produced using the function of RGB channels rotation in Image Enhancer and Adobe Photoshop (see attachment G). Some differences are enhanced and immediately distinguishable, due to an unusual perception of the colour by the eyes of the observer. The function of Edge detection, by the means of Image Enhancer (for the image processing descriptions see attachment G), showed potentialities in recognition of the discontinuities in pixels distribution. The brighter is the area, the more discontinuities in pixel values distribution are detected there. Brighter areas may indicate the presence of changes in surface orientation, material properties and scene illumination.

Among the tested functions, subtraction and difference algorithms between visible and infrared images were applied in the comparison between Adobe Photoshop and ImageJ. Fig. 52 shows the result of difference function by the means of ImageJ between the visible (VIS) and infrared (IR2) images which were previously converted to a grayscale mode using Image Enhancer. The Fig. 53 shows the result of difference function by the means of Adobe Photoshop between the visible (VIS) and infrared (IR2) images which were previously converted to a grayscale mode using Image Enhancer.



Figure 52. Result of Difference function, applied to the non-elaborated visible and infrared images, by the means of ImageJ. Fragment of the Dedication scene.



Figure 53. Result of subtraction between visible and infrared non-elaborated images, using Adobe Photoshop. Fragment of the bottom part of the Coronation scene. The red arrows indicate the presence of discontinuities which may help in locating possible stitches of the mosaic fragments.

Qualitative analysis by the means of Profilocolore dedicated software

The results of qualitative and semi-quantitative analysis by Profilocolore dedicated software were used to compare the informativity between the calibrated and non-calibrated images, as well for the evaluation of reliability, potentialities and limits of alternative software tools. The

result of PCA 4 analysis [19] clearly shows differences in the characteristics of mosaic tesserae in the left bottom part of the Coronation scene.

Combinations of three bands by the means of alternative free software tools were also tested. The ultraviolet, visible and infrared images were converted to grayscale mode using Image Enhancer. The resulting image contained the combined information from the three bands: the difference in pixel brightness values between visible and infrared images, with the addition of brightness values of a grayscale UV image. The tests were performed by the means of ImageJ and Adobe Photoshop. The selection of these spectral bands is due to the fact that differences between the visible and infrared image may indicate the presence of distinct material composition and the brightness parameters of the ultraviolet image reflect the superficial distribution of eventual organic restoration and consolidation materials. All these photos are non-calibrated and acquired at the same lighting conditions. Any type of information from the non-calibrated spectral images should be analyzed considering that the differences can be partially related to the artefacts produced by the inhomogeneity of illumination and irregularity of the surface. These transformations helped enhance the differences in mosaic technique between areas that can indicate presumably original and reshuffled areas. It is shown by the comparison of image analysis results by the means of Profilocolore software (Fig. 54a) and alternative image analysis tools (Fig.54b). As shown by comparison in Fig. 54, the results of calculations performed on non-calibrated spectral images contain noise since the frame resolution varies between different bands, and artefacts, which derive from the inhomogeneous lighting conditions (Fig. 54b).

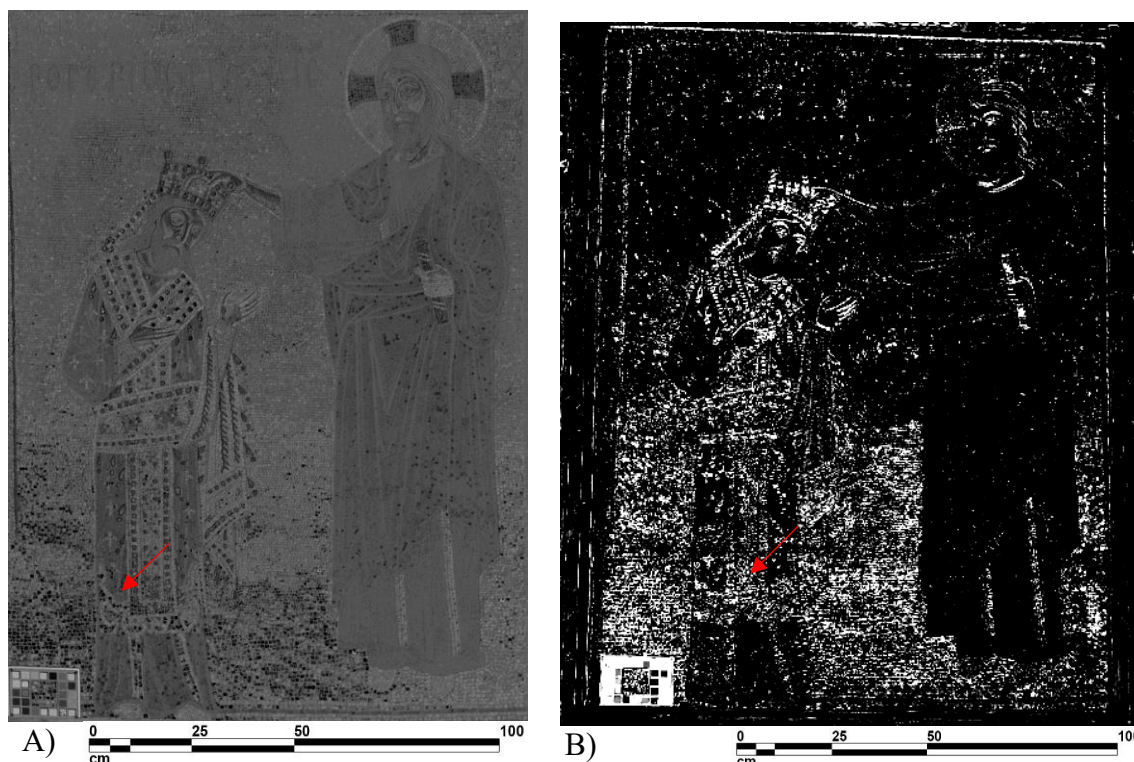


Figure 54. Coronation scene, combined analysis of several spectral bands: a) result of a Principal component analysis (PCA 4) performed on calibrated spectral images by the means of Profilocolore software; b) Combined analysis, performed on non-calibrated spectral images by the means of ImageJ (difference between the pixel values in visible and infrared images and addition of pixel value sin the ifnrared range).

Therefore, the combination of more than two non-calibrated images cannot be considered as a reliable scientific tool for the analysis of multispectral images in this case study.

Differentiation between similar tesserae in the Dedicatory panels

Detailed qualitative analysis approach was tested for differentiation between similar tesserae. Visual observation and integration of simple image processing algorithms were used for the evaluation of homogeneity in the distribution of red, black and golden tesserae on the mosaic panels. This approach allowed preliminary evaluation of homogeneity in the gilded tesserae of the background.

The red tesserae employed in the “Dedication of the church to the Virgin” and in the “Coronation of King Roger” are of glass paste and characterized by a highly smooth and very glossy surface. Some of the red tesserae respond with a glare, due tho the differences in angle of inclination of tesserae. From this point of view, the comparison and analysis of reflectance values of singular tesserae without complementary information about the surface morphology

cannot be reliable and scientifically correct. In terms of size, two types of red tesserae can be distinguished: tiny tesserae (5 x 5 mm), used for the face features and hands contour, and big tesserae (10 x 10 mm) for the halo, vestments and feet.

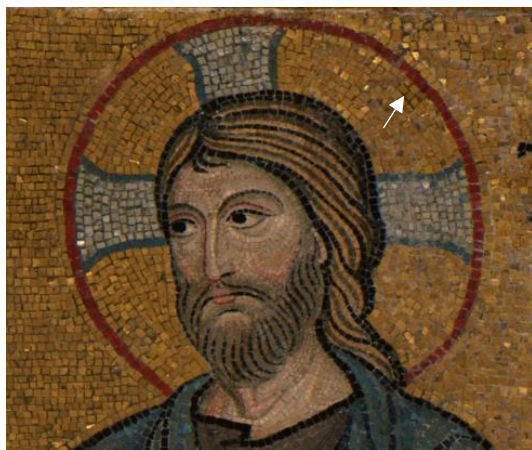
In the infrared range, big red tesserae in the halos of the Virgin and of the Christ are indistinguishable from the golden background (Fig. 55). The infrared image in both cases shows more inhomogeneities in the surface reflectance of the background (gilded tesserae) and of the Halo of the figures. The inhomogeneities between the red tesserae are enhanced in the infrared range, as shown in Fig. 56.



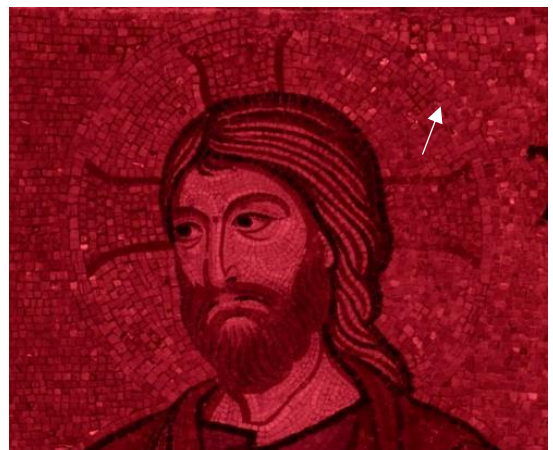
A)



B)



C)



D)

Figure 55. Halos of the figures. Comparison of raw non-elaborated images: a) Virgin Mary, fragment of the Founder's Panel, raw non-elaborated visible image (VIS); b) Virgin Mary, fragment of the Founder's Panel, raw non-elaborated infrared image (IR2); c) Jesus Christ, fragment of the Coronation scene, raw non-elaborated visible image (VIS); d) Jesus Christ, fragment of the Coronation scene, raw non-elaborated infrared image (IR1). The arrows indicate the red tesserae that in the infrared range appear indistinguishable from the gilded background.

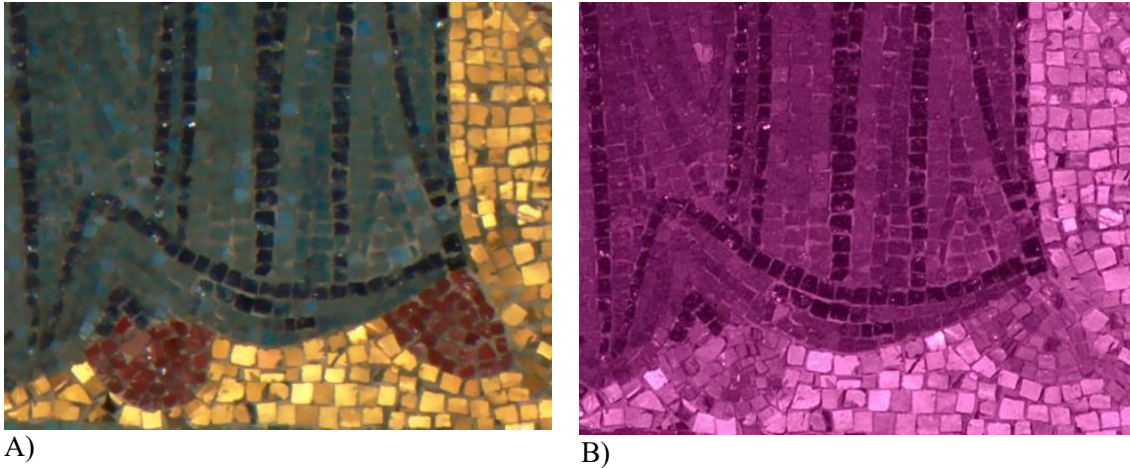


Figure 56. Feet of Virgin, Dedication scene. Differences in red tesserae: a) raw non-elaborated visible image (VIS); b) raw non-elaborated infrared (IR2) image.

Acquisitions of multispectral images on curved decorated surfaces inside the church

Multispectral acquisitions on other mosaics inside the Church of Santa Maria dell’Ammiraglio were complicated by the following factors:

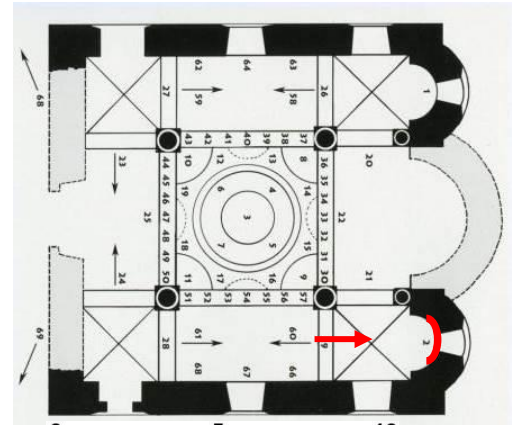
- **shape of the decoration support:** curved apse or vault;
- **site conditions**, i.e. non adequate artificial lighting, limited physical accessibility, distance and structural obstacles.

In this specific case, it was not possible to mitigate these factors. Complementary methods may be necessary to discriminate between real anomalies (i.e. different material composition) and artefacts that may appear due to the geometrical features of the supporting structure and site conditions. In this specific case, the impact of the curved form is very strong, particularly in MI acquisitions on the mosaic of Saint Anna, located in the southern apse of the church (Fig. 57). The acquisitions on the apse mosaic were performed following the standard acquisition geometry. The distance from the camera to the apse mosaic was approximately 7.5 m.

Observation of spectral images showed that all the gold tesserae (background, vestments and halo) are relatively homogeneous in their form and size. Many of them miss the final golden leaf cover, resulting in a shimmering effect on the background. It is possible that partially the absence of golden leaf in some of the tesserae was intentional.



A)



B)

Figure 57. Apse mosaic of Saint Anna: a) visible image; b) position of the mosaic in the church nucleus



A)



B)



C)

Figure 58. Apse mosaic of Saint Anna, face details fragment: a) raw non-elaborated ultraviolet image; b) raw non-elaborated visible image (VIS); c) raw non-elaborated infrared image (IR1).

Big red and gold tesserae appear similar in the infrared range. They present similar distribution of variabilities in infrared reflectance values, comparable to the tesserae used in the Dedication and Coronation scenes. The tesserae of the vestment of Saint Anna show inhomogeneous reflectance values in the infrared range (Fig. 59). The most pronounced discontinuities between visible and infrared ranges, however, were observed in the blue tesserae, as indicated by a white arrow in the Fig. 59a and 59b. Some blue tesserae of the sleeve edge of Saint Anna, indistinguishable in the visible range, are of different composition and most probably not original (substituted or overpainted). They show stronger reflectance values in the infrared range. The red tesserae of the halo are clearly visible in the visible range but indistinguishable from the gold tesserae in the infrared range (Fig. 60a and 60b).

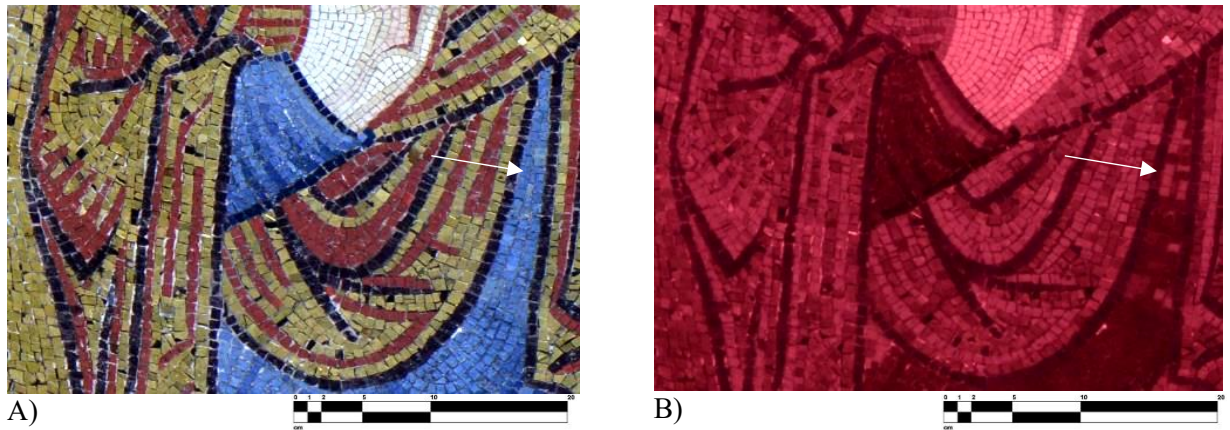


Figure 59. Fragment of the vestment of Saint Anna in non-elaborated visible (a) and infrared IR1 (b) images. Infrared image reveals inhomogeneities in the distribution of tesserae. The white arrows indicate the location of blue tesserae showing different reflectance values in the infrared range.

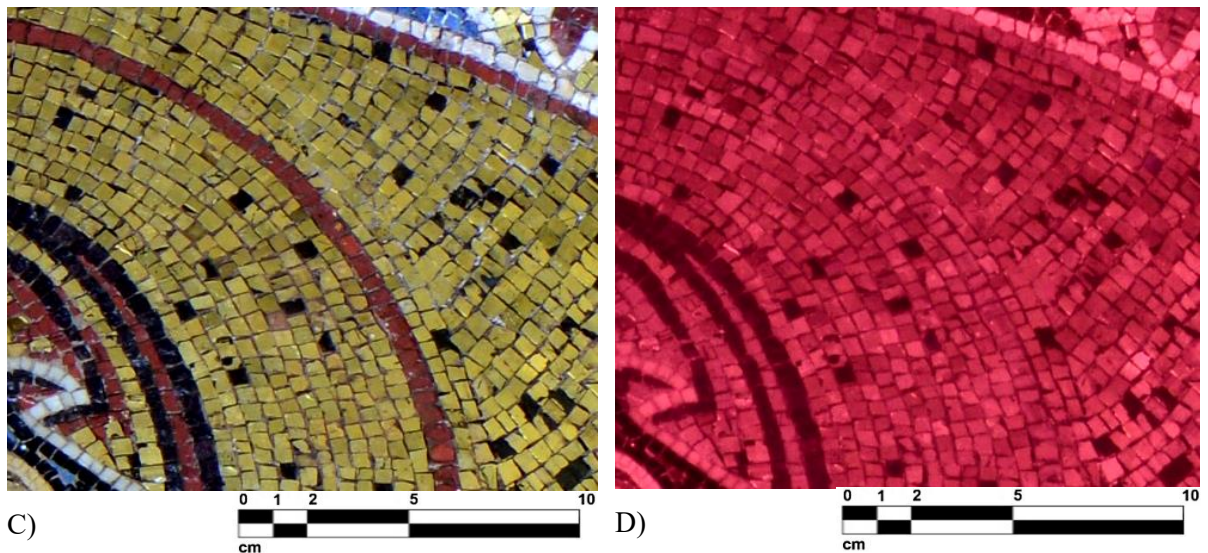


Figure 60. Fragment of the halo of Saint Anna. Red tesserae appear indistinguishable from the gold tesserae in the infrared range. a) non-elaborated visible image; b) non-elaborated infrared image (IR1).

The smooth and glossy tiny dark black tesserae are used for the eyes, eyebrows and in the area around the face of Saint Anna, as shown in Fig. 61. More rough big black tesserae (dark grey) are found in folds of the vestment and letters on the golden background. The differences are enhanced in the infrared range.

In Fig. 62, the white arrow shows some of the tiny red tesserae that present distinct reflectance values in the infrared range. Entire rounded tesserae were used for each of the eye pupils and they are characterized by slight asymmetry in form.

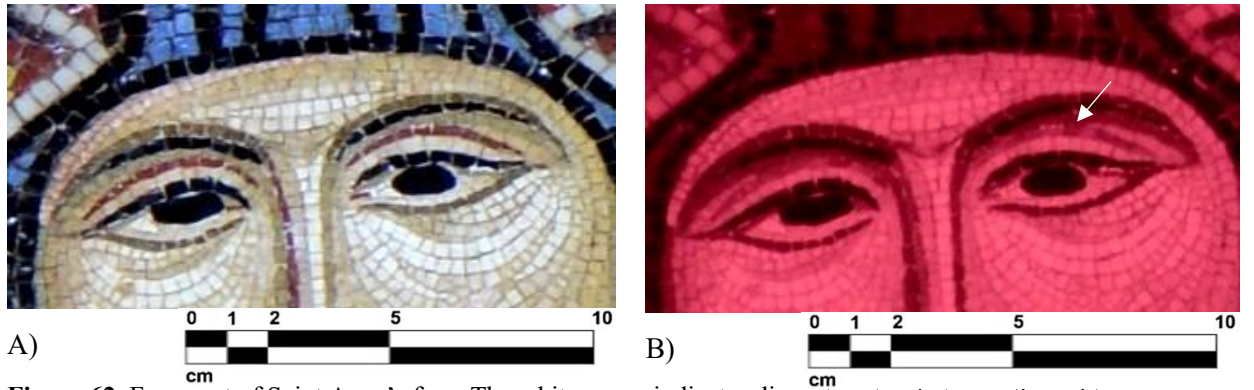


Figure 62. Fragment of Saint Anna's face. The white arrow indicates discontinuities between the red tesserae, detectable in the infrared range: a) raw non-elaborated visible image (VIS); b) raw non-elaborated infrared image (IR1).

The same acquisition and analysis procedure was followed for the Saint Apostles mosaics, located in the southern nave of the church (Fig. 63). The distance from the camera to the vault mosaics was approximately 7 m.

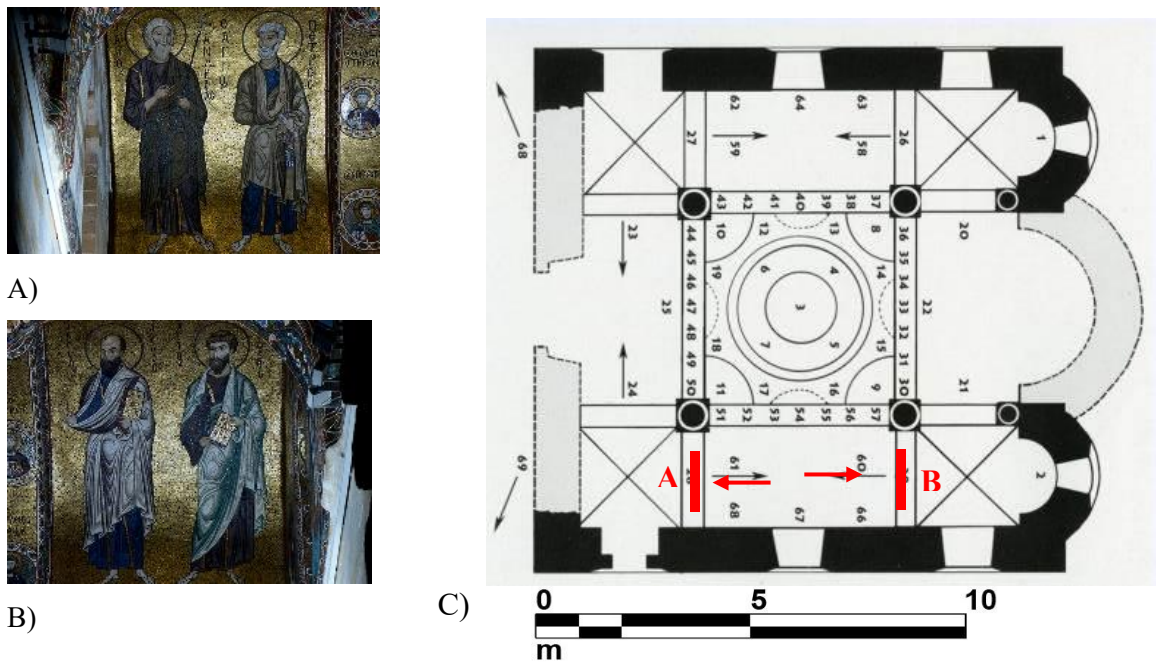


Figure 63. Saint Apostles vault mosaics. a) Saint Andrew and Saint Peter; b) Saint Jacobus and Saint Paul; c) Position of the mosaics inside the byzantine part of the church.

Unlike the red tesserae in the halos of the mosaic panels and in the halo of Saint Anna, the red tesserae in the halo contour of the Saint Apostles appear clearly distinguishable on the golden background in the infrared range (Fig.64).

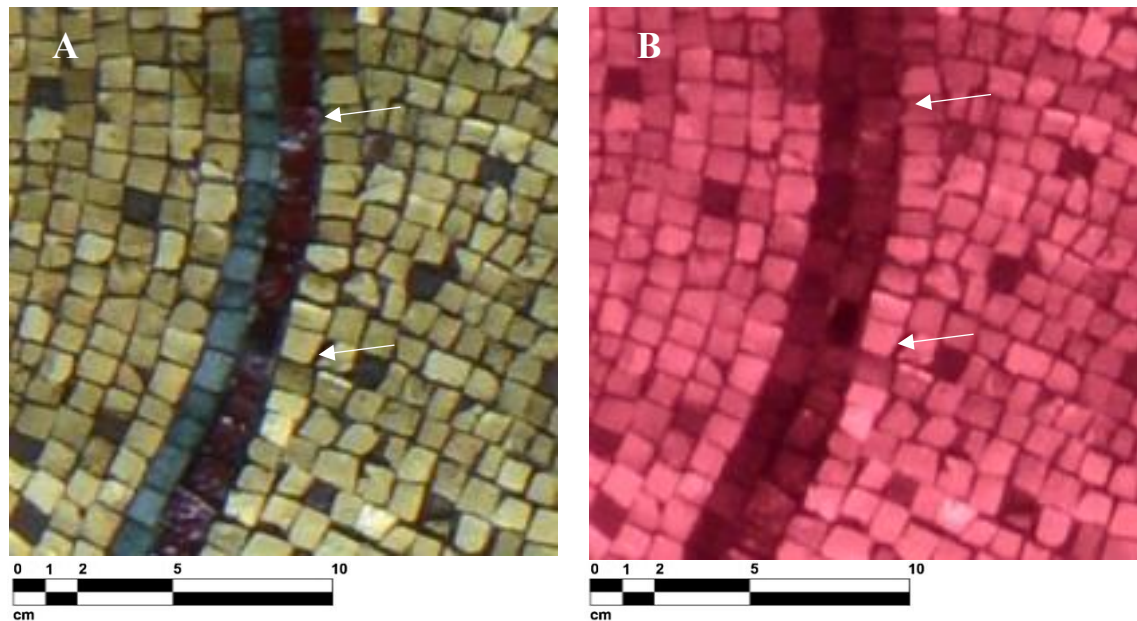


Figure 64. Saint Apostle Paul, fragment, red tesserae on the golden background. a) non-elaborated visible image; B) non-elaborated infrared image. The arrows indicate the location of red tesserae showing different reflectance properties in the infrared range.

The red tesserae in the face contour of Saint Apostles appear homogeneous and they show similar IR reflectance values to the grey tesserae of the beard and hair of the figures, but some of the red tesserae in the feet contour appear differently in the infrared range like shown in the Fig. 65, on the example of Saint Paul's foot. This can be an indication of non-original, probably, substituted tesserae.

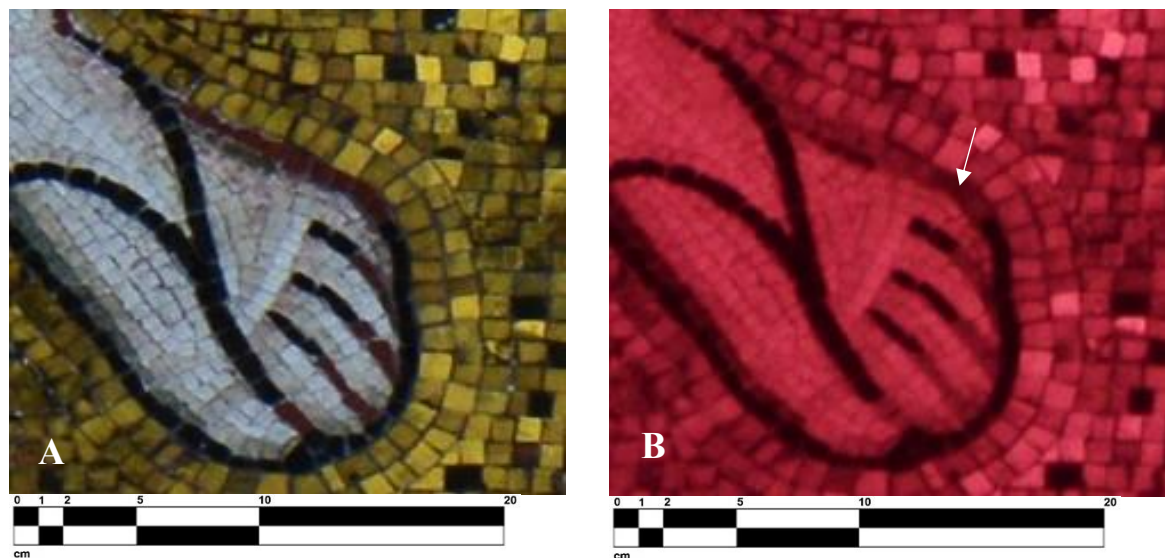


Figure 65. Saint Paul, detail of the foot, raw non-elaborated images: A) visible image (VIS); B) infrared image (IR1). The arrows indicate the location of red tesserae showing anomalous reflectance properties in the infrared range.

The differences between black tesserae (more glossy deep black and rough dark-grey) are enhanced in the infrared range. Both types of black tesserae were used for the vestment contour around the neck of Saint Apostle Andrew (Fig.66).

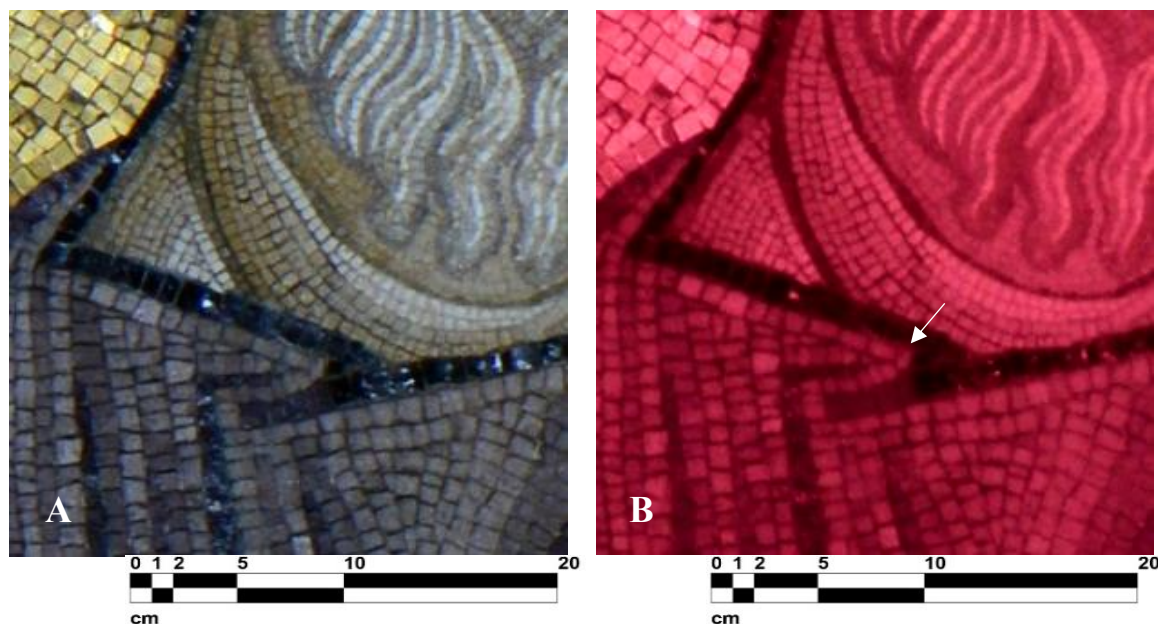
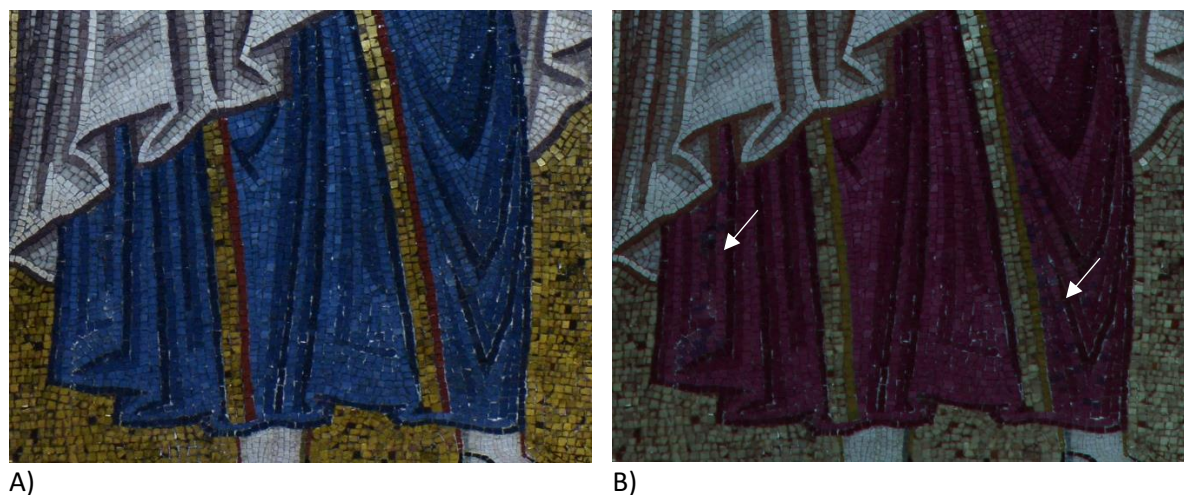


Figure 66. Collar detail of Saint Andrew raffiguration, raw non-elaborated images. a) visible image; b) infrared image (IR1).

The most evident differences between were detected in the blue tesserae of Saint Paul's vestment. Comparison between visible and infrared images allowed mapping of presumably substituted blue tesserae (Fig.67).



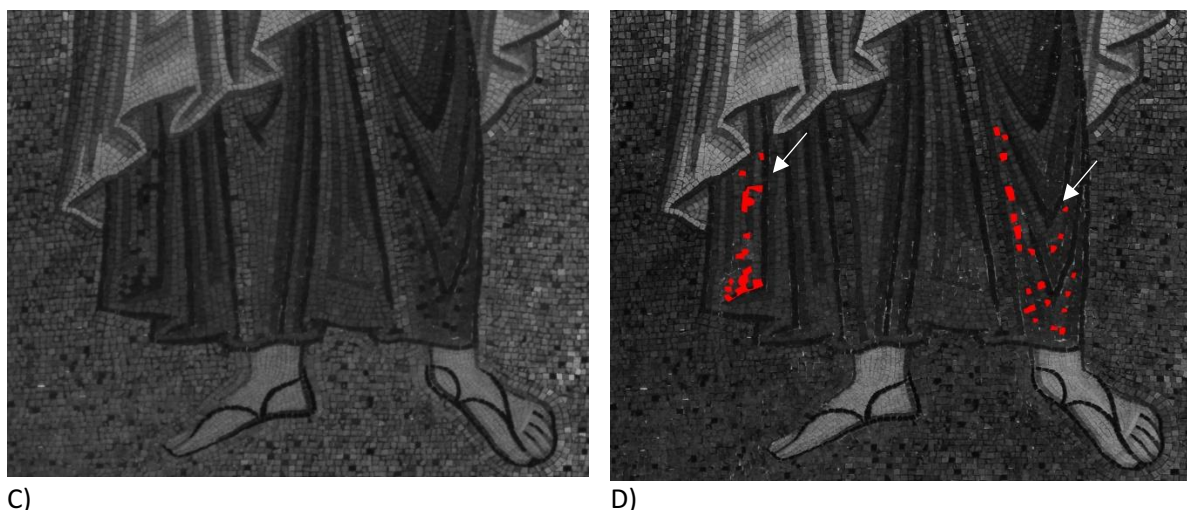


Figure 67. Saint Jacobus, mosaic fragment. Mapping of anomalous blue tesserae of the vestment of Saint Paul. a) non-elaborated visible image; b) false colour infrared image (by the means of Adobe Photoshop); c) grayscale infrared image (IR2); d) grayscale infrared image with mapping of anomalous tesserae.

5.1.3 Discussion of the results

The analysis of multispectral images in the church of Santa Maria dell’Ammiraglio proved its usefulness as a pre-screening tool for wall mosaic decorations to identify areas of interest for art historical and material study.

Differences observed by comparison between the visible and ultraviolet spectral images indicate inhomogeneities on the uppermost superficial layer. The identified differences may be related to the presence of organic materials (for example, linseed oil residues from the restorations of the 19th century, synthetic resins from the most recent consolidation treatments). This information can be useful for the planning of future conservation treatments and for the studies about the reconstruction of the mosaic panel history.

Differences observed by comparison between the visible and infrared images indicate discontinuities in the composition of the tesserae surface. In the case of gilded background or vestment’s tesserae, this inhomogeneity may be explained by the presence of different, eventually reintegrated tesserae. These differences were particularly evident on the reshuffled cloak of the Admiral in the Dedication panel (black tesserae) and on the vestements of Saint Anna and Saint Apostle Paul (blue tesserae). Eventual presence of an overpaint, e.g. on the face of the Virgin in the Dedication scene and of the Christ in the Coronation scene, may indicate the presence of later retouchings or may lead to further debate on the original appearance of the faces.

The information, which was retrievable from the observation of non-elaborated raw images in the given case study, is summarized in Table 14.

Table 14. Informativity of on-site non-elaborated and non-calibrated spectral images

Band	Detectable information
UV	- Enhanced differences in the gold tesserae, which can be related also to the irregularity of the surface (the ultraviolet image is usually darker and the discrimination between details is difficult)
VIS	- high resolution visible image for observation of the details and development of technical documentation ; - Reference image for the evaluation and comparison of different spectral bands
IR	- Distinct reflectance/absorbance values of visibly similar material only in the IR range , useful for the identification of reintegrated/restored areas (the problem of irregularity of the surface persists but with less impact if compared to the UV band); - Enhanced differences in gold tesserae , also detectable in UV and VIS band (discrimination between real differences and irregularities of the surface is still difficult).

Qualitative evaluation of multispectral images (without the use of color checker and semi-quantitative image analysis tools) is not capable of providing information about the exact molecular or elemental composition of original and substituted tesserae, though it can give preliminary information about their spatial distribution and number of types of tesserae.

Combined examination of two different spectral bands (VIS and IR, VIS and UV) can be performed by simply comparing raw or desaturated images or by basic image processing transformations using free or commonly available softwares: Image Enhancer, ImageJ, Adobe Photoshop (see attachments F and G). The methodology of combining different spectral bands, already described in the chapters 4.1-4.4 for wall paintings, was tested on wall mosaics. This approach proved its usefulness for enhancement of differences and facilitating general evaluation of surface homogeneity. Blending of visible and infrared images in luminosity mode by the means of Adobe Photoshop is recommended for immediate in-situ identification of

reintegrated/non-original tesserae. The use of RGB channels transformations, False-Colour Infrared and False Colour Ultraviolet mode proved their usefulness in the immediate mapping of areas of interest (distinct material), even when applied to non-calibrated images.

The main limitations of the informativity of spectral images, as shown by this investigation campaign, were the lighting conditions during the acquisition and geometry/irregularity of the surface. Complementary methods (profilometry), naked eye detailed observation or different acquisitions at a closer distance to the object may be needed to discriminate between real anomalies and artefacts related to the surface form and geometry. Combined examination of three or more spectral bands may produce artefacts in the resulting maps of spectral intensities if non-calibrated images were used. Depending on the art historical or conservation problem, quantitative or semi-quantitative analysis software may be introduced into the workflow of mosaic examination, with the specific function and algorithm for statistical mapping of certain tesserae types and for differentiation between similar tesserae. It is recommended to perform the combination of three or more spectral images, semi-quantitative image processing algorithms (i.e. PCA) only on the images, acquired in the presence of a colour reference chart, after calibration of lighting conditions.

The recommended image acquisition and analysis workflow and the selected image processing procedure can be found in attachments D and F respectively. The detailed description of each of the image processing functions, tested in this project, is reported in the attachment G.

The application of Infrared Thermography in passive mode did not reveal inhomogeneities in the subsurface structure of the mosaic decorations, due to insufficient thermal gradient (the tests were performed in February 2016).

The first application of Holographic Subsurface Radar (HSR) was tested on a small area of Dedication scene but it could not provide clear about the internal subsurface structure, due to the strong signal reflection from the gilded surface. This result led to the conducting of laboratory simulation tests, described in Chapter 6.

The brief observations of the research questions of this case study are summarized in table 15.

Table 15. Results of the acquisitions in the Church of Santa Maria dell' Ammiraglio, Palermo

Research question	Results and observations
- Can Multispectral Imaging be used in this case study to differentiate between original and	Yes, even in the absence of a color reference chart: by comparison of different spectral bands (VIS and IR for tesserae, VIS and UV

restored/reintegrated mosaic areas (tesserae and binder)?	for interstitial material), facilitated and enhanced by the means of free and/or commonly available software tools
- Can Multispectral Imaging be used in this case study to differentiate between similar tesserae of distinct composition?	Yes/no. Some differences have been identified, even in the absence of a color reference chart: by comparison and combined analysis of VIS and IR bands by the means of free and/or commonly available software tools. More tests are needed.
- Can Multispectral Imaging be used in this case study to identify the composition of the tesserae?	Yes/no. The analysis of mineralogical composition can be performed only by the means of dedicated Proficolore or ENVI image processing software, in the presence of relative database of minerals (stone tesserae) and metal oxides (glass paste tesserae) The comparison was not performed in this case study. More tests are needed.
- Can Multispectral Imaging be used in this case study without a color reference chart? If yes, what are the potentialities and limitations?	Yes. The enhancement of differences in tesserae surface characteristics, tesserae and binder constituent material and subsequent mapping of inhomogeneities can be performed in the absence of a color reference chart. The main limitations include the distance from the camera to the studied mosaic surface and geometry/irregularity of the surface
- Can passive Infrared Thermography be used in this case study to reveal information about the homogeneity in the mosaic subsurface and about stability/preservation state of the structural support (wall, vaults etc.)?	Yes/no. In this case, in February 2016 the available thermal gradient was not sufficient to reveal subsurface and structural inhomogeneities

<p>- Can Holographic Subsurface Radar be used in this case study to reveal discontinuities and defects in the mosaic subsurface layers?</p>	<p>Unknown. In this case study, the first tests were performed only on the gilded background fragments of the Dedicatory panels. More tests are needed</p>
<p>- What are the main limitations of Multispectral Imaging, Infrared Thermography and Holographic Subsurface Radar techniques when applied in-situ to wall mosaics?</p>	<p>For MI: Limited access (only during the opening hours to the public), impossibility to completely darken the environment (for the use of MI in fluorescence mode) and impossibility to use the complete set of recommended acquisition arrangement (color checker and positioning the flashlights), non planar geometry of the mosaic surface</p> <p>For IRT: Insufficient natural thermal gradient</p> <p>For HSR: Impossibility to use contact method in the areas of interest, presence of gold tesserae in the mosaic layer</p>

5.2 Palatine Chapel (Palermo, Italy)

5.2.1 Case study description

The *Cappella Palatina* (Palatine Chapel) was the royal chapel of the Norman kings of Kingdom of Sicily, part of the architectural complex of the Norman Palace. It has the shape of western basilica with three naves (Fig.68).

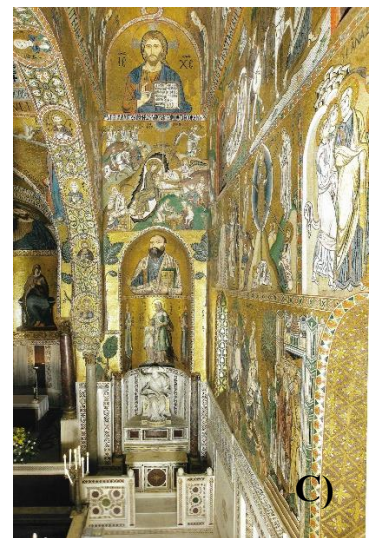
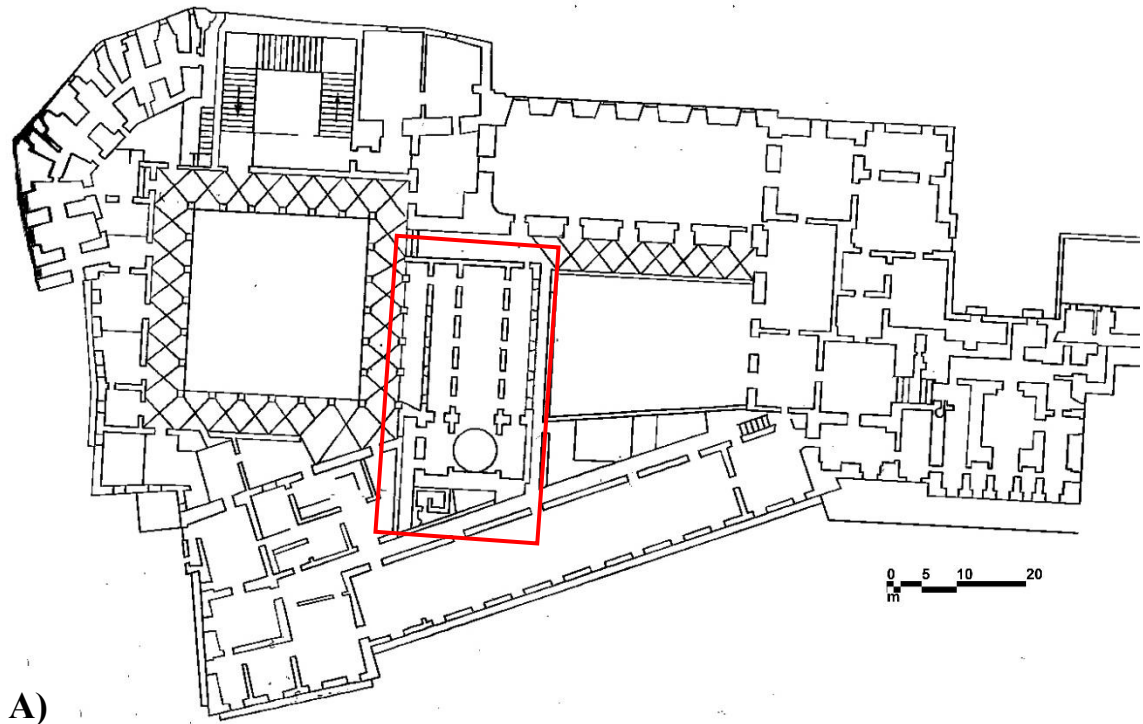


Figure 68. Palace of the Normans (*Palazzo dei Normanni*): a) groundfloor plan at the level of Parliamentary Chamber, current state. The red frame indicates the location of Palatine Chapel within the architectural complex; b) External view of the Palace, Southern facade; c) Interior of the Palatine Chapel, Southern transept [199].

Characterized by rich wall mosaics, wooden ceilings (muqarnas) and stone decorations (intarsia marbles), the Chapel is inscribed in UNESCO's World Heritage List [200]. Nowadays Palazzo Normanni, also called Royal Palace, houses the Sicilian Regional Assembly, the parliament of Italy's largest semi-autonomous regional government.

The Palace was originally built for the Arab emirs and their harems in the 9th century, on a site earlier occupied by Roman and Punic fortresses. Eventually abandoned by arabs, it was subsequently restored by Normans. The Royal Chapel was commissioned by King Roger II and built in the first half of the 12th century. However, the exact year of its foundation is not known. It was believed for a long time that the year has been indicated 1132 when Archbishop Pietro di Palermo elevated in the parish church a chapel dedicated to the apostle Pietro in the royal palace of Palermo.

The researchers Zorič and Brenk do not agree with this hypothesis and attribute the consecration of 1132 to the lower Church, already dedicated to the Mother of God (Odigitria). According to B. Brenk's studies [199], the construction of the new Palatine Chapel started two to four years before its consecration on April 28, 1140. The work on mosaic decorations continued over a longer period. The mosaics of the presbytery are attributed to the first phase of the building of the Palatine Chapel, still during the reign of Roger II (22 December 1095 – 26 February 1154) [201], the mosaics of the nave and aisles were most likely made later, during the rule of William I (1154-1166). After the Normans left, the palace experienced several centuries of serious decay until the second half of the 14th century, when the seat of Spanish viceroys was transferred into the Norman Palace. The first restoration of the Chapel, promoted by Elisabeth of Bavaria, queen mother of King Ludwig, testified by an inscription on the western wall of the north aisle, refers to the date 1345 [200]. A wider restoration campaign of mosaic decorations was implemented in the XV century, under the rule of John I Aragon. After a century of decline, in 1555, when Normanni Palace was chosen by viceroys as the main residence once again, a big restoration campaign was started. The Chapel, that was previously isolated, became literally incorporated into the new volume of buildings: to the west by the volume of Sala d'Ercole, to the north by the Fontana courtyard, to the south by the porch of the Maqueda courtyard and to the east by the building facing Piazza della Vittoria. The lighting conditions inside the chapel were drastically modified: the windows of the apses lose their original function and, by the second half of the 18th century, they were all closed and decorated by new mosaic integrations. In the 18th century, the restoration school was installed. Its first restorations, guided by Mario Morretti, are indistinguishable by naked eye observation from the Byzantine original parts of

the mosaics, due to precision and high imitation level. The next main restorer Santi Cardini from Arezzo is characterized by particular pictorial plastic style, and these restorations can be found in the three mosaic raffigurations between the windows of the north wall of the central nave, created probably to fill the void after the demolition of a small balcony. The restoration campaigns were implemented under the supervision of Giuseppe Paticolo from the end of the 19th century when some not original structures were demolished. In the 1980s the old roof was replaced by a structure of wooden trusses and polycarbonate sheets. In 2002, after an earthquake, small repairs were carried out. In 2005 a detailed restoration campaign started, on donations by Reinhold Wurth, which ended in 2009 [200].

The wall mosaics of Palatine Chapel represent a complex case study because of numerous reshufflments and restorations. A documentation of presbytery mosaics by from the first half of the 19th century show some significant differences with the current arrangement mosaic program. Fig. 69 shows two documentations: fig.69a from 1935 and fig.69b from 1838 [201]. Significant differences are observed in the mosaic depicting nowadays Virgin and Saint John Baptist analysed within this acquisition campaign. Many questions are posed by contemporary art historians to the possible substitutions and transfers of mosaic parts inside the iconographic program of the chapel (eventual presence of a Virgin in place of Christ Pantokrator or of Saint Peter in place of Saint Andrew).

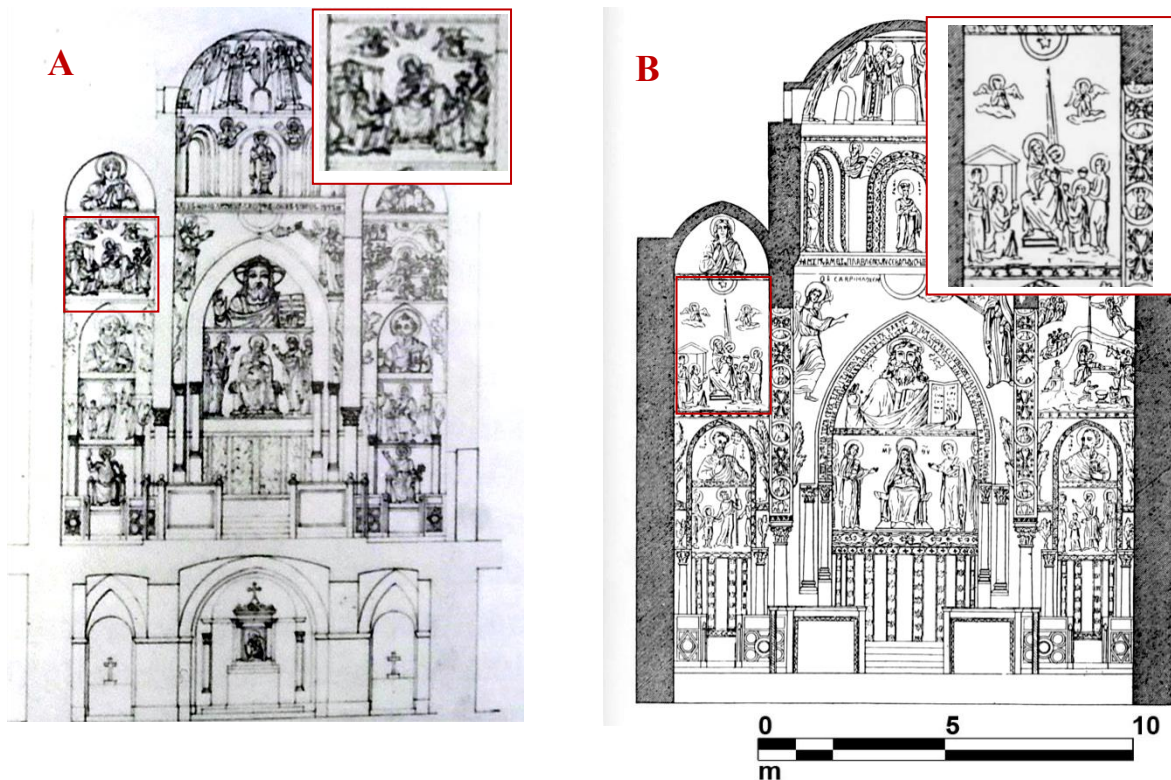




Figure 69. 1935 Documentation of the mosaics from the 19th century in the Northern transept: a) view towards the presbytery, northern transept, from 1835, after Hittorf and Zanth [201]; b) the same view, after Domenico Lo Faso Pietrasanta Duca di Serradifalco, 1938 [201]; c) current situation, visible image.

The experimentation was focused on the potentialities of the technique as a non-invasive as an easy portable prescreening tool in the analytical investigation, aimed to provide initial stage support to the iconographic study and material characterization study of the wall mosaics.

The main research questions of these case studies are reported as follows:

The main research questions of this case study are the following:

- Can Multispectral Imaging be used in this case study to differentiate between original and restored/reintegrated mosaic areas (tesserae and binder)?
- Can Multispectral Imaging be used in this case study to differentiate between similar tesserae of distinct composition?
- Can Multispectral Imaging be used in this case study to identify the composition of the tesserae?
- Can Multispectral Imaging be used in this case study without a color reference chart? If yes, what are the potentialities and limitations?

- What are the main limitations of Multispectral Imaging technique when applied in-situ to wall mosaics?

5.2.2 Acquisition and analysis of multispectral images

The instrument Nikon D800 FR (Full range) camera with 36-megapixel sensor was used. The camera has been modified, removing the internal UV and IR filters, to collect different images in the UV-VIS-IR range using specific external band-pass filters. A couple of modified Nikon speedlight flashes (Nikon SB 910) including excitations in the UV and NIR ranges was also used. During the acquisition, these flashes are in general positioned at 45° with respect to the measured surface, whereas the camera is placed between the flash lights and pointed orthogonally to the surface. Five external band-pass filters were used in this case to take the pictures in the UV-Vis-NIR ranges: one for the UV range (350-420 nm), one for the visible range (about 400-700 nm) and three different filters for the near infrared range (IR1= 720 nm, IR2= 850 nm, IR3= 950 nm). The use of a color reference chart was not possible in this case study, due to the accessibility restrictions (height at which the wall mosaics are located and absence of scaffoldings).

Before analysing in alternative software tools, the collected photos were converted from raw images (.NEF) to 16-bit Tagged Image File Format (TIFF) with minimal processing (without white balance and brightness corrections or stretching or pixel rotations) using the NX Viewer free software.

The list of multispectral acquisitions, according to the research questions of art historian Professor Beat Brenk (University of Basel, Switzerland), performed inside the Palatine Chapel, are shown in Fig. 70 and 71.

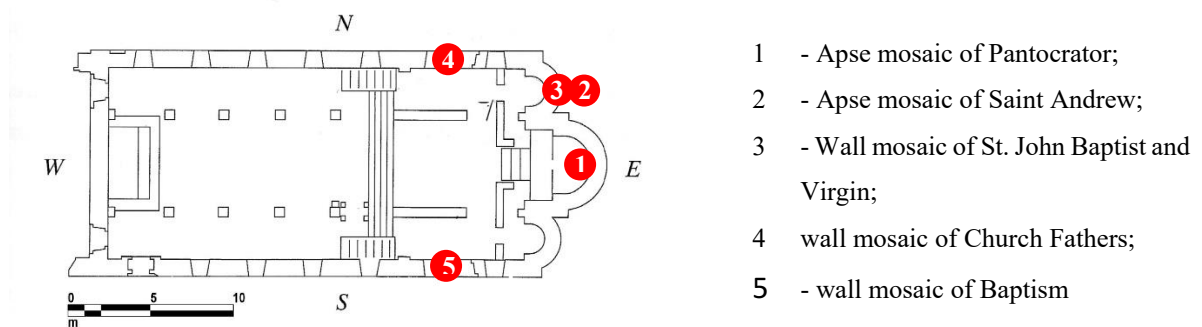
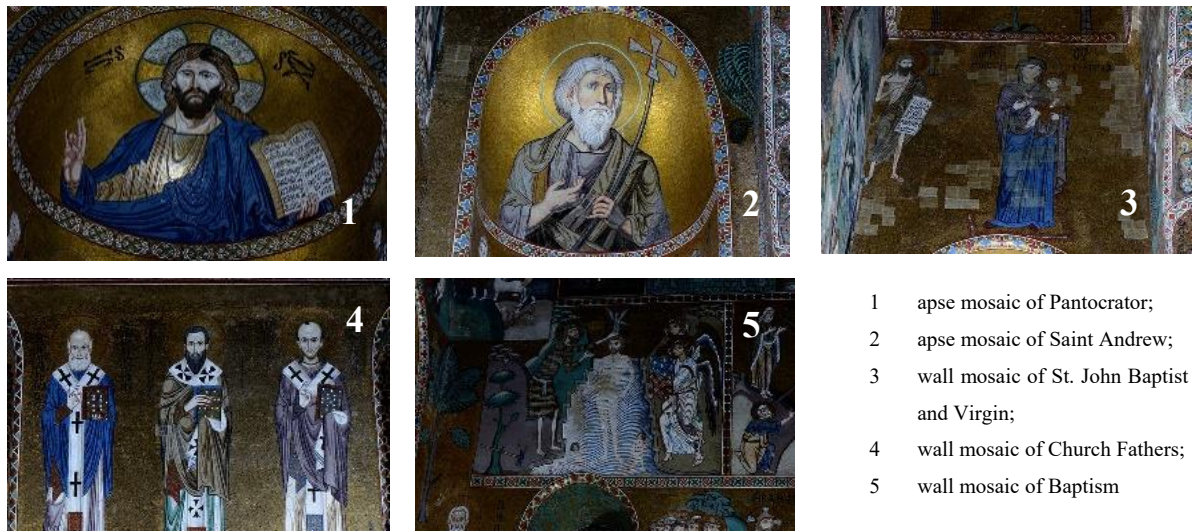


Figure 70. Palatine Chapel, floor plan. The red dots and nubers indicate the position of the investigated wall mosaics inside the Chapel.



- 1 apse mosaic of Pantocrator;
- 2 apse mosaic of Saint Andrew;
- 3 wall mosaic of St. John Baptist and Virgin;
- 4 wall mosaic of Church Fathers;
- 5 wall mosaic of Baptism

Figure 71. Non-elaborated visible images of the wall mosaics inside the Palatine Chapel.

The analysed raffigurations are located at the height from 3.5 m (northern and eastern apse mosaics) to 8-10 m (southern wall of the clerestory, scenes from the Old Testament) [199]. Due to logistical limitations (i.e. absence of scaffoldings and inaccessibility of some areas), it was not possible to follow the suggested geometry of acquisition and all the necessary calibration steps (e.g. use of a colour reference chart) for further quantitative image analysis on all the analysed mosaic decorations.

The qualitative examination procedure started with the observation of raw images using Nikon dedicated visualization software NX viewer. Subsequently, common image editing software programs (open source: Image Enhancer; ImageJ, commercial: Adobe Photoshop) were tested for calibration, enhancement and preliminary examination of acquired images.

Apse mosaic of Christ Pantokrator

In the central raffiguration of Christ Pantokrator (images acquired at the distance of 7.5 m following standard geometry of flashlight sources in the absence of a color checker), the tesserae, especially in the areas of the gilded background, can be characterized as generally inhomogeneous. Most of the discontinuities detectable in the visible range and are confirmed by the observation of the other spectral images. Further differences between visibly homogeneous black tesserae could be detected in the infrared band, which indicate possible substitutions during restoration interventions in the past.

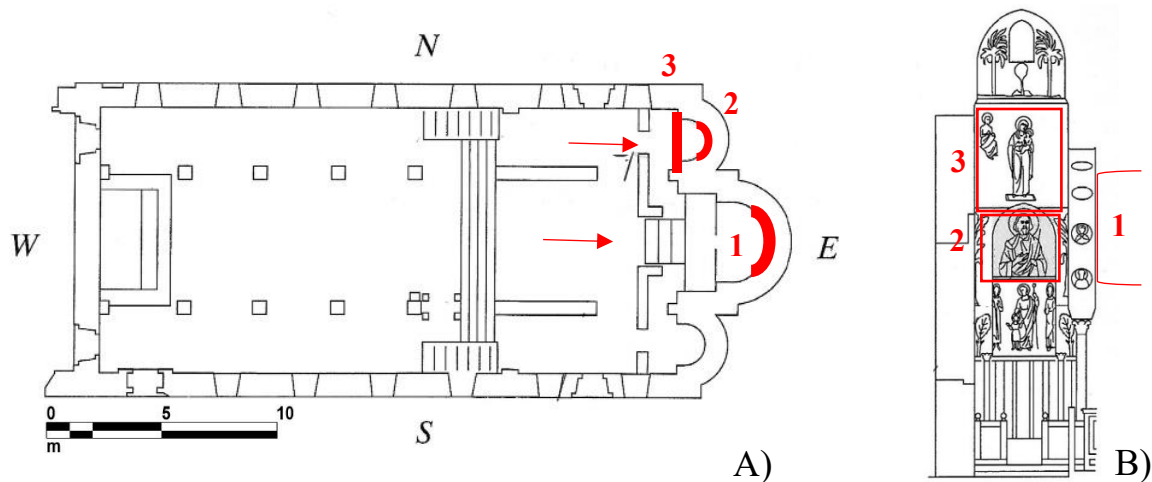
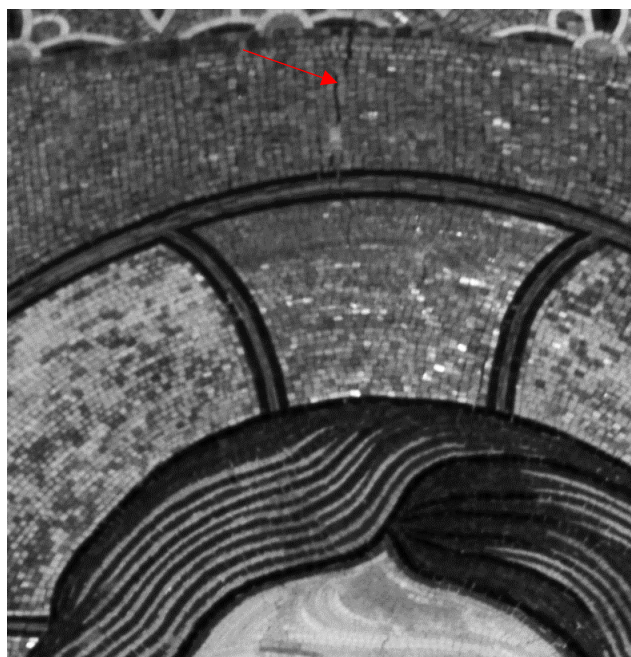
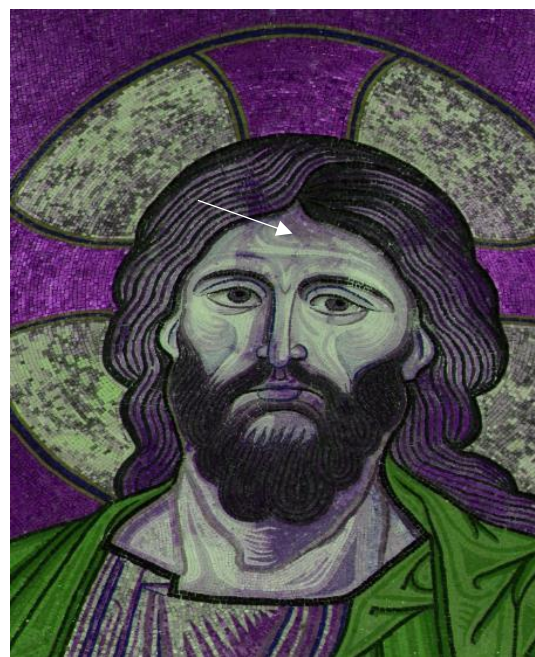


Figure 72. Mosaics of Christ Pantokrator (1), Saint Apostle Andrew (2) and the scene with St. John Baptist and Virgin (3). a) Floor plan of the Palatine Chapel; b) view towards the Northern transept [199].

Already in the visible range, it was possible to observe the presence of cracks on the mosaic surface. Figure 72 shows a fragment in the upper part of Christ’s face and halo, where several cracks are observed, more enhanced in the three infrared bands (fig. 72a). Some areas appear darker (“wet” effect”), in all the three bands. These differences were enhanced when processed in Image Enhancer or Adobe Photoshop, by applying contrast correction and False Colour mode (Fig. 72b). For the description of these image processing functions please see attachment F.



A)



B)

Figure 72. Detail of Christ Pantokrator mosaic. a) Infrared image (IR2), the red arrows indicate the presence of cracks; b) visible image, converted to False Colour mode, by the means of Image Enhancer. The arrow indicates the darker areas, detectable in visible and ultraviolet ranges.

Apse mosaic of Saint Apostle Andrew

The raffiguration of Saint Apostle Andrew belongs to a later integration, recognizable through a distinct iconographic style. Some of the art historians [199, 200] presumed that originally there was the figure of Saint Peter in the place of Saint Andrew. The preliminary in-situ qualitative analysis of multispectral images cannot provide sufficient scientific data to confirm or reject the hypothesis.

Some areas of tesserae inhomogeneity (in terms of brightness, colour, proportions, orientation, angle and regularity) could be detected in all the analysed bands: ultraviolet, visible and infrared. For example, some differences detectable in the visible light were confirmed and furtherly enhanced in the reflected infrared light image:

- Variability in tesserae colour, brightness and orientation in the vestment of Saint Andrew (see Fig. 73a);
- Differences in size and brightness of the tesserae of the halo and background adjacent to the figure of Saint Apostle Andrew (see fig.73b).

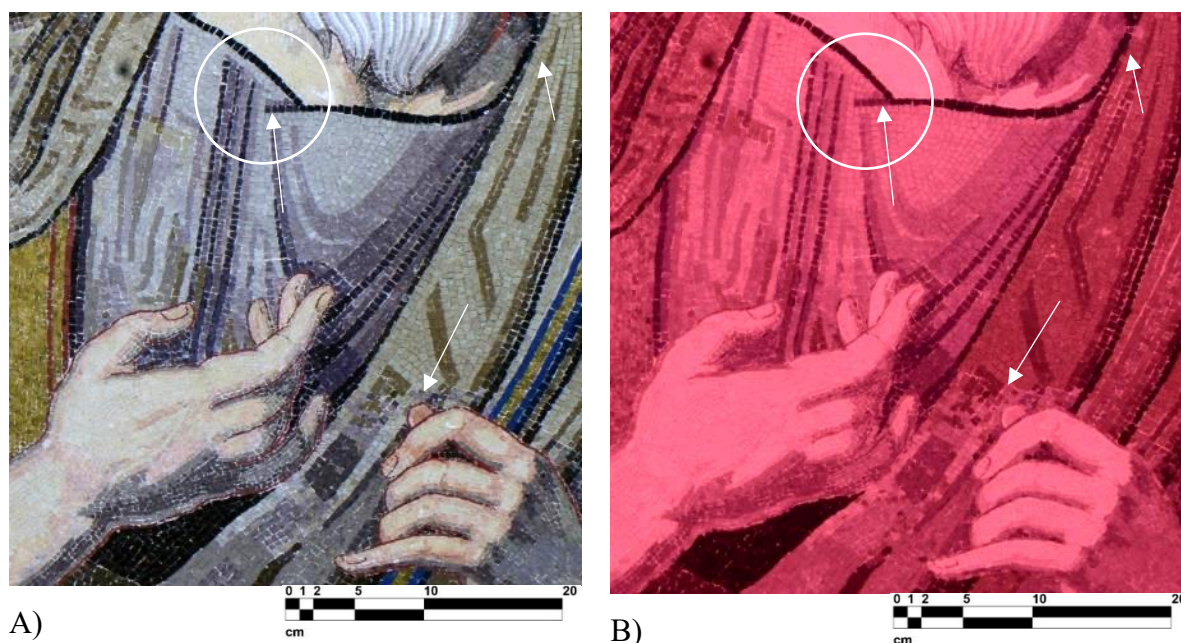


Figure 73. Tesserae discontinuities in the mosaic of the Apostle Saint Andrew, raw non-elaborated images. A) visible image (VIS); B) infrared (IR1) image. The arrows indicate the differences enhanced in the infrared range.

Through comparison of different bands, it was possible to observe black tesserae in the vestment and face contour, which appear identic or very similar in the visible range, but show different reflectance properties in the infrared range (Fig. 74).

The differences, detectable outside the visible range, in particular, in the infrared band (IR1-IR3), indicate the presence of different constituent material of the tesserae. The singular identic tesserae with different reflectance properties in the infrared range indicate, most probably, not original areas and/or integrations.

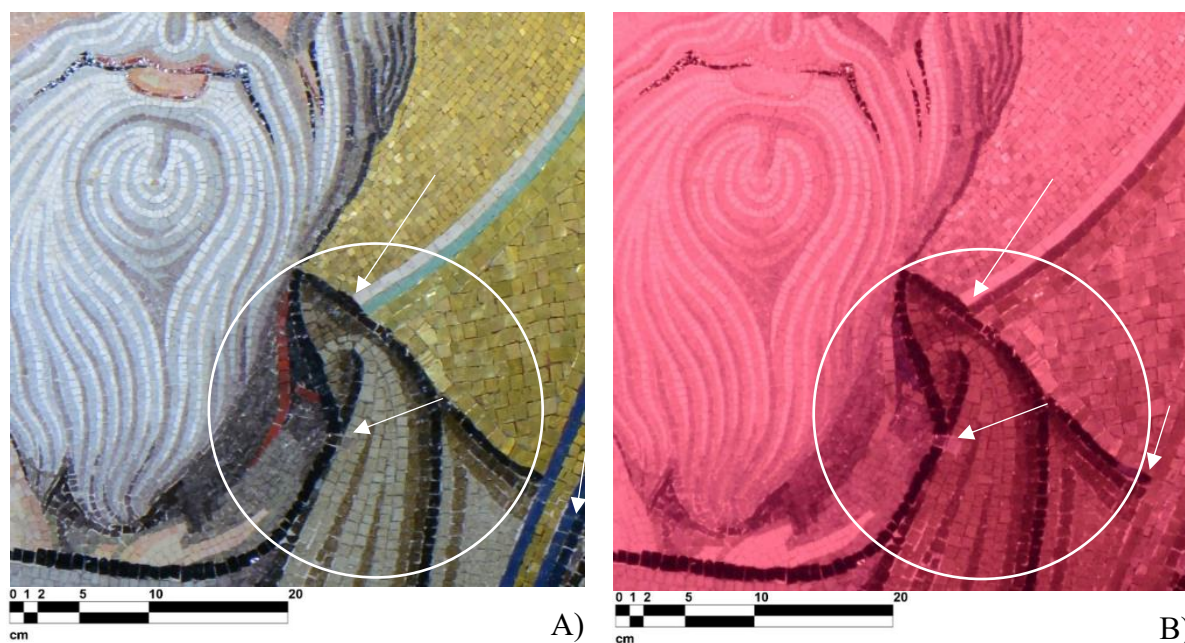


Figure 74. Visibly homogeneous tesserae that present distinct reflectance properties in the infrared range. Mosaic of Saint Apostle Andrew. A) non-elaborated visible image; B) non-elaborated infrared (IR1) image. The arrows indicate the differences detectable in the infrared range.

The discontinuities in the size and proportions, orientation and regularity of tesserae may indicate the areas of previous restorations (reintegration of reused or new tesserae).

Wall mosaic St. John Baptist and Virgin “Odigitria”

The wall mosaic of St. John Baptist and Virgin (Odigitria), as illustrated in the introduction of this case study (Fig. 69), was heavily reshuffled over the years. The whole area of the mosaic composition nowadays is characterized by numerous variations in tesserae size, proportions and color. The differences are detectable in the visible image and significantly enhanced in the infrared reflected light images. The Fig.75a shows the infrared light image of the current state of the mosaic decoration. The Fig. 75b shows the the left part of the mosaic in the Southern transept, acquired in the visible range and converted to False Colour mode (by the means Image

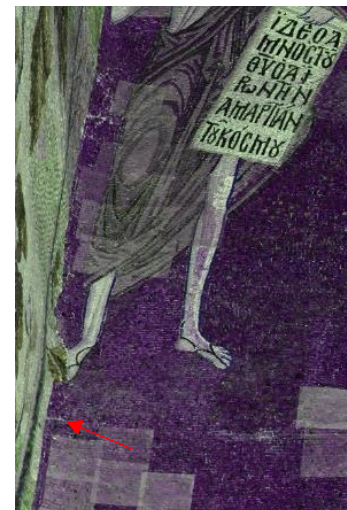
Enhancer through rotation of RGB channels filter (see attachment F). The enhanced “stitches” of different areas, composed by groups of tesserae with similar characteristics, enhanced in the infrared range, as well as clear iconographic discontinuities (overlap of a later mosaic from the sidewall, indicated by a red arrow in the Fig. 75b) are important for:

- mapping of the original and reintegrated areas;
- virtual reconstruction of the presumed original iconographic program;
- understanding of the wall mosaic history and study of the provenience of used mosaic fragments.

Fig. 76a and 76b show the discontinuities between tesserae of the gilded background, enhanced in the infrared range. In particular, the figure shows the stitches between gold tesserae with different characteristics in the central part of the mosaic, near the figure of Virgin (fig. 76a) and in the bottom part of the mosaic, near the feet of St. John Baptist (fig. 76b). The presence of white interstitial material is enhanced in the infrared image, as shown by red arrows in Fig. 76b.



A)



B)

Figure 75. St. John Baptist and Virgin (Odigitria) mosaic: a) non-elaborated infrared image (IR1); b) visible image, converted to False Colour, by the means of Image Enhancer. The arrow in image 75b indicates the overlap of the mosaic scenes.



A)

B)

Figure 76. St. John Baptist and Virgin (Odigitria). Fragments of grayscale infrared images (IR2), showing discontinuities and stitches between different areas in the golden background.

Wall mosaic of the Church Fathers

The observation of raw spectral images of the wall mosaics raffigurating three Fathers (Fig.77) of the Church allowed stating a high level of inhomogeneity in this wall mosaics (Fig.78 and 79).

In a similar way to the Odigitria and St. John Baptist, main differences are detectable in the visible range. The stitches between areas of golden background constituent by groups of different tesserae are shown in Fig. 78a. These differences are detectable in the visible light image and enhanced in the infrared. The Fig. 78b shows a fragment of the wall mosaics in False Colour Infrared Mode, where the combination of visible and infrared bands in RGB channels was applied to enhance the differences between tesserae and binding material in the interstitial areas.

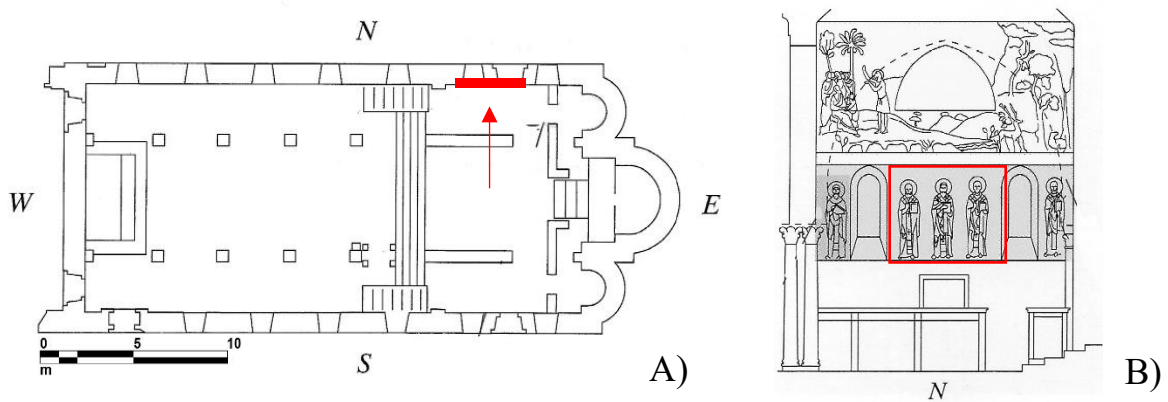


Figure 77. Wall mosaic depiction the Fathers of the Church inside the Palatine Chapel: a) floor plan of the Palatine Chapel, the position and direction of MI acquisition in indicated in red; b) view towards the wall mosaic, northern transept [199]



A)

B)

Figure 78. Inhomogeneity of the wall mosaics of Church Fathers: a) raw non-elaborated visible image with the mapping of different areas; b) fragment of the central figure, False Colour Infrared Image (IR2, without calibration).

The detected inhomogeneities can be evaluated in relation to the visible differences: the figures are characterized by variable height, proportions of the heads (the head of the right figure is bigger than the heads of the left and central figures). The differences in gold tesserae areas of different characteristics, stitched together, are enhanced in the infrared image (Fig. 79 and 80). Close observation and comparison between visible and infrared even non calibrated and non elaborated images revealed a high level of inhomogeneity and variations in tesserae of the background and halos around the faces of the Saints, indicating the areas of previous integrations and reshufflements in the mosaic.

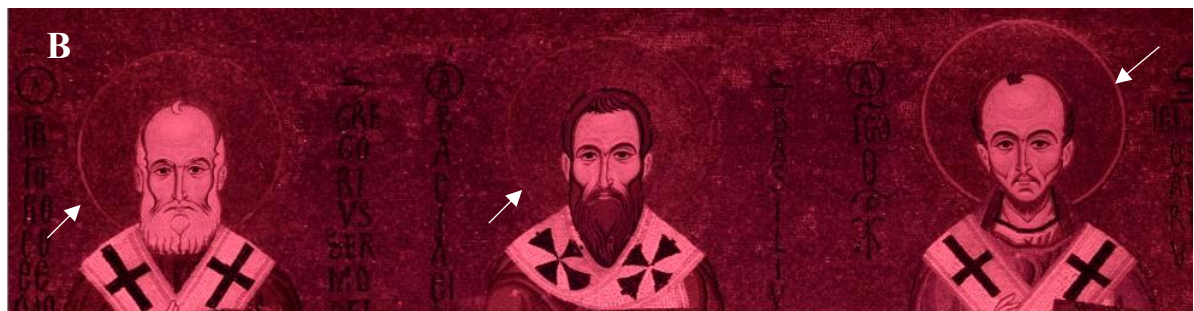


Figure 79. Fragment of wall mosaics. Comparison of faces and halos of the Church Fathers. The arrows indicate visibly homogeneous red tesserae that present different reflectance values in the infrared range: a) non-elaborated visible image; b) non-elaborated infrared image.

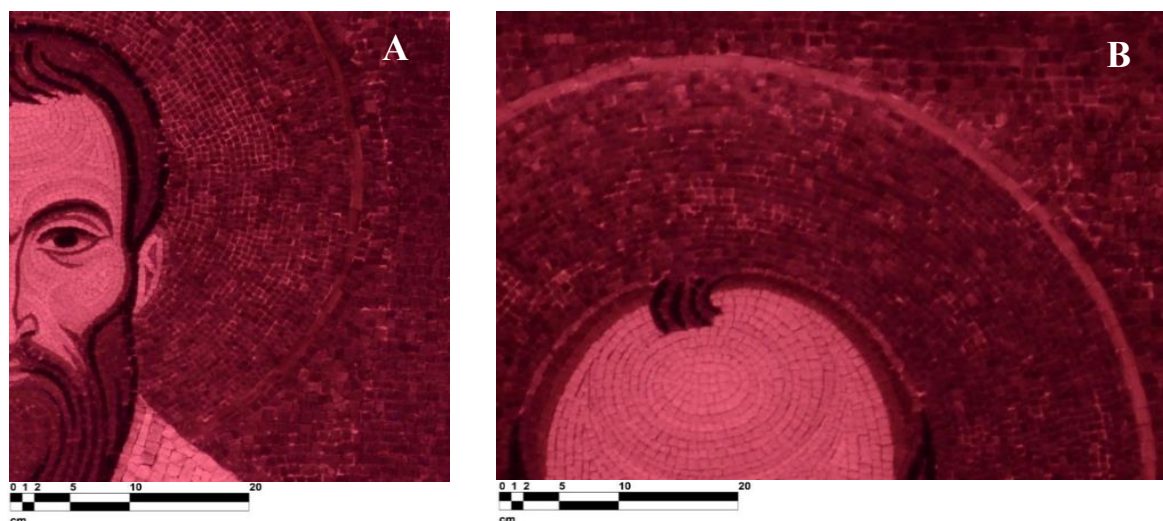


Figure 80. Comparison of halos of the central and right figure in non-elaborated infrared images (IR1). a) fragment of the face and halo of the central figure; b) fragment of the head and halo of the right figure.

Differences between red tesserae are detectable also in Gospel book and vestment details, as shown by the fragment of the left figure (Fig.81), similar to the chaotic distribution of red and golden tesserae, already detected in the vestments of Saints in the Church of Santa Maria dell’Ammiraglio (e.g. in the vestment of Saint Anna), see chapter 5.1.

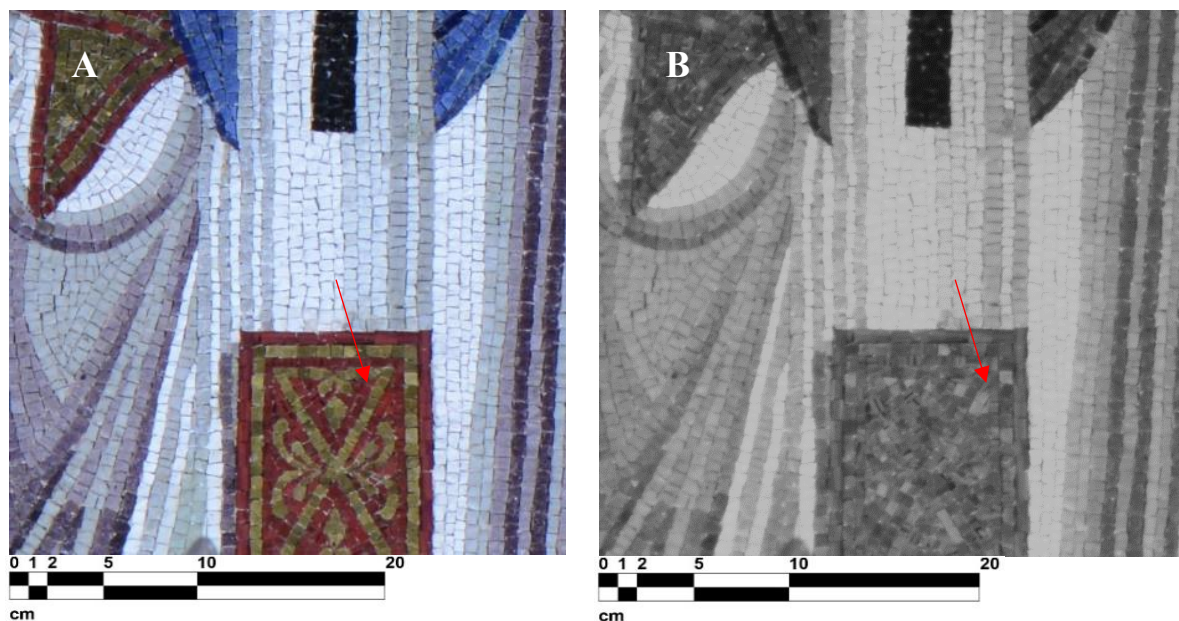


Figure 81. Detail of vestment. Revealing tesserae inhomogeneities in the infrared range. a) visible image; b) grayscale infrared image (IR2).

Baptism scene

The wall mosaic representing the Baptism scene of Jesus Christ (Fig. 82) is the most recent among the analysed mosaics. The general distribution of tesserae materials within separate compositional parts of the depiction, as shown by comparison of visible and infrared images, can be evaluated as homogeneous. Some differences, which may indicate the most recent consolidation or restoration interventions, were enhanced in the ultraviolet range and they are, instead, almost undetectable in the infrared range (fig. 83c and 83f).

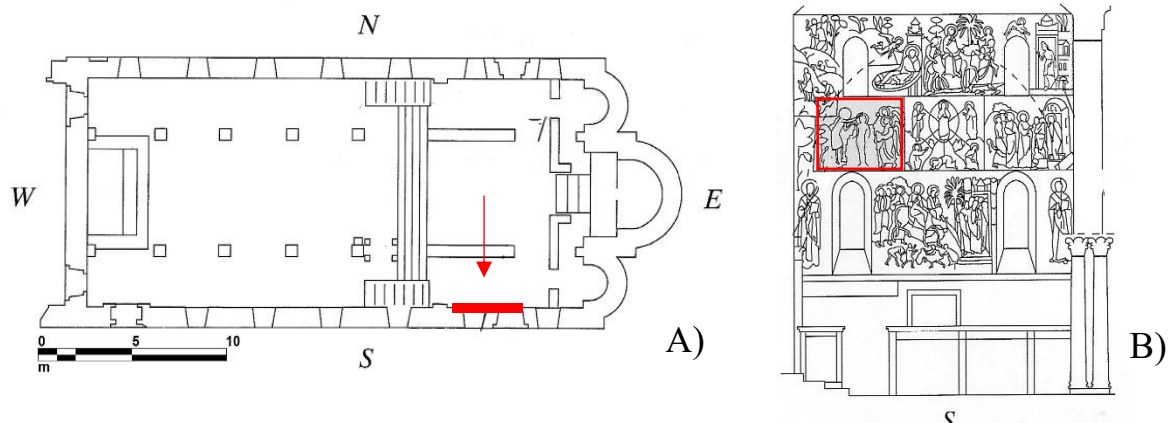


Figure 82. Wall mosaic depiction of the Baptism scene inside the Palatine Chapel. A) floor plan of the Palatine Chapel; B) view towards the wall mosaic, Southern transept [199]

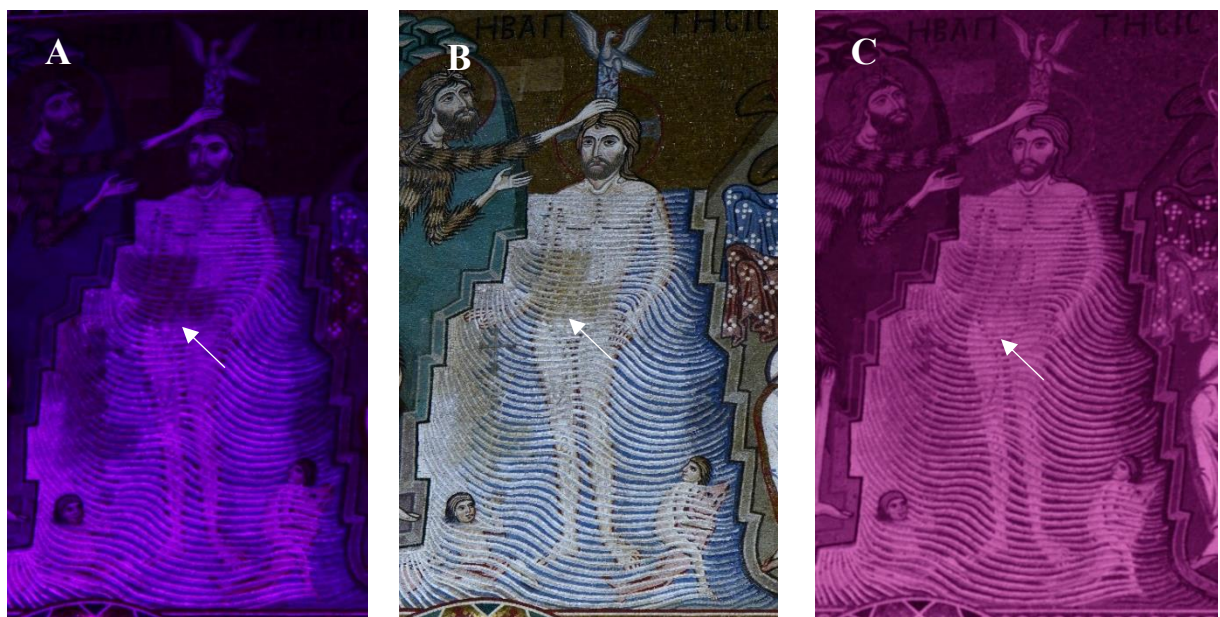




Figure 83. Enhancement of differences on the surface of the mosaic layer, indicated by arrows. a) ultraviolet (UV) image; b) visible image; c) infrared (IR2) image; d) detail of the UV image; e) detail of the visible image; f) detail of the infrared image.

5.2.3 Discussion of the results

The analysis of multispectral images in the Palatine Chapel showed high potentiality of the technique as a pre-screening tool for in-situ mosaic diagnostics, even without the application of image processing tools.

The informativity of ultraviolet range in this specific case was limited if compared to the infrared. However, the differences detected on the wall mosaics of Baptism scene can be helpful in the mapping of recent treatments with the use of organic materials.

Differences observed by comparison between the visible and infrared images may indicate the presence of tesserae of distinct composition, probably reintegrated. These differences were particularly evident in the wall mosaic depicting the Church Fathers, highlighting in the infrared range the distinct features of tesserae reflectance values, proportions and orientation. In all the analyzed mosaic panels, the IR1 band showed itself to be the most informative, if compared to IR2 and IR3.

The brief summary of the information obtainable from observation and comparison of raw spectral images (without further elaboration in image processing software), acquired in the Palatine Chapel, is summarized in Table 16.

Table 16. Case study observations. Non-elaborated and non-calibrated spectral images of mosaics

Band	Detectable information
UV	<ul style="list-style-type: none"> - Enhanced differences of tesserae surface properties (smoothness, gloss, inclination) and interstitial areas, - Identification of organic residues on the mosaic surface
VIS	<ul style="list-style-type: none"> - Reference image for comparison of different bands, improved readability of details for technical documentation, recognition of cracks and mapping of visible differences
IR 1-3 (particularly IR1)	<ul style="list-style-type: none"> - Distinct reflectance/absorbance values of visibly similar material only in the IR range, useful for the identification of reintegrated/restored areas (the problem of irregularity of the surface persists but with less impact if compared to the UV band); - Enhanced differences in gold tesserae, also detectable in UV and VIS band (discrimination between real differences and irregularities of the surface is still difficult).

Combination of different bands, using False-Colour Infrared mode allowed more rapid enhancement and recognition of differences between the visible and infrared images.

Qualitative evaluation of multispectral images is not capable of providing information about the exact molecular or elemental composition of original and substituted tesserae, though it can give preliminary information about their spatial distribution and types of tesserae. More sophisticated software tools can be applied to the semi-quantitative analysis of acquired images (by Profilocore or ENVI softwares) or to point-like elemental or molecular analysis (by portable XRF, Raman, etc.). The results of the initial stage analysis of multispectral images can be used for identification of areas of interest for further point-like analysis or even, if allowed, for sampling.

The main limitations of the informativity of spectral images, as shown by this investigation campaign, were the lighting conditions during the acquisition and geometry of the surface. Combined examination of different spectral bands can be performed by simply comparing raw non-elaborated spectral images or by basic image processing transformations using free or commonly available softwares. Depending on the art historical or conservation problem, quantitative or semi-quantitative analysis software may be introduced into the workflow of mosaic examination, with the specific function and algorithm for statistical mapping of certain tesserae types and for differentiation between similar tesserae.

The recommended image acquisition and analysis workflow and the selected image processing procedure can be found in attachments D and F respectively. The detailed description of each of the image processing functions, tested in this project, is reported in the attachment G.

The brief observations of the research questions of this case study are summarized in table 17.

Table 17. Results of the acquisitions in the Palatine Chapel, Palermo

Research question	Results and observations
- Can Multispectral Imaging be used in this case study to differentiate between original and restored/reintegrated mosaic areas (tesserae and binder)?	Yes, even in the absence of a color reference chart: by comparison of different spectral bands (VIS and IR for tesserae, VIS and UV for interstitial material), facilitated and enhanced by the means of free and/or commonly available software tools
- Can Multispectral Imaging be used in this case study to differentiate between similar tesserae of distinct composition?	Yes/no. Some differences have been identified, even in the absence of a color reference chart: by comparison and combined analysis of VIS and IR bands by the means of free and/or commonly available software tools. More tests are needed.
- Can Multispectral Imaging be used in this case study to identify the composition of the tesserae?	Yes/no. The analysis of mineralogical composition can be performed only by the means of dedicated Proficolore or ENVI image processing software, in the presence of

	relative database of minerals (stone tesserae) and metal oxides (glass paste tesserae) All the images were acquired in the absence of a color reference chart.
- Can Multispectral Imaging be used in this case study without a color reference chart? If yes, what are the potentialities and limitations?	Yes/no. The enhancement of differences in tesserae surface characteristics, tesserae and binder constituent material and subsequent mapping of inhomogeneities can be performed in the absence of a color reference chart. The main limitations include the distance from the camera to the studied mosaic surface and geometry/irregularity of the surface
- What are the main limitations of Multispectral Imaging technique when applied in-situ to wall mosaics?	Limited access, impossibility to completely darken the environment (for the use of MI in fluorescence mode) and the impossibility to use the complete set of recommended acquisition arrangement (color checker and positioning the flashlights), non planar geometry of the mosaic surface

5.3 The main porch of the Basilica of Saint Mark in Venice (Italy)

5.3.1 Case study description

The *Basilica di San Marco* (St. Mark's Basilica) in Venice is one of the most important monuments in Italy. It is the main church of Venice, very famous for its art historical importance and for the richness of exterior and interior wall and floor decorations. As for now, it is decorated by approximately 8500 m² of mosaic on a gilded ground. In this dissertation, the study is focused on the mosaic decoration of the inner porch of the Basilica di San Marco, entrance to the Dogal chapel of Venice, consecrated to Saint Mark (see Fig. 84).

The basic structure of today's cathedral was completed by the end of the 13th century, although minor adjustments to the façade and mosaics were made after the Venetian led conquests of Constantinople in the Fourth Crusade. This study is focused on the main portal.

History of the main porch of the Basilica

The first phase of mosaic decoration was started in the last decades of the 11th century, with the figures of Apostles and Virgin in the main entrance (the main porch examined within this project). The start of the second phase dates to 1106 of when restoration works were necessary after a fire [202].

The architectural arrangement of the porch decoration consists nowadays of three tiers. There were however four of them before a vault was demolished in the 16th century in order to open a lightwell (italian: "pozzo"). In the third level above the main entrance to the Dogal Chapel, there is a standing figure of Saint Mark, orant, in episcopal robes. This mosaic was concluded in 1545 by the brothers Francesco and Valerio Zuccati, who probably used a carton of their friend Titian to make the portrait of the main patron saint of Venice [203]. The inner porch was used during the main processions, when all the citizens and important guests, as emperors, popes, ambassadors, were involved to celebrate magnificent religious feasts and civil events.

Two extensive studies about the porch were implemented by Otto Demus [202] and by Renato Polacco [204]. Both scholars sustain that the two levels were built separately, in two different periods. According to both of them, the original portal was composed of a single row of arches. Demus sustains that the original porch served as the main entrance to San Marco in the 10th century and had only the second tier of arches, decorated by mosaics in the last quarter of the 11th century. The first mosaic decoration, according to him, included the figures of the Virgin and Child, in the central part of the composition, and eight apostles, four on each of the sides. Subsequently, the four evangelists should have been added in the lower row. At the same time, according to Renato Polacco, the portal consisted only of the lower row and served initially as a façade portal. The scholars have different opinions about the possible original shape of the portal and the mosaics chronology. Both of them base their hypothesis on the apparent non-conformity of the mosaics within the arches, from dissimilarities in marbles manufacturing of the two levels, from differences between the two rows of mosaics, from the use of different colors and various alphabets (Greek and Latin), as well as different mosaic execution styles [203].

The results of non-invasive acquisitions, discussed within this thesis, are part of an interdisciplinary project, conducted by the University of Padua (Italy): Department of Cultural

Heritage and Geosciences. The in-situ measurements were conducted during the restoration works in progress on the main porch of the Basilica, at a very short distance from the mosaics (less than 1 m), determined by the presence of covered scaffoldings and general geometry of the porch. The involved methods include: Multispectral Imaging, Holographic Subsurface radar and Ground Penetrating Radar.

The main research questions, considered in this thesis, include the following:

- Can Multispectral Imaging be used in this case study to differentiate between original and restored/reintegrated mosaic areas (tesserae and binder)?
- Can Multispectral Imaging be used in this case study to differentiate between similar tesserae of distinct composition?
- Can Multispectral Imaging be used in this case study to identify the composition of the tesserae?
- Can Multispectral Imaging be used in this case study without a color reference chart? If yes, what are the potentialities and limitations?
- What are the main limitations of Multispectral Imaging technique when applied in-situ to wall mosaics?
- Can HSR be helpful in this case study to reveal subsurface and structural discontinuities underneath the decoration layer?

The multispectral images were acquired on the second tier of the porch. The HSR acquisitions were performed on the apse mosaic of Saint Mark but did not produce any contribution to the study. The physical contact to the surface of the central mosaic part (figure of Saint Mark) was not allowed. The results of lateral acquisitions on the gilded background (similarly to those already discussed in chapter 5.1) led to the implementation of laboratory simulation tests (see chapter 6).

5.3.2 Acquisition and analysis of multispectral images

The instrument Nikon D800 FR (Full range) camera with 36-megapixel sensor was used. The camera has been modified, removing the internal UV and IR filters, to collect different images in the UV-VIS-IR range using specific external band-pass filters. A couple of modified Nikon speedlight flashes (Nikon SB 910) including excitations in the UV and NIR ranges was also used. During the acquisition, these flashes are in general positioned at 45° with respect to the measured surface, whereas the camera is placed between the flash lights and pointed orthogonally to the surface. The multispectral images were acquired in the presence of a

colorchecker provided with the camera and placed close to the wall paintings during the acquisition. Five external band-pass filters were used in this case to take the pictures in the UV-Vis-NIR ranges: one for the UV range (350-420 nm), one for the visible range (about 400-700 nm) and three different filters for the near infrared range (IR1= 720 nm, IR2= 850 nm, IR3= 950 nm).

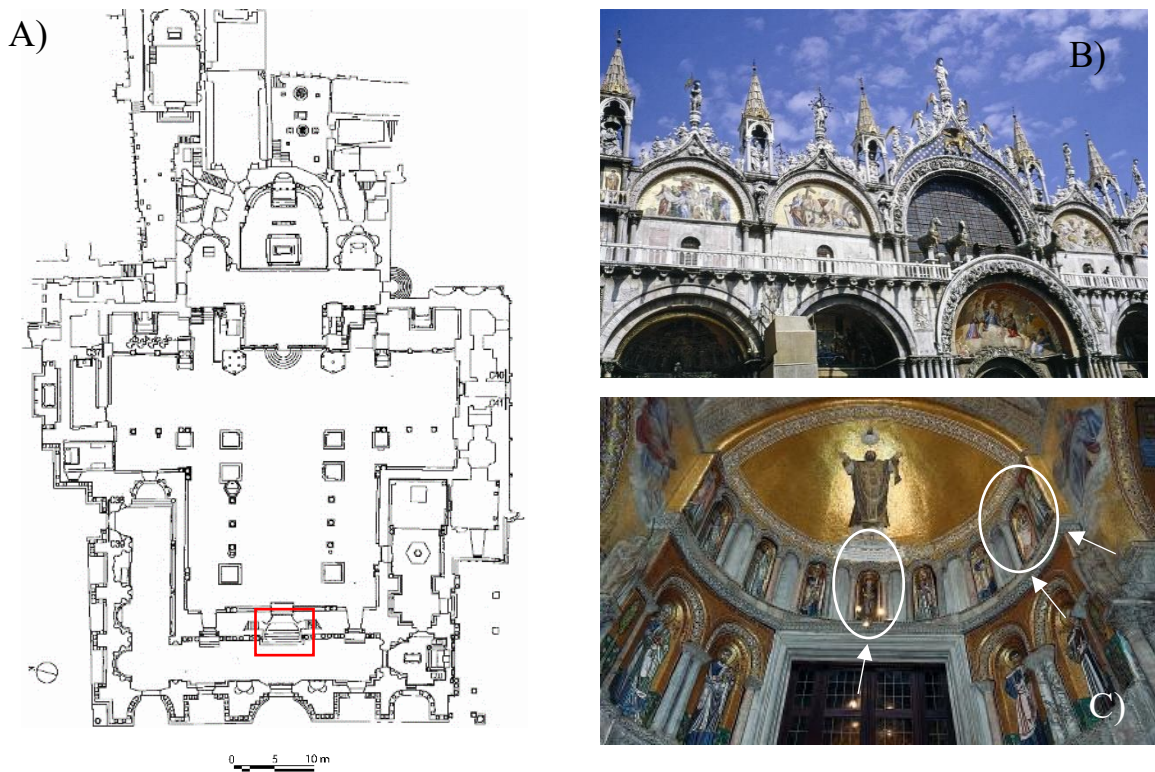


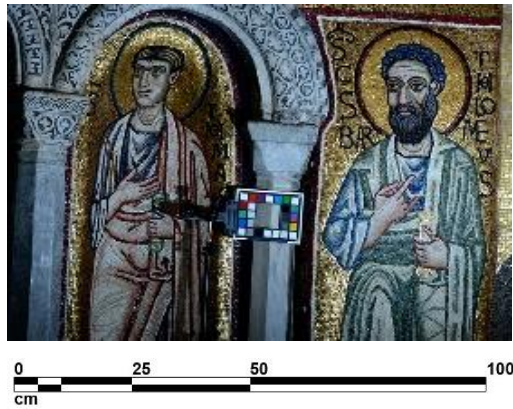
Figure 84. The analyzed main porch within the structure of the Basilica of Saint Mark: a) Groundfloor plan [204]; b) Western facade of the Basilica, actual state; c) Main porch after restoration (2018) [205]

The images were acquired at a very close distance (1 m) of the camera from the mosaic surface, due to the limited availability of the space on the scaffoldings during the restoration works. Only qualitative analysis of multispectral images was performed. The qualitative examination procedure started with the observation of raw images using Nikon dedicated visualization software NX Viewer. Subsequently, common image editing software programs (open source: Image Enhancer; ImageJ, commercial: Photoshop) were tested for calibration, enhancement and preliminary examination of acquired images.

The multispectral images were acquired and analysed on three mosaics of the second tier of the main porch (Fig.84):

- Virgin and Child (the central niche in the Fig.84; Fig. 85b);

- Saint Apostle Thomas (in the right side of the portal, as shown in the Fig.84; Fig. 85a)
- Saint Apostle Bartholomew (in the right side of the portal, as shown in the Fig.84; Fig.85a)



A)



B)

Figure 85. Non-elaborated visible images of the wall mosaics of the main porch of Saint Mark: a) Saint Apostles Thomas and Bartholomew; b) Virgin and Child.

Niche mosaic of Virgin and Child

The observation and comparison of visible and infrared images of the mosaic raffigurating the Virgin and Child in the main porch did not reveal significant changes in constituent material of mosaic areas. The gilded tesserae are characterized by irregular placement, proportions and size, especially in the corners. Some of the tesserae are present very irregular form (triangular, prolonged, etc.) or miss the finishing golden leaf cover.

The red tesserae show high variability in colour and surface characteristics in the visible range. The surface features, in particular, darker veins or surface “stripes”, were enhanced in the infrared range (Fig. 86c).

The black tesserae used for eye apples (big and rounded) are very particular. For both of the faces, different surface characteristics between the two eyeapples were detected: one is glossy deep black, the other is faded and rough (Fig. 87).

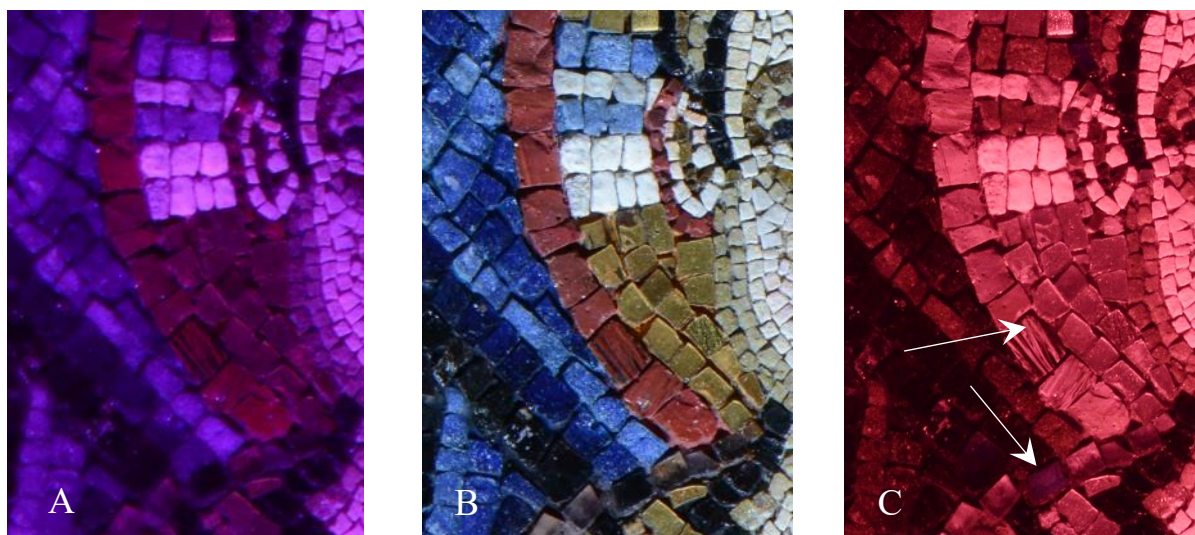


Figure 86. Detail of the Child's raffiguration. Differences between similar tesserae, enhanced in the ultraviolet and infrared ranges, raw non-elaborated images: a) ultraviolet image (UV); b) visible image (VIS); c) infrared image (IR1).

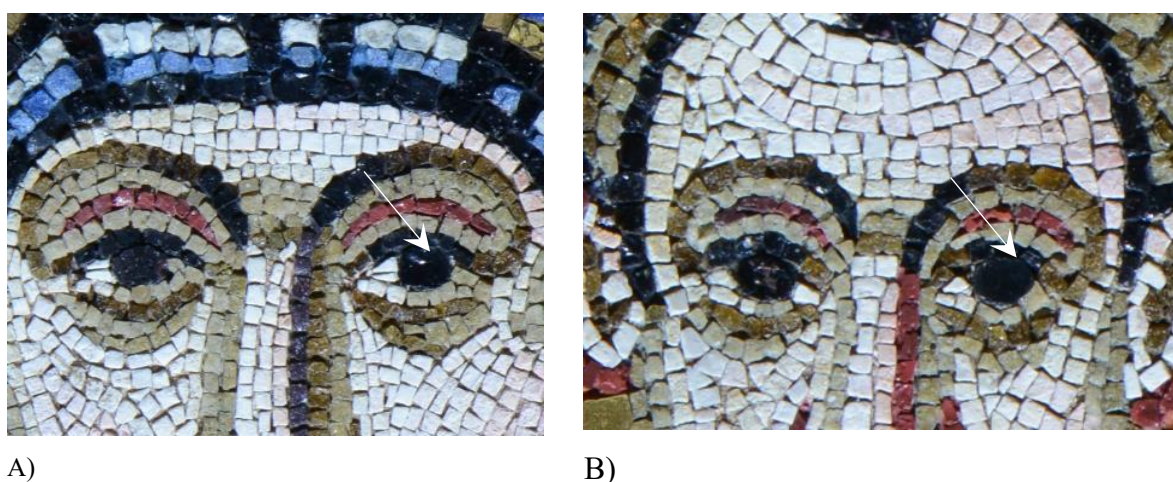


Figure 87. Details in the faces of Virgin (a) and Child (b). Non-elaborated visible images showing asymmetric use of black rounded tesserae.

Mosaics of Saint Thomas and Saint Bartholomew

The differences between gold tesserae inside and outside the halo of Saint Bartholomew are detectable in the visible range and enhanced in the infrared and ultraviolet bands (Fig. 88).

In infrared range, the differences in the surface characteristics of the gold tesserae and in interstitial material for both of the Saint Apostles raffigurations are enhanced (Fig. 88). The infrared band allowed also localization of some tesserae of different reflectance values (distinct composition) in the homogeneous areas of vestment details (Fig. 89). Also, the surface irregularities appeared more enhanced in the infrared image.



Figure 88. Comparison of gilded tesserae inside the halo of Saint Bartholomew and outside it (background), raw non-elaborated images: a) visible image (VIS); b) non-elaborated infrared image (IR1).

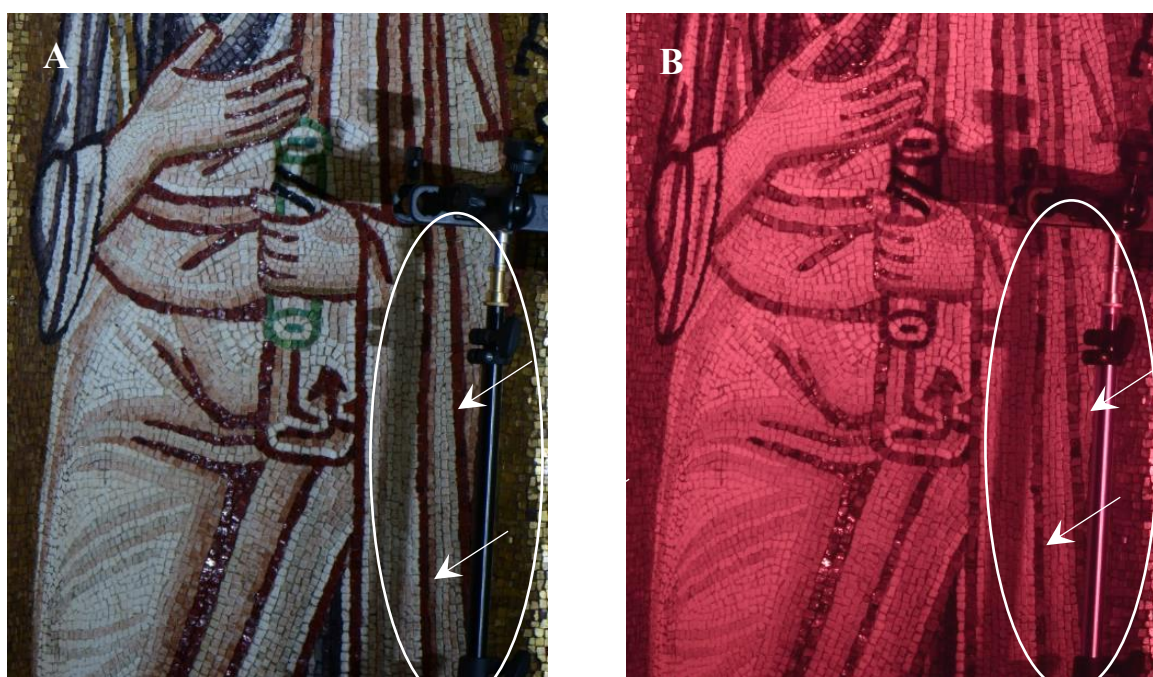


Figure 89. Differences in IR reflectance values of visibly homogeneous red tesserae in the Figure of Saint Bartholomew, raw non-elaborated images: a) visible image (VIS); b) infrared image (IR1).

Observation and acquisition of the tesserae at close distance in this case study (on scaffoldings) allowed observation of particularly variable colour and surface characteristics (lines, holes) in red tesserae. Some colour and brightness differences, clearly observed in the visible range, are

not detectable in the infrared range: visibly different tesserae appear homogeneous in the infrared range.

5.3.3 Discussion of the results

In this case study, the acquisitions by Holographic Subsurface Radar and Ground Penetrating Radar were not applicable on the part of mosaics depicting figures. At the same time, the HSR acquisitions on a gilded surface of the mosaic background did not reveal information about the underlying substrate layers. The holographic images showed dense repetitive inhomogeneity and the results are not presented here. As demonstrated by the laboratory simulation tests (chapter 6), it can be explained by the absence of the signal penetration into the surface surface beneath the gold tesserae.

Analysis of in-situ multispectral images showed also in this case study that there is a strong potentiality of the method in detailed comparison of iconographic features, materials and execution technique of the mosaics. The method can be used as a pre-screening tool for identification of areas of interest for subsequent point-like non-invasive or (if allowed) micro-invasive analysis. A short distance from the object allowed better observation and detailed comparison of the mosaic tesserae. Observation of raw non-elaborated images allowed to reveal some differences between similar tesserae, through variations in reflectance values between visible and infrared ranges. The IR1 band was more informative in enhancing these differences, if compared to IR2 and IR3.

The brief summary of the information obtainable by observation and comparison of non-calibrated and non-elaborated spectral images of the mosaics in the main porch of the Basilica is reported in Table 18.

Table 18. Informativity of non-elaborated and non-calibrated spectral images in the given case study

Band	Detectable information
UV	- Low informativity or unclear differences
VIS	- Reference image for comparison of different bands, improved readability of details for technical documentation.
IR 1-3	- Distinct reflectance/absorbance values of some visibly similar material only in IR range , useful for

	<p>the identification of reintegrated/restored areas (the problem of irregularity of the surface persists);</p> <ul style="list-style-type: none"> - Enhanced differences in gold tesserae, also detectable in UV and VIS band (discrimination between real differences and irregularities of the surface is still difficult).
--	---

In this particular case study, the processing of different spectral images (e.g. blending mode in Adobe Photoshop or False Colour Infrared transformations) did not significantly contribute to revealing discontinuities between different spectral ranges. The results, therefore, are not presented here.

The brief observations of the research questions of this case study are summarized in Table 19.

Table 19. Results of the acquisitions in the Catholikon of Dafni Monastery, Athens

Research question	Results and observations
- Can Multispectral Imaging be used in this case study to differentiate between original and restored/reintegrated mosaic areas (tesserae and binder)?	Yes, even in the absence of a color reference chart: by comparison of different spectral bands (VIS and IR for tesserae, VIS and UV for interstitial material), in this case, it was neither facilitated nor enhanced by the means of image processing tools
- Can Multispectral Imaging be used in this case study to differentiate between similar tesserae of distinct composition?	Yes/no. Some differences have been identified, even in the absence of a color reference chart: by comparison and combined analysis of VIS and IR bands. But additional methods to discriminate these differences from the surface irregularity, angle of tesserae placement etc. In this case, use of image processing tools did not contribute to increasing the informativity of spectral images

<p>- Can Multispectral Imaging be used in this case study to identify the composition of the tesserae?</p>	<p>Yes/no. The analysis of mineralogical composition can be performed only by the means of dedicated Profilocolore or ENVI image processing software, in the presence of relative database of minerals (stone tesserae) and metal oxides (glass paste tesserae) These tests were not performed in this case study.</p>
<p>- Can Multispectral Imaging be used in this case study without a color reference chart? If yes, what are the potentialities and limitations?</p>	<p>Yes. The enhancement of differences in tesserae surface characteristics, tesserae and binder constituent material and subsequent mapping of inhomogeneities can be performed in the absence of a color reference chart. The main limitations include the distance from the camera to the studied mosaic surface and geometry/irregularity of the surface</p>
<p>- Can Holographic Subsurface Radar be used in this case study to reveal discontinuities and defects in the mosaic subsurface layers?</p>	<p>Unknown. In this case study, the first tests were performed on the gilded background fragments of the mosaic (the areas not of the main interest). Some difficulties were encountered in the interpretation of results.</p>
<p>- What are the main limitations of Multispectral Imaging and Holographic Subsurface Radar techniques when applied in-situ to wall mosaics?</p>	<p>For MI: Limited access and space for the instrumentation (limited opening hours and restoration works in progress), impossibility to completely darken the environment (for the use of MI in fluorescence mode), non planar geometry of the mosaic surface For HSR: Impossibility to use contact method in the areas of interest, presence of gold tesserae in the mosaic layer</p>

5.4 Investigations in the Catholikon of Dafni Monastery (Athens, Greece)

5.4.1 Case study description

The history of Dafni monastery and its Catholikon was briefly introduced in chapter 4.4.

The non-invasive acquisitions presented in the given project were performed in July 2017 within the frames of regular monitoring activities held by the Ministry of Culture, Ephorate of Antiquities of West Attika, Piraeus and Islands, in collaboration with the Non-Destructive testing techniques Laboratory of the National Technical University of Athens (NTUA, Greece). Referring to the conservation state of wall mosaics in Catholikon, the main problem was the appearance of salts efflorescence, observed on the mosaic surface in the Church interior. The phenomenon had been observed on the interior mosaic surface, in correspondence to the external surfaces, which have undergone different restoration procedures. The efflorescence of mosaic tesserae surface may have been caused by the moisture content, trapped inside the wall structure. The surface was cleaned from the salts formation and, subsequently, regular control on-site and preventive monitoring of wall decorations has been implemented.

In this case study, the main research questions, referring to wall mosaics (for wall paintings see chapter 4.4), are the following:

- Can Multispectral Imaging be used in this case study to differentiate between original and restored/reintegrated mosaic areas (tesserae and binder)?
- Can Multispectral Imaging be used in this case study to differentiate between similar tesserae of distinct composition?
- Can Multispectral Imaging be used in this case study to identify the composition of the tesserae?
- Can Multispectral Imaging be used in this case study without a color reference chart? If yes, what are the potentialities and limitations?
- Can passive Infrared Thermography be used in this case study to reveal information about the homogeneity in the mosaic subsurface and about stability/preservation state of the structural support (wall, vaults etc.)?
- What are the main limitations of Multispectral Imaging and Infrared Thermography techniques when applied in-situ to wall mosaics?

5.4.2 a) Acquisition and analysis of multispectral images

The instrument Nikon D800 FR (Full range) camera with 36-megapixel sensor was used. The camera has been modified, removing the internal UV and IR filters, to collect different images

in the UV-VIS-IR range using specific external band-pass filters. A couple of modified Nikon speedlight flashes (Nikon SB 910) including excitations in the UV and NIR ranges was also used. During the acquisition, these flashes are in general positioned at 45° with respect to the measured surface, whereas the camera is placed between the flash lights and pointed orthogonally to the surface. The multispectral images were acquired in the absence of color reference chart. Five external band-pass filters were used in this case to take the pictures in the UV-Vis-NIR ranges: one for the UV range (350-420 nm), one for the visible range (about 400-700 nm) and three different filters for the near infrared range (IR1= 720 nm, IR2= 850 nm, IR3= 950 nm). Before analysing in alternative software tools, the collected photos were converted from raw images (.NEF) to 16-bit Tagged Image File Format (TIFF) with minimal processing (without white balance and brightness corrections or stretching or pixel rotations) using the NX Viewer free software.

The distance from the camera to mosaic decoration was approximately 8 m.

The stack of spectral images was acquired only on the apse mosaic depicting Saint Nicolas (Άγιος Νικόλαος), in the apse of Catholikon of the Dafni Moastery. The acquisitions were performed without a color reference chart and at a big distance from the decoration, in the absence of scaffoldings. The given on-site conditions drastically limited the informativity of the technique.

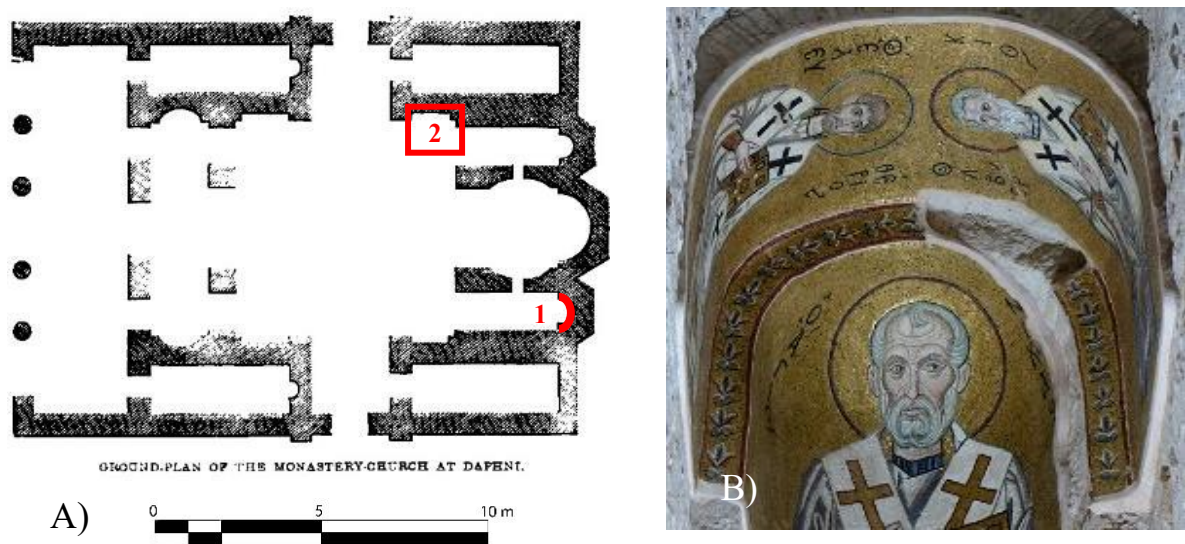


Figure 90. Acquisitions on wall mosaics inside the Catholikon of Dafni Monastery. a) Ground plan with indicated location of examined wall mosaic of Saint Nicolas by the means of Multispectral Imaging (1) and by the means of Infrared Thermography (2), presented here [191]; b) raw non-elaborated visible image of examined wall mosaic.

The examination started with a comparison of raw images using Nikon dedicated visualization software (NX Viewer). Similar to previously described case studies, detailed observation of differences in the face of Saint Nicolas, detectable between the visible and the infrared range, allowed localization of singular tesserae that are indistinguishable in the visible or in the infrared range, which show different reflectance properties in the infrared range. The differences between dark tesserae of the face features were enhanced in the infrared range (Fig. 91). The discrimination between real differences and artefacts is difficult, due to unknown detailed morphology of the surface, presence of glares on the mosaic surface and long distance.

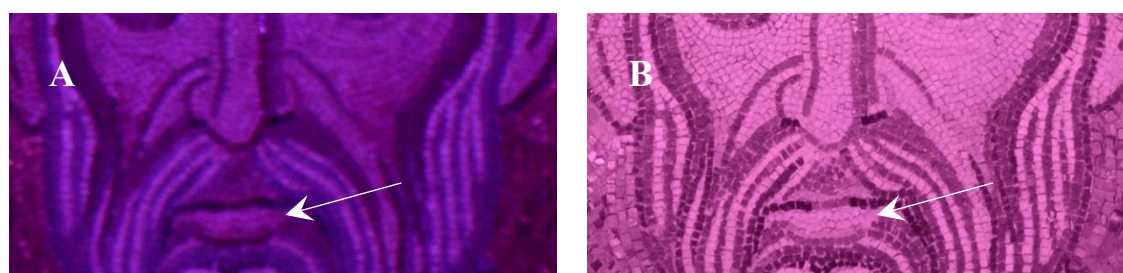


Figure 91. Saint Nicolas face details, raw non-elaborated images: A) ultraviolet image (UV); B) infrared image (IR2).

According to the previous micro-invasive analysis performed on the mosaic tesserae in the Catholikon [118], the lead-free glass samples were identified as mostly original. The 19th century glass tesserae were characterized by a low percentage of magnesium and potassium oxide and by a higher presence of lead oxides in tesserae constituent material [207].

Common image editing software programs (open source: Image Enhancer; ImageJ, commercial: Photoshop) were tested for calibration, enhancement and preliminary examination of acquired images. Qualitative multispectral imaging approach, however, was not capable to provide useful data that can help differentiate between different types of tesserae, in view of in-situ conditions limitations.

Fig. 92 shows the comparison of face mosaic execution technique between the three case studies:

- the main porch of Saint Mark Basilica (Virgin's face with the absence of colour gradations on the skin tone);
- the Catholikon of Dafni Monastery (St. Nicholas' face);
- the Church of Santa Maria dell'Ammiraglio (George of Antioch).

The comparison of visible images reveals similar features in the mosaics of Saint Nicolas of Dafni Monastery in Athens (Greece) and George from Antioch of La Martorana Church in Palermo (Italy). In these case studies, visible range shows a wide range of skin colour and brightness gradation and detailed elaboration of faces. In both case studies, IR range does not reveal these gradations. The tesserae form only a schematic outline of the face. The mosaic raffigurations of the Basilica of Saint Mark in Venice (Italy) appear more schematic both in the visible and in the infrared range (see Fig. 92).

The combination of tested image processing functions did not contribute significantly to the informativity of the acquired image of the mosaic. No information about degraded or any eventually substituted tesserae was obtained.

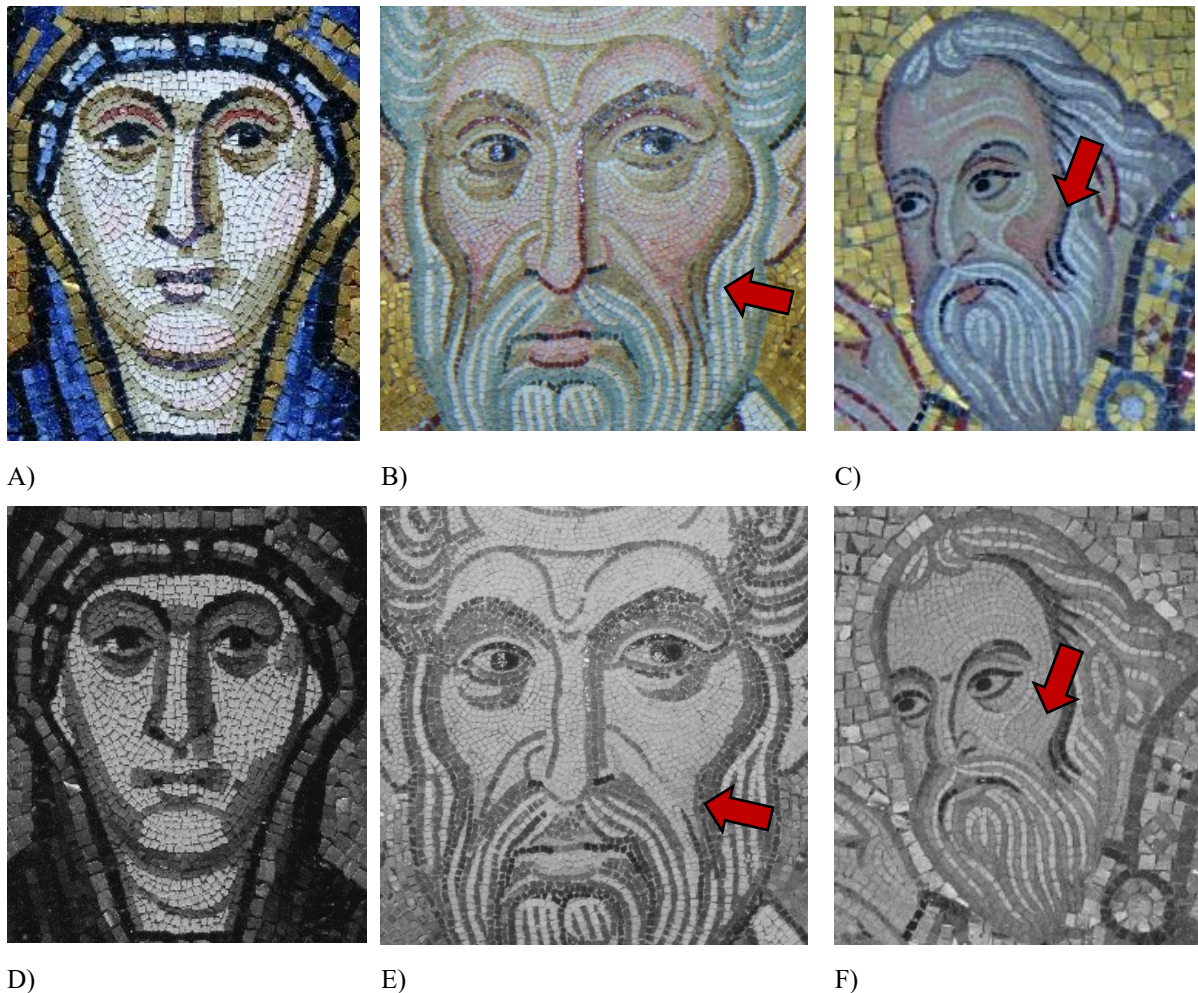


Figure 92. Comparison of mosaic execution techniques between different case studies, visible raw non-elaborated and infrared grayscale images: a) face of the Virgin in the main porch of Saint Mark Basilica; b) face of Saint Nicholas in the Catholikon of Dafni Monastery; c) face of George from Antioch in the Church of Santa Maria dell'Amiraglio. The arrows indicate the areas with wide tone and color gradation, detectable in the visible and ultraviolet ranges (b and c) and not detectable in the infrared range (e and f).

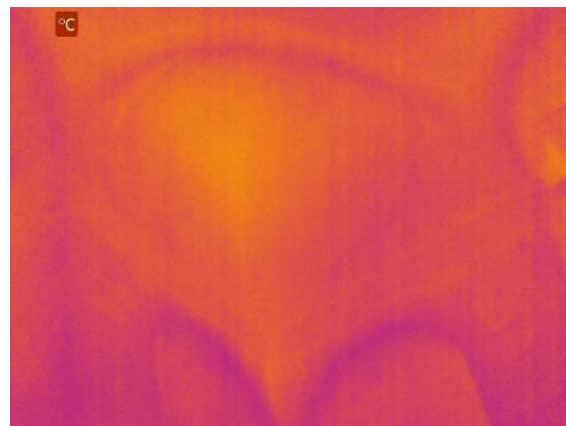
5.4.2

b) Infrared Thermography acquisitions

The in-situ tests were performed with the FLIR ThermaCAM SC640 in July 2017, property of the Non-Destructive Testing techniques Laboratory of the National Technical University of Athens (Greece), in collaboration with the Ephorate for Antiquities of Attica Region, in charge for the preservation of Daphni Monastery, in July 2017.

In this case study, external thermal excitation sources could not be used. It was observed that the absence of strong natural thermal gradient and big distance from the investigated objects can strongly limit the informativity of acquired thermal images. According to the preliminary results of passive IR Thermography inspection, there are no thermal contrasts within the upper and medium levels in the church's architectural structure. The conservation state of wall subsurface and its structural support can be characterized by the absence of serious structural damage or moisture rising. Additional tests, with the use of external thermal excitation source (IR lamps), may be needed to confirm the stable equilibrium of the walls.

The presence of moisture beneath the decoration layers, referred to during the previous inspections, was not detectable anymore by visual observation of thermal images acquired in passive mode (Fig. 93).



A)

B)

Figure 93. Transfiguration mosaic of the Catholikon, Dafni Monastery (Athens, Greece): a) Visible image; b) thermal image

5.4.3

Discussion of the results

Both Multispectral Imaging and Passive Infrared Thermography techniques, full-field and non-contact, were applied in challenging and very limiting in-situ conditions. Unlike the wall paintings, the mosaics are located at a long distance (8-10 m), the view is partially inhibited by scaffolding in use by conservators-restorers. The stacks of spectral images were acquired only in reflected light mode on the only one mosaic of Saint Nicholas in the apse of Catholikon. The brief summary of the information obtainable by observation and comparison of raw non-elaborated spectral images of this apse mosaic raffiguration is reported in Table 20.

Table 20. Informativity of non-calibrated and non-elaborated spectral images in the given case study

Band	Detectable information
UV	Low informativity, due to long distance from the object and irregularity of the surface (enhanced variability of skin brightness and colour gradation)
VIS	Reference image for comparison of different bands, improved readability of details for technical documentation
IR 1-3	Low informativity, due to long distance from the object and irregularity of the surface (information about differences in IR reflectance values of tesserae, which do not correspond to the differences observed in other ranges)

Experiments with the elaboration of different spectral images (e.g. blending mode in Adobe Photoshop or False Colour Infrared transformations) did not significantly improve the informativity of the multispectral images in this case. Simple observation of spectral images was useful, however, to enhance some differences between visually similar tesserae, highlighting possible discontinuities in their composition due to the discontinuities detectable in the infrared range. Further tests at a shorter distance to the mosaic with the use of a color reference chart might be useful for improvement of the on-site preliminary characterization procedure.

In this and in the other wall mosaic case studies, the infrared and ultraviolet ranges were helpful to enhance the details related to iconographic features and mosaic execution techniques.

The in-situ passive infrared thermography inspection inside the Catholikon of the Dafni Monastery (Athens, Greece) was performed in the absence of sufficient thermal difference between the outside and interior conditions of the church. In these conditions, the technique showed its limited applicability for rapid on-site preliminary structural and subsurface diagnostics by solely visual observation of thermal images. Under natural conditions, no temperature contrasts could be observed. Further tests might be needed for in-depth study and confirmation of the subsurface and structural condition of wall decoration support.

The brief observations of the research questions of this case study are summarized in Table 21.

Table 21. Results of the acquisitions in the Catholikon of Dafni Monastery, Athens

Research question	Results and observations
- Can Multispectral Imaging be used in this case study to differentiate between original and restored/reintegrated mosaic areas (tesserae and binder)?	Yes/no. In this case study, it is difficult due to the long distance from the object and impossibility to control lighting conditions
- Can Multispectral Imaging be used in this case study to differentiate between similar tesserae of distinct composition?	Yes/no. Some differences have been identified, even in the absence of a color reference chart, but more tests are needed.
- Can Multispectral Imaging be used in this case study to identify the composition of the tesserae?	Yes/no. In this case study, due to long distance, uncontrolled and low lighting, absence of a color checker it was impossible. The analysis of mineralogical composition can be performed only by the means of dedicated Profilocolore or ENVI image processing software, in the presence of relative database of minerals (stone tesserae) and metal oxides (glass paste tesserae)

<p>- Can Multispectral Imaging be used in this case study without a color reference chart? If yes, what are the potentialities and limitations?</p>	<p>Yes/no. The enhancement of differences in tesserae surface characteristics, tesserae and binder constituent material and subsequent mapping of inhomogeneities can be performed in the absence of a color reference chart. The main limitations include the distance from the camera to the studied mosaic surface and geometry/irregularity of the surface</p>
<p>- Can passive Infrared Thermography be used in this case study to reveal information about the homogeneity in the mosaic subsurface and about stability/preservation state of the structural support (wall, vaults etc.)?</p>	<p>Yes/no. In the given case study, the available thermal gradient was not sufficient or the system was characterized by the absence of subsurface structural inhomogeneities. More tests are needed</p>
<p>- What are the main limitations of Multispectral Imaging and Infrared Thermography and techniques when applied in-situ to wall mosaics?</p>	<p>For MI: long distance, limited access (only during the opening hours to the public), impossibility to completely darken the environment (for the use of MI in fluorescence mode) and impossibility to use the complete set of recommended acquisition arrangement (color checker and positioning the flashlights), non planar geometry of the mosaic surface</p> <p>For IRT: Insufficient natural thermal gradient</p>

6. LABORATORY SIMULATION TESTS

Series of laboratory tests were performed before and during in-situ acquisition campaigns. The experiments were aimed at testing and comparing the applicability of selected methods, at evaluation and selection of the most informative parameters for applications on real cases, taking in consideration the acquisition conditions, characteristics of the examined objects and questions by conservators and art historians.

For wall paintings, the tests were aimed at selection of the best parameters for in-situ acquisitions on wall paintings, aimed at their immediate characterization as a whole system, at different depths.

- 1) Diagnostics and characterization of the decoration layer by a modified camera (Multispectral Imaging):
 - recognition and quick mapping of certain in-situ pigments;
 - tests for efficient in-situ identification of the areas of interest for sampling with subsequent laboratory analysis.
- 2) Diagnostics and characterization of the subsurface structure by the HSR technique:
 - Testing of the innovative technique for subsurface investigations on a fresco sample, selection of the most appropriate acquisition parameters;
 - detection of shallow subsurface inhomogeneities underneath the pictorial layer.

For wall mosaics, the laboratory tests were aimed at evaluation the HSR technique for mosaic subsurface diagnostics:

- 1) Testing of the HSR technique for subsurface investigations on a mosaic model, evaluation of applicability limitations, selection of the most appropriate acquisition parameters;
- 2) Complementary use of HSR and two additional methods (DHSPI and SIRT), already well known in the field of artwork diagnostics.

The performed laboratory experiments include:

- Multispectral imaging tests in infrared fluorescence mode on archaeological fresco fragments from Sarno Baths (Pompeii), aimed at selection of the most appropriate illumination source for on-site acquisitions (see chapter 4.1);

- Holographic Subsurface Radar tests on the detection of hidden metallic elements underneath a fresco sample;
- Holographic Subsurface Radar tests on simplified laboratory models simulating hidden elements underneath plasterboard sheets and a gilded wooden icon
- Holographic Subsurface Radar, Digital Holographic Speckle Pattern Interferometry and Stimulated Infrared Thermography acquisitions on a custom-built mosaic model with buried elements, irregular surface and complex subsurface structure (performed at the Department of Cultural Heritage of the University of Padova and at the Holography Metrology Laboratory of the Institute of Electronic Structure and Laser).

Particular attention was dedicated to the Holographic Subsurface Radar technique, which was aimed at:

- 1) selection of the most appropriate acquisition parameters for each typology of studied wall decorations (paintings or mosaics), as well as for each specific case study under examination;
- 2) development of the safest and possibly non-contact acquisition procedure;
- 3) recognition of eventual drawbacks of the given technique and testing possible solutions;
- 4) evaluation of the technique's complementarity with different non-invasive and non-destructive methods.

During the internship at the Remote Sensing Laboratory of Bauman Technical University (Moscow, Russian Federation), implemented in March 2016, some preliminary simplified laboratory tests were performed on buried objects made of different materials (wood, metal, ceramic and glass), positioned underneath one or more layers of plasterboard.

Already during the first tests, the technique proved its efficiency in the detection of buried elements that are characterized by high contrast in dielectric permittivity within the investigated medium and by the size bigger than the step of acquisition of the instrument (5 mm). Subsequently, a new series of tests on a wall painting and wall mosaic laboratory models were performed at the Department of Cultural Heritage of the University of Padova. As shown by the preliminary laboratory and on-site tests, some fundamental problems in the application of Holographic Subsurface Radar are related to the manual acquisition: high sensitivity of the instrument to any deviation from the parallel acquisition paths and reflections while acquiring on non-planar surfaces.

For this purpose, a resistant solid plexiglass shield (dimensions 50x70x10 mm) with engraved parallel guiding lines (each 5 mm) was prepared and used for the next series of laboratory HSR acquisitions at the University of Padova (Fig. 95-97).

Table 22 reports a brief description of each laboratory sample and main objectives of the implemented experimental procedure.

Table 22. Samples for laboratory tests

Laboratory sample	Objectives of the experiments
Fragments of real wall fresco paintings	Selection of the most appropriate parameters for on-site identification of Egyptian Blue pigment
Fresco sample: two lime mortar layers (arricio and intonachino) on a strandboard, without integrated defects	Evaluation of the HSR technique, influence of the surface characteristics and selection of the most efficient parameters for the detection of hidden discontinuities underneath the wall fresco painting, in correlation to previous restoration interventions and state of conservation
Mosaic sample: variable thickness from one to three mortar layers upon a plywood support; integrated buried objects	Evaluation of the HSR technique's applicability to wall mosaics, influence of the surface characteristics, selection of the most informative parameters for the detection of hidden discontinuities underneath the mosaic decoration layer, differences in mortar application and material properties, in correlation to previous restoration interventions and state of conservation
Gilded icon on a wood panel: wooden support, golden leaf and paint layer	Additional tests aimed to check the limitations of the HSR when applied to gilded surfaces (thin metallic leaf tesserae of the Martorana church, Palatine Chapel, Basilica of Saint Mark and in metal decoration details of wall paintings in Scrovegni Chapel)

Multispectral Imaging tests on wall painting fragments

As shown by various studies [49, 50], Egyptian blue, widely used in Roman wall paintings, is one of the pigments that show specific fluorescence in the infrared range, induced by the visible light.

In the given project, the modified multispectral camera was evaluated as a portable tool for on-site detection and mapping of Egyptian blue pigment. In particular, the tests were performed on wall paintings of the Frigidarium of Sarno Baths (Archaeological site of Pompeii, Italy), described in Chapter 4.1 of this thesis. As shown by the first in-situ tests, the natural lighting conditions inside the Frigidarium were too low for collecting near-infrared fluorescence from

the Egyptian Blue pigment, induced by the natural visible light. Therefore, several tests were performed at the University of Padova, aimed at selection of the most appropriate additional sources of visible light. Six (6) blue fragments of Roman fresco wall paintings were used for the laboratory experimentation: three of them containing Egyptian Blue and three of them not containing Egyptian Blue pigment. These blue fragments are collected on the archaeological site of Pompeii. The exact provenience details (i.e. building, wall, Roman period and style attribution) are unknown.

In order to study the mineralogical composition and to confirm analytically eventual presence of Egyptian Blue pigment, the samples were examined by different laboratory methods (XRD, Raman, FORS, pXRF, SEM and OM).

The Egyptian Blue shows the strongest visible induced near- infrared fluorescence at around 910 nm [208]. Therefore, the bandpass filter IR2 (with the central wavelength at 850 nm) was selected for the experimentation. The T8 fluorescent tube, color temperature of 4000 K (natural white), namely the model F38t8 of cH lighting, proved to induce sufficient near-infrared fluorescence in the Egyptian blue for its recognition, as indicated by white arrows in the Fig. 94c. It was selected for the in-situ multispectral imaging acquisitions on the archaeological site of Pompeii.



Figure 94. Visible induced infrared fluorescence mode, IR2 bandpass filter. a) Visible light image; b) Near-infrared (IR2) image under natural light conditions; c) Near-infrared (IR2) image when illuminated by a fluorescent lamp (T8 fluorescent tube). The arrows indicate the wall painting fragments with the painting layer containing different concentrations of Egyptian blue.

Holographic Subsurface Radar tests on wall painting sample

A fresco sample of the size 25x25x2,5 cm, realized at the Accademia dell’Affresco (Padova, Italy), was used for A strandboard (thickness 1 cm) was used as structural support, covered by two layers of lime mortar: *arricio* and *intonachino* (total thickness of mortar layers 1,5 cm). The preparatory drawing was applied by tracing technique. The painting was executed by *buon fresco* technique (without retouchings) applying only one layer of alkaline-resistant mineral pigments (green earth, red and yellow ochre).

Several metal nails and mounting plates of different size were placed underneath the fresco sample. They are characterized by strong dielectric contrast to mortar/air and simulate the presence of different fixing elements, which can be found inside the wall after structural interventions (metallic ropes, fixing anchors and nails, etc.). Their detectability by HSR technique was investigated through a series of simplified tests using different acquisition parameters.

The first acquisition was performed over the fresco sample with buried defects placed underneath it. The second acquisition was performed over the same defects in the same position, after removing the fresco sample. A transparent plexiglass sheet (0,5 cm thick) was used as an intermediate support for manual acquisition over the fresco surface and a non-transparent plywood sheet (0,5 cm thick) was used as the support for additional manual acquisition directly over defects. The additional acquisition was aimed to evaluate better the influence of the fresco sample medium on the resulting holographic image. The acquisition step and the measurement resolution (in planar direction) used are of 0,5 cm.

The presence of strong dielectric contrast bigger larger than 0,5 cm (measurement resolution) was detected in each of the acquired holographic images.

Figure 95 shows the acquisition process and the resulting holographic images, using the defects represented by two steel mounting plates (one 1,5 x 3,0 cm and the other 3,0 x 7,0 cm).

Fig. 95d shows the holographic image, acquired on the defects underneath the fresco sample and the Fig. 95e shows the holographic image, acquired on the defects directly, without it. Comparison of the obtained results shows that the signal was disturbed by non-planarity of the sample surface and by the highly porous and irregular internal structure of the strandboard support. The presence of metal elements was, however, still detectable underneath the laboratory fresco sample.

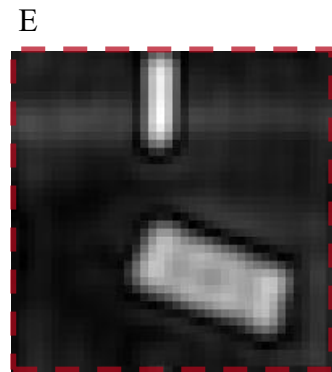
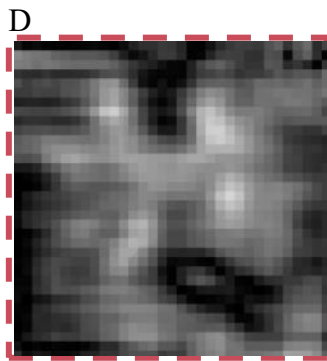
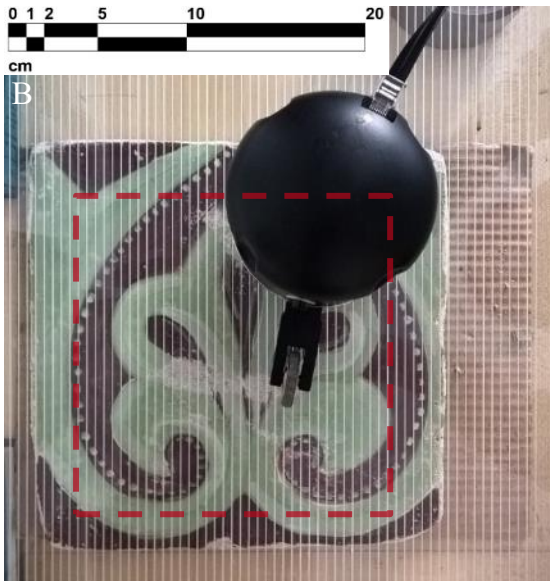
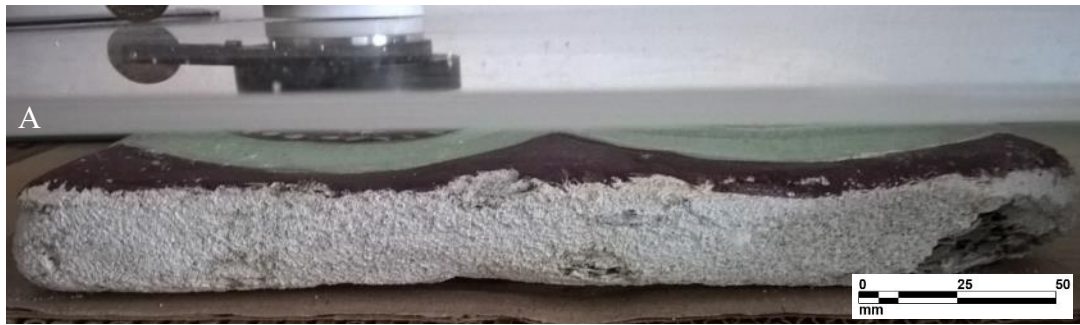


Figure 95. Rascan 5/7000 laboratory tests on a fresco sample. a) Lateral view during the acquisition procedure; b) manual acquisition procedure, the red dashed line shows the area of interest; c) Position of buried elements (2 mounting steel plates of dimensions 1,5 x 3,0 cm and 3,0 x 7,0 cm); d) Rascan image at 6.8 GHz, focused at 1,5 cm depth, acquired on a fresco sample covering the hidden objects , after processing in Q-Rascan software; e) Rascan image at 6.7 GHz, focused at 1,0 cm depth, acquired on the objects, covered by a plywood sheet, after processing in Rascan-Q software.

Additional tests were dedicated to the alternative ways of post-processing of HSR data. Comparison of splitted non-processed images at different showed to be a useful tool for additional help in discrimination between the overlap of discontinuities shown by a processed rascan image (Fig. 96).

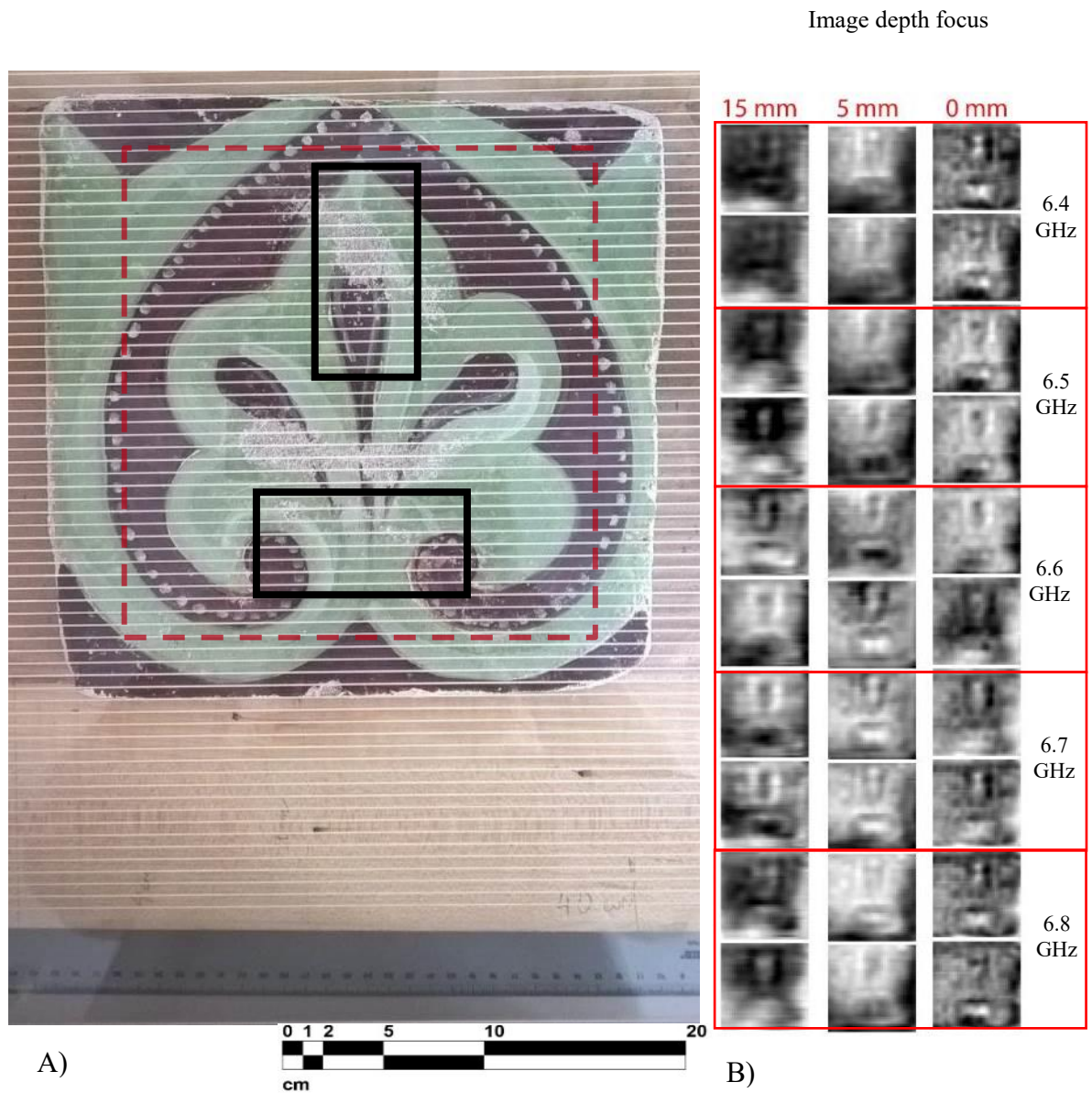


Figure 96. Alternative ways of data visualization: a) image of the fresco sample with the position of acquisition frame 20x20 cm (dashed red line), hidden defects (showed by black contour); b) comparison of in-phase and quadrature components of the signal at three different depths from the lower point of the fresco sample: on the surface, inside the medium and immediately underneath the fresco layer.

Subsurface structural diagnostic tests on a mosaic laboratory model

The experiments were aimed at evaluation of the informativity of Holographic Subsurface Radar (HSR) and Digital Holographic Speckle Pattern Interferometry with Stimulated Infrared Thermography (DHSPI and SIRT) to provide crucial information about the subsurface structure at different depth levels. Their informativity is evaluated in terms of capability to address the specific needs of historical mosaic conservation: on-site detection of hidden structural inhomogeneity and defects, cracks, voids, detachments, identification of deteriorated, previously restored or reshuffled areas.

An experimental mosaic model was realized at the Orsoni Foundry in Venice (Italy), following traditional procedures of historical Venetian artisanal workshop of the 19th century [209]. The foundry was established in 1895, having maintained since then the same procedure of glass manufacture till now.

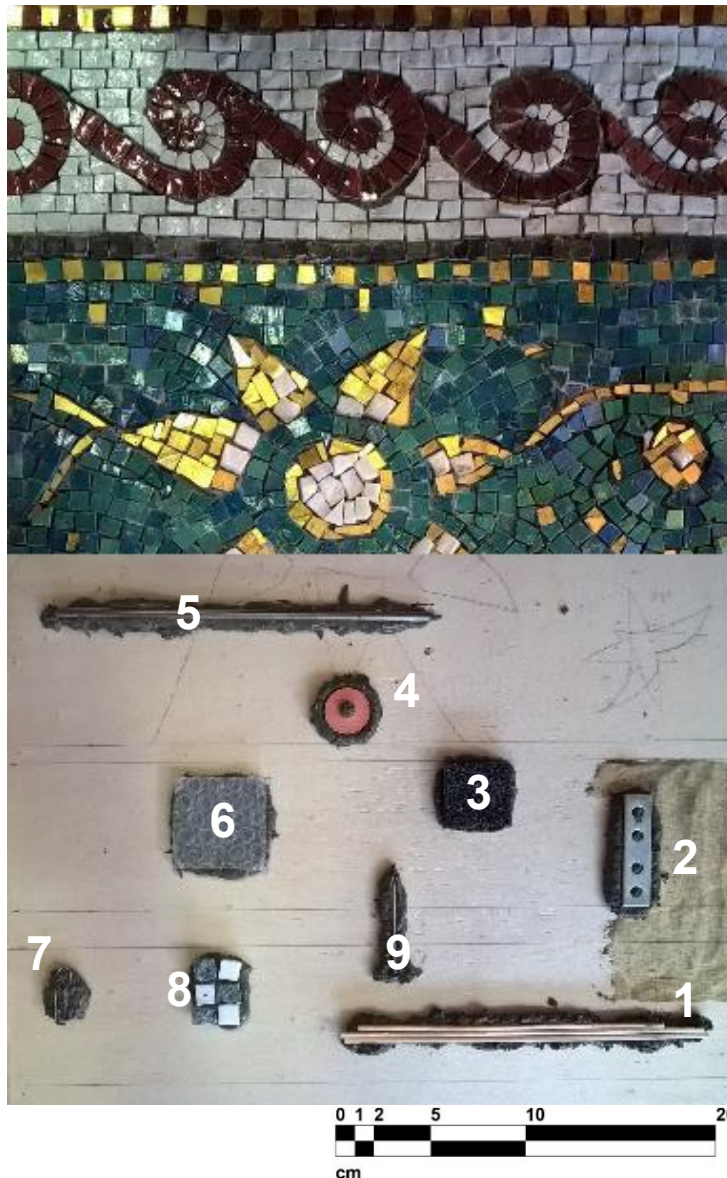
The mosaic model consists of three main parts: the support, the substrate and the decoration layer. A plywood sheet of the dimensions 400 x 600 mm x 5 mm provides the structural support for the sample's transportation. The thickness of the preparation layer varies from the bottom to the top of the mosaic model, starting from 3 layers in the bottom part up to 1 layer in the upper part of the mosaic, with a maximum difference of 20 mm.

Upon the first bedding layer, several known defects (Fig. 97) were placed and subsequently covered by another layer of cement based mortar:

- 5) metallic elements: steel stick, stainless steel inox plate, steel nail, bended thin metallic wire;
- 6) thick (synthetic sponge) and thin detachments or adhesion loss (airbubble wrap);
- 7) other elements present inside the mortar structure (wooden sticks, rubber ring, mosaic tiles etc.).

It should be added that buried metallic elements of known thickness, form and size simulate the presence of fixing elements and joints underneath the decoration. Mosaic tiles represent residues of plastered layers (stone and glass) materials underneath. Wooden sticks are the elements that can be present inside the historical Byzantine mortars. The air bubble wrap represents a loss of adhesion between layers (very shallow detachment), while a semi-rigid synthetic sponge (mix of air and plastic) simulates a bigger detachment. The presence of plastic in the wrap and in the sponge was necessary for the formation of the defect with the necessary thickness and its persistence after the mortar setting down. A shallow rubber ring represents a

non-original material with very different dielectric and thermal properties if compared to the surrounding medium. This material is not expected to be encountered within the historical or archaeological structure and acts as a reference for testing the performance of different techniques.



1. three *wooden sticks* (diameter around 3 mm, length 200 mm);
2. one *steel inox plate*, with four holes (15 x 60 x 1mm);
3. one semi-rigid *synthetic sponge* (35 x 35 x 5 mm);
4. one *rubber ring*, with central hole (diameter 25 mm, thickness 3 mm);
5. one *metallic stick* (diameter 5 mm, length 200 mm).
6. *air bubble wrap* (45 mm x 50 mm, thickness 1-5 mm);
7. one *metallic clip*, steel wire (30 x 10 mm, 1 mm thick);
8. three *marble* and three *glass tiles* (each around 10x10x10 mm).
9. *steel nail* (45 mm length, diameter 2 mm, head diameter 5 mm)

Figure 97. Buried defects inside the mortar subsurface structure: a) photo of the defects; b) list of defects.

The upper decoration layer consists of three types of tesserae:

- manually cut glass paste tesserae manufactured by Orsoni Foundry (different colours);
- manually cut stone tesserae (carrara and verona marble, grey basalt);
- golden leaf tesserae (cartellina).

The colours of the glass-paste tesserae used in the decoration layer of the mosaic model include: several shades between light and dark blue tesserae, light and dark green tesserae, white and a

few tones. The colours of the stone tesserae used in the decoration layer of the mosaic model include: white carrara marble, light red verona marble, dark and light grey basalt tesserae.

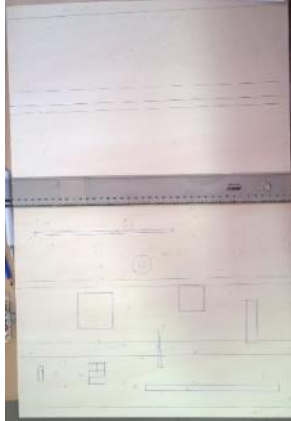
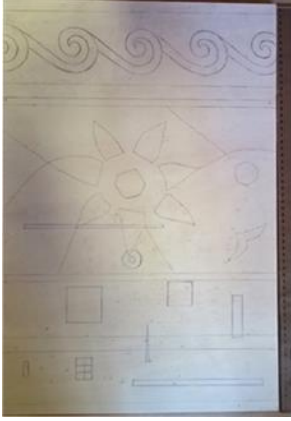

The application of mortar was performed in different ways:



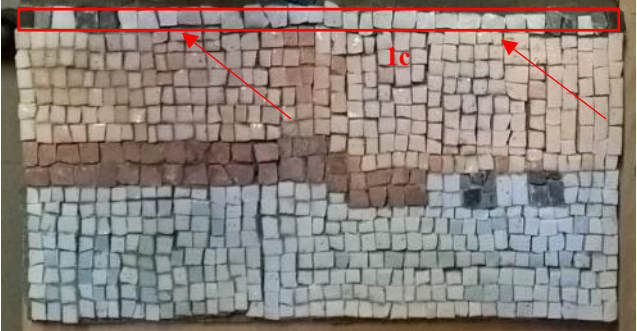
- in homogeneous flattened layers in the bottom part of the mosaic;
- by inhomogeneous inlays in the central and upper part of the mosaic.



The simulated and documented differences in mortar application represent possible structure inside the historical mosaics, with eventual consolidation injections, rearrangements and mosaics integrations.

The detailed timeline of mosaic model realization is presented in Table 23.

Table 23. Documentation of mosaic sample realization

Procedure	Description	Photographic documentation	
1 step Preparation of the plywood support	<p>The design scheme was transferred from a sheet of paper to the plywood sheet (by tracing technique). The distribution of hidden elements was traced in a different color. The plywood support was treated by vinavil and subsequently dried (48 hours).</p> <p><i>Dates: 26-27.09.2016</i></p>		
2 step Placement of defects	<p>First, a 5 mm layer of cement based mortar was laid upon the plywood sheet. The objects that represent the defects were placed over the first preparation layer and subsequently covered by 5 mm of cement based mortar.</p> <p><i>Dates: 28-29.09.2016</i></p>		

<p>3 step Realization</p> <p>Section 1a-b</p>	<p>The application of mortar started from the half-part of the mosaic that contains hidden defects (400 mm width, 300 mm height). This section contains mostly glass-paste tesserae, with addition of stone tesserae inclusions in the decoration layer.</p> <p><i>Dates: 30.09 – 04.10.2016</i></p>	
<p>3 step Realization</p> <p>Section 2</p>	<p>Simultaneously, the realization of the upper part of the mosaic started (400 mm width, 200 mm height). Its structure in the upper part of the mosaic contains only one thin layer of cement based mortar (2-3 mm). The hand-cut glass-paste tesserae are placed directly on one preparation layer on the plywood sheet. It is considered to be homogeneous.</p> <p><i>Dates: 30.09 – 07.10.2016</i></p>	
<p>3 step Realization</p>	<p>When the section 1a-b was finished, the row of stone tesserae was applied over 10-15 mm cement based mortar layer (section 1c).</p> <p><i>Date: 05.10.2016</i></p>	

	<p>In the central area of the mosaic, the mortar was applied in pieces, following the lines of decoration layer pattern.</p> <p>The first figure shows the first areas applied in the central part of the mosaic.</p> <p><i>Date: 06.10.2016</i></p>	
	<p>These two figures show an intermediate step and the last day in the application of mortar.</p> <p>07-10.10.2016; 11.10-14.10.2016.</p>	

Summarising the complexity of the model, it can be presented as a system of three levels:

1. Differences in subsurface structure: mortar proportional composition and application (Fig. 98a).
2. Differences in tesserae color and composition: glass paste, stone and gilded tesserae (Fig. 98b).
3. Differences in surface topography: irregularity of the surface and tesserae pacement (Fig. 98c).

Aiming at the evaluation of the limits of applicability of the holographic radar to the irregular (in terms of planarity) and inhomogeneous surfaces (in terms of the composition of constituent materials), three-dimensional scanning survey on the mosaic model was performed by the means of scanner "Chronos Dual" produced by Open Technologies. The visual representation of model surface irregularity was performed by the means of the commercial software Cinema 4D.

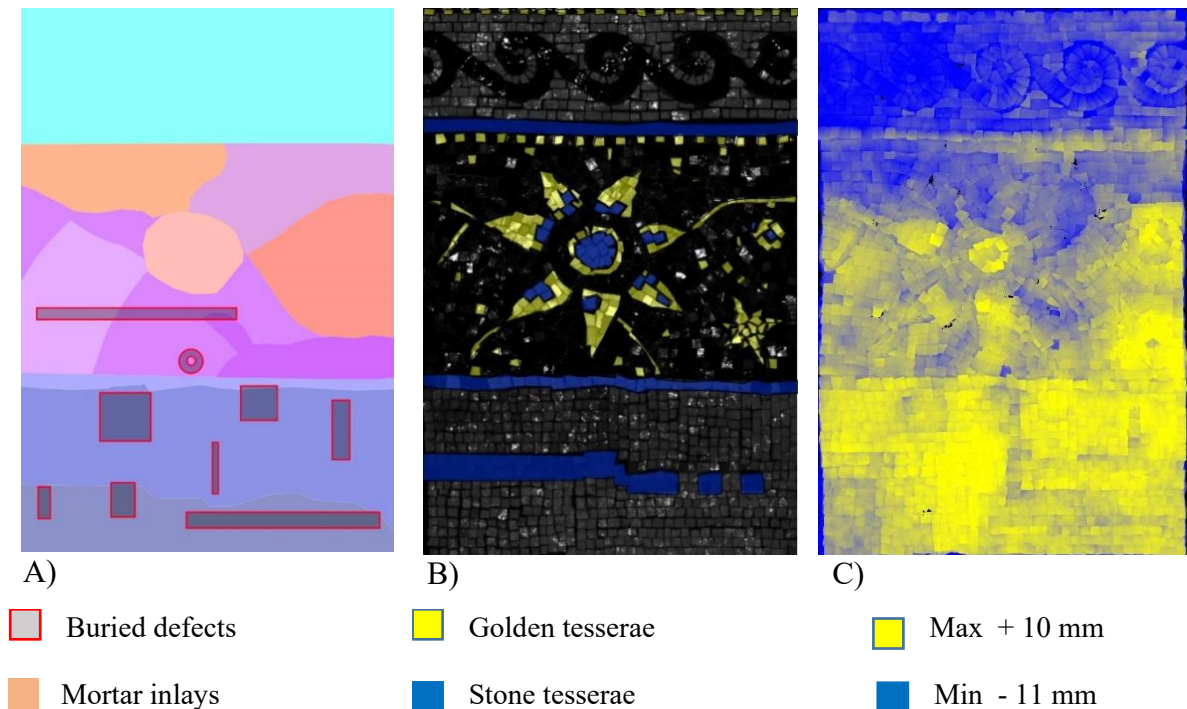


Figure 98. The structure of the mosaic sample: a) position of buried defects and structure of mortar; b) scheme of golden (yellow) and stone (blue) tessera; c) topography of the surface, obtained by 3D laser scanner survey. The color gradient map shows the differences in height on the surface of the mosaic model.

The three methods, selected for the laboratory study, exploit the interaction of electromagnetic radiation with the matter, but are based on different physical principles:

- Holographic subsurface radar method, the main technique of the experimental study, which is based on the detection of contrasts in dielectric permittivity of different materials;
- Simultaneous application of Digital Holographic Speckle Pattern Interferometry and Stimulated Infrared Thermography, which provide complementary information on the subsurface structure, based on differences in thermal expansion behavior (DHSPI) and thermal conductivity properties (SIRT).

The list of relative physical properties for the subsurface medium and buried defects are reported in Table 24 [210-217]. These values are approximate and are aimed to give a general idea of differences in physical values between the defect and the medium. The exact values of thermal conductivity, thermal expansion coefficient and dielectric permittivity constant should be measured for the given combination of the objects' characteristics.

Table 24. Summary of physical properties for subsurface elements

Number	Element	Material	Thermal conductivity, k [W/(mK)] [100, 101]	Linear thermal expansion coefficient (volumetric expansion coefficient is indicated in brackets) [102,103]	Dielectric permittivity Constant [104, 105]
-	substrate	cement based mortar	1.4- 1.75	11-14	2.2
1	wooden sticks (3)	unknown wood	0.05-0.14	30	2.3
2	metallic plate (1)	stainless steel	16	18.5 (55.5)	infinite
3	semi-rigid fiber sponge (1)	unkown rigid plastic and air	0.2 for glass fiber and 0.03 for air	40-120 and 0.034	1.2 and 1
4	rubber ring (1)	rubber	0.045	(80)	2.5-4.6
5	metallic stick (1)	stainless steel	16	18.5 (55.5)	infinite
6	air bubble wrap (1)	air	0.33 for plastic and 0.03 for air	108-120 and 0..034	2.2-2.4 and 1
7	metallic bended wire (1)	steel	16	9.9 – 14.8 (29.7 – 44.4)	infinite

8	tesserae (6)	marble, glass	3.14 for marble and 0.96 for glass	5.5-14.1 and 5.9	8 and 6.9
----------	---------------------	------------------	--	---------------------	-----------

Holographic Subsurface Radar tests

The reconstruction of a microwave image in the system was complicated by reflections from the irregular surface which usually dominate the reflections from the subsurface target. More, in the specific case of a mosaic decoration layer, many tesserae tesserae are characterized by high metal oxides content (for example, up to 19% lead oxide) or contain metal leaf (golden tesserae). The surface is complex (due to the variable size of tesserae and interstitial areas). The glass paste material is characterized by high metal oxides content (for example, up to 19% lead oxide) or contains metal leaf (gold). The golden tesserae are widely used in Byzantine mosaics for background areas and for details in the figures of Saints.

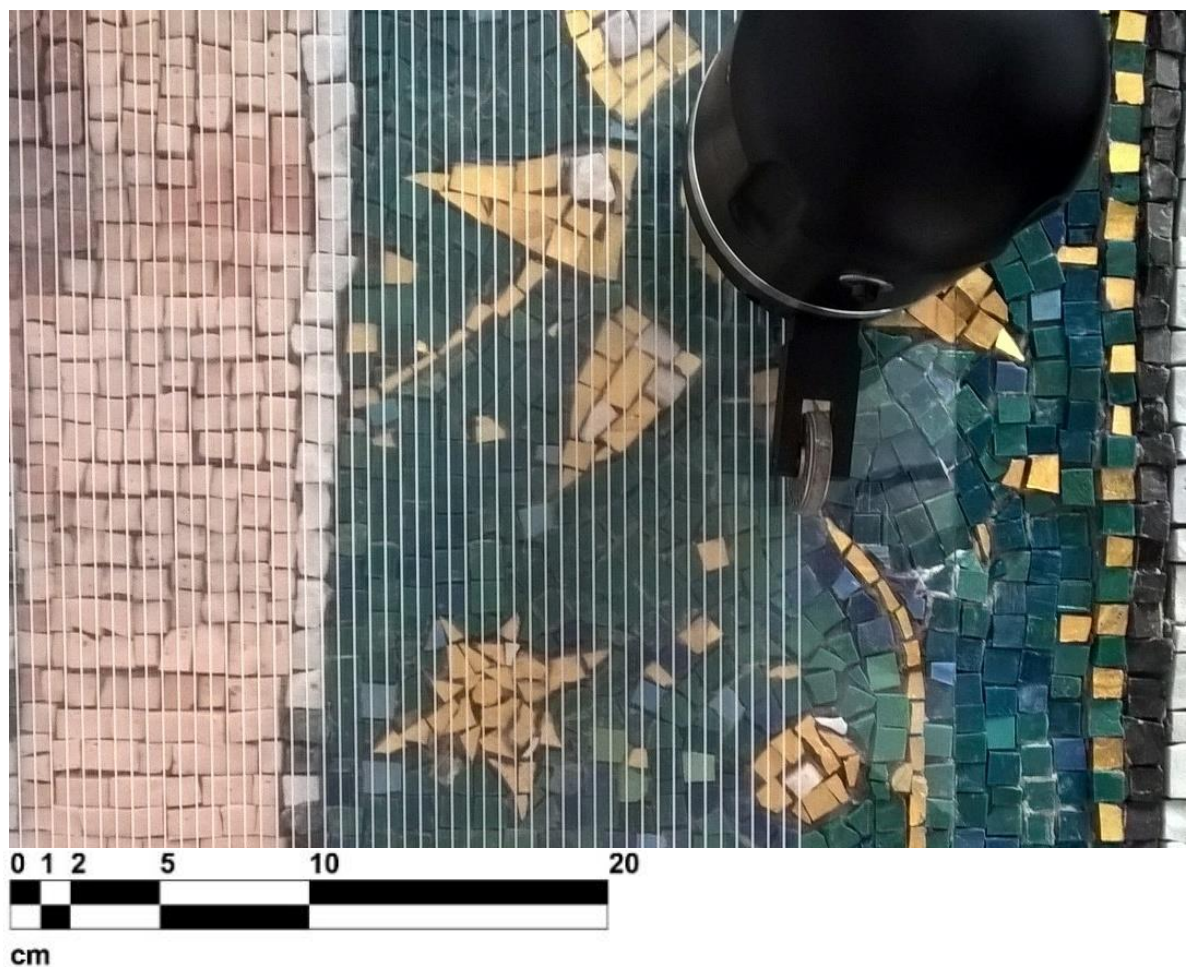


Figure 99. Manual operation of the Rascan 5/7000 a laboratory mosaic model with the use of plexiglass sheet containing incised acquisition guiding lines.

Figure 100c shows the stitched combination of six small area acquisitions (25x25 cm, 20x30 cm), with the operating frequencies 6.7 and 6.8 GHz, focused at different depths from 1,5 to 2 cm below the surface of the mosaic sample.

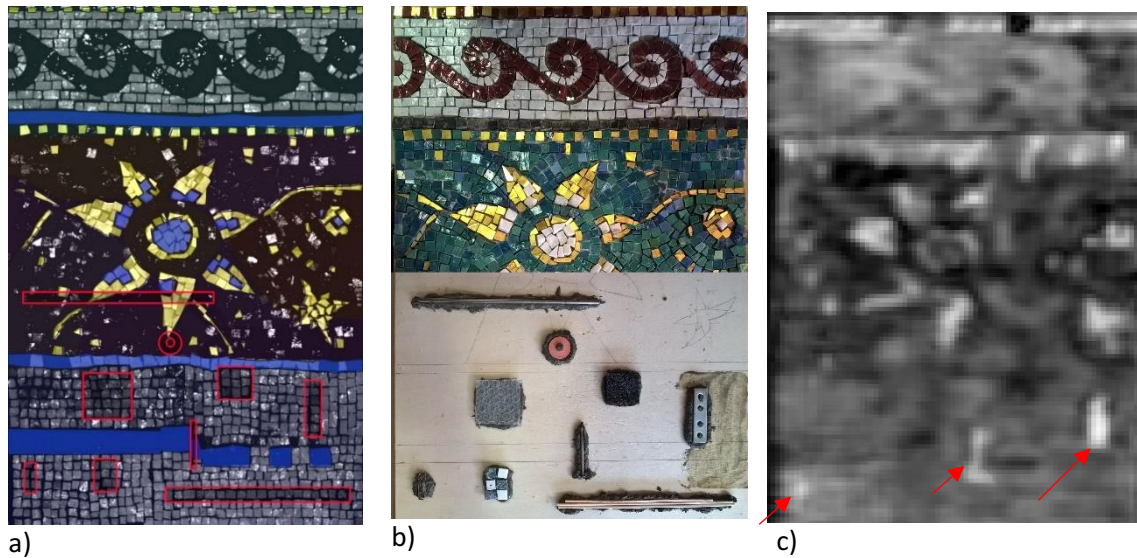


Figure 100. Mosaic inhomogeneities and rascan image. a) Scheme of the mosaic sample showing the position of different tesserae and different mortar portions; b) Buried defects in the subsurface structure; c) Rascan image at 6.7-6.8 GHz.

Though the surface height of the mosaic sample is variable (the difference between the lowest and the highest points is of 21 mm), the acquisitions were performed on small acquisition areas. The most appropriate depth value was selected for each acquisition area, in order to focus on the planar depth containing the buried defects. Focusing on the given depth levels was performed by the means of Rascan-Q software.

The results are visualized as “in-plane” horizontal maps of the intensity of the waves, which contain a sum of reflections from different depth levels. Switching the frequencies and with a known dielectric permittivity of the constituent material, it is possible to focus the image at the specific depth. The strongest differences will correspond to the selected level. The image, however, will still contain the sum of reflections that come from different depths.

The obtained Rascan images represent the complex inhomogeneity of the custom-built sample. The stitches in the mortar and the minimal differences in composition are not detectable by HSR technique, since they do not show the contrast in dielectric permittivity.

The signal phase shift, observed on the HSR image as grayscale contrast, may indicate the presence of the known buried objects, but at the same time may be related to other factors (surface irregularity, mortar structure), coming from different depths. It is not possible to discriminate between these anomalies without the use of complementary techniques or precise information about the subsurface structure.

The strongest reflection in the obtained Rascan image comes from the surface golden leaf tesserae of the decorative layer. The two buried metal elements, namely the steel plate with

holes and the steel nail, are detectable underneath stone and glass paste tesserae of the decoration layer and inside relatively homogeneous mortar medium. At the same time, the reflections from the metal stick are predominantly overlapped by the reflections from the golden tesserae of the decorated surface.

The observed inhomogeneity areas in the Rascan image may indicate the presence of metal clips, of a synthetic sponge and of a simulated shallow detachment (air bubble wrap). Nevertheless, discrimination is not possible without the use of additional complementary techniques.

In the given experiment, due to the phase shift of the signal and its reconstruction by Rascan-Q software, the signal reflections from metallic elements appear as bright areas, the reflections from the simulated void/detachment and from the semi-rigid synthetic sponge appear as dark areas. Comparison of the 3D virtual model of the mosaic to the HSR resulting image allowed a better understanding of the influence of surface irregularity on the experimental results (Fig. 101).

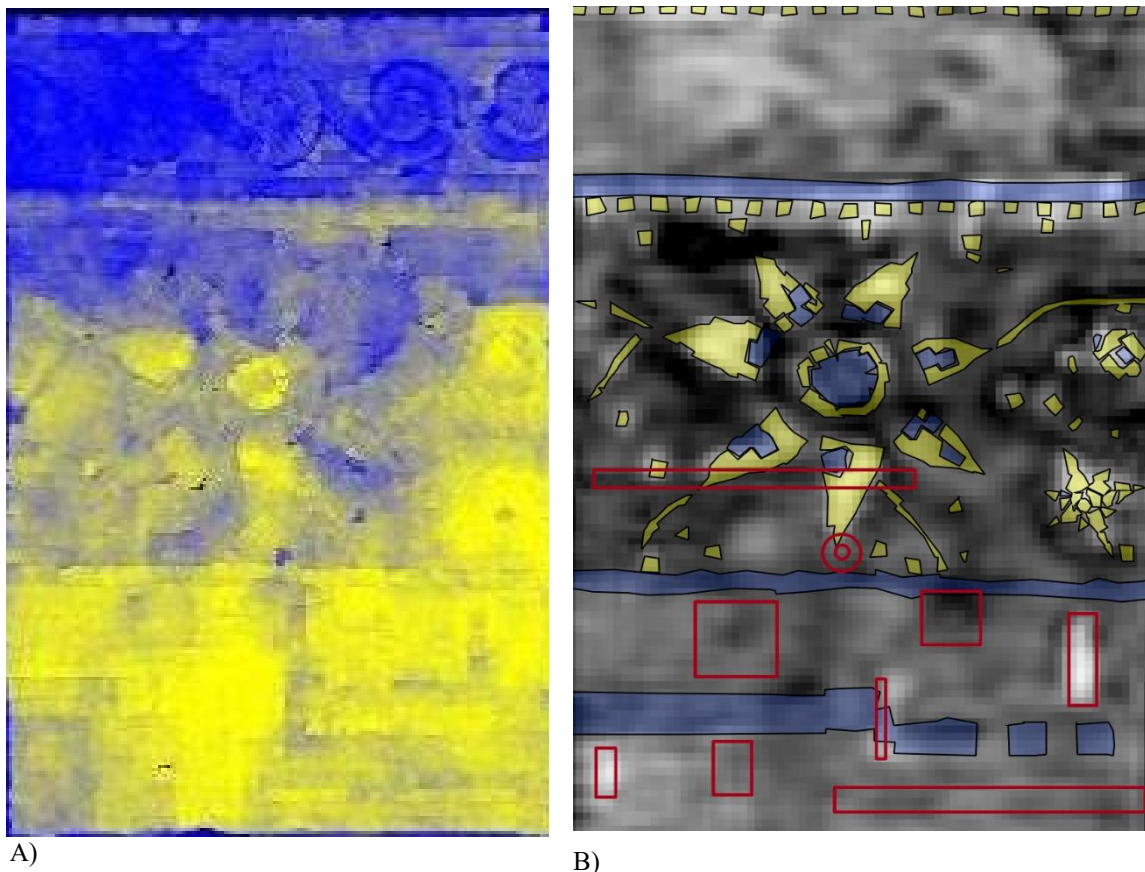


Figure 101. Comparison of mosaic surface topography image, acquired by 3D laser scanner survey (a), and the Rascan image, 6.7-6.8 GHz (b). The image 6.8b shows an overlap of strong reflections from the mosaic surface (golden leaf tesserae indicated in yellow and stone tesserae in light blue) compared to the position of buried defects (red contour).

Additional tests on a gilded icon

The fact that the signal does not penetrate underneath the metal leaf surface represents a strong limitation of the technique’s application in the field of Byzantine wall mosaic diagnostics. It was confirmed experimentally by the tests on a gilded icon on a wood panel. A steel plate was placed under the icon: completely underneath the gilded area, at the edge between the gilded and painted areas, underneath the paint layer. The experimental results confirmed that the metal plate was detectable only underneath the painted area. In the case of gilding, the signal was completely reflected from the surface and did not penetrate (Fig. 102b). The part of the steel plate underneath the gilded background was not detected.

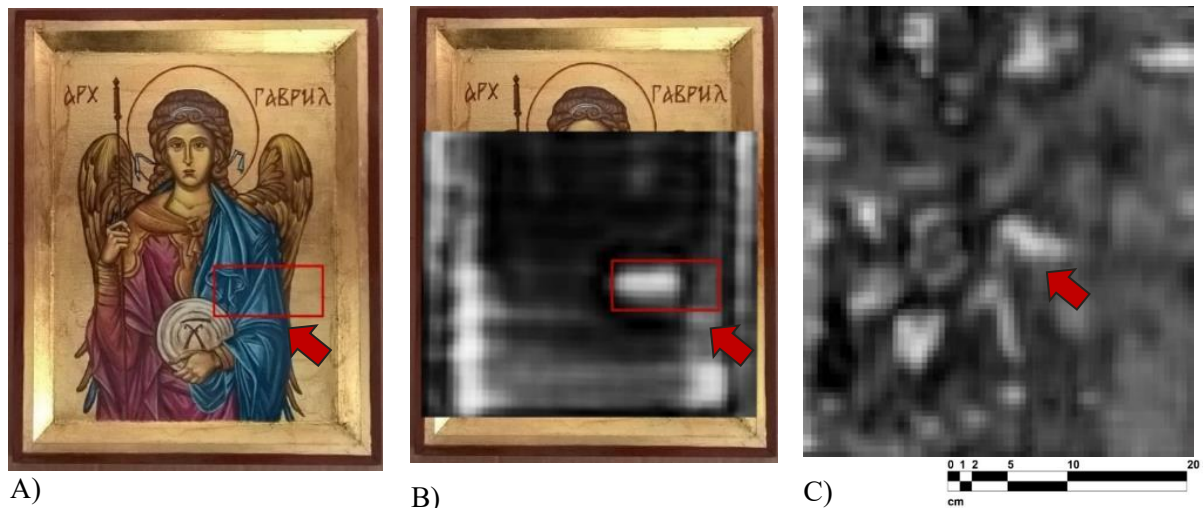


Figure 102. Some experimental tests illustrating the limitations of the technique when applied to golden tesserae and gilded details in wall mosaics decorations: a) Position of the hidden metallic plate under the icon; b) Result of Rascan acquisition at 6.5 GHz, focused at the depth of 1 cm, where only the part of the metallic plate under painted surface is detected; c) case study reflections from the gilded tesserae surface.

The summary of experimental results on detectability of known defects by the means of HSR technique is reported in Table 25.

Table 25. Experimental results of HSR acquisitions

Buried defects	HSR informativity	Possible explanation
Differences in composition and stitches of mortar	not detectable	-
1) Wooden sticks	not detectable	not sufficient contrast in dielectric permittivity

2) Steel plate	detectable	high contrast in dielectric permittivity
3) Semi-rigid synthetic sponge	not detectable	Reflections from irregular surface and other factors to be defined
4) rubber ring	not detectable	Reflections from irregular surface and other factors to be defined
5) steel stick	not detectable	high contrast in dielectric permittivity but overlap of strong surface reflections
6) air bubble wrap	not detectable	Reflections from irregular surface and other factors to be defined
7) metal clip	detectable	high contrast in dielectric permittivity
8) steel nail	detectable	high contrast in dielectric permittivity
9) glass and marble tiles	not detectable	Reflections from the surface, signal attenuation and other factors to be defined

Digital Holographic Speckle Pattern Interferometry and Stimulated Infrared Thermography tests

The experimental tests on the combined use of DHSPI-SIRT were performed at the Holography Metrology Laboratory of the Institute for Electronic Structure and Laser, Foundation for Research and Technology (IESL-FORTH), Heraklion (Crete, Greece) during March-April 2018.

The experimental set-up, used for laboratory experiments, was designed for simultaneous recording of micro-deformation and thermal responses of the sample with the objective to acquire real-time holographic and thermal recordings of the thermomechanical effects on the object after thermal excitation by infrared irradiation. The description of the two system operation can be found in Chapter 2.3. the experimental set-up of simultaneous DHSPI-SIRT acquisition, developed at IESL-FORTH and used in these tests, is illustrated in Fig. 103.

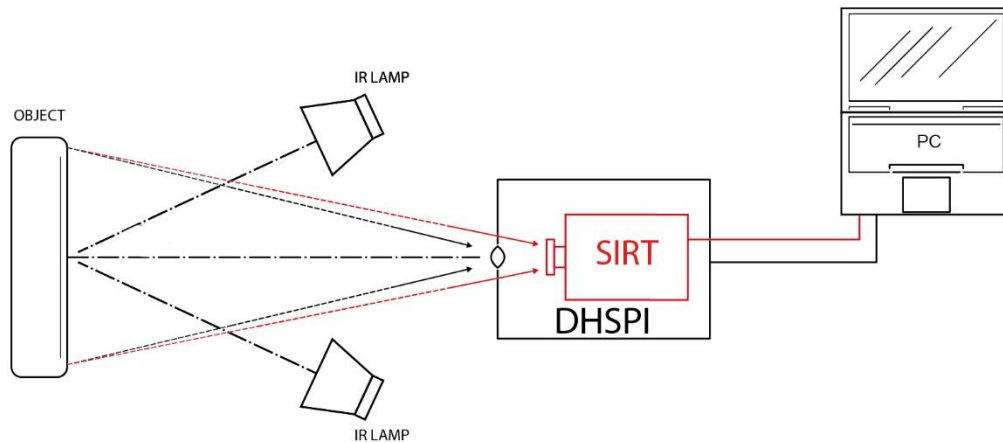


Figure 103. Scheme of the experimental set-up of simultaneous DHSPI-SIRT acquisition.

Two infrared lamps of 175 mW were placed on the same angular setting to the orthogonal axis of the object's surface (from 20 to 45°), in order to provide homogeneous thermal excitation to the whole investigated surface. The temperature increase of the surface is recorded by a thermometer device, connected to the pc and recording the surface temperature continuously from the beginning of the experiment. Other sensors connected to the same pc, in particular, a thermometer and a relative humidity meter, are recording the environmental RH/T values before the excitation and throughout the experiment. The operation of both systems in the laboratory is shown in Fig. 104.

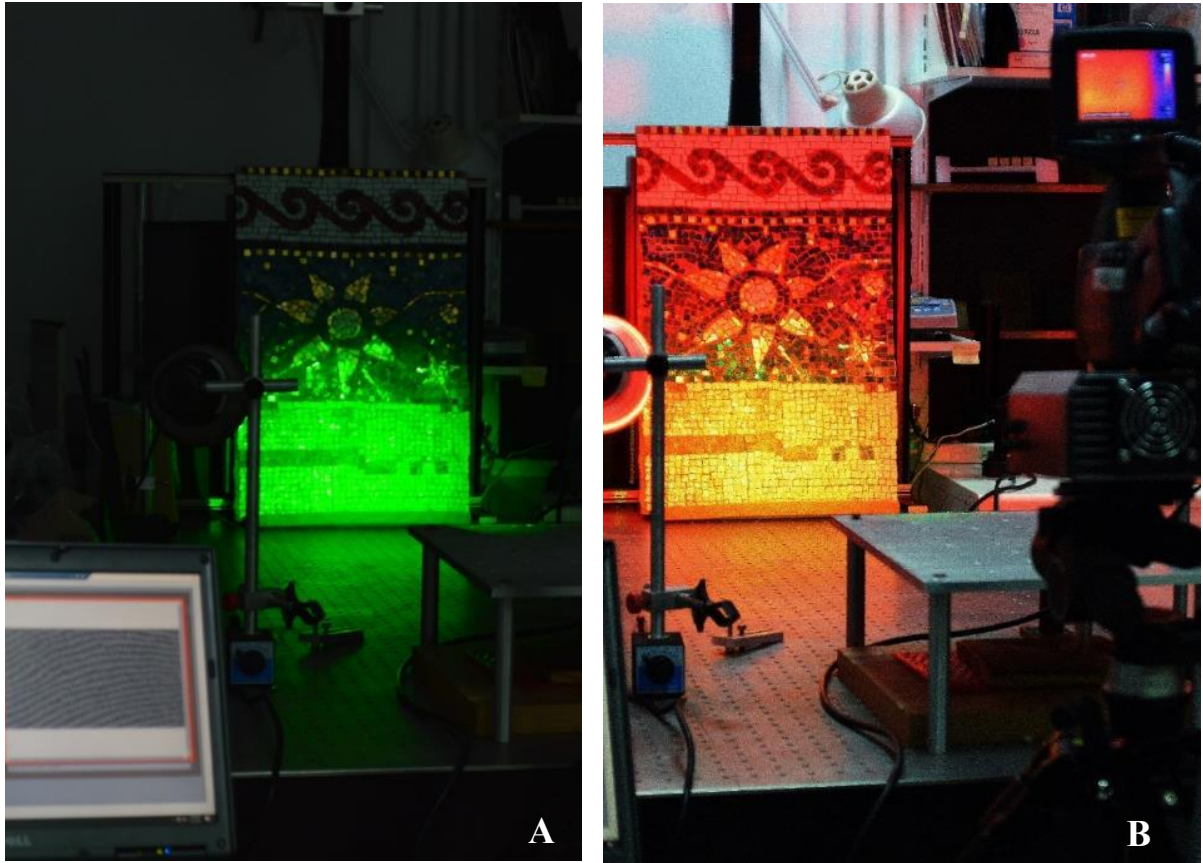


Figure 104. Simultaneous DHSPI and SIRT laboratory acquisitions. a) Digital Holographic Speckle Pattern Interferometry; b) Stimulated Infrared Thermography.

The mosaic sample was fixed firmly on a holder. By the DHSPI the first reference image was acquired before the IR lamps were switched on. SIRT and DHSPI systems started recording simultaneously as soon as the lamps are switched off. In full-field acquisitions, the DHSPI and SIRT systems were placed at a distance of 95 cm from the object. For detailed area acquisitions, the distance varied in the range 45-50 cm from the object.

DHSPI results of detailed area investigations

Among the known defects, the synthetic sponge is detectable through open curves of fringes starting from approximately 120 seconds of cooling down monitoring after induced thermal impact $\Delta t=1.0^{\circ}\text{C}$ (60 seconds of IR excitation at a distance of 50 cm). This pattern can be classified as “internal crack or detachment” (structural diagnostics fresco) and this discontinuity was the earliest to appear among the detected defects. Air bubble wrap gave impact on the surface as an open curve starting from 200 seconds after induced thermal impact of $\Delta t=1.4^{\circ}\text{C}$ (after 80 seconds of IR excitation). Other defects were also detectable, for example, the rubber

ring as an irregular circular fringe within a complex morphology of fringes pattern and the steel stick as a change in the direction curves. The detectability of the nail through a slight direction change in the direction of fringes was achieved by longer thermal excitation, $\Delta t=2.1\text{ }^{\circ}\text{C}$ (after 160 seconds of infrared excitation). The defects simulating detachments, for example, synthetic sponge, appear on the interferograms as open curves after lower thermal impact and as closed curved fringes after higher thermal impact (Fig. 105a and 106), indicated by red arrows.

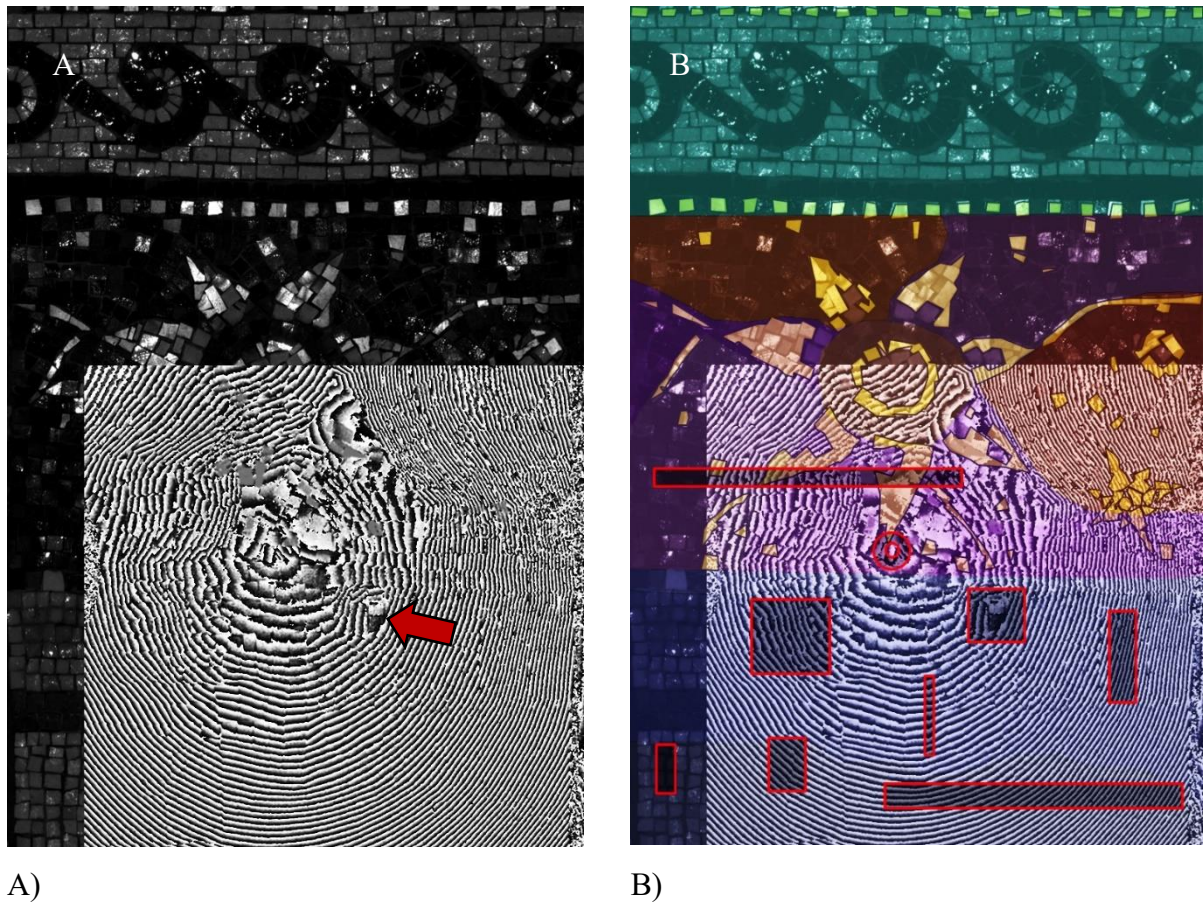


Figure 105. Detailed DHSPI acquisition after 160 seconds of thermal excitation (induced thermal impact of $\Delta t=2.1\text{ }^{\circ}\text{C}$). a) interferogram at 200 seconds after thermal excitation placed over a white light reference image; b) overlay of complex sample inhomogeneity over the interferogram captured at 200 seconds after thermal excitation.

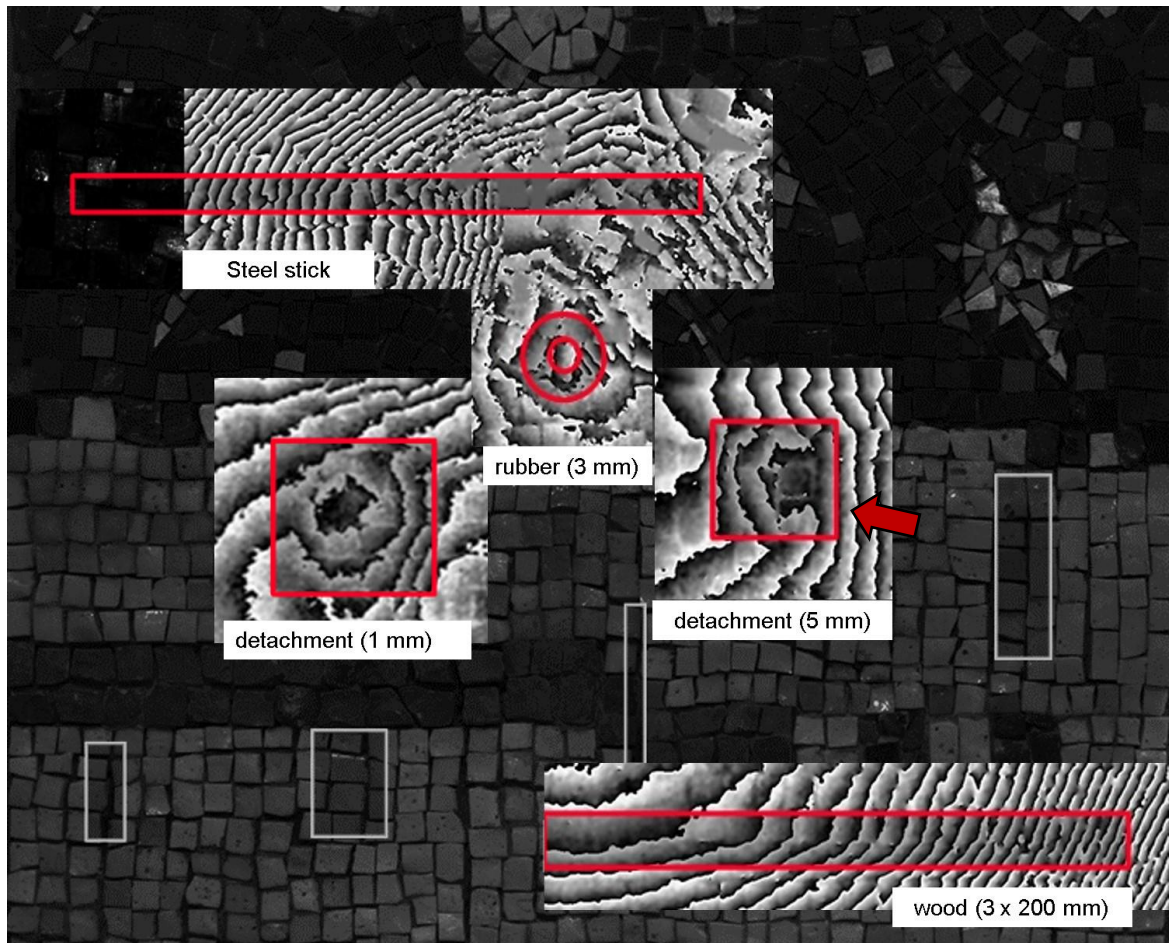


Figure 106. Summary of detected known defects in small area acquisitions with thermal excitation of 2.1 to 3.1 °C.

The presence of a flat steel inox plate was not detected by the DHSPI system by detailed area acquisitions. The thermal excitation induced on the buried defect did not induce sufficient deformation in vertical direction, in order to provide an impact on the mosaic surface.

Besides the known defects, the system allowed to distinguish areas, characterized by distinct density and inclination of fringes, as well as discontinuities formed by parallel dead-end fringes. Generally, the changes in fringes density may be correlated to the different properties in underlying materials (their composition and microstructure). The dead-end fringes may indicate the presence of cracks.

The acquired interferogram, already shown in Fig. 105, revealed presence of unknown (or at least unintentionally present) defects. These are abrupt dead-ends of the fringes indicating the presence of cracks (shown by a red arrow) and small closed curves of the fringes indicating the presence of small voids between the tesserae and mortar or inside the mortar structure (showed by a white arrow). These discontinuities are detected in the areas where the mortar was applied

quickly, using a higher proportional amount of acrylic glue and water, and without pressing/flattening of the layers.

At the same time, the areas with different density and direction of inclination of fringes corresponding to the different portions of mortar, prepared and applied separately and in a different manner. These pieces of mortar are characterized by a different ratio of cement powder, water and acrylic glue. The first differences were observed in detailed acquisitions after 40 seconds of thermal excitation, with the thermal gradient of only 0.5 °C. Fig. 107 illustrates the detection of subsurface crack and inhomogeneous microstructure in the central part of the mosaic, with no hidden elements underneath.

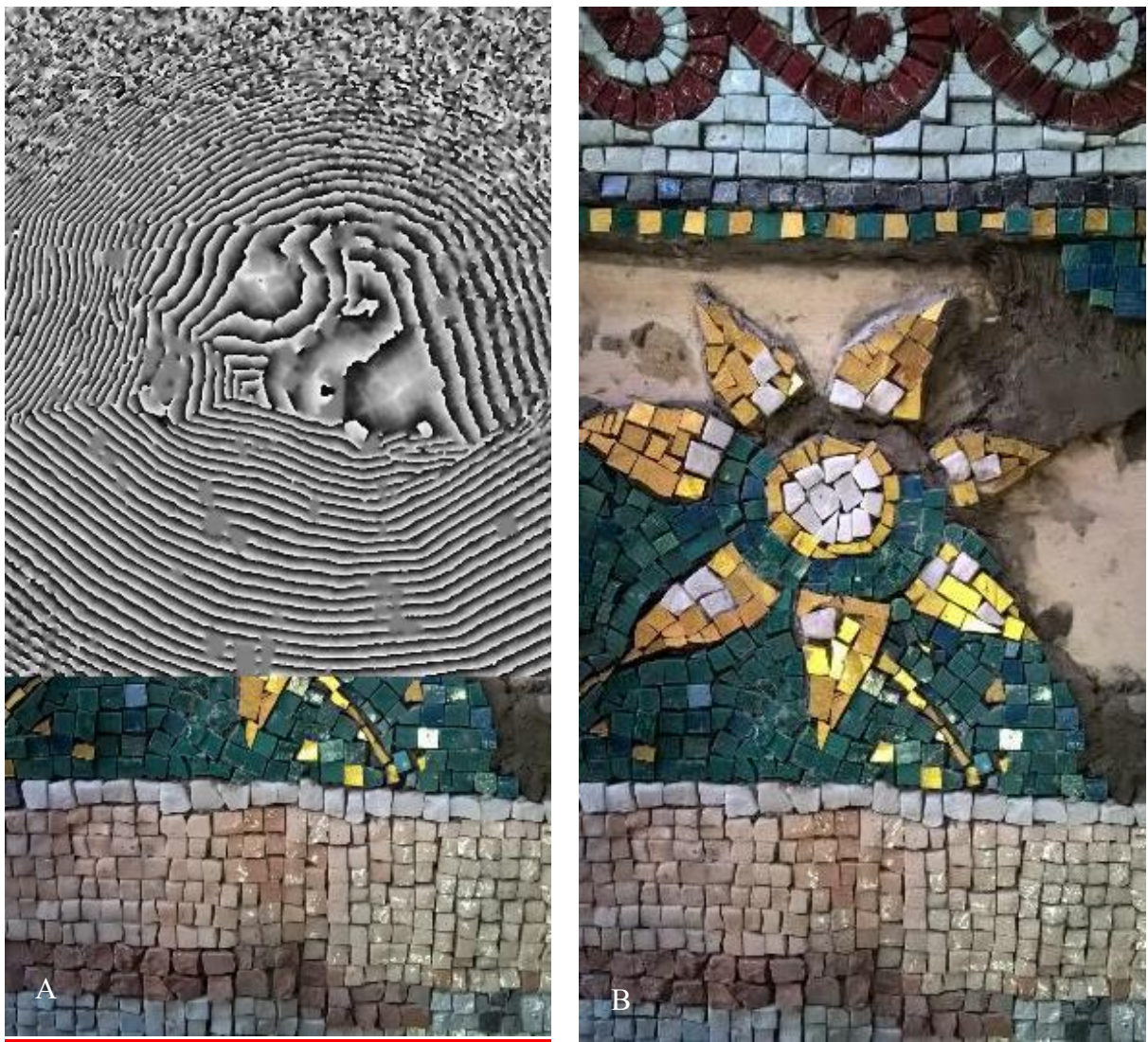
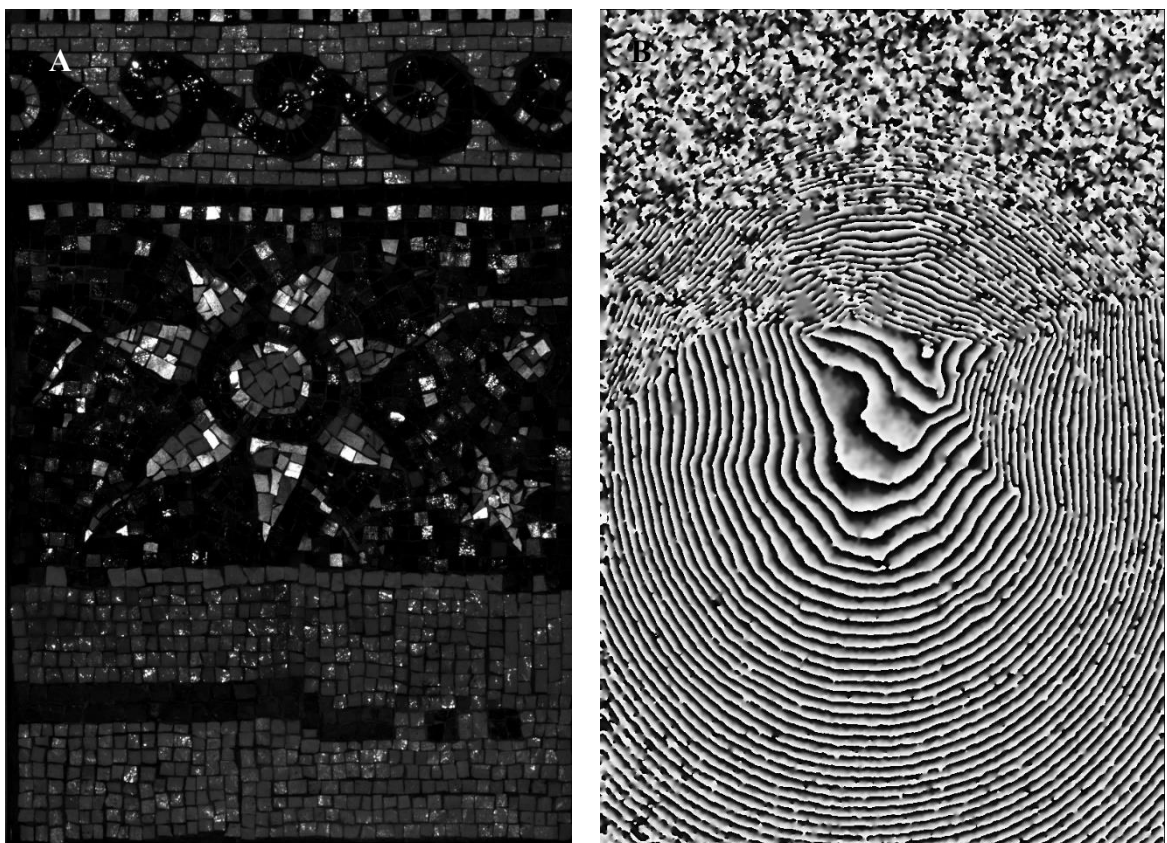


Figure 107. Mosaic model in process, upper part. A) Sample preparation in progress, detail of mortar application; B) Interferogram at 170 seconds after $\Delta t=3.1$ thermal excitation (80 sec.).

The interferogram pattern shows the curved stitch of the mortar layers along the decoration design, as well as horizontal discontinuity at the boundary between the central and upper part of the mosaic.

Results of overall acquisitions

After 60 seconds of thermal excitation on the whole sample from the distance of 900 cm, when the sample's surface temperature increased of $\Delta T=0.6$ °C, the interferograms started to show clear differences in fringes pattern density and directions. In order to compare the revealed differences to the known discontinuities in the subsurface structure, the documentation scheme of mortar distribution was overlaid on the interferogram captured at 49 seconds of cooling down monitoring, using 50% layer transparency mode in Adobe Photoshop (fig.108a). The direction changes in fringes, according to the developed classification for fresco structural diagnosis (DHSPI structural diagnosis), may indicate the presence of material change inside the sample's structure. As shown in Fig.108b, these changes predominantly match the known stitches of mortar.



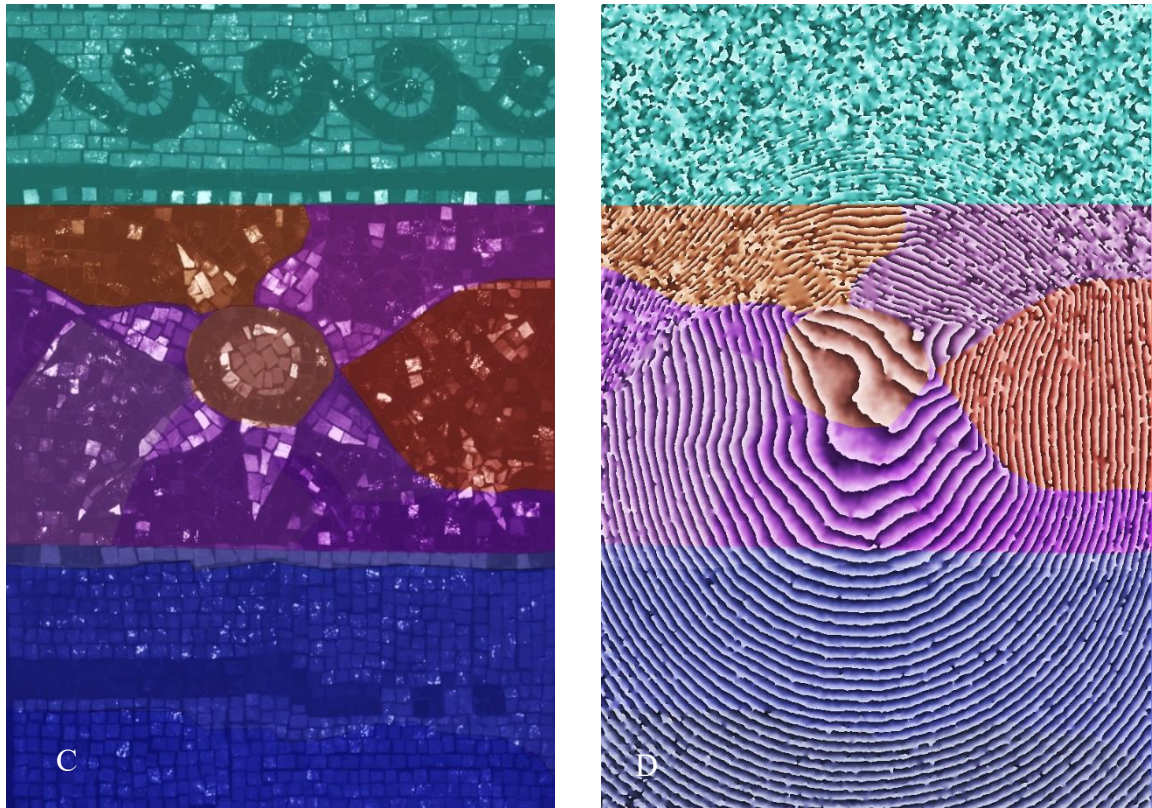


Figure 108. Overall acquisition on a mosaic sample.

- A) White light image;
- B) Interferogram at 49 seconds of cooling down monitoring after $\Delta t=1.4^{\circ}\text{C}$ (80 seconds of excitation),
- C) Overlap of the subsurface mortar structure scheme and the white light image, using Photoshop layers blending mode (50% transparency) ;
- D) Interferogram at 49 seconds of cooling down monitoring after $\Delta t=1.4^{\circ}\text{C}$ (80 seconds of excitation) overlap using Photoshop layers blending mode (50% transparency).

The system has not been applied before on mosaic sample of this complexity level (mortar, defects, irregularity of the thickness and materials of the decoration layer), and further tests may be needed for correct interpretation of fringes pattern discontinuities, detected during investigations of mosaic surfaces.

The summary of the detectability of known defects by DHSPI technique is presented in Table 26.

Table 26. Detectability of known defects by DHSPI

Buried defects	DHSPI informativity	Fringes pattern and possible explanation
Differences in composition and stitches of mortar	detectable	change in fringes direction and density
(1) Wooden sticks	detectable in a small area acquisition	slight change in fringes direction
(2) Steel plate	not detectable	not sufficient thermal expansion in vertical direction, no impact on the surface

(3) Semi-rigid synthetic sponge	detectable in detailed acquisitions	closed curves (detachment or void)
(4) rubber ring	detectable in detailed acquisitions	closed curves (detachment or void)
(5) steel stick	detectable in detailed acquisitions	change in fringes direction
(6) air bubble wrap	detectable in detailed acquisitions	change in fringes direction
(7) metal clip	not detectable	Too small, not sufficient thermal expansion in vertical direction, no impact on the surface
(8) steel nail	not detectable or hardly detectable	slight change in fringes direction
(9) glass and marble tiles	not detectable	not sufficient thermal expansion in vertical direction, no impact on the surface

SIRT data

Analysis of detailed SIRT acquisitions

The thermal images revealed differences in the surface temperature distribution, which can be related both to surface and subsurface characteristics of the mosaic. As mentioned before, the decoration layer consists of marble tesserae (thermal conductivity 3.14), glass paste tesserae (thermal conductivity is to be estimated due to variable contents of lead and other metal oxides) and metal leaf under a thin layer of glass (thermal conductivity is to be estimated). The tesserae are of different colors and are placed at different angles. Some of the tesserae act as mirrored surface (creating a shimmering effect of reflections on the thermogram), see Fig. 109.

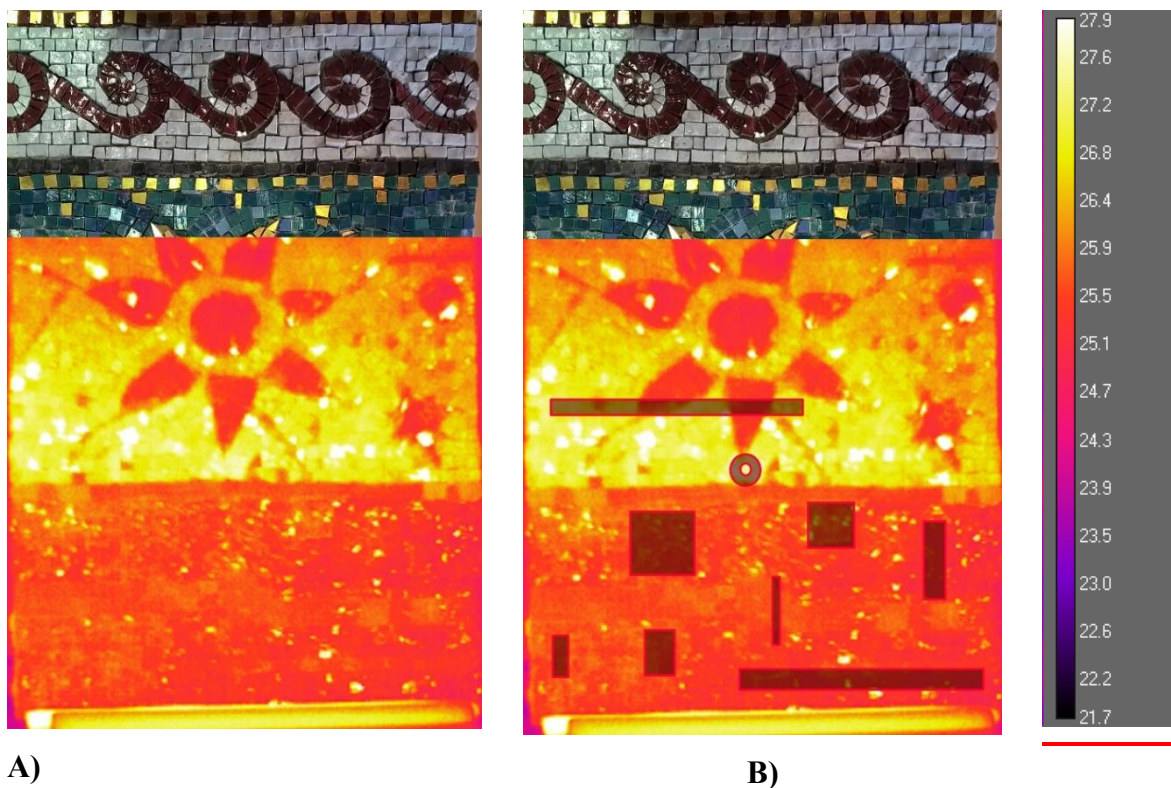


Figure 109. a) Thermal image at 1st second after 180 sec. by IR excitation ($\Delta T= 0.8$ °C); b) the same image showing the position of the hidden defects.

Due to the inhomogeneity of the mosaic surface, the presence of buried objects is hardly detectable (synthetic sponge, wooden sticks) or not detectable (steel inox plate) by solely visual observation of thermal images (Fig. 109). The discrimination between the thermal contrasts and their interpretation requires their simultaneous correlation to the visible observation of the mosaic: surface topography, material color and composition, thickness of the sample. More, the correlation of the results to other techniques (DHSPI and HSR) can be useful.

Processing of SIRT data

Rectangular regions of interest (ROI) were drawn upon the sample’s surface: one ROI covering exactly the area above a buried defect with two ROIs in its proximity, covering the surrounding areas without buried objects. Average temperature values, subsequently called *mean temperature* values, were detected for each of the analyzed areas. The mean temperature over time analysis by the means of Research IR FLIR software is presented for the selected defects: three wooden sticks (called defect 1), steel plate (called defect 2) and synthetic fiber sponge (called defect 3). The size of each rectangular area corresponds to the size of the correspondent defect underneath the decoration surface:

- 3x10 mm rectangular areas covering the wooden sticks and two equal surrounding areas;
- 10x50 mm rectangular areas covering the steel plate and two equal surrounding areas;
- 30x30 mm rectangular areas covering the synthetic sponge and two equal surrounding areas.

At the 1st second of excitation, each of the three defected areas shows higher mean temperature values than their surrounding areas (detectable by visual observation of thermal images for defect 1 and 3, not visible for defect 2). The temperature values of each defected area and its thermal gradient with the surrounding areas at the start and at the end of cooling down monitoring are reported in the tables 27-29.

Table 27. Mean temperature per area inside and outside the defect 1

Defect 1 (wood)	T ₁ at the 1st sec., [°C] Start of the cooling down monitoring	T ₂ at the 360 sec., [°C] End of the cooling down monitoring	Δt (T ₁ - T ₂)
Defected area	25.47	24.62	0.85
Non-defected top	25.38	24.70	0.68
Non-defected bottom	25.37	24.51	0.86

Table 28. Mean temperature values per area inside and outside the defect 2

Defect 2 (steel)	T ₁ at the 1st sec., [°C]	T ₂ at the 360 sec., [°C]	Δt (T ₁ - T ₂)
------------------	--------------------------------------	--------------------------------------	--

	Start of the cooling down monitoring	End of the cooling down monitoring	
Defected area	25.40	24.51	0.89
Non-defected left	25.33	24.71	0.62
Non-defected right	25.28	24.67	0.61

Table 29. Mean temperature values per area inside and outside the defect 3

Defect 3 (plastic and air)	T ₁ at the 1st sec., [°C] Start of the cooling down monitoring	T ₂ at the 360 sec., [°C] End of the cooling down monitoring	Δt (T ₁ - T ₂)
Defected area	25.83	25.08	0.75
Non-defected left	25.61	24.93	0.68
Non-defected right	25.52	24.81	0.71

Fig. 110 shows the position of the analyzed ROIs for the comparison of mean temperature values inside and outside the defect 1. On the right part of the mosaic sample, the central ROI covers only the defected area 1, two equal ROIs are located to the top and to the bottom from it, without buried objects underneath. The analysis was performed on three equal ROIs, placed symmetrically on the left side of the sample, partially covering the position of mosaic tiles and of a metallic clip underneath the decoration layer.

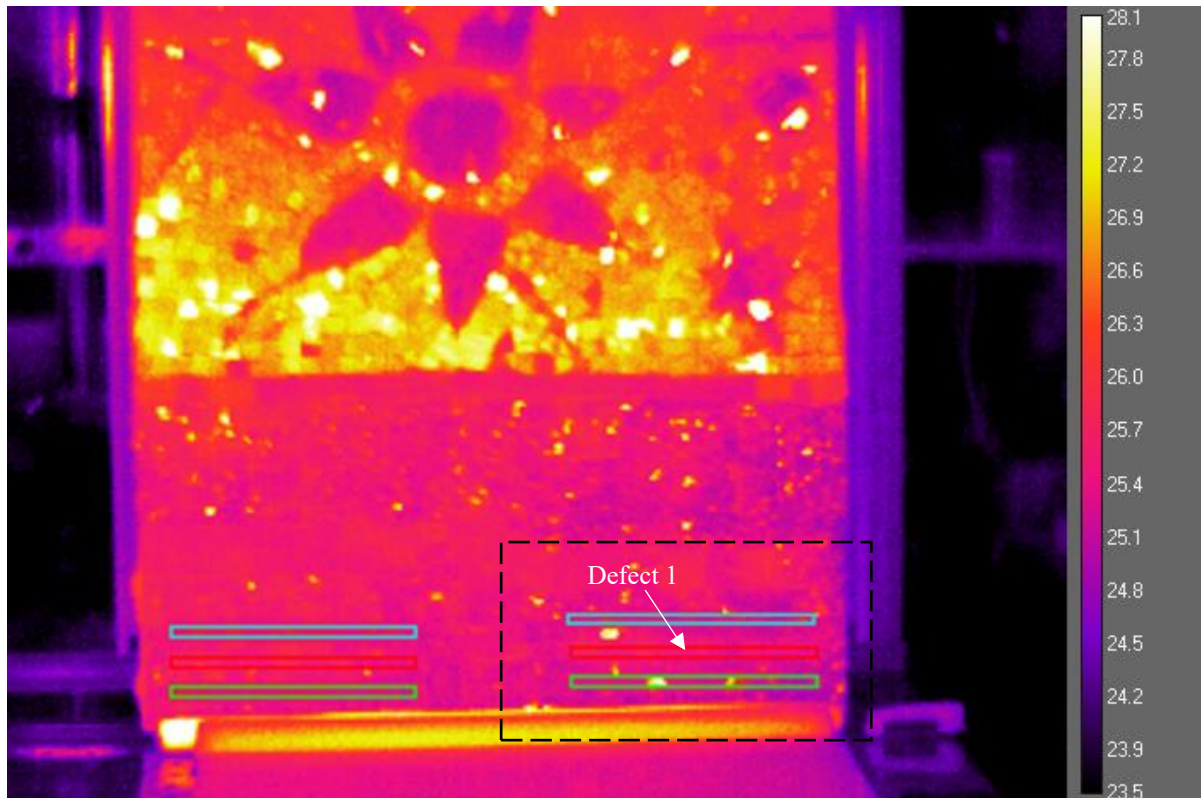


Figure 110. The position of the ROIs inside and outside Area 1 (outlined by a black dashed rectangle). The thermal distribution between the ROIs on the right side of the sample is compared to symmetrically placed ROIs on the left side of the sample.

The comparison of thermal plots for the two sets of three ROIs, on the left and on the right side of the mosaic sample shows that:

- on the left side of the mosaic, without wooden sticks in the subsurface layer, the plots show the distribution of values, expected for a sound area of the mosaic (the presence of buried mosaic tiles and a metallic clip is not detectable);
- on the right side of the mosaic, where the buried wooden sticks are located, the higher mean temperature at 1st second after excitation is detected in the defected area (25.47 °C), compared to defect-free areas (25.37 and 25.38 °C respectively). The temperature inside the defect equalizes with the values of the defect-free area at 110 seconds after excitation. At the end of the cooling down monitoring the distribution of values reaches the distribution similar to the left part, dependin solely on the geometry of the sample, materials on the surface and thermal excitation homogeneity.

The increase in surface temperature above the area covering the buried wooden sticks can be explained by the lower thermal conductivity of the wood elements, compared to the thermal conductivity of the cement mortar binding medium (0.05-0.14 and 1.4-1.75 respectively).

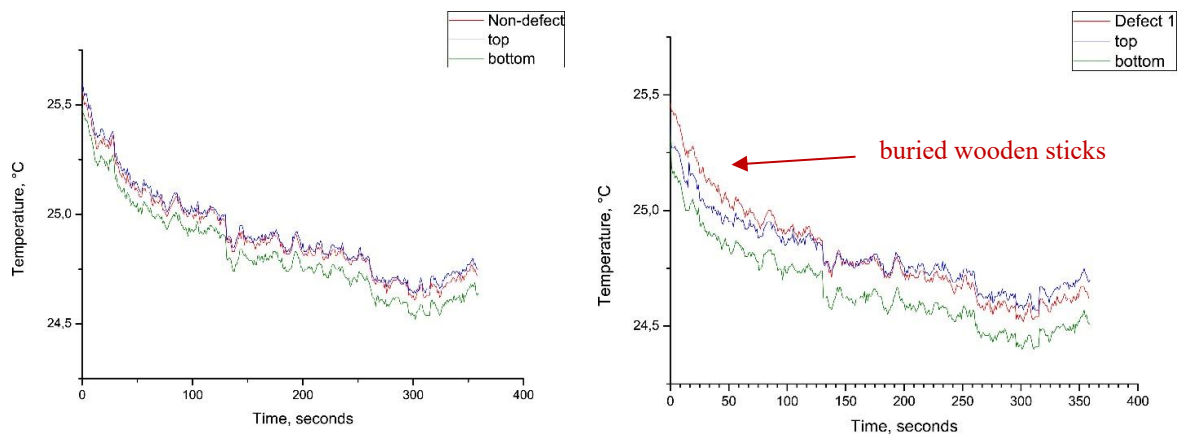


Figure 111. Temperature over time plots: a) Left part of the mosaic, where mosaic tiles and metallic clip are hidden in the subsurface structure. b) The right part of the mosaic, where wooden sticks are hidden in the subsurface structure.

Fig. 112 shows the position of the ROIs for the measurement of mean temperature values over time inside and outside of the defect 2 (metallic plate) and of the defect 3 (synthetic sponge). As shown by the temperature plot (Fig. 113), at the 1st second after thermal excitation, the area upon the stainless steel plate shows slightly higher mean temperature values than its surrounding areas (difference of 0.2 °C) and it is not detectable by visual observation of thermal images. Already at 30 seconds of cooling down monitoring, temperature equalization of the surface occurs and, subsequently, starting from 92 seconds, the inverted distribution of temperature values is maintained until the end of cooling down monitoring. At 300 seconds of cooling down monitoring its difference, however, is very low (0.1 °C). It can be explained by the fact that the metal with higher thermal conductivity ($k=16 \text{ W}/(\text{mK})$) heats faster and cools down faster than the surrounding medium, characterized by lower thermal conductivity ($k=1.75 \text{ W}/(\text{mK})$).

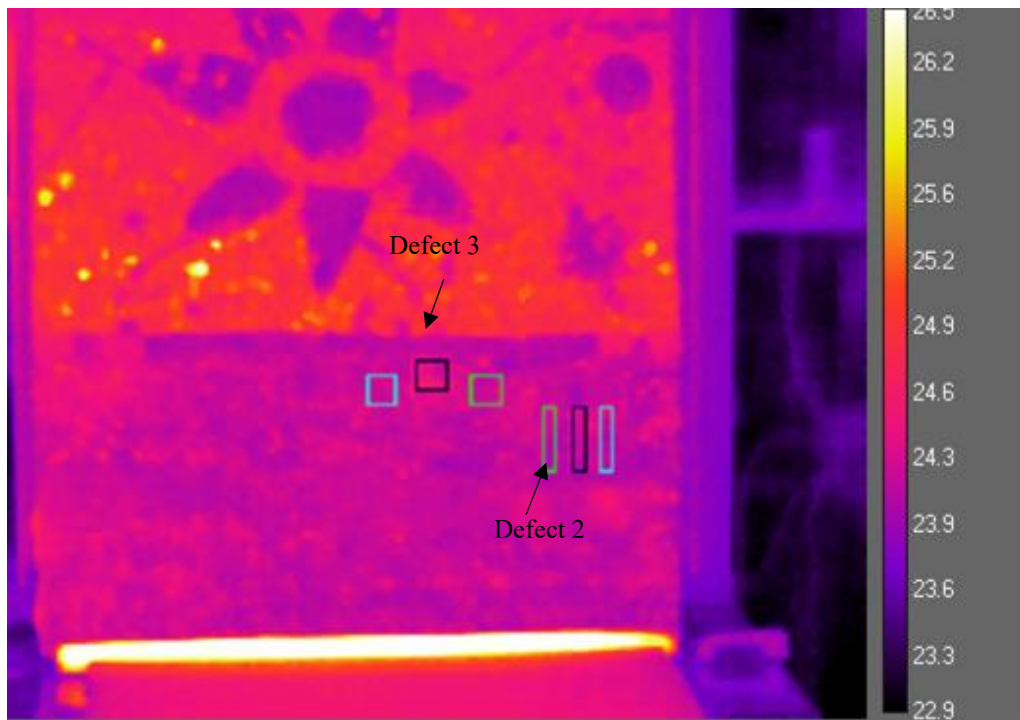


Figure 112. The position of the two defects and analyzed ROIs for the defects 2 and 3.

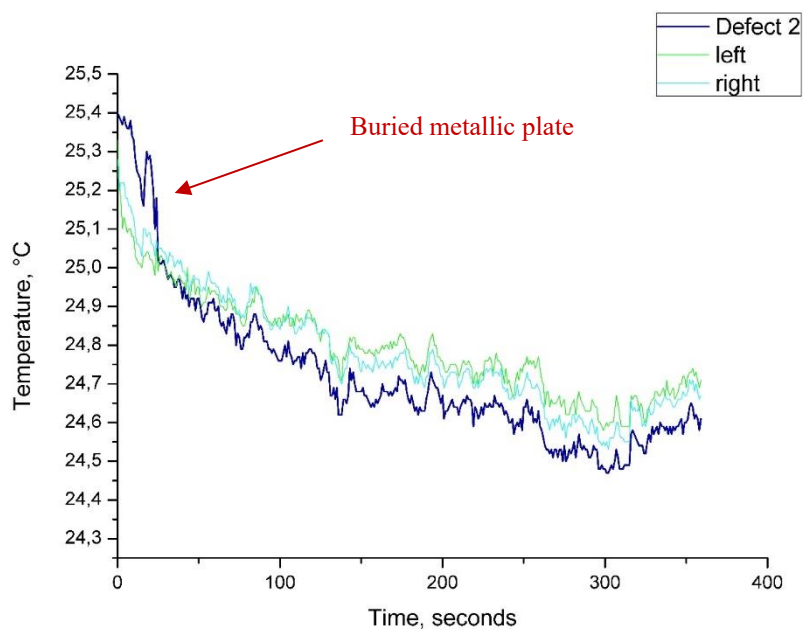


Figure 113. Mean temperature over time for the area upon the buried metal object (blue line) and two surrounding areas of equal dimensions and form.

Additionally, thermal plots for two points inside and outside of the position of steel plate were calculated and plotted. Point 1 is located within the defected area and point 2 is located in the

proximity outside it, in the direction of the bottom of the sample. Both points are located above the glass paste tesserae, point 2 in very close to the stone tesserae.

The temporal plots for the two points inside and outside the area the area of defect 2 confirmed the inversion of absolute temperature values, observed in graphs of the mean temperature per area (Fig. 114).

At 1st second after thermal excitation, the point temperature within the defected area 2 (steel plate) is 0.17 °C higher than of the point outside it (25.45 and 25.27 °C respectively). The temperature inversion occurs at 31 seconds after excitation and the difference remains persistent until the end of cooling down monitoring, with the maximum $\Delta t = 0.12$ °C.

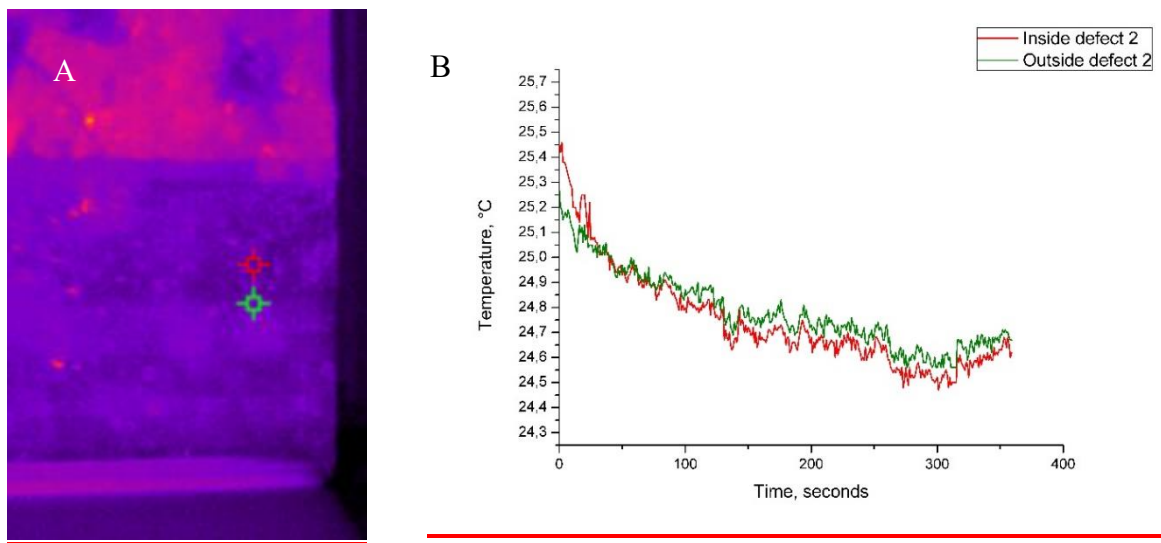


Figure 114. Temporal plots for thermal point analysis: a) The position of analyzed points (3x3 pixel); b) Point temperature measurement over time.

The defect 3 is detectable by simple visual observation of thermal images, through higher temperature than of the surrounding area, being similar to the common thermal effect of voids or detachments. However, in the temporal graphs, unlike the wooden sticks or steel plate, the exchange in temperature values between the defected and non-defected areas is yet not observed until the end of cooling down monitoring at 360 seconds. The thermal conductivity values for the synthetic sponge are low. It contains air and plastic ($k=0.026$ W/(mK) and $k=0.2-0.3$ W/(mK) respectively). The thermal energy remains blocked inside the sponge and longer monitoring time may be needed in order to observe the inversion of temperature between the defect and its surroundings.

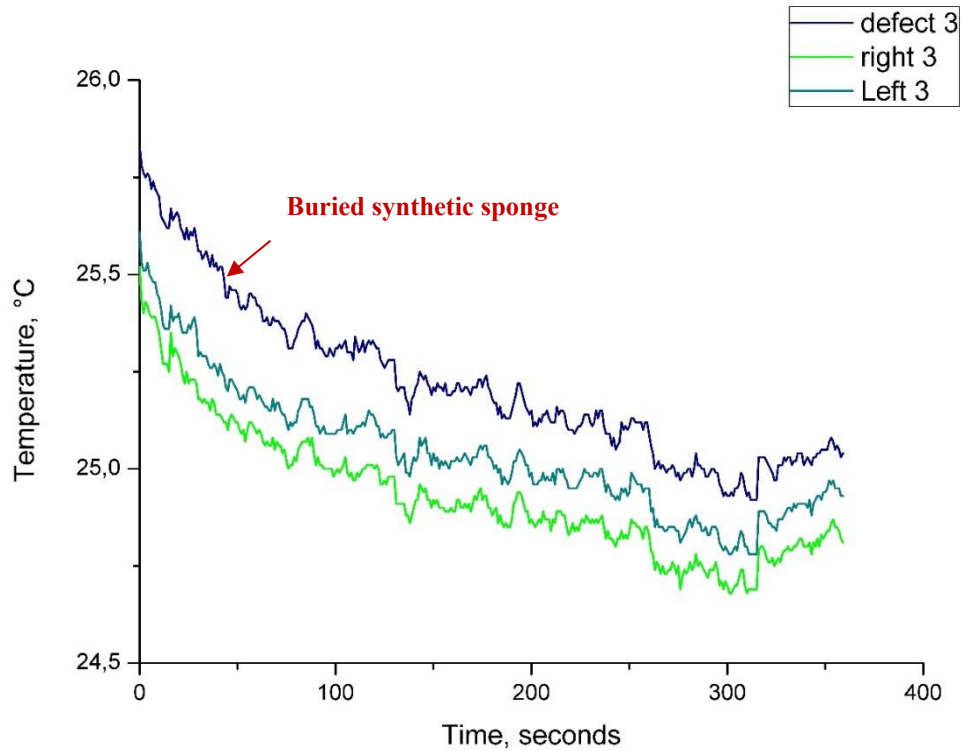


Figure 115. Mean temperature over time for the area upon the defect 3 (buried synthetic sponge) and two surrounding areas of equal dimensions and form

The summary on detectability of known hidden defects by the means of Stimulated Infrared Thermography is presented in Table 30.

Table 30. Experimental results of SIRT acquisitions

Buried defects	SIRT informativity	Detection
Differences in composition and stitches of mortar	not detectable	Absence of sufficient contrast in thermal conductivity
1) Wooden sticks	detectable	Visual observation of thermal images, data processing
2) Steel plate	detectable	Only through data processing by Research IR software
3) Semi-rigid synthetic sponge	detectable	Visual observation of thermal images, data processing
4) rubber ring	detectable	Visual observation of thermal images, data processing
5) steel stick	not detectable	Almost completely covered by metal leaf tesserae, thin diameter and high inhomogeneity of the surface
6) air bubble wrap	not detectable	High influence of the surface inhomogeneity

7) metal clip	not detectable	Absence of sufficient contrast in thermal conductivity due to the small size of the target and high influence of surface characteristics
8) steel nail	not detectable	Absence of sufficient contrast in thermal conductivity due to the small size and influence of surface characteristics
9) glass and marble tiles	not detectable	Absence of sufficient contrast in thermal conductivity, small size of buried elements

Discussion of the experimental results

The three techniques, operating with different principles, provided complementary information on the subsurface homogeneity and structural stability of the custom-built mosaic model. The acquisitions were performed as non-contact full-field investigations by DHSPI and SIRT and as detailed contact investigations by HSR.

Study of the subsurface mortar structure

The DHSPI system showed its high potentiality for the study of subsurface medium homogeneity. By observation of the interferograms over time, it was possible to reconstruct the known internal structure of mortar and differentiate between its distinct portions, applied one after another. The system was capable in recognizing the differences in the proportions of mortar's composition and in the way it had been applied (flattened, regular vs. rapid, and irregular), as well as the stitches between different parts.

Detachments, voids, adhesion loss and different inclusions in the mosaic subsurface structure

Observation of fringes morphology over time in DHSPI results allowed localizing the defects that simulate the presence of adhesion loss, detachments and voids. The biggest of these defects was localized by simple observation of SIRT images, the other well-known technique in the study of this type of defects.

Metal objects

Regarding the hidden metal objects, the steel plate was not detected: neither by the examination of interferograms pattern nor by solely visual observation of thermal images. The metal plate, simulating the presence of fixation joints or other elements underneath the decoration layer, was revealed subsequently by post-processing of thermal data over time. Thermal excitation did not provoke vertical displacement in the metal sample, therefore, no impact on the surface could be detected by the Digital Holographic Speckle Pattern Interferometry. The heating may have induced the change in length of the metal plate, which cannot be detected by the given

system. The steel plate and the steel nail were, however, immediately detectable by the third complementary technique – HSR. This method showed high potentiality in the detection of high contrasts in dielectric permittivity when the object width in planar surface is bigger than the acquisition step of the technique. The signal is reflected from a metal interface without any further penetration inside the medium, which represent, from one side, an advantage in the detection of hidden metal elements and a disadvantage, from the other side, during acquisitions upon signal reflective surfaces. This signal does not penetrate underneath the golden tesserae layer, which is a strong limitation for the field of Byzantine wall mosaics diagnostics. The signal is strongly attenuated through superficial reflections from the irregular mosaic tesserae surface with high metal oxides content (average 18-20%).

The detectability of each known defect is discussed and reported in the Tables 31-40. The summary of the results on known defects is presented in attachment H.

Table 31. Detectability of mortar inhomogeneities

Defect	Detectability by complementary techniques		
	DHSPI	SIRT	HSR
Differences in composition and stitches of mortar	Detectable, both differences in microstructure and mortar stiches: through the direction of fringes inclination and density	Not detectable	not detectable, but there is information about general inhomogeneity
Possible explanation	Impact on the surface due to different z-displacement values induced by differences in thermal expansion of different mortar portions	The differences in composition are too small, no significant cracks or detachments between the mortar portions	No contrast in dielectric permittivity

Table 32. Detectability of synthetic sponge

Defect	Detectability by complementary techniques		
	DHSPI	SIRT	HSR
Synthetic sponge	Detectable through circular fringes	Detectable through thermal gradient on the surface	Not detectable or not clearly detectable: difference in signal intensity may come from the irregular surface reflections
Notes /explanation	Difference in thermal expansion properties:	Difference in thermal conductivity	Probably, the signal is attenuated too much by the superficial layer

	impact on the surface due to different z-displacement values		
--	--	--	--

Table 33. Detectability of plastic material

Defect	Detectability by complementary techniques		
	DHSPI	SIRT	HSR
rubber ring	Detectable through circular fringes, within a very complex pattern of fringes	Detectable	Not detectable
Notes / explanation	Difference in thermal expansion behavior, different impact on the surface	Difference in thermal conductivity	Strong signal attenuation, reflections from the irregular surface

Table 34. Detectability of shallow detachments

Defect	Detectability by complementary techniques		
	DHSPI	SIRT	HSR
Air bubble wrap	Detectable through open curves in fringes	Not detectable or not clearly detectable	Not detectable
Notes / explanation	Difference in thermal expansion behaviour, different impact on the surface	The detachment is too thin, high influence of the surface	Strong signal attenuation, reflections from the irregular surface

Table 35. Detectability of a metallic stick

Defect	Detectability by complementary techniques		
	DHSPI	SIRT	HSR
steel stick	Detectable through fringes direction change	Not detectable	Not detectable
Notes / explanation	Difference in thermal expansion behaviour, different impact on the surface	High influence of the surface	Located in a parallel direction to the acquisition line, high attenuation of the signal, reflections from the irregular surface and metallic tesserae

Table 36. Detectability of a metallic plate

Defect	Detectability by complementary techniques		
	DHSPI	SIRT	HSR

Stainless steel inox plate	Not detectable	Detectable through detailed SIRT data processing	Detectable
Notes / explanation	The heating does not provoke an expansion of the material in the vertical direction (z-displacement)	Difference in thermal conductivity between the metal and cement based mortar	Good contrast in dielectric permittivity

Table 37. Detectability of metallic nails

Defect	Detectability by complementary techniques		
	DHSPI	SIRT	HSR
Steel nail	Not detectable or just a possible indication in the change of fringes direction	Not detectable	Detectable
Notes / explanation	The heating does not provoke an expansion of the material in the vertical direction (z-displacement)	Too small in size for revealing thermal conductivity between the metal and cement based mortar	High contrast in dielectric permittivity

Table 38. Detectability of a metallic wire

Defect	Detectability by complementary techniques		
	DHSPI	SIRT	HSR
metal clip (30x10mm, thickness less than 1 mm)	Not detectable or just a possible indication in the change of fringes direction	Not detectable	Not detectable
Notes / explanation	The heating does not provoke sufficient expansion of the material in the vertical direction (z-displacement)	Too small in size for revealing differences in thermal conductivity between the metal and cement based mortar	Small size, reflections from the irregular surface and signal attenuation

Table 39. Detectability of wooden sticks

Defect	Detectability by complementary techniques		
	DHSPI	SIRT	HSR
three wooden sticks (diameter 2-3)	Detectable in small area acquisitions	Detectable	not detectable

mm, length 16 cm)			
Notes / explanation	Slight difference in thermal expansion behaviour, different impact on the surface	Difference in thermal conductivity	Small size, reflections from the irregular surface and signal attenuation

Table 40. Detectability of plastered small stone and glass tiles

Defect	Detectability by complementary techniques		
	DHSPI	SIRT	HSR
6 mosaic tiles (3 glass and 3 marble tiles 1x1 cm)	not detectable	Not detectable	not detectable
Notes / explanation	The heating does not provoke sufficient expansion of the material in the vertical direction (z-displacement)	High influence of the surface, low contrast in thermal conductivity	Small size, reflections from the irregular surface and strong signal attenuation

As shown by experimental results, each of the tested techniques is characterised by certain advantages and limitations. The main considerations for each technique are reported below and briefly summarized in chapter 7.

Holographic Subsurface radar (HSR)

Limitations:

- contact method, high influence of surface geometry and material transparency to the microwave signal;
- no penetration under the golden leaf tesserae;
- possible errors during manual acquisition;
- discrimination between real defects and artefacts is difficult;
- no information about mortar differences.

Advantages:

- good detection of metal elements larger than the resolution step of the instrument even under irregular mosaic tesserae surface.

This technique can be useful in real cases for the detection of any metallic structures underneath, potentialities for smaller area acquisitions and detailed information about the form of hidden defects/anomalous elements.

Digital Holographic Speckle Pattern Interferometry (DHSPI)

Limitations:

- detection of only z-microdisplacement, the elements without impact on the surface will not be detected (like the metal plate in the specific laboratory case study).

Advantages:

- full-field, non-contact method;
- appropriate for irregular surfaces & good penetration underneath the metal leaf and other types of tesserae;
- immediate information about detachments, cracks, differences in mortar distribution.

This technique is potentially useful in real cases for subsurface structural diagnostics of mosaics and for discrimination between reshuffled and original areas in a wall mosaic.

Stimulated Infrared Thermography (SIRT):

Limitations:

- Eventual limits in maximum thermal excitation, allowed on real cases of highly valuable wall decorations;
- Presence of low thermal conductivity material in the superficial decoration layer

Advantages:

- Immediate non-contact detection of contrasts in thermal conductivity, good potentiality for the study of shallow depth detachments and voids;
- more informativity if combined to simultaneous DHSPI acquisitions.

As shown by the laboratory study, in real cases the non-contact full-field techniques DHSPI and SIRT should be applied in combination as first pre-screening tools for mapping the areas of interest in the subsurface of mosaics for further detailed acquisitions. Depending on the available historical documentation, conservation issues and first full-field results, the further procedure of detailed area acquisitions may be different.

The HSR technique proved its usefulness for the detection of metallic elements, which can be useful on-site for revealing nails and anchors in the mosaic subsurface. SIRT could be useful too if metallic elements are of sufficient dimensions and if thermal excitation is allowed.

If the presence of detachments, cracks, other non-metallic material inclusions are suspected, DHSPI-SIRt should be added.

More, DHSPI technique showed its high potentiality in the detection of mortar inhomogeneities underneath the decoration layer. It should be furtherly tested in-situ as a tool for immediate non-contact differentiation between original and reshuffled areas in historical mosaics.

5 SUMMARY AND CONCLUSIONS

In this research project, several non-invasive methods based on EM signal propagation have been experimentally tested, in order to highlight the advantages and limitations of their use in non-invasive measurements on ancient wall paintings and mosaics.

In particular, for the first part of the research concerning the on-site non-invasive acquisitions, four different methods were tested:

- Multispectral imaging (MI), using a modified camera with visible, infrared and ultraviolet filters, 300-1000 nm), applied to analysis of the decoration layer;
- Holographic subsurface radar (HSR), with 6.4-6.8 GHz antenna), applied to analysis of the shallow subsurface layers;
- Infrared thermography (IRT), applied to analysis of the subsurface structure;
- High resolution ground penetrating radar (GPR), with a full polar 2 GHz antenna for the investigation of the internal structure of the wall.

In the second part of this work, the in-situ measurements were integrated with experimental laboratory tests, where the measurements were performed with other non-invasive techniques on a mosaic model with known anomalies. In particular, the qualitative and quantitative Multispectral Imaging approach for the surface analysis was integrated and compared to X-Ray Fluorescence and Fiber Optics Reflectance Spectroscopy measurements. The subsurface diagnostic was finally integrated by another innovative technique, named Digital Holographic Speckle Pattern Interferometry, simultaneously applied with the Stimulated Infrared Thermography.

The analysis of the state of art in this matter highlights that the Multispectral Imaging is already a known tool for the preliminary study of wall paintings, however, still not for wall mosaics. At the same time, Holographic Subsurface Radar represents a very new technique in the field of subsurface diagnostics of all types of wall decorations.

The experimental results confirmed that Multispectral Imaging and passive Infrared Thermography are both full-field non-invasive and easily portable methods. Both of the techniques proved to be effective pre-screening tools to identify areas of interest for further analysis (the first technique for the surface and the second one for the subsurface analysis) when applied to both types of the wall decorations: paintings and mosaics. The usefulness of the information provided by these techniques, was confirmed by the experimental results, that also revealed as this method is strongly influenced by the site conditions (e.g. lighting control for MI and temperature contrast for IRT) and by the shape, and surface general characteristics of the wall decoration and its internal layers and support. The other two methods, included in the

non-invasive approach here proposed, are represented by contact techniques, providing the information about the homogeneity of the subsurface layers and of the inner structural support. They can be applied only in the cases, where direct contact to the surface is allowed.

In particular:

a) **Summarizing in-situ multispectral imaging (MI) results on wall paintings**, obtained in this project, it is possible to state that the qualitative analysis provided by this method is useful for:

- on-site fast and clear visualization of presumed original and restored areas;
- identification of the pigments in case studies with limited palette (e.g. Roman wall paintings);
- enhancement of lost details in degraded wall paintings;
- revealing of the underdrawings.

On the other hand, the semi-quantitative analysis of multispectral images provided more information on relative distribution of pigments. This step could be performed only by means of specific software tools (camera dedicated software or commercially distributed sophisticated spectral analysis software) and after calibration of lighting conditions.

b) **Summarizing in-situ multispectral imaging (MI) results on wall mosaics**, obtained in this project, it is possible to state that the qualitative analysis provided by this method is useful for:

- on-site fast and clear visualization of supposed original and restored areas;
- fast identification of possibly reintegrated tesserae (restorations).

As discussed before for the wall paintings, also, in this case, the semi-quantitative analysis of multispectral images of wall mosaics could provide more information about the differences between presumably original and restored areas. This step could be performed only by means of specific software tools (camera dedicated software or commercially distributed sophisticated spectral analysis software) and after calibration of lighting conditions.

As demonstrated by the experimental approach, used in this research project, the correct calibration of the images for quantitative analysis about the distribution of pigments or different tesserae, generally needs detailed information about the geometry of the surface. The wall decoration surfaces are in fact often characterized by high irregularity (degraded surface in wall paintings, tesserae inclination in wall mosaics) and by the non-planar shape of the structural elements (e.g. decoration of the apses or vaults).

As to the passive infrared thermography, the experimental results demonstrate some limitations of its efficiency, generally due to the absence of sufficient thermal contrasts. Therefore, only the results of passive infrared thermography inspections in the Scrovegni Chapel (Padua, Italy) and in the Catholikon of the Dafni Monastery (Athens, Greece) have been presented and discussed in this thesis.

The passive on-site thermography inspections (IRT), in the presence of sufficient temperature contrast, provides useful information for:

- mapping of the areas affected by moisture rise;
- presence of different materials in the subsurface underneath the decoration layer;
- location of structural anomalies;
- modification in the buildings due to previous restoration (e.g. walled doors or windows);
- possible cracks and detachments;
- anomalies in material and/or thickness of the structure.

With regards to the applicability of the HSR to the issues discussed in this project, it is possible to state that this contact method is not easily applicable: first, due to the high value of the painting and/or mosaic decoration; second, due the reflections of the signal from the gilded surfaces (golden leaf mosaic tesserae). This instrument proved its capability in the metal elements detection through the very high dielectric permittivity of the metals. The metallic elements are detectable even underneath irregular and lead-rich mosaic tesserae, but not detectable underneath the gilded tesserae. On the other hand, the experimental results showed that detection of anomalies, which are characterized by lower contrast in dielectric permittivity compared to the surrounding medium, was not clearly possible: the signal from the inner anomalies is not detectable or mixed with the signal artefacts generated by the irregularity of the surface. Another limitation, observed during the laboratory tests both for fresco and mosaic samples, is related to the resolution of HSR images, both along and across the orientation of the acquisition lines, as well as by the orientation and dimension (thickness and shape) of the hidden defect. Furthermore, the results are highly influenced by the manual precision in the acquisition procedure.

As shown by the experimental results on the custom-built mosaic sample, the additional method here proposed, DHSPI -SIRT has been capable to detect:

- all the simulated detachments, voids and cracks;
- organic solid materials, including rubber, plastic and wood;
- stitches and differences in the subsurface medium proportional composition (different portions of mortar).

The thin metallic elements, in which the micro-deformation in the vertical direction is too small to produce an impact on the surface, were not detected by DHSPI. The metallic plate, however, could be detected by the processing of thermal images over time (SIRT), using FLIR Research IR software.

The coupled use of DHSPI-SIRT was useful in the detection of differences in mortar structure, revealing the portions of mortar, applied separately, simulating the restoration intervention. More, it proved good capability in the detection of known and unknown cracks, voids, detachments.

These results of the laboratory tests are very important for planning further in-situ acquisitions. A proposed scheme illustrating the applicability of the methods used in this research is presented in the attachment H.

A brief summary including the considerations about the applicability and limitations of each non-invasive EM technique, tested here, is reported in Table 41.

Table 41. Application, advantages and limitations of tested EM non-invasive methods

METHOD	Characteristics	Application	Advantages	Limitations
Ground Penetrating Radar (GPR) 2 GHz	<p>Contact method</p> <p>Impulse- radar</p> <p>Result: 2D vertical section of the investigated subsurface (for each line)</p> <p>Detection of contrasts in dielectric permittivity properties distribution</p> <p>(vertical resolution= 10 cm – max depth of investigation=1.5 m)</p>	<p>Identification of the anomalies in the internal deeper structural support and their correlation with surface degradation phenomena or restoring operations</p>	<ul style="list-style-type: none"> - good penetration into the structure of the wall; - Possibility to estimate the distance to the target if the material properties are known; - identification of deep structural anomalies and humidity 	<ul style="list-style-type: none"> - Not applicable to highly valuable and/or degraded surfaces; - insufficient resolution for the detection of shallow depth discontinuities and thin/small defects
Holographic subsurface radar (HSR) 6.4-6.8 GHz	<p>Contact method</p> <p>Continuous wavelet radar (5 frequencies)</p> <p>Holographic principle of image formation: horizontal sections</p> <p>Detection of contrasts in dielectric permittivity properties distribution</p> <p>(horizontal resolution=0.5 cm – max depth of investigation= 20 cm)</p>	<p>Identification of anomalies in the shallow subsurface (preparation layer) on wall paintings and their correlation with the preservation state of the decorated surface</p>	<ul style="list-style-type: none"> - High efficiency in the detection of metallic elements and humidity; - Possibility to reconstruct the exact horizontal dimensions and shape of the detected targets. 	<ul style="list-style-type: none"> - Not applicable to highly valuable and/or degraded surfaces; - Not applicable on gilded decorated surface and almost not applicable on lead-rich mosaic tesserae; - time-consuming acquisition, requiring precision; - Results high influenced by the accuracy in the acquisition - Low resolution along and across the acquisition lines (need to acquire in two perpendicular directions) - production of artefacts by an irregular surface; - difficult interpretation of the results
Infrared thermography (IR)	<p>Non-contact method</p> <p>Measurement of thermal variations on the investigated surfaces</p> <p>Image: distribution map of the temperature on the decorated surface</p>	<p>Examination of the surface and subsurface anomalies and their correlation with surface degradation phenomena or restoration interventions</p>	<ul style="list-style-type: none"> - High efficiency in detection of detachments, voids, cracks and humidity; - Efficiency in the detection of metallic elements in the shallow subsurface. 	<ul style="list-style-type: none"> - Necessity of thermal contrast (naturally present or intentionally induced); - high influence of differences in surface morphology surface thermal properties

	<p>Detection of anomalies related to different thermal properties, i.e. thermal conductivity of materials</p> <p>(vertical resolution= n.a. – max depth of investigation= 0.5 cm)</p>			<p>(material and color);</p> <ul style="list-style-type: none"> - strong reflections from tesserae in mosaic acquisitions - Difficult recognition of small temperature differences by simple observation of thermal images.
<p>Multispectral imaging (VIS-UV-IR) 300-1000 nm</p>	<p>Non-contact method</p> <p>Measurement of the amplitude reflection in different bands of the electromagnetic spectrum (range 300-1000 nm)</p> <p>Image different pictures for each band (UV, VIS, IR)</p> <p>(vertical resolution= n.a. – max depth of investigation= n.a.) their correlation with surface degradation phenomena or restorations</p>	<p>Presence of anomalies in the surface and their correlation with degradation phenomena or restoring.</p> <p>UV – superficial coatings, binders, organic treatments (more informative when applied in fluorescence mode);</p> <p>IR – revealing underdrawings, enhancement of lost details, mapping of restored areas, identification of certain pigments (fluorescence mode)</p>	<ul style="list-style-type: none"> - Easy interpretation and comparison of the results; - Fast mapping of similar pigments or tesserae with the different composition; - Quick identification of areas for further analytical interest; - Identification of different pigments in limited palettes 	<ul style="list-style-type: none"> - High influence of uncontrolled lighting and logistics problems (e.g. surface distance, shape and irregularity of the surface);
<p>Digital holographic speckle pattern interferometry* (VIS) Monochromatic light source 532 nm</p>	<p>Full-field or detailed Remote control Non-contact method</p> <p>Measurement of surface micro-displacement (induced by thermal or mechanical stress)</p> <p>Image formation: monochromatic light source (532 nm), holographic principle, superposition of interferometric fringes.</p> <p>When coupled to SIRT, detection of differences in thermal expansion coefficient</p> <p>(vertical resolution= 266 nm – max depth of investigation= n.a.)</p>	<p>Revealing the subsurface discontinuities and defects, their correlation with surface degradation phenomena or restoring.</p>	<ul style="list-style-type: none"> - No influence of surface geometry (it can be applied to curved, sculpted and irregular surfaces); - Easy and immediate visualization of the results; - Possibility to obtain quantitative information defects' location, size measurement and exact positioning within the structure of the object; - Possibility to differentiate between the types of defects, by comparison to the developed fringes pattern classification 	<ul style="list-style-type: none"> - High sensibility of the instrument to surrounding vibrations; - only deformations in the vertical direction can induce impact on the surface and therefore be detected

*additional technique used in laboratory simulation tests

Preliminary recommendations for non-invasive in-situ diagnostics of wall paintings

The experimental results obtained in this research project, confirm the role of multispectral imaging as a non-invasive, contactless method, efficient tool in the prescreening phase for the identification of the areas of interest for more detailed or analytical investigations. In most of the cases, with or without calibration of lighting conditions, it is helpful for enhancement of degraded iconographic features, revealing underdrawings and highlighting original and retouched areas. As the next step, further point-like analysis (e.g. portable XRF, FORS and Raman) can be applied to the wall decoration study, if the conservation issue refers to the surface, its preservation, the analysis of the artist's technique and the pigments distribution. If further sophisticated tests are needed and if micro-sampling is allowed, multispectral imaging can be used for the identification of most reasonable sampling areas.

If the conservation issue refers to the shallow subsurface layer, non-contact infrared thermography can be used. If the environmental temperature contrast is sufficient, this method can be applied in passive mode to reveal the surface temperature anomalies, probably indicating areas with presence of humidity, different materials distribution, subsurface detachments and/or cracks. If the natural temperature contrast is not sufficient, it is possible to apply this method in active mode (Stimulated Infrared Thermography). Digital Holographic Speckle Pattern Interferometry, coupled to Stimulated Infrared Thermography, allows in-situ immediate and full-field visualization of subsurface hidden discontinuities, particularly in the detection of differences in the subsurface material, stitches between different materials, cracks and detachments.

Holographic Subsurface radar and high frequency Ground Penetrating radar techniques usually cannot be applied to highly valuable wall paintings. However, if physical contact to the surface is allowed, Holographic Subsurface radar can be applied for detection of shallow metallic anomalies. For the detection and more detailed study of anomalies in the deeper layers (structural support), in this case, high frequency Ground Penetrating Radar is recommended.

In general, all of these techniques are characterized by some limitations, however, as the whole, the proposed non-invasive approach can be used to different case studies and can provide preliminary information about the decoration and its support in completely non-invasive way, in order to improve the conservation planning of wall paintings of high historical and archaeological interest.

Preliminary recommendations for non-invasive in-situ diagnostics of wall mosaics

As previously discussed for the wall paintings, thanks to the experimental results of this research project, the multispectral imaging confirms its characteristics of non-invasive, contactless method, efficient as a prescreening tool for identifying areas of interest also for detailed analytical investigations in wall mosaics. In fact, it is helpful in revealing anomalies in mosaic execution technique, in most of the cases, even without calibration of lighting conditions. In particular, it can be helpful in the identification of apparently identic tesserae, or in the recognition of original and rearranged (reintegrated) mosaic parts. Infrared thermography can be applied also in this case as a non-contact diagnostic technique. It can be applied in passive mode if the natural temperature contrast is sufficient for the detection of anomalies in thermal distribution on the mosaic surface, related to moisture rise, differences in mortar, detachments and cracks. In general, for the mosaic studies is better to use the Infrared Thermography in active mode (Stimulated Infrared Thermography) if additional thermal excitation sources can be used on-site. Also, in this case, Digital Holographic Speckle Pattern Interferometry, coupled to Stimulated Infrared Thermography, as shown by the laboratory simulation test results, its capability in the analysis of mosaics, especially for the detection of anomalies in subsurface materials, stitches between different materials, cracks and detachments.

The last two techniques, presented in this project (GPR and HSR), require direct contact with the surface of wall mosaic decoration and therefore, cannot be applied in many real cases (due to the distance of the surface (e.g. vaults), surface irregularity and geometry, as well as due to the preservation condition. But if allowed, Holographic Subsurface Radar should be used for the detection of metallic elements in the shallow subsurface (e.g. the for anchoring the mortar layer to the wall or apse support). For the detection and more detailed study of any discontinuities in the deeper layers (structural support), also in this case, as for the wall paintings, the use of high frequency Ground Penetrating Radar is recommended.

Some of the important issues that emerged during the experimental procedure and that are worth being studied in more detailed are reported as follows:

- This experimental study included laboratory tests of multispectral imaging (MI) applied to wall painting fragments but could not be performed on mosaic laboratory samples. These tests might be useful for testing a semi-quantitative approach to the differentiation and mapping of different types of mosaic tesserae.

- In view of the constant development of available software tools, further tests on different imaging processing algorithms can be useful for the improvement of data elaboration procedure.
- The laboratory tests on a mosaic sample showed good potentiality of the Digital Holographic Speckle Pattern Interferometry (DHSPI) for the differentiation between original and reintegrated (reshuffled) areas of mosaic decoration. Further tests on real case studies can be useful.
- The Holographic Subsurface Radar (HSR) showed strong limitations in its applicability to a custom-built complex laboratory model and to real cases of wall decorations. Further simplified laboratory tests and real case acquisitions might be needed.
- Further integrations with complementary methods and alternative instrumentations are recommended.

REFERENCES

1. ICOMOS Charter (2003), Principles for the Preservation and Conservation-Restoration of wall paintings. Ratified by the ICOMOS 14th General Assembly in Victoria Falls, Zimbabwe (2003)
2. Vitruvius: *Ten Books on Architecture*, translated by Ingrid D. Rowland, commentary and illustrations by T. Noble Howe, Cambridge, University Press (1999)
3. *Arte e tecnologia nel mosaico*, Fiorentini Roncuzzi I., Longo, 1971. - 205 p (1971)
4. *Scientific Examination for the Investigation of Paintings: A Handbook for Conservators-restorers*, Pinna D., Galeotti M., Mazzeo R., Publisher Centro Di (2011), ISBN: 8870384581
5. *Analytical Chemistry for Cultural Heritage*, Mazzeo R., Springer International Publishing Switzerland (2017), <https://doi.org/10.1007/978-3-319-52804-5>
6. Mosca S., Alberti R., Frizzi T., Nevin A., Valentini G., Comelli D., *A whole spectroscopic mapping approach for studying the spatial distribution of pigments in paintings*, in: Applied Physics A 122, 815 (2016)
7. Vallet J.-M., Detalle V., De Luca L., Bodnar I.-L., Guillon O., Trichereau B., Mouhoubi K., Martin-Beaumont N., Syvilay D., Giovannacci D., Stefani C., Walker G., Feillou M., Martos-Le Vif D., Marron P., De Banès Gardonne F., *Development of a NDT toolbox dedicated to the conservation of wall paintings: Application to the frescoes chapel in the Charterhouse of Villeneuve-lez-Avignon (France)*, in: Digital Heritage (2) (2013): 67-74
8. *Dalla conservazione alla storia dell'arte. Riflettografia e analisi non invasive per lo studio dei dipinti*, Poldi, G., Villa G.C.F., Edizioni della Normale (2006) (Italian), ISBN 8876422056
9. *Scientific Methods and Cultural Heritage: An introduction to the application of materials science to archaeometry and conservation science*, G. Artioli, Oxford University Press (2010) EAN: 9780199548262
10. Piovesan R., Siddall R., Mazzoli C., Nodari L., *The Temple of Venus (Pompeii): A study of the pigments and painting techniques.*, in: Journal of Archaeological Science (38), pp. 2633–2643.
11. Prati S., Joseph E., Sciuotto G., Mazzeo R., *New advances in the application of FTIR microscopy and spectroscopy for the characterization of artistic materials*, in: Accounts of Chemical Research 43 (2010) 792–801.
12. *IR and Raman Spectroscopy*, Wartewig S., Schorn C., Bigler P., (2003) Book (IR), 191, <https://doi.org/10.1002/3527601635>
13. *Introduction to X-Ray Powder Diffractometry*, Jenkins R., Snyder R. L., Wiley J., New York (1996), ISBN 0 471 51339 3, 403+XXIII pp.
14. Lange G., Seidel K., *Electromagnetic Methods*, in: Environmental Geology, Springer, Berlin, Heidelberg
15. Kouis D., Giannakopoulos G., *Incorporate Cultural Artifacts Conservation Documentation to Information Exchange Standards – The DOC-CULTURE Case*, In: Proceedings of the 3rd International Conference on Integrated Information. Prague, Czech Republic, September 5-13, 2013.
16. Kouis D., Vassilakaki E., Vraimaki E., Cheilakou E., Saint A.C., Sakkopoulos E., Viennas E.; Pikoulis E.V., Nodarakis N., Achilleopoulos N., Zervos S., Giannakopoulos G., Kyriaki-Manessi D., Tsakalidis A. K., Kouis M., *Standardizing NDT & E Techniques and Conservation Metadata for Cultural Artifacts*, in: 9th Metadata and Semantics Research Conference (MTSR 2015), Garoufallou E., Eds. Springer: Manchester, UK (2015); Communications in Computer and Information Science (CCIS), vol 544.
17. *Theory of electromagnetic wave propagation*, Herach Papas C., Dover Publications, New York (2011), pp. 272, ISBN: 0486656780
18. *Civil Engineering Applications of Ground Penetrating Radar*, Benedetto A., Pajewskiy L., Springer International Publishing (2015), ISBN 978-3-319-04813-0
19. Melis M., Miccolib M., Quarta D., *Multispectral Hypercolorimetry and automatic guided pigment identification some masterpieces case studies*, in: SPIE Optical Metrology 2013, International society for Optics and Photonics (2013)
20. Blažek J., Soukup J., Zitová B., Flusser J., Tichý T., Hradilová J., *Low-cost mobile system for multispectral cultural heritage data acquisition*, in: Digital Heritage International congress, Marseille, France, 28 Oct – 1 Nov 2013. Digital Heritage 2013, DOI: 10.1109/DigitalHeritage.2013.6743715
21. Cosentino A., *Panoramic, Macro and Micro Multispectral Imaging: An Affordable System for Mapping Pigments on Artworks*, in: Journal of Conservation and Museum Studies. 13(1), p.Art. 6 (2015). DOI: <http://doi.org/10.5334/jcms.1021224>
22. Cosentino A., *Multispectral imaging system using 12 interference filters for mapping pigments*, in: Conservar Património 21 (2015), 25-38
23. Cheilakou E., Troullinos M., Kouis M., *Identification of pigments on Byzantine wall paintings from Crete (14th century AD) using non-invasive Fiber Optics Diffuse Reflectance Spectroscopy (FORS)*, in: Journal of Archaeological Science 41 (2014) 541–555.
24. Saint A.C., Cheilakou E., Dritsa V., Kouis M., Kostanti K., Christopoulou A., *The combined use of XRF and VIS-NIR FORS spectroscopic techniques for the non-invasive identification of pigments on archaeological*

- works of art*, in: Technart 2015- No-destructive and microanalytical techniques in art and cultural heritage, Catania, Italy (2015)
25. Valentini F.; Calcaterra A.; Antonaroli S.; Talamo M., *Smart Portable Devices Suitable for Cultural Heritage: A Review*, in: *Sensors* (2018), 18, E2434.
 26. Conti C., Striova J., Aliatis I., Colombo C., Greco M., Possenti E., Realini M., Brambilla L., Zerbi G., *Portable Raman versus portable mid-FTIR reflectance instruments to monitor synthetic treatments used for the conservation of monument surfaces*, in: *Anal. Bioanal. Chem.* 405, 1733–1741 (2013)
 27. Fukunaga K., Hosako I., *Innovative non-invasive analysis techniques for cultural heritage using terahertz technology*, *Comptes Rendus Physique*, Volume 11, Issues 7-8, (2010), Pages 519-526
 28. Cosentino A., *Terahertz and Cultural Heritage Science: Examination of Art and Archaeology*, *Technologies* (2016), 4(1)
 29. Mercuri F., Cicero C., Orazi N., Paoloni S., Marinelli M., Zammit U., *Infrared Thermography Applied to the Study of Cultural Heritage*, in: *Int J Thermophys* (2015), 36.5-6:1189–1194.
 30. Candoré J. C., Bodnar J. L., Detalle V., P. Grossel, *Characterization of defects situated in a fresco by stimulated infrared thermography*, in: *EPJ Applied Physics* 57(1) (2012).
 31. Bodnar J. L., Nicolas J. L., Mouhoubi K., Detalle V., *Stimulated infrared thermography applied to thermophysical characterization of cultural heritage mural paintings*, in: *EPJ Applied Physics* 60(2) (2012).
 32. Moropoulou A., Avdelidis N.P., Delegou E.T., Aggelakopoulou E., Karoglou M., Haralampopoulos G., Griniezakis S., Kouli M., Karmis P., Aggelopoulos A., Karagianni E.A., Georgiadi Ch., N.K. Uzunoglou N.K., *NDT investigation on Hagia Sophia mosaics*, in: *Research Work*, NTUA (2000)
 33. Theodorakeas P., *Quantitative Analysis and Defect Assessment Using Infrared Thermographic Approaches*, PhD Thesis, NTUA (2013)
 34. Martinho E., Dionísio A., *Main geophysical techniques used for non-destructive evaluation in cultural built heritage: a review*, in: *Journal of Geophysics and Engineering*, 11, pp. 1-15 (2014)
 35. Santos-Assunção S., Perez-Gracia P., Caselles O., Clapes J., Salinas V., *Assessment of Complex Masonry Structures with GPR Compared to Other Non-Destructive Testing Studies*, in: *Remote Sensing*, 6, pp. 8220-8237 (2014).
 36. Côte P., Dérobert X., Miltiadou-Fezans A., Delinikolas N., Durand O., Alexandre J., Kalagri A., Savvidou M., Chryssopoulos D., Anamaterou L., Georganis F., *Application of non-destructive techniques at the Katholikon of Dafni Monastery for mapping the mosaics substrata and grouting monitoring*, in: D'Ayala, D. and Fodde, E. (Eds.) *Structural Analysis of Historic Construction*, Taylor and Francis: London, pp. 1149-1156 (2007).
 37. Ranalli D., Scozzafava M., Tallini M., *Ground penetrating radar investigations for the restoration of historic buildings: the case study of the Collemaggio Basilica (L'Aquila, Italy)*, in: *Journal of Cultural Heritage*, 5:1, pp.91-99 (2004).
 38. Kosma K., Andrianakis M., Hatzigiannakis K., Tornari V., *Digital holographic interferometry for cultural heritage structural diagnostics: A coherent and a low-coherence optical set-up for the study of a marquetry sample*, *Strain* 54 (part 1), doi: 10.1111/str.12263
 39. Tornari V., *Optical and digital holographic interferometry applied in art conservation structural diagnosis*, in: *e-Preservation science*, (2006), 3, 51-57
 40. Tornari V., *On development of portable Digital Holographic Speckle Pattern Interferometry system for remote-access monitoring and documentation in art conservation*, *Strain* 201, DOI:10.1111/str.12288
 41. *Fully non contact holography-based inspection on dimensionally responsive artwork materials*, V. Tornari, E. Bernikola, A. Nevin, E. Kouloumpi, M. Doulgeridis, C. Fotakis, in: *Sensors*, 2008, 8, DOI 10.3390/SENSORS (2008) “Laser Interference-Based Techniques and Applications in Structural Inspection of Works of Art”, V. Tornari, *Analytical and Bioanalytical Chemistry*; 387, 761-780 (2007)
 42. Schirripa Spagnolo G., Guattari G., Grinzato E., *Frescoes Diagnostics by electro-optic holography and infrared thermography*, in: *Proc I the 6th World Conference on NDT and Microanalysis in Diagnostics and Conservation of Cultural and Environmental Heritage*, Rome (1999), p. 385-398.
 43. De Stefano A., Matta E., Clemente P., *Structural health monitoring of historical heritage in Italy: some relevant experiences*, in: *Journal of Civil Structural Health Monitoring* 6(1):83–106 (2016)
 44. Clemente P., *Extending the life-span of cultural heritage structures*, in: *Journal of Civil Structural Health Monitoring* 8 (5):83–106 (2016)
 45. Schirripa S. G., Ambrosini D., Paoletti D., *Optical methods for mosaic diagnostics*, in: *J Opt* 29:394–400 (1998)
 46. Castellini P., Paone N., *Development of a Measurement Procedure for Non-invasive Detection of Frescoes' Detachments*, in: *Proceedings of SPIE - The International Society for Optical Engineering*, (1995)
 47. Del Vescovo D., Fregolent A., *Assessment of fresco detachments through a non-invasive acoustic method*, in: *Journal of Sound and Vibration* 284: 1015-1031.

48. Razevig V.V., Ivashov S.I., Vasiliev I.A., Zhuravlev A.V., Bechtel T., Capineri L., Falorni P., *RASCAN Holographic Radars as Means for Non-Destructive Testing of Buildings and Edificial Structures*, in: Proceedings of the Structural Faults and Repair-2010, 15th - 17th June 2010, Edinburgh, Scotland, UK.
49. Ivashov S.I., Makarenkov V.I., Masterkov A.V., Razevig V.V., Sablin V.N., Sheyko A.P., Tchaporovski V.V., Vasiliev I.A., *Concrete Floor Inspection with Help of Subsurface Radar*, in: Proceedings of 6th Meeting Environmental and Engineering Geophysics. Bochum, Germany, September 3-7 (2000) P-GR04.
50. Ivashov S., Razevig V., Sheyko A., Vasilyev I., Zhuravlev A., Bechtel T., *Holographic Subsurface Radar Technique and its Applications*, in: Proceedings of the 12th International Conference on Ground-Penetrating Radar, GPR 2008, 16-19 June 2008, University of Birmingham, UK.
51. Capineri L., Falorni P., Borgioli G., Bulletti A., Valentini S., Ivashov S., Zhuravlev A., Razevig V., Vasiliev I., Paradiso M., Inagaki M., Windsor C., Bechtel T., *Application of the RASCAN Holographic Radar to Cultural Heritage Inspections*, in: Archaeological Prospection 16, pp. 218-230 (2009)
52. Capineri L., Falorni P., Ivashov S., Zhuravlev A., Vasiliev I., V. Razevig, V., Bechtel T., Stankiewicz G., *Combined Holographic Subsurface Radar and Infrared Thermography for Diagnosis of the Conditions of Historical Structures and Artworks*, in: European Geosciences Union, General Assembly 2009, Vienna, Austria (2009)
53. Melis M., Miccoli M., *Trasformazione evolutiva di una fotocamera reflex digitale in un sofisticato strumento per misure fotometriche e colorimetriche*, in: IX Conferenza del Colore - Firenze, 19 – 20 settembre (2013)
54. <http://www.profilocolore.com>
55. Chaban A., Deiana R., Parisatto M., Asscher Y., *Analysis of on-site multispectral images: a case study of degraded wall paintings in Sarno Baths, Pompeii*, in: ACTA ARTIS ACADEMICA (2017) "Painting as a story", Academy of Fine Arts in Prague ISBN: 978-80-87108-75-8, pp. 151-160
56. Papadakis, V.M., Orphanos, Y., Kogou, S., Melessanaki, K., Pouli, P., Fotakis, C.: *IRIS: a novel spectral imaging system for the analysis of cultural heritage objects*. In: Proc. SPIE. 8084, 80840W (2011)
57. Φτίκου Α. Ζ., Κριτηρια επιλογής υλικών και τεχνικών για την αποκατάσταση του υποστρώματος ιστορικών ψηφιδωτών, PhD, NTUA (2016)
58. Theodorakeas P., Cheilakou E., Ftikou E., Kouli M., *Passive and active infrared thermography: an overview of applications for the inspection of mosaic structures*, in: 33rd UIT (Italian Union Thermo-Fluid Dynamics Heat Transfer Conference 655 (2015)
59. Avdelidis N.P., Kouli M., Ibarra-Castaneda C, Maldague X., *Thermographic studies of plastered mosaics*, in: J. Infrared Physics and Technology, Vol. 49, pp. 254-256 (2007)
60. Razevig V.V., Ivashov S.I., Vasiliev I.A., Zhuravlev A.V., Bechtel T., Capineri L., Falorni P., *RASCAN Holographic Radars as Means for Non-Destructive Testing of Buildings and Edificial Structures*, in: Proceedings of the Structural Faults and Repair-2010, 15th — 17th June 2010, Edinburgh, Scotland, UK.
61. Ivashov S.I., Makarenkov V.I., Masterkov A.V., Razevig V.V., Sablin V.N., Sheyko A.P., Tchaporovski V.V., Vasiliev I.A., *Concrete Floor Inspection with Help of Subsurface Radar*, in: Proceedings of 6th Meeting Environmental and Engineering Geophysics. Bochum, Germany, September 3-7 (2000) P-GR04
62. Ivashov S., Razevig V., Sheyko A., Vasilyev I., Zhuravlev A., Bechtel T., *Holographic Subsurface Radar Technique and its Applications*, in: Proceedings of the 12th International Conference on Ground-Penetrating Radar, GPR 2008, 16-19 June 2008, University of Birmingham, UK.
63. Capineri L., Falorni P., Borgioli G., Bulletti A., Valentini S., Ivashov S., Zhuravlev A., Razevig V., Vasiliev I., Paradiso M., Inagaki M., Windsor C., Bechtel T., *Application of the RASCAN Holographic Radar to Cultural Heritage Inspections*, in: Archaeological Prospection 16, pp. 218-230 (2009)
64. Capineri L., Falorni P., Ivashov S., Zhuravlev A., Vasiliev I., V. Razevig, V., Bechtel T., and Stankiewicz G., *Combined Holographic Subsurface Radar and Infrared Thermography for Diagnosis of the Conditions of Historical Structures and Artworks*, in: European Geosciences Union, General Assembly 2009, Vienna, Austria (2009)
65. Tornari V., Tsiranidou E., Bernikola E., *Interference fringe-patterns association to defect-types in artwork conservation: an experiment and research validation review*, in: Applied Physics A 106(2), 397-410 (2012).
66. Tornari V., Bernikola E., Tsigarida N., Andrianakis M., Hatzigiannakis K., Leissner J., *Preventive deformation measurements on cultural heritage materials based on non-contact surface response of model samples*, in: Studies in Conservation, Volume 60, Issue S1 (August, 2015), pp. S143-S158
67. Bernikola E., Nevin A., Tornari V., *Rapid initial dimensional changes in wooden panel paintings due to simulated climate-induced alterations monitored by digital coherent out-of-plane interferometry*, in: Applied Physics A 95, pp. 387-399 (2009).
68. Tornari V., Andrianakis M., Hatzigiannakis K., Kosma K., Detalle V., Bourguignon E., Giovannacci D., Brissaud D., *Complementarity of digital holographic speckle pattern interferometry and simulated infrared*

- thermography for Cultural Heritage structural diagnostic research*, in: International Journal of Engineering Research & Science (IJOER) ISSN: [2395-6992] [Vol-2, Issue-11 (2016)]
69. Gaburro N., Marchioro G., Daffara C., *A versatile optical profilometer based on conoscopic holography sensors for acquisition of specular and diffusive surfaces in artworks*, in: Optics for Arts, Architecture, and Archaeology VI 2017
 70. Proietti N., Capitani D., Di Tullio V., *Applications of Nuclear Magnetic Resonance Sensors to Cultural Heritage*, in: Sensor (2014), 14, 6977–6997
 71. Baias M., *Mobile NMR: An essential tool for protecting our cultural heritage*, in: Magn. Reson. Chem. (2017), 55, 33–37.
 72. Cucci C., Delaney J.K., Picollo M., *Reflectance hyperspectral imaging for investigation of Works of Art: old master paintings and illuminated manuscripts*, in: Acc Chem Res. (2016); 49:2070–9. doi: 10.1021/acs.accounts.6b00048
 73. Kubik M., *Hyperspectral Imaging: a new technique for the non-invasive study of artworks*, in: Creagh D., Bradley D., editors., in: Physical techniques in the study of art, archaeology and cultural heritage, Oxford: Elsevier (2007), p. 199–259.
 74. *Conservation of Wall Paintings*, Mora P., Mora L. and Philippot P., Sevenoaks: Butterworths (1984). ISBN 0-408-10812-6
 75. Geneste J.-M., Mauriac M., *The Conservation of Lascaux Cave, France*. In Saiz-Jimenez, C., Ed. The Conservation of Subterranean Cultural Heritage, CRC Press: New York (2014); pp. 165-172.
 76. Davy H., *Some Experiments and Observations on the Colours Used in Painting by the Ancients*, in: Phil. Trans. R. Soc. London, 1815, 105, 97-124
 77. *Historical Painting Techniques, Materials and Studio Practice*, Wallert A., Hermens E., Peek M. (Eds.), (1995), preprints of a symposium held at the University of Leiden, the Netherlands, 26-29 June, 1995. Getty Conservation Institute: Malibu. ISBN 9780892363223
 78. Marey H.M., Kantiranis N., Ali M., Stratis J., *Characterization of Ancient Egyptian Wall Paintings, the Excavations of Cairo University at Saqqara*, in: International Journal of Conservation Science, 2(3), (2011), pp. 145-154.
 79. Cameron A.S., Jones R.E., Philippakis S.E., *Scientific Analyses of Minoan Fresco Samples from Knossos*, The Annual of the British School at Athens, Vol. 72 (1977), pp. 121-184.
 80. Tsairis G., Palamara E., Zacharias N., Cosmopoulos M., *A non-destructive technological study of three fresco fragments from Iklaina, Pylos, Greece*, in: STAR: Science & Technology of Archaeological Research, 3:2, 418-427, DOI: [10.1080/20548923.2017.1395153](https://doi.org/10.1080/20548923.2017.1395153) (2017)
 81. Ling R., Ling L., *Wall and panel painting*, in: Making classical art: process and practice, edited by R. Ling, London, p.47-61.
 82. Winfield D.C., *Middle and Later Byzantine wall painting methods — a comparative study*, Dumbarton oaks paper 22:61–142 (1968)
 83. Cennini C., *The craftsman's handbook 'Il Libro dell'Arte' Cennino d'Andrea Cennini* (translated by D.V. Thompson). Dover, New York (1960)
 84. Colalucci G., *Michelangelo in the Sistine Chapel: painting technique and technique of restoration, Case studies in the conservation of stone and wall paintings*, in: Contributions to the 1986 IIC Congress, Bologna, p.46-47 (1986)
 85. *Giotto nella Cappella Scrovegni: Materiali per la tecnica pittorica, Studi e ricerche dell'Istituto Centrale per il Restauro*, A cura di Basile G., Istituto Poligrafico e Zecca dello Stato (2005)
 86. Van den Berg J.D.J., *Analytical chemical studies on traditional linseed oil paints*, PhD thesis, University of Amsterdam (2002)
 87. *Analytical techniques in materials conservation*, Stuart B., Chichester, England, Hoboken, NJ: John Wiley & Sons, (2007)
 88. *The Materials of the artist and their use in painting*, Doerner M., A Harvest book, Harcourt Brace & Co: 265 (1984)
 89. Piovesan R., Mazzoli C., Maritan L., Cornale P., *Fresco and Lime Paint: an Experimental Study and Objective Criteria for Distinguishing Between These Painting Techniques*, in: Archaeometry 54 (4), pp. 723–736
 90. *Metodologia e Restauro delle Pitture Murali*, Botticelli G., Edizioni Centro Di, 1992
 91. *The Grove Encyclopedia of Materials and Techniques in Art*, Front Cover, Gerald W.R., Ward. Oxford University Press (2008) - Art - 828 pages
 92. *Light: its Interaction with Art and Antiquities*, Brill T.B., Springer US, (1980)
 93. *I Colori Pompeiani*, Augusti S., De Luca., Roma (1967), 51-61
 94. Bearat H., *Quelle est la gamme exacte des pigments romains? Confrontation des resultats d'analyse et des textes de Vitruve et de Pline*, in: Proceedings of the International Workshop on Roman Wall Painting, Fribourg (1996), 16-24

95. *I colori degli antichi*, Colombo L., Nardini, Roma (1995)
96. *I pigmenti nell'arte: dalla preistoria alla rivoluzione industriale*, Bevilacqua N., Borgioli L., Adrover Garcia I., Il Prato (2010), 302 p., ISBN:8863360901
97. *La chimica del restauro*, Matteini M., Moles A., Nardini, Roma, (2002)
98. Grossi C.M., Brimblecombe P., Bonazza A., Sabbioni C., Zamagni J., *Sulfate and carbon compounds in black crusts from the cathedral of Milan and Tower of London*, in: Proceedings of the International Conference on Heritage, Weathering and Conservation, HWC 2006, Volume 1, p.441-446 (2006)
99. Sotiropoulou S., Sciutto G., Tenorio A.L., Mazurek J., Bonaduce I., Prati S., Mazzeo R., Schilling M., Colombini M.P., *Advanced analytical investigation on degradation markers in wall paintings*, in: *Microchem J.* (2018);139:278–94.
100. Zucconi L., Gagliardi M., Isola D., Onofri S., Andaloro M.C., Pelosi C., Pogliani P., Selbmann L., *Biodeterioration agents dwelling in or on the wall paintings of the Holy Saviour's cave (Vallerano, Italy)*, in: *International Biodeterioration & Biodegradation*, Volume 70 (2012), Pages 40-46, [https://doi.org/10.1016/0048-9697\(95\)04587-Q](https://doi.org/10.1016/0048-9697(95)04587-Q)
101. Garg K.L., Jain K., Mishra A.K., *Role of fungi in the deterioration of wall paintings*, in: *Science of The Total Environment*, Volume 167, Issues 1–3, 1 (1995), Pages 255-271
102. Chelazzi D., Poggi G., Jaidar Y., Toccafondi N., Giorgi R., Baglioni P., *Hydroxide nanoparticles for cultural heritage: consolidation and protection of wall paintings and carbonate materials*, in: *J Colloid Interface Sci.* (2013) Feb 15;392:42-49. Epub 2012, doi: 10.1016/j.jcis.2012.09.069
103. Turton C.E., *Plan for the Stabilization and Removal of Wall Paintings at Çatalhöyük*, Msc Thesis (Historic Preservation), University of Pennsylvania, Philadelphia, USA (1998)
104. *Conservation-restoration of wall paintings, Ratified by the ICOMOS 14th General Assembly in Victoria Falls, Zimbabwe, in 2003 (2003).*
105. *Glossario tecnico-storico del mosaico: con una breve storia del mosaico*, Farneti M., Longo, 236 pages (1993)
106. *A Handbook of Roman art: a comprehensive survey of all the arts of the Roman world*, Henig M., Ithaca N.Y., Cornell University Press (1983)
107. Fiorentini Roncuzzi I., Fiorentini E., *Mosaic: materials, techniques and history*, MWeV, (2002).
108. Demus O., *Byzantine Mosaic Decoration: Aspects of Monumental Art in Byzantium*, (London) (1948).
109. Demus O., *The mosaics of Norman Sicily*, Byzantium (London) (1950)
110. *The Mosaics of San Marco in Venice*, Demus O., Chicago and London, Washington (1984), pp. 358, 495
111. Bovini G., Kitzinger E., Oicard G.C., s.v. *Mosaico*, in: *EUA*, cit. vol. IX, p.672-706
112. *Mosaici minuti romani dei secoli XVIII e XIX (I)*, Petochi D., Alfieri M., Branchetti M.G., ISBN: 978-8870470185 (1981)
113. Arletti R., Fiori G., Vandini M., *Mosaic glass from St. Peter's, Rome: manufacturing techniques and raw materials employed in late 16th-century Italian opaque glass*, in: *Archaeometry*, 53 (2011), 364–386.10.1186/s40494-016-0085-2.
114. *Storia sociale dell'arte Volume secondo Rococo Neoclassicismo Romanticismo Arte moderna e contemporanea*, Hauser A., Piccola Biblioteca Einaudi, Torino (1976)
115. *Verità M., Mosaico vitreo e smalti: la tecnica, i materiali, il degrado, la conservazione*, in: *I colori della luce: Angelo Orsoni e l'arte del mosaico*, ed. Moldi C. Ravenna, Venice: Marsilio (1996), pp. 41–97.
116. *Glass science (2nd edition)*, Doremus R.H., Wiley (1994)
117. *Glas in Antike und Mittelalter. Geschichte eines Werkstoffes*, Wedepohl K.H., Schweizerbarische Verlagsbuchhandlung (2003)
118. *The Science and Archaeology of Materials: An Investigation of Inorganic Materials*, Henderson J., Routledge, xvi, 334 p., ISBN: 0415199344 (2000)
119. *Arte e tecnologia nel mosaico*, Fiorentini Roncuzzi I., Longo, 1971. - 205 p (1971)
120. Kaplan Z., Ipekoglu B., Boke H., *Characteristics of Mortars of Mosaics From A Roman Villa in Antandros Ancient City, Turkey*, Conference: 6th International Congress on Science and Technology for the Safeguard of Cultural Heritage in Mediterranean Basin, Athens (2013)
121. Von Landsberg D., *The history of lime production and use from early times to the industrial revolution*, Wiesbaden, Zement-Kalk-Gips 45, Wiesbaden Baurverlag, pp.199-203 (1992)
122. *Τα ψηφιδωτά της νεας Μονής Χίου (Διτομο)*, Μουρική Ντούλα, βυζαντινά μνημεία, 600 σ. (1985)
123. Silvestri A., Molin G., Salviulo G., *Archaeological glass alteration products in marine and land-based environments: morphological, chemical and microtextural characterization*, in: *Journal of Non-Crystalline Solids*, vol. 351, issue 16-17, pp. 1338-1349
124. *Science and conservation for museum collections*, edited by Fabbri B., Firenze, Nardini (2012)
125. *Lessons Learned: Reflecting on the Theory and Practice of Mosaic Conservation*, Ben Abed A., Demas M., Roby T., Getty Conservation Institute, Los Angeles (2008), pp.440
126. *Teoria e pratica per la conservazione del mosaico*, Vandini M., Fiore C., Il Prato, Padova, (2002)

127. <https://parcodeinebrodi.blogspot.com/2018/06/il-palazzo-disvelato-il-palazzo-reale.html>
128. Takahashi K., Igel J., Preetz H., Kuroda S., *Basics and application of ground-penetrating radar as a tool for monitoring irrigation process*, in: Problems, Perspectives and Challenges of Agricultural Water Management, 160, InTech (2012).
129. *Ground Penetrating Radar (2nd Edition)*, Daniels D.J. (Ed.), IEE, ISBN 0-86341-360-9, London (2004)
130. Lizuka K., Freundorfer A.P., *Detection of non-metallic buried objects by a step frequency radar*, in: Proceedings of IEEE, Vol.71, N.2, pp.276-279 (1983).
131. *An introduction to applied and environmental geophysics*, Reynolds J.M., Wiley-Blackwell (2011)
132. Barone P.M., Di Matteo A., Graziano F., Mattei E., Pettinelli E., *GPR application to the structural control of historical buildings: two case studies in Rome, Italy (2006)*
133. D'Aranno P.J.V., De Donno G., Marsella M., Orlando L., Renzi B., Salviani S., Santarelli M.L., Scifoni S., Sonnessa A., Verri F., Volpe R., *High-resolution geomatic and geophysical techniques integrated with chemical analyses for the characterization of a Roman wall*. *Journal of Cultural Heritage* (2015). doi:10.1016/j.culher.2015.06.005
134. Vasiliev I.A., Ivashov S.I., Makarenkov V.I., Sablin V.N., Sheyko A.P., *RF Band High Resolution Sounding of Building Structures and Works*, in: IEEE Aerospace & Electronic Systems Magazine (1999), Vol. 14, No. 5, pp. 25-28.
135. Razevig V.V., Ivashov S.I., Vasiliev I.A., Zhuravlev A.V., Bechtel T., Capineri L., *Advantages and restrictions of holographic subsurface radars. Experimental evaluation*, in: Proceedings of the XIII International Conference on Ground Penetrating Radar, Lecce, Italy, 21–25, June 2010, pp. 657–662.
136. Ivashov S.I., Makarenkov V.I., Masterkov A.V., Razevig V.V., Sablin V.N., Sheyko A.P., Tchapourski V.V., Vasiliev I.A., *Concrete Floor Inspection with Help of Subsurface Radar*, in: Proceedings of 6th Meeting Environmental and Engineering Geophysics, Bochum, Germany, September 3-7 (2000) P-GR04.
137. Ivashov S., Razevig V., Sheyko A., Vasilyev I., Zhuravlev A., Bechtel T., *Holographic Subsurface Radar Technique and its Applications*, in: Proceedings of the 12th International Conference on Ground-Penetrating Radar, GPR 2008, 16-19 June 2008, University of Birmingham, UK.
138. Ivashov S.I., Capineri L., Bechtel T. *Holographic subsurface radar technology and applications*, in: UWB radar Applications and Design, Taylor J.D. /Boca Raton, FL: CRC Press), pp.421-444 (2012).
139. Ivashov S.I., Sablin V.N., *New technologies in humanitarian demining operations*, ISTAS (2000): 101-10.
140. Falorni P., Capineri L., *Optical method for the positioning of measurement points*, in: International Workshop on Advanced Ground Penetrating Radar (IWAGPR), Florence, July 7–10, 2015
141. Razevig V.V., Zhuravlev A.V., Bugaev A.S., Chizh M.A., Ivashov S.I., *Imaging under irregular surface using microwave holography*, in: Progress in Electromagnetics Research Symposium - Fall (PIERS - FALL), Singapore, (2017), pp. 172-177. Doi: [10.1109/piers-fall.2017.8293132](https://doi.org/10.1109/piers-fall.2017.8293132)
142. Junkin G., Anderson A.P., *Limitations in microwave holographic synthetic aperture imaging over a lossy half-space*, in: Communications, Radar and Signal Processing, IEE Proceedings F, Volume 135, Issue 4 (1988), pp. 321 – 329.
143. Vasiliev I.A., Ivashov S.I., Makarenkov V.I., Sablin V.N., Sheyko A.P., *RF band high resolution sounding of building structures and works*, in: IEEE Aerospace & Electronic Systems Magazine, Vol.14, N. 5, pp.25-28, May (1999).
144. http://www.rslab.ru/english/downloads/rascan-5_manual_en.pdf
145. Capineri, L., Arezzini, I., Calzolari, M., Windsor C.G., Inagaki, M., Bechtel, T. D. and Ivashov S. I., High resolution imaging with a holographic radar mounted on a robotic scanner, *PIERS Proceedings*, pp. 1583–1585, August 12–15, Stockholm, (2013).
146. Jo Y.H., *Study on Applicability of Passive Infrared Thermography Analysis for Blistering Detection of Stone Cultural Heritage*, *Journal of Conservation Science*, Vol. 29, Issue 1, pp.55-67, The Korean Society Of Conservation Science For Cultural Properties. Doi: 10.12654/JCS.2013.29.1.06 (2013)
147. Liou K.N., *An Introduction to Atmospheric Radiation (2nd Edition)*, in: International Geophysics Series Vol. 84, Elsevier Science, California, USA (2002)
148. *Theory and Practice of Infrared Technology for Nondestructive Testing*, Maldague X.P., ISBN: 978-0-471-18190-3 (2001)
149. Carlomagno G.M., Cardone G., *Infrared Thermography for convective heat transfer measurements*, in: J. of Experiments in Fluids, Vol.49 (10), pp.1887-1218
150. Titman D.J., *Applications of Thermography in Non-Destructive Testing of Structures*, NDT&E International, Vol. 34, pp.149-154 (2001)
151. Ibarra-Castaneda C., Gonzalez D., Klein M., Pilla M., Vallerand S., *Infrared image processing and data analysis*, *Infrared physics & technology* 46 (1-2), 75-83 (2004)
152. Dyer J., Verri G., Cupitt J., *Multispectral imaging in reflectance and photo-induced luminescence modes: a user manual*, in: 7th framework program of charisma Project, The British Museum (2013), p 184

153. *Digital Image Processing (3rd edition)*, R.C. Gonzalez, R.E. Woods, Prentice-Hall (2008)
154. MacDonald L. W., Vitorino T., Picollo M., Pillay R., Obarzanowski M., Sobczyk J., Nascimento S., Linhares J., *Assessment of multispectral and hyperspectral imaging systems for digitisation of a Russian icon*, *Heritage Science* (2017) 5:41 pp. 1-16. DOI 10.1186/s40494-017-0154-1
155. <https://chsopensource.org/multispectral-imaging-system/>
156. Balas C., *A Novel Hyper-Spectral Imaging Apparatus for the Non-Destructive Analysis of Objects of Artistic and Historical Value*, in: *Journal of Cultural Heritage* 4, n. 1(2003):330-37.
157. <http://www.iesl.forth.gr/downloads/projects/general/IRIS.pdf>
158. https://www.hyspex.no/products/vnir_1600.php
159. <http://www.specim.fi/>
160. <http://www.specim.fi/products/pfd-65-v10e/>
161. Groves M. et al., *Damage and deterioration monitoring of artwork by data fusion of 3D surface and hyperspectral measurements*, in: *Proc. SPIE 9141, 91411E* (2014)
162. *Understanding Digital Raw Capture*, Fraser B., Adobe. Whitepaper (2004)
163. Accorsi G., Verri G., Bolognesi M., Armaroli N., Clementi C., Miliani C., Romani A., *The exceptional near-infrared luminescence properties of cuprorivaite (Egyptian blue)*, in: *Chemical Communications* (2009)
164. Thoury M., Delaney J.K., Rie E.R., Palmer M., Morales K., Krueger J., *Near-infrared luminescence of cadmium pigments: in situ identification and mapping in paintings*, *Applied Spectroscopy* 65(8) (2011)
165. <http://www.profilocolore.com/wp-content/uploads/2013/07/Profilocolore-Nikon-eXperience-Fotocamera-Full-Range-e-SB.pdf>
166. <https://archive.codeplex.com/?p=imageenhancer>
167. <https://chsopensource.org/chsos-technical-photography-kit/>
168. Cosentino A., Stout S., *Photoshop and Multispectral Imaging for Art Documentation*, in: *e-Preservation Science*, 11, 91–98 (2014).
169. Schneider C.A., Rasband W.S., Eliceiri K.W., *NIH Image to ImageJ: 25 years of image analysis*, in: *Nature Methods* (volume 9), pages 671–675 (2012)
170. <https://www.harris.com/solution/envi>
171. Tornari V., *Laser interference-based techniques and applications in structural inspection of works of art*, in: *Analytical and bioanalytical chemistry* 387 (3), 761-780
172. *Holographic interferometry*, Vest, C.M., John Wiley and Sons, Inc. (1979).
173. Ioppolo G. (ed.), *Le terme del Sarno a Pompei. Iter di un'analisi per la conoscenza, il restauro e la protezione sismica del monumento*, in: *Monografie* 5, "L'Erma di bretscheider", Soprintendenza Archeologica di Pompei (1992), p 191.
174. Pugliese Carratelli G., Baldassare I. (ed.), *Pompei: pitture e mosaici, V. VIII*, Istituto della Enciclopedia italiana (1981).
175. Niccolini F. and Niccolini A., *Le case ed i monumenti di Pompei. Disegnati e descritti* (reprint), F. Di Mauro, (2003).
176. Verri G., Saunders D., Ambers J., Sweek T., *Digital mapping of Egyptian Blue: conservation implications*, in: *Studies in Conservation* 55, sup. 2 (2010), 220-224.
177. *Giotto Architetto*, Gioseffi D., Giotto, Edizioni di comunità (1963).
178. Bellinati C., *Nuovi studi sulla Cappella di Giotto all'Arena di Padova (25 marzo 1303-2003)*, in «Quaderni dell'Archivio Vescovile e della Biblioteca Capitolare di Padova», 2, Il Poligrafo, Padova (2003).
179. *Padova – Piante e vedute (1449-1865) con saggio di Giuliana Mazzi*, Gironi S., Panda Edizioni, Padova (1985).
180. *Scrovegni commission. (1305-1306). Arena Chapel, exterior front and side. [Architecture]*, Retrieved from https://library.artstor.org/asset/ASJAMES_10313459950
181. *Scrovegni commission. (1305-1306). Arena Chapel, exterior front and side. [Architecture]*, Retrieved from https://library.artstor.org/asset/ASJAMES_10313459950
182. *Giotto. La Cappella degli Scrovegni*, Basile G., Electa, Milano (1992), p. 9.
183. *Giotto nella Cappella Scrovegni: Materiali per la tecnica pittorica, Studi e ricerche dell'Istituto Centrale per il Restauro*, a cura di G. Basile, Istituto Poligrafico e Zecca dello Stato (2005)
184. *Relazione sul restauro del Giudizio Universale di Giotto nella Cappella degli Scrovegni a Padova*, manoscritto, Brandi C., Istituto Centrale per il Restauro (1958).
185. *Da Giotto a Padova al cantiere di restauro dei dipinti*, Basile G., in: *Il restauro della Cappella degli Scrovegni. Indagini, progetti, risultati*, Ministero per i beni e le Attività Culturali, Skira, Milano (2003)
186. *The Franciscans and Art Patronage in Late Medieval Italy*, Bourdua L., Cambridge and New York: Cambridge University Press, (2004)
187. *Giotto e il suo tempo*. Sgarbi V. Federico Motta Editore, Milano, (2000)
188. Baggio L., *Iconografia di sant'Antonio al Santo di Padova nel XIII e XIV secolo: Spazi, funzioni, messaggi figurati, committenze*, Tesi di dottorato, Università di Padova (2014)

189. <http://geostatsrl.it/2016/05/rilievi-architettonici/>
190. Miltiadou-Fezans A., A *multidisciplinary approach* for the *structural Restoration* of the *Katholikon* of *Daphni Monastery* in *Attica Greece*, in: *Structural Analysis of Historic Construction*, D'Ayala & Fodde (editors), Taylor & Francis Group, London, (2008). ISBN 978-0-415-46872-5
191. Delinikolas N., Miltiadou-Fezans A., Chorafa E., Zaroyianni E., *Study on restoration of the Katholikon of Dafni Monastery: Phase A – Architectural and historical Survey*. Hellenic Ministry of Culture (2003)
192. Georgopoulos A., *Novel survey and digital photogrammetry methods for geometrical and architectural digital survey of Byzantine monuments*, in: *The case Dafni Monastery*. Research Report, NTUA and Hellenic Ministry of Culture, Athens (2003)
193. www.gtp.gr
194. *The mosaics of St. Mary's of the Admiral in Palermo*, Kitzinger E., Dumbarton Oaks, Washington (1990).
195. *Byzantine mosaic decoration: aspects of monumental art in Byzantium*, Demus O., Boston Book & Art Shop, (1955).
196. Nave. [Architecture], Retrieved from https://library.artstor.org/asset/HARTILL_12316474
197. *Palermo guida della città e dei dintorni*, Bellafiore G., Palermo 2009
198. *Two images of the Virgin in the Dumbarton Oaks Collection*, Der Nersessian S., DOP, 14 (1960), p. 69.
199. *Mirabilia Italia, La Cappella Palatina di Palermo*, A cura di Brenk B., Modena: Franco Cosimo Panini (2010), p.31-33
200. Cannella M., *La Cappella Palatina di Palermo: misura, interpretazione, rappresentazione*, in: *Rivista semestrale del Dipartimento di Storia, Disegno e Restauro*, 43, (2011)
201. *Palace of the Normans*. [Architecture], Retrieved from https://library.artstor.org/asset/HARTILL_12316459
202. *The Mosaics of San Marco in Venice*, Demus O., Chicago and London, Washington (1984), pp. 358, 495
203. Cantone V., *On the Mosaic of the Main Porch of San Marco in Venice: Towards a Multi-methodological Approach in Mosaics Studies*, in: *Actual Problems of Theory and History of Art, VI*, ed. by Maltseva S.V., Zakharova A.V., Staniukovich-Denisova E.Iu., ISSN 2312-2129, St. Petersburg (2016), pp. 143-149, tav. p. 870.
204. *La Basilica d'oro*, Polacco R., Milano, Berenice Publ. (1991), 352 p., p.30-34 (in Italian)
205. *La Basilica di San Marco* in Venezia illustrata nella storia e nell'arte da scrittori veneziani, Camillo B., Ongania, Venezia, 1888.
206. <https://www.pressreader.com/italy/corriere-di-verona/20180130/281857233972943>
207. Arletti R., Fiori C., Vandini M., *A Study of Glass Tesserae from Mosaics in the Monasteries of Daphni and Hosios Loukas (Greece)*, in: *Archaeometry*, Vol. 52, issue 5 (2010), <https://doi.org/10.1111/j.1475-4754.2009.00504>
208. Pozza G., Ajò D., Chiari G., De Zuane F., Favaro M., *Photoluminescence of the inorganic pigments Egyptian blue, Han blue and Han purple*, in: *Journal of Cultural Heritage*, 1(4), 393-398, (2000)
209. www.orsoni.it
210. *University Physics (7th Edition)*, Young H.D., Addison Wesley (1992)
211. *CRC Handbook of Chemistry and Physics* (1983) CRC Press Inc., Florida
212. *Engineering ToolBox*, (2003). *Coefficients of Linear Thermal Expansion*. [online], retrieved from: https://www.engineeringtoolbox.com/linear-expansion-coefficients-d_95.html [Accessed 01/09/2018]
213. *Introduction to Heat Transfer*, Incropera, F., De Witt, D., 2nd Edition, John Wiley and Sons, 1990
214. *Engineering ToolBox*, (2009). *Volumetric - or Cubic Thermal Expansion*. [online], retrieved from: https://www.engineeringtoolbox.com/volumetric-temperature-expansion-d_315.html [Accessed 01/09/2018]
215. *Engineering ToolBox*, (2010). *Relative Permittivity - the Dielectric Constant*. [online], retrieved from: https://www.engineeringtoolbox.com/relative-permittivity-d_1660.html [Accessed Day Mo. Year]
216. Von Hippel A.R., *Dielectric Materials and Applications*, in: *The International Critical Tables*, Chapman & Hall, London (1954)

Acknowledgments

Firstly, I would like to express my sincere gratitude to all my supervisors who advised me during the implementation of my PhD project with their immense knowledge, continuous support and patience.

I thank so much my supervisor Prof. Rita Deiana and my co-supervisor Prof. Gilberto Artioli at the University of Padua, who followed my work during all the three years of the PhD project.

I am very grateful for the extraordinary support, time and valuable advice by Dr. Vivi Tornari and by Mr. Michalis Andrianakis during and even after my stay at the IESL-FORTH (Heraklion, Crete - Greece).

I would like to thank very much Prof. Maria Koui for her supervision and valuable support and availability for my research period at the NTUA (Athens, Greece).

I would like to thank the whole team of Orsony foundry, in particular Ms. Liana Melchior and Ms. Antonella Gallenda for their availability and fruitful collaboration.

I would like to thank Prof. Valentina Cantone, Dr. Yotam Asscher for their input and professional advice. I would like to express my gratitude to Prof. Sergey Ivashov, Prof. Vladimir Razevig and all the other academic colleagues who contributed to my work with their professional support.

There are no words to express my biggest sincere gratitude to my family and to my dearest friends.

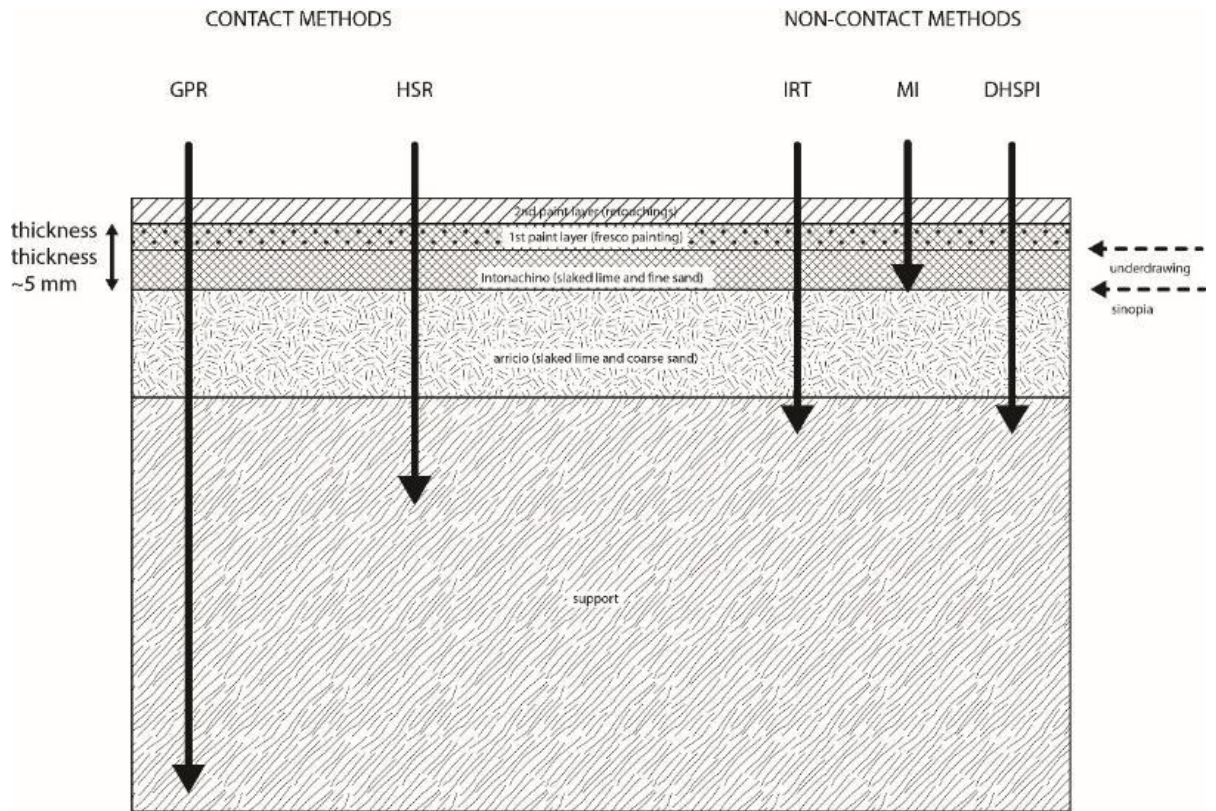
Finally, I would like to thank my external reviewers Prof. Roger Groves and Prof. Asterios Bakolas for their constructive criticism and insightful comments at the stage of the external review, which helped me to improve the structure of this thesis.

Attachment A. List of case studies and applied methods

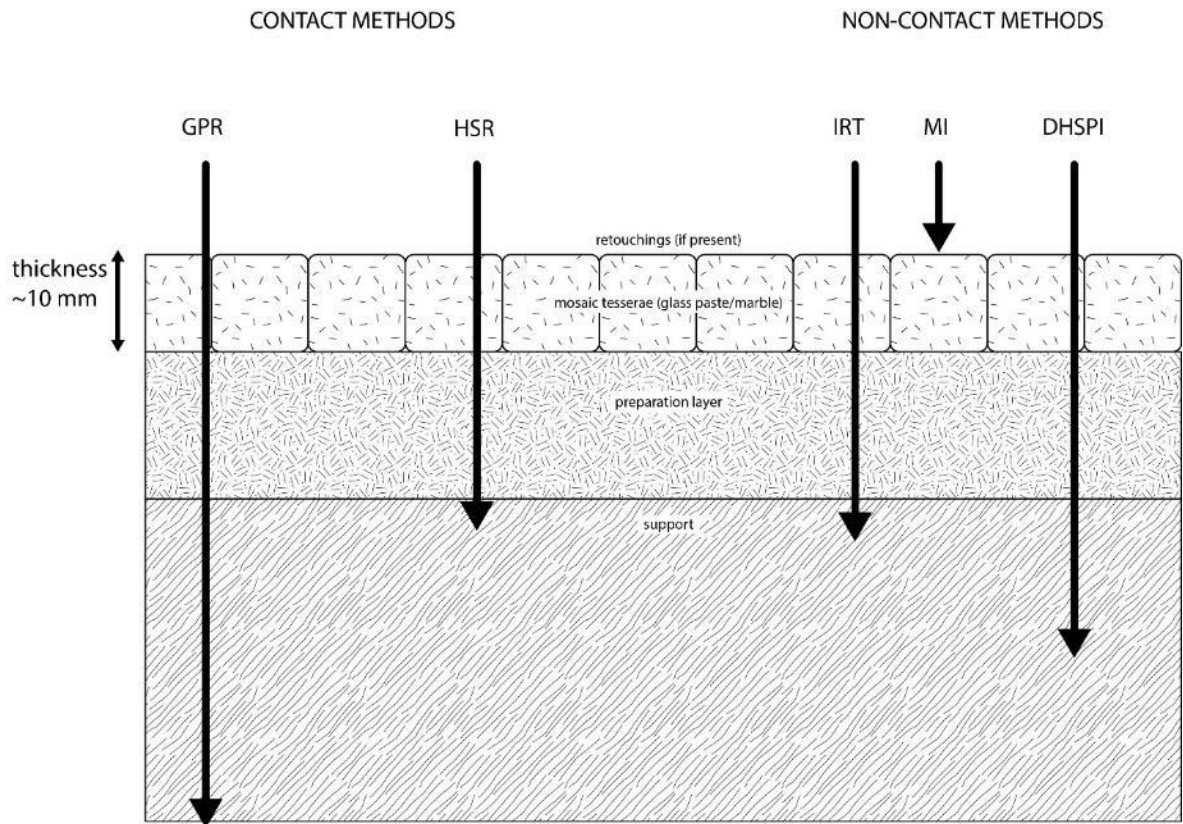
TYPE OF WALL DECORATION	CASE STUDY	APPLIED METHODS
WALL PAINTINGS	Scrovegni Chapel (Padua, Italy)	MULTISPECTRAL IMAGING, IR THERMOGRAPHY
	Sarno Baths (Pompeii, Italy)	MULTISPECTRAL IMAGING, IR THERMOGRAPHY
	Sala del Capitolo (Chapterl Hall), Basilica of Saint Anthony (Padua, Italy)	MULTISPECTRAL IMAGING, HSR, GPR
	Catholikon of Dafni Monastery (Athens, Greece)	MULTISPECTRAL IMAGING, IR THERMOGRAPHY

TYPE OF WALL DECORATION	CASE STUDY	APPLIED METHODS
WALL MOSAICS	Church of Santa Maria dell'Ammiraglio, "La Martorana" (Palermo, Italy)	MULTISPECTRAL IMAGING, HSR, INFRARED THERMOGRAPHY
	Palatine Chapel (Palermo, Italy)	MULTISPECTRAL IMAGING
	Basilica of Saint Mark (Venice, Italy)	MULTISPECTRAL IMAGING, GPR, HSR
	Catholikon of Dafni Monastery (Athens, Greece)	MULTISPECTRAL IMAGING, IR THERMOGRAPHY

Attachment B. Penetration depth of electromagnetic methods, employed in the experimental study to the diagnostic of wall paintings

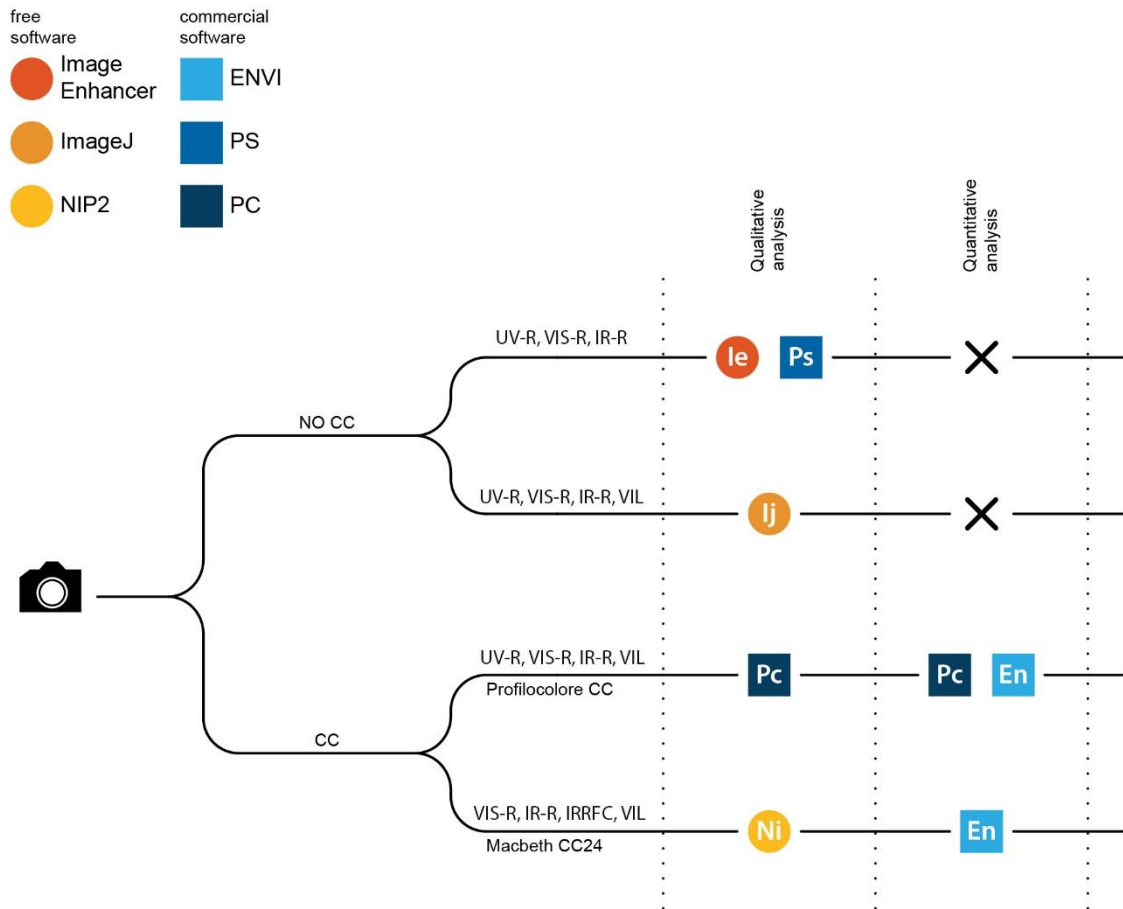


Attachment C. Penetration depth of electromagnetic methods, employed in the experimental study to the diagnostic of wall mosaics



Attachment D. Experimental results of in-situ MI acquisitions on wall decorations.

Recommended workflow



No CC – in the absence of a colour checker;

CC – in the presence of a colour checker;

UV-R – ultraviolet-reflected images;

VIS-R – visible reflected images;

IR-R – infrared-reflected images;

IRRFC – infrared false colour images;

VIL – visible induced infrared luminescence images

Attachment E. Multispectral Imaging Methodology applied to wall paintings

CASE STUDY		Conservation issue	Spectral band	Selected image processing procedure	Software tools
Roman wall paintings Frigidarium, Sarno Baths (Archaeological site of Pompeii, Italy)	Western Wall Painting (CC Profilocolare, CC Macbeth)	Enhancement, revealing of the underdrawings and lost details due to the degradation	IR VIS + IR	Remapping of image tonalities, contrast enhancement and RGB transformations (IE or Ps) Blending of layers in luminosity mode (Ps)	IE, Photoshop
		Differentiation between similar pigments	VIS, IR VIS + IR	<i>After calibration of lighting conditions:</i> remapping of image tonalities (IE or Ps) False Colour Infrared mode (NIP2)	IE, NIP2, Ps
		Identification and mapping of specific pigments in limited palettes (Egyptian Blue)	VIL	Enhancement (IE, Ps) and Subtraction (ImageJ)	IE or Ps and ImageJ
		Semi-quantitative analysis, relative	VIS, IR, VIL	<i>After calibration of lighting conditions:</i> Spectral analysis, statistical mapping, PCA	PrC and/or ENVI

		concentration of Egyptian Blue pigment			
		Enhancement of details and study of the underdrawings	UV, VIS, IR	Not efficient due to advanced degradation state	-
	Eastern Wall Painting (CC Profilocolore)	Identification and mapping of certain pigments (Egyptian Blue)	VIL	Enhancement and Subtraction	ImageJ
		Semi-quantitative analysis (concentration of Egyptian Blue)	VIS, IR, VIL	<i>After calibration of lighting conditions:</i> Spectral analysis, statistical mapping, PCA	PrC, ENVI
		Enhancement of details, support to the iconographic study	UV, VIS, IR	Enhancement, remapping of image tonalities and RGB transformations	IE and/or Ps
Late medieval wall paintings by Giotto Main Nave, Scrovegni Chapel (Padua, Italy)	Southern Wall Lunette painting Presbytery (CC Profilocolore)	Revealing hidden painting layers, enhancement of brush movements and artist's technique	IR VIS +IR	Remapping of image tonalities, contrast enhancement and RGB transformations (IE or Ps) Blending of layers in luminosity mode (Ps)	IE, Ps
		Enhancement of details, preliminary differentiation between original and retouched areas	UV, VIS, IR VIS +IR	False Colour Infrared, False Colour Ultraviolet mode through RGB channels transformations (Ps); Blending of layers in luminosity mode (Ps)	Ps

		Differentiation and mapping of pigments, semi-quantitative analysis	UV, VIS, IR	<i>After calibration of lighting conditions:</i> Spectral analysis, statistical mapping, PCA	PrC and/or ENVI
	Seven vices and seven virtues (No CC)	Enhancement of painting details and surface characteristics (texture, thickness, irregularities and fractures)	UV, VIS, IR	Convolution, Edge detection, remapping of image tonalities, RGB transformations	IE, Ps
		Enhancement of underdrawings, preliminary differentiation between original and retouched areas	IR VIS +IR(1-2)	Remapping of image tonalities, contrast enhancement and RGB transformations (IE or Ps) Blending of layers in luminosity mode (Ps)	IE, Ps
		Enhancement of lost details and improvement of script readability	IR VIS +IR(2)	Enhancement and Subtraction	ImageJ
Late medieval wall paintings, attributed to the hand of Giotto, covered by 16th century wall painting Basilics of Sant' Antonio, Sala del Capitolo (Padua, Italy)	Southern wall painting (Profilocolore CC)	Enhancement, revealing of the underdrawings and lost details	IR VIS +IR(1)	Remapping of image tonalities, contrast enhancement and RGB transformations (IE or Ps) Blending of layers in luminosity mode (Ps)	IE, Ps
		Differentiation and mapping of pigments, semi-quantitative analysis	UV, VIS, IR	<i>After calibration of lighting conditions:</i> Spectral analysis, statistical mapping, PCA	PrC and/or ENVI

<p>Wall paintings (16th century)</p> <p>Daphni Monastery, Catholikon (Athens, Greece)</p>	<p>Vault Painting Unknown Saint (No CC)</p>	<p>Enhancement, revealing of the underdrawings and lost details due to the degradation</p>	<p>IR VIS + IR</p>	<p>Remapping of image tonalities, contrast enhancement and RGB transformations (IE or Ps) Blending of layers in luminosity mode (Ps)</p>	<p>IE, Photoshop</p>

Attachment F. Multispectral Imaging methodology applied to wall mosaics

CASE STUDY		Conservation issue	Spectral band	Selected image processing procedure	Software tools
Church of Santa Maria dell’Ammiraglio (La Martorana), Palermo (Italy)	“Dedication of the Church to Virgin” (CC Profilocolore)	Enhancement of surface irregularities and differences in interstitial material; Eventually, enhancement of organic stains; Enhancement of color and hue variations on the tesserae surface; eventual presence of overpaints	UV, VIS+UV	Remapping of image tonalities, contrast enhancement and RGB transformations (IE or Ps)	IE and/or Ps
		Enhancement of surface irregularities; Revealing the	IR, VIS + IR	Good informativity without image processing , improved through:	- IE and/or Ps

		tesserae micromorphology		Remapping of image tonalities, contrast enhancement and RGB transformations (IE or Ps) Blending of layers in luminosity mode (Ps)	
		Enhancement of differences between tesserae; Differentiation between visibly identical tesserae of distinct composition	IR, VIS + IR	Good informativity without image processing , improved through: Remapping of image tonalities, contrast enhancement and RGB transformations (IE or Ps) Blending of layers in luminosity mode (Ps)	- IE and/or Ps
		Enhancement of differences in tesserae and in execution technique; Differentiation between presumably original and reshuffled/rearranged areas	VIS + IR UV+VIS+IR	Edge detection (IE) Subtraction, difference (ImageJ)	IE ImageJ
		Semi-quantitative analysis, mapping of certain types of tesserae; differentiation between original and reshuffled areas	UV, VIS, IR; UV+VIS+IR	<i>After calibration of lighting conditions:</i> Spectral analysis, statistical mapping, PCA	Profilocolore

	<p>“Coronation of King Roger” (CC Profilocolore)</p>	<p>Enhancement of surface irregularities and differences in interstitial material</p>	<p>UV, VIS+UV</p>	<p>Remapping of image tonalities, contrast enhancement and RGB transformations (IE or Ps) Blending of layers in luminosity mode (Ps)</p>	<p>IE and/or Ps</p>
		<p>Enhancement of surface irregularities, revealing of tesserae micromorphology</p>	<p>IR, VIS + IR</p>	<p>Good informativity without image processing, improved through: Remapping of image tonalities, contrast enhancement and RGB transformations (IE or Ps) Blending of layers in luminosity mode (Ps)</p>	<p>- IE and/or Ps</p>
		<p>Differentiation between visibly homogeneous (identical) tesserae of distinct composition: small black tesserae of Christ’s face features</p>	<p>IR, VIS + IR</p>	<p>Good informativity without image processing, improved through: Remapping of image tonalities, contrast enhancement and RGB transformations (IE or Ps) Blending of layers in luminosity mode (Ps)</p>	<p>- IE and/or Ps</p>
		<p>Mapping of differences in tesserae and execution technique; Differentiation between presumably original and reshuffled areas</p>	<p>VIS + IR UV+VIS+IR</p>	<p>Edge detection (IE) Subtraction, difference, multiplication (ImageJ)</p>	<p>IE ImageJ</p>

		Semi-quantitative analysis: mapping of certain types of tesserae; - differentiation between original and reshuffled areas	UV, VIS, IR; UV+VIS+IR	<i>After calibration of lighting conditions:</i> Spectral analysis, statistical mapping, PCA	Profilocolore
Apse Mosaic Saint Anna (No CC)		Enhancement of color and hue variations in the face of Saint Anna, eventual presence of an overpaint; Enhancement of differences in interstitial material (binding medium)	UV, VIS+UV	Remapping of image tonalities, contrast enhancement and RGB transformations (IE or Ps)	IE and/or Ps
		Differentiation between visibly identical tesserae that have distinct composition : small tesserae in face features; common size tesserae of the vestment	IR, VIS + IR	Good informativity without image processing , improved through: Remapping of image tonalities, contrast enhancement and RGB transformations (IE or Ps) Blending of layers in luminosity mode (Ps)	- IE and/or Ps
		Enhancement of differences in	UV, VIS, IR; VIS + UV;	Good informativity without image processing , improved through:	- IE and/or Ps

		tesserae and execution technique; preliminary evaluation of preservation state, documentation of cracks	VIS + IR	Remapping of image tonalities, contrast enhancement and RGB transformations (IE or Ps) Blending of layers in luminosity mode (Ps) Subtraction of spectral images (ImageJ)	ImageJ
Vault mosaics Saint Apostles Andrew and Peter, Saint Apostols Paul and Jacobus; Nativity scene (No CC)		Enhancement of color and hue variations in the faces; enhancement of differences in the interstitial areas	UV, VIS + UV	Remapping of image tonalities, contrast enhancement and RGB transformations (IE or Ps)	IE and/or Ps
		Differentiation between visibly identical tesserae of different composition: small tesserae in face features; common size tesserae of the vestment	IR, VIS + IR	Good informativity without image processing , improved through: Remapping of image tonalities, contrast enhancement and RGB transformations (IE or Ps) Blending of layers in luminosity mode (Ps)	- IE and/or Ps
		Evaluation of differences in tesserae material and execution technique, documentation of	UV, VIS, IR; VIS + UV; VIS + IR	Good informativity without image processing , improved through: Remapping of image tonalities, contrast enhancement and RGB transformations (IE or Ps)	- IE and/or Ps ImageJ

		the preservation state		Blending of layers in luminosity mode (Ps) Subtraction of spectral images (ImageJ)	
Palatine Chapel, Palermo (Italy)	Christ Pantokrator (No CC)	Enhancement of colour and hue variations; Eventually, enhancement of organic stains	UV; VIS + UV	Good informativity without image processing , improved through: Remapping of image tonalities, contrast enhancement and RGB transformations (IE or Ps)	- IE and/or Ps
		Differentiation between visibly similar (identical) black tesserae of the background	IR, VIS + IR	Good informativity without image processing , improved through: Remapping of image tonalities, contrast enhancement and RGB transformations (IE or Ps)	- IE and/or Ps
		Evaluation of differences in tesserae material and execution technique; Documentation of the general preservation state and mapping of cracks	UV, VIS, IR; VIS + UV; VIS + IR	Good informativity without image processing , improved through: Remapping of image tonalities, contrast enhancement and RGB transformations (IE or Ps) Blending of layers in luminosity mode (Ps) Subtraction of spectral images (ImageJ)	- IE and/or Ps ImageJ
	Apostle Saint Andrew (No CC)	Differentiation between visibly similar (identical)	IR, VIS + IR	Good informativity without image processing , improved through:	IE and/or Ps

		black tesserae of the vestment contour and of the letters		Remapping of image tonalities, contrast enhancement and RGB transformations (IE or Ps)	
		Evaluation of differences in tesserae material and execution technique; Documentation of the general preservation state and mapping of cracks	UV, VIS, IR; VIS + UV; VIS + IR	Good informativity without image processing , improved through: Remapping of image tonalities, contrast enhancement and RGB transformations (IE or Ps) Blending of layers in luminosity mode (Ps) Subtraction of spectral images (ImageJ)	IE and/or Ps ImageJ
	St. John Baptist and Virgin (No CC, long distance)	Enhancement of differences in tesserae and execution technique; Documentation of the mosaic preservation state and support to the reconstruction of the original iconographic scheme	UV, VIS, IR; VIS + UV; VIS + IR	Good informativity without image processing , improved through: Remapping of image tonalities, contrast enhancement and RGB transformations (IE or Ps) Blending of layers in luminosity mode (Ps) Subtraction of spectral images (ImageJ)	IE and/or Ps ImageJ
	Church Fathers (No CC)	Enhancement of differences in the interstitial material	UV; VIS + UV	Good informativity without image processing , improved through:	- IE and/or Ps

				Remapping of image tonalities, contrast enhancement and RGB transformations (IE or Ps)	
		Differentiation between visibly similar tesserae (red tesserae of the halos, red and golden tesserae of the vestments)	IR, VIS + IR	Good informativity without image processing , improved through: Contrast enhancement, remapping of image tonalities and RGB transformations (IE or Ps)	- IE and/or Ps
		Enhancement of differences in tesserae (size, reflectance values, form) and execution technique; Documentation of the mosaic preservation state and support to the reconstruction of the original iconographic scheme	UV, VIS, IR; VIS + UV; VIS + IR	Good informativity without image processing , improved through: Remapping of image tonalities, contrast enhancement and RGB transformations (IE or Ps) Blending of layers in luminosity mode (Ps) Subtraction of spectral images (ImageJ)	- IE and/or Ps ImageJ
	Baptism scene (no CC, long distance)	Enhancement of superficial stains	UV; VIS + UV	Good informativity without image processing , improved through:	- IE and/or Ps

				Contrast enhancement remapping of image tonalities, and RGB transformations (IE or Ps)	
Saint Mark Basilica, main porch, Venice (Italy)	Niche mosaic Virgin and Child (Profilocolore CC, short distance)	Enhancement of differences in tesserae surface characteristics (gloss/roughness), tone/hue and angle of inclination; Enhancement of differences in the interstitial material	UV; VIS + UV	Good informativity without image processing , improved through: Contrast enhancement, remapping of image tonalities, and RGB transformations (IE or Ps)	- IE and/or Ps
		Enhancement of differences in tesserae surface micromorphology (stripes of veins)	IR, VIS + IR	Good informativity without image processing , improved through: Contrast enhancement, remapping of image tonalities and RGB transformations (IE or Ps)	- IE and/or Ps
	Niche mosaics Saint Apostles Thomas and Bartoholomew (Profilocolore CC, short distance)	Enhancement of differences in execution technique, general evaluation of mosaic homogeneity	UV, VIS, IR	Good informativity without image processing , improved through: Contrast enhancement, remapping of image tonalities and RGB transformations (IE or Ps)	- IE and/or Ps
		Enhancement of differences in tesserae surface characteristics	UV; VIS + UV	Good informativity without image processing , improved through:	- IE and/or Ps

		(gloss/roughness), tone/hue and angle of inclination; Enhancement of differences in the interstitial material		Contrast enhancement, remapping of image tonalities, and RGB transformations (IE or Ps)	
		Differentiation between visibly similar tesserae (red tesserae of the vestment of Saint Bartholomew)	IR, VIS + IR	Good informativity without image processing , improved through: contrast enhancement, remapping of image tonalities and RGB transformations (IE or Ps)	- IE and/or Ps
Daphni Monastery, Catholikon, Athens (Greece)	Apse mosaic Saint Nicholas (No CC, long distance)	Evaluation of general homogeneity, evaluation and documentation of the mosaic preservation state	UV, VIS, IR	Good informativity without image processing , improved through: contrast enhancement, remapping of image tonalities and RGB transformations (IE or Ps)	- IE and/or Ps
		Enhancement of differences in tesserae surface characteristics (gloss/roughness), tone/hue and angle of inclination	UV; VIS + UV	Good informativity without image processing , improved through: Contrast enhancement, remapping of image tonalities, and RGB transformations (IE or Ps)	- IE and/or Ps

Attachment G. Description of image processing tools selected for the qualitative analysis of multispectral images

Table 1. NX Viewer

NX Viewer Image format: .NEF			
Function	Description of the function	Spectral range of applicability	Scope of use/information obtainable
CONVERSION OF IMAGE FORMATS	Conversion of the input file using raw format (.NEF) to an output file which can be elaborated in different image processing softwares (.TIFF or .JPEG)	UV; VIS; IR	Pre-processing step
INFORMATION ABOUT ACQUISITION PARAMETERS	Data visualization	UV; VIS; IR	Documentation purposes
BRIGHTNESS/CONTRAST (available also in Adobe Photoshop)	This tool adjusts the tonal range of an image. The brightness slider increases/decrease tonal values and expands image highlights/shadows. The contrast slider expands or shrinks the overall range of tonal values in the image	UV; VIS; IR	Enhancement of contrast and improvement of image readability

Table 2. Image Enhancer 1.0.0

Image Enhancer 1.0.0 Image format: .TIFF, .JPEG			
Filter	Description of the image processing algorithm	Spectral range of applicability	Scope of use/information obtainable
INVERT	Inversion of RGB channels	VIS	Inverted colors, providing a different (complementary) view on the image;
CONVOLUTION	A convolution is done by multiplying a pixel's and its neighboring pixels color value by a matrix (see " <i>Satellite Digital Image Analysis</i> ", Jamie Ludwig, Portland State University) Implementation of the algorithm calculating each pixel of the result image as weighted sum of the correspondent pixel and its neighbors in the source image	UV; VIS; IR	The resulting image is grayscale Enhancement of the surface microstructure, relief
CONTRAST CORRECTION	Increasing RGB values of bright pixels and	Grayscale UV; VIS;	Enhancement of contrast

	decreasing RGB values of dark values	Grayscale IR (“Burning” and “wild” colors when applied to raw (not grayscale) UV and IR bands)	
CONTRAST STRETCHING	Called also simply “normalization”, improvement of the contrast in an image by 'stretching' the range of intensity values it contains to span a desired range of values, e.g. the full range of pixel values that the image type concerned allows.	UV, VIS, IR	Enhancement of differences, correction of colors, increase of intensity and tones graduation
CANNY EDGE DETECTION	Detection of the edge of a binarized image using Canny Method	UV; VIS; IR	- Discontinuities in material properties; - variations in illumination; - differences in surface orientation and depth
SOBEL EDGE DETECTION	Detection of the edge of a binarized image using Sobel Method	UV; VIS; IR	MORE enhanced in comparison to Canny Edge detection White edges on black background EDGES INFORMATION: - discontinuities in material properties; - variations in illumination; - differences in surface orientation and depth
GRAYSCALE	Conversion to grayscale image (each pixel carries only intensity information)	UV; VIS; IR	Simple operation, helpful to focus on the pixels brightness in the resulting images
ROTATE RGB CHANNELS	Red channel is replaced by green, green by blue, blue by red	VIS	False Colour Mode Differentiation between similar pigments (through color components per pixel) and/or their concentrations
SATURATION CORRECTION	Adjustment of the pixel’s saturation value, increasing or decreasing it by specified operation HSL color space	VIS Often error in the UV band	Enhancement of color zones
SHARPEN	Preservation of the sharp edges of the input image. Identification and enhancement of edges (brightness discontinuities)	UV; VIS; IR	Enhancement of brightness discontinuities

EXTRACT CHANNEL (available also in Adobe Photoshop and ImageJ)	Replacement of the specified RGB channel with grayscale	VIS	Information about color pixel distribution (suggested for calibrated spectral images)
EDGE DETECT TYPE 1	Detection of the object edges by calculating maximum difference between pixels in 4 directional pixel processing technique	UV; VIS; IR	Helpful in detection of edges (sharp discontinuities)
GAUSSIAN BLUR	Application of Gaussian Blurring using the convolution kernel	UV; VIS; IR	Smoothing, reduction of noise
EDGE DETECT TYPE 2	Detection of object edges calculating the maximum difference of processing pixel with neighboring pixels in 8 directions	UV; VIS; IR	Helpful in detection of edges (sharp discontinuities)
CONSERVATIVE SMOOTHING	Noise reduction technique that derives its name from the fact that it employs a simple, fast filtering algorithm that sacrifices noise suppression power in order to preserve the high spatial frequency detail (e.g. sharp edges) in an image.	UV; VIS; IR	Noise reduction
MEDIAN FILTER	Nonlinear digital filtering technique used to remove noise	UV; VIS; IR Applicable to all the band, useful as pre-processing filter	Noise reduction, pre-processing step to improve the results of later processing (for example, edge detection on an image)

Table 3. Adobe Photoshop/ GIMP

Adobe Photoshop Image format: .TIFF, .JPEG			
Function	Description of the image processing algorithm	Spectral range of applicability	Scope of use/information obtainable
CURVES ADJUSTMENT	A linear function correlates input and output values. The horizontal axis of the graph represents the input and the vertical axis represents the output levels. As control points are added and moved to the line, the shape of the curve changes, reflecting the image adjustments (https://helpx.adobe.com/photoshop/using/curves-adjustment.html)	UV; VIS; IR	Transformations of brightness values. In wall paintings, this function is particularly useful for inversion of tones in the visible image before its blending with the infrared (for enhancement of underdrawings underneath dark pictorial areas)
BRIGHTNESS CONTRAST ADJUSTMENT	This tool makes non-linear (default) and linear adjustments to the tonal range of an image. The brightness slider increases/decrease tonal values and expands image highlights/shadows. The contrast	UV; VIS; IR	Enhancement of contrast and improvement of image readability

	slider expands or shrinks the overall range of tonal values in the image (https://helpx.adobe.com/photoshop/using/apply-brightness-contrast-adjustment.html)		
RGB CHANNELS: Rotation (available also in Image Enhancer and NIP2)	Channels represent and allows the manipulations in grayscale of the different components of the colors in the RGB system. Other channels can be added to enhance information and manipulation capabilities. The rotation function allows shift and exchange of reflectance values between RGB channels of one or more spectral images: the choice and order of shifting the channels can be changed (more options if compared to Image Enhancer and NIP2) (https://helpx.adobe.com/it/photoshop/using/channel-basics.html)	VIS; VIS + UV (False Colour UV); VIS + IR (False Colour IR)	Differentiation between similar pigments and/or their concentrations
RGB CHANNELS: Extraction (available in Image Enhancer and ImageJ)	Channels represent and allows the manipulations in grayscale of the different components of the colors in the RGB system. Other channels can be added to enhance information and manipulation capabilities. The rotation function allows to shift and exchange reflectance values between RGB channels of one or more spectral images (https://helpx.adobe.com/it/photoshop/using/channel-basics.html) The function extraction allows replacement of the specified RGB channel with grayscale	VIS	Information about the distribution of each RGB channel component (suggested for calibrated spectral images)
BLENDING OF LAYERS: Luminosity mode	Creates a result color and brightness from the hue and saturation of the base color and the brightness (luminance) of the blend color (https://helpx.adobe.com/it/photoshop/using/blending-modes.html)	VIS (base layer) + UV (blend layer); VIS (base layer) + IR (blend layer)	Enhancement of underdrawings in wall paintings
BLENDING OF LAYERS: Subtraction mode	Looks at the color information in each channel and subtracts the blend color and brightness information from the base color or brightness (https://helpx.adobe.com/it/photoshop/using/blending-modes.html)	UV+VIS; VIS + IR; IRF (visible induced infrared fluorescence)	Enhancement of differences in reflectance values between different spectral bands
BLENDING OF LAYERS: Difference mode	Either looks at the color information in each channel and subtracts the blend color and brightness from the base color or the base color from the blend color and brightness, depending on which has the greater brightness value (https://helpx.adobe.com/it/photoshop/using/blending-modes.html)	UV+VIS; VIS + IR; IRF (infrared fluorescence)	Enhancement of differences in reflectance values between different spectral bands

Table 4. ImageJ

ImageJ Image format: .TIFF			
Function	Description of the image processing algorithm	Spectral range of applicability	Scope of use/information obtainable
EXTRACTION OF RGB CHANNELS (available also in Image Enhancer and Adobe Photoshop)	The function saves each Channel to an external file with grayscale representation	VIS	Information about color pixel distribution (suggested for calibrated spectral images)
SUBTRACTION MODE for a stack of	The digital numeric value of each pixel in the image	UV+VIS; VIS + IR;	Enhancement of differences between spectral images

spectral images (at least 2)	is subtracted from another image	IRF + IR (infrared fluorescence)	
DIFFERENCE MODE for a stack (at least 2) of spectral images	The resulting image consists of differences in digital numeric value per each pixel of two images	UV+VIS; VIS + IR; IRF (infrared fluorescence)	Pixel difference value between spectral images

Table 5. NIP2

NIP2 (only in presence of Macbeth Color Checker) Image format: .TIFF			
Function	Description of the image processing algorithm	Spectral range of applicability	Scope of use/information obtainable
CALIBRATION OF LIGHTING CONDITIONS	The function uses another image, acquired at the same conditions, to eliminate the differences in color and brightness connected to the irregularity	UV; VIS; IR	Useful for the evaluation of color components, pre-processing step for differentiation between similar pigments
ROTATION OF RGB VALUES	Red channel is replaced by green, green by blue, blue by red (VIS) Blue channel is replaced by UV image, the green channel is replaced by blue, the red channel is replaced by green Red channel is replaced by IR image, the green is replaced by red, the blue is replaced by green (False Colour IR)	VIS; VIS + UV (False Colour UV); VIS + IR (False Colour IR)	Differentiation between similar pigments and/or their concentrations
SIMILAR COLOUR	Upon the defined threshold of digital numeric values deviation, the pixels are selected that correspond to the selected range of values	VIS	Statistical mapping of image pixels with similar color

Attachment H. Subsurface diagnostic Laboratory simulation tests results

Table 1. Detectability of known hidden defects in a mosaic subsurface

	Detachments, voids	Plastic, rubber	Wood	Metal	Stone and glass	Medium inhomogeneities
DHSPI	●	●	●	●	●	●
SIRT	●	●	●	●	●	●
HSR	●	●	●	●	●	●

Table 2. Applicability of methods to mosaic surface

	Portable and non-invasive	Full field	Contact less	Irregular, inhomogeneous surfaces	Under metal leaf	Resolution
DHSPI	●	●	●	●	●	●
SIRT	●	●	●	●	?	●
HSR	●	●	●	●	●	●

Figure 1 Experimental results. Recommended non-invasive approach

